

MECHANISMS REGULATING THE CIRCANNUAL RHYTHM OF HIBERNATION

By

Carla Frare, B.S., M.Sc.

A Dissertation Submitted in Partial Fulfillment of the Requirements

for the Degree of

Doctor of Philosophy

in

Biochemistry and Neuroscience

University of Alaska Fairbanks

August 2019

APPROVED:

Kelly L. Drew, Committee Chair

Abel Bult-Ito, Committee Member

Thomas K. Green, Committee Member

Thomas B. Kuhn, Committee Member

Thomas K. Green, Chair

Department of Chemistry and Biochemistry

Leah W. Berman, Dean

College of Natural Science and Mathematics

Micheal A. Castellini, Dean of the Graduate School

Abstract

Hibernation is a unique adaptation to conserve energy entering a hypometabolic (low metabolic rate) and hypothermic (low body temperature) state called torpor. Torpor is characterized by a drop in metabolism to 1-2% of basal metabolic rate and a decrease in body temperature to one to two degrees above ambient temperature. Metabolic rate is restored to basal metabolic rate and body temperature increases from 2-3°C to 36°C during the regularly timed arousal. The adenosine A₁ receptor agonists promote the onset of hibernation and torpor in different species, through a yet undefined neuronal circuit. In the Arctic ground squirrel, CHA, an adenosine A₁ receptor agonist, induces hibernation during the winter- hibernation season but not in summer even when the environmental conditions are kept constant (ambient temperature of 2°C and a light cycle of 4L:20D). Thus, the phenomenon of CHA-induced hibernation is entrained to an endogenous circannual rhythm. In this work, I aim to identify the changes in neuronal activation that reflect the circannual rhythm regulating the seasonal difference in response to CHA. Arctic ground squirrels, housed at constant ambient temperature (2°C) and light cycle (4L:20D), were implanted with body temperature transmitters. I collected tissue during Summer, Fall, Winter and Torpor conditions for seasonal analysis. For treatment analysis, I collected tissue from animals treated with CHA or vehicle in Summer and Winter. Primarily, I used immunohistochemistry to identify cell groups affected by season and treatment. I used cFos to identify neuronal activity and other immunohistochemical markers to identify neuronal phenotypes, based on specific cytoplasmic proteins. An overall seasonal decrease in thermogenesis, measured as reduced neuronal activity in the thermoregulatory pathways, and increase in vasoconstriction reflected the higher order processing necessary for CHA-induced hibernation. CHA inhibited the histaminergic neurons in the hypothalamus suppressing wakefulness and dis-inhibited the nucleus tractus solitarius, further suppressing thermogenesis. Preliminary data also suggested a seasonal change in the adenosine metabolic pathway, which may have increased adenosine receptor sensitivity during the hibernation season. Our results suggest that histaminergic neurons in the hypothalamus and the nucleus tractus solitarius are likely targets to manipulate metabolic demand in the clinical setting inducing therapeutic hypothermia or increasing metabolic rate.

Al mio papa`, to my dad

La nebbia a gl'irti colli
piovigginando sale,
e sotto il maestrone
urla e biancheggia il mar;

ma per le vie del borgo
dal ribollir de' tini
va l'aspro odor de i vini
l'anime a rallegrar.

Gira su' ceppi accesi
lo spiedo scoppiettando:
sta il cacciator fischiando
sull'uscio a rimirar

tra le rossastre nubi
stormi d'uccelli neri,
com'esuli pensieri,
nel vespero migrar.

San Martino da Rime Nuove, Giosue` Carducci, 1883.

Table of Content

	Page
Abstract.....	iii
Table of Content	v
List of Figures	ix
List of Tables	xi
List of Appendices	xiii
Acknowledgment	xiv
Chapter 1: General introduction.....	1
1.1 The phenomenon of hibernation.....	1
1.2 Medical application.....	3
1.2.1 Obesity	3
1.2.2 Therapeutic hypothermia	4
1.3 Adenosine, a potential mediator of hibernation	5
1.3.1 Adenosine biosynthesis in the brain	5
1.3.2 Adenosine and energy metabolism	6
1.3.3 Adenosine and sleep	6
1.3.4 Adenosine, hibernation and torpor	7
1.4 Research objectives	8
1.5 References	12
Chapter 2: The raphe pallidus and the hypothalamic-pituitary-thyroid axis gate seasonal changes in thermoregulation in the hibernating Arctic Ground Squirrel (<i>Urocitellus Parryii</i>).	17
2.1 Abstract.....	17
2.2 Introduction	18
2.3 Materials and Methods.....	19
2.3.1 Animals.....	19
2.3.2 Seasonal changes in the HPT-axis	19
2.3.3 Changes in the HPT-axis after CHA-induced cooling.....	20
2.3.4 Drugs	20
2.3.5 Brain tissue processing.....	21
2.3.6 Immunohistochemistry	21

2.3.7 Image analysis	22
2.3.8 Thyroid tissue processing and image analysis	22
2.3.9 TH analysis.....	23
2.3.10 Statistical analysis	24
2.4 Results.....	24
2.4.1 Seasonal changes in the HPT-axis	24
2.4.2 CHA-induced cooling.....	25
2.4.3 Changes in the HPT-axis after CHA-induced cooling.....	26
2.4.4 Seasonal changes in the SNS and in CHA-induced cooling	26
2.5 Discussion.....	27
2.6 Author contributions.....	30
2.7 Funding	30
2.8 Conflict of interest statement.....	31
2.9 Acknowledgments.....	31
2.10 References	41
Chapter 3: Seasonal decrease in thermogenesis and increase in vasoconstriction explain seasonal response to N ⁶ -cyclohexyladenosine -induced hibernation in the Arctic Ground Squirrel (<i>Urocitellus parryii</i>).....	45
3.1 Abbreviations	45
3.2 Abstract.....	46
3.3 Introduction	47
3.4 Materials and Methods.....	48
3.4.1 Animals.....	48
3.4.2 Surgery	49
3.4.3 Oxygen consumption	50
3.4.4 Experimental procedure	50
3.4.5 Drugs	51
3.4.6 Brain tissue processing.....	52
3.4.7 Immunohistochemistry	52
3.4.8 Double-labeled immunohistochemistry	53
3.4.9 Antibody characterization.....	53
3.4.10 Cell counting procedures	55

3.4.11 Statistical analysis	57
3.5 Results.....	58
3.5.1 Effect of handling on torpor bout in Winter AGS	58
3.5.2 Seasonal changes in euthermic T_b	58
3.5.3 Effect of treatments on T_b and metabolic rate	59
3.5.4 Effect of season on sleep-wake and thermoregulatory pathways	59
3.5.5 Effect of CHA on sleep-wake pathways	59
3.5.6 Effect of CHA on thermoregulatory pathways.....	60
3.5.7 Interaction of CHA and season on sleep-wake and thermoregulatory pathways	61
3.6 Discussion.....	61
3.6.1 Seasonal modulation of thermoregulatory response to CHA underlies onset of hibernation..	61
3.6.2 Thermolytic and somnogenic effects of CHA promote the onset of hibernation	63
3.6.3 Seasonal decrease in thermogenesis is required for the onset of hibernation.....	65
3.6.4 Seasonal differences in neuronal activation within the SCN unrelated to CHA	66
3.7 Acknowledgments and conflict of interest	67
3.8 References	88
Chapter 4: Seasonal changes in adenosine kinase in tanycytes underlie the possible mechanism of adenosine-induced hibernation in the Arctic Ground Squirrel (<i>Urocitellus parryii</i>).....	95
4.1 Abstract.....	95
4.2 Introduction	96
4.3 Materials and Methods.....	97
4.3.1 Animals.....	97
4.3.2 Brain tissue processing.....	98
4.3.3 Immunohistochemistry	98
4.3.4 Image analysis	99
4.3.5 Statistical analysis	99
4.4 Results.....	100
4.4.1 Seasonal changes alter tanycytes process width, but not length in the 3V.	100
4.4.2 Tanycytes express ADK	101
4.4.3 ADK expression in the tanycyte-like cells in the AP and 4V.....	101
4.5 Discussion.....	102
4.6 Conflict of Interest	105

4.7 Funding	105
4.8 Acknowledgments.....	105
4.9 References	115
Chapter 5: General conclusions	119
5.1 References	122
Appendices.....	125

List of Figures

	Page
Figure 1.1: Circannual rhythm in the AGS.....	9
Figure 1.2: Seasonal change in T_b in the AGS.....	10
Figure 1.3: ATP-Adenosine formation and catabolism.	11
Figure 2.1: HPT-axis is active in summer and winter euthermia, but not in torpor.	33
Figure 2.2: CHA, adenosine A1 receptor agonist, promotes onset of hibernation in a seasonally dependent manner.	34
Figure 2.3: CHA activates HPT axis more in winter than in summer.	36
Figure 2.4: Sympathetic tone decreases in winter.	37
Figure 2.5: Seasonal modulation of thermoregulation in hibernation.....	38
SI Figure 2.1: Level of reverse triiodothyronine (rT3) pharmacologically inactive hormone.	39
SI Figure 2.2: During torpor HPT axis is downregulated.	39
SI Figure 2.3: Higher concentration of TT3 and TT4 are associated with low T_b consistent with higher circulating levels at minimum T_b during torpor.	40
Figure 3.1: Graphical abstract.....	68
Figure 3.2: CHA promotes the onset of hibernation in a seasonally dependent manner.....	69
Figure 3.3: Regions of interests investigated in this study.	71
Figure 3.4: CHA reduces neuronal activity in the histaminergic neurons of the TMN.	72
Figure 3.5: Regions in the thermoregulatory pathway show differential activation in CHA groups compared to VEH.	75
SI Figure 3.1: Characterization of the antibodies used in the hypothalamus.....	81
SI Figure 3.2: Characterization of the antibodies used in the brainstem.	82
SI Figure 3.3: CHA induces a decrease in subcutaneous T_b (T_{sc}) that resembles the effect of CHA on core T_b	83
SI Figure 3.4: Representative images showing the seasonal changes in cFos expression.....	84
SI Figure 3.5: Representative images showing changes in neuronal activation in the CHA and VEH groups.	85
Figure 4.1: Tanycytes process' width does change between seasons, but not tanycytes length.	107
Figure 4.2: ADK is present in the cell body of the tanycytes.	108
Figure 4.3: ADK levels are lower in Winter compared to Summer in the tanycytes cell bodies.	110

Figure 4.4: Tanycyte-like cells and ADK are present in the AP. 111

SI Figure 4.1: Tanycytes morphology in the Torpor group. 113

SI Figure 4.2: Tanycytes morphology in the Fall group. 114

SI Figure 4.3: Tanycytes width decreased in Winter IBA. 115

List of Tables

	Page
Table 2.1: Characteristics of each seasonal phenotype.....	38
Table 3.1: Physiological parameters of Summer and Winter euthermic AGS.	76
Table 3.2: List of primary antibodies used to identify cFos and phenotypic markers, Research Resource Identifier (RRID).	77
Table 3.3: Seasonal changes in cFos expression.	78
Table 3.4: Treatment induced changes in neuronal activation, measured as cFos activation, in the paraventricular nucleus of the hypothalamus (PVN).....	79
Table 3.5: Treatment induced changes in neuronal activation, measured as cFos activation, in the nucleus tractus solitarius (NTS).....	79
SI Table 3.1: Brain regions in the AGS that do not show any differences between groups.	86
SI Table 3.2: List of primary antibody not showing immunoreactivity in AGS brain tissue.	87
Table 4.1: Physiological characteristics of the animals.....	112

List of Appendices

	Page
Appendix A: Protocols.....	125
Appendix A 1: IACUC Approval Letter for Research Protocol.....	125
Appendix A 2: AGS Husbandry Protocol	126
Appendix A 3: Protocol for Experiment and Animal Handling.....	131
Appendix A 4: Perfusion Protocol	134
Appendix A 5: Brain Processing Protocol.....	136
Appendix A 6: General Immunohistochemistry Protocol	139
Appendix A 7: Specific Immunohistochemistry Protocol for anti-Histamine Ab	142
Appendix A 8: Double-labeling Immunofluorescence Protocol.....	144
Appendix A 9: Abdominal Transmitter Protocol.....	145
Appendix B: Syllabi.....	147
Appendix B 1: Biology of Torpor Syllabus	147
Appendix B 2: Attending a Conference Syllabus.....	155
Appendix B 3: Neurochemistry Research Syllabus	157
Appendix B 4: Neuroendocrinology Syllabus.....	162
Appendix B 5: Teachable Unit Optogenetics	164
Appendix C: Mentoring Resources.....	166
Appendix C 1: General Introduction to Immunohistochemistry	166
Appendix C 2: Undergraduate Research Mentoring Contract.....	188
Appendix C 3: Student's Performance Evaluation	190
Appendix C 4: Mentor-Mentee Closure Assesment	192

Acknowledgment

I want to thank my adviser K. Drew, from whom I learn to love the complexity and the beauty of the brain. She gave me the opportunity to be part of the Drew lab, where I have grown to be an independent and critical scientist. I thank my lab partners, who have been supportive, fun to work with and who listen to any comments I had (and someday I had many..): B. Barati, L. Bogren, S. Bohwmick, Z. Carlson, M. Jenkins, B. Laughlin, J. Moore, L. Moore, C. Murphy, S. Rice. I would like to thank my past and present committee members, A. Bult-Ito, B. Edmonds, T. Green, T. Kuhn, for their support, comments and advice along the road. I thank the IACUC committee and the Animal Resources Center, who taught me the challenges of doing animal research and that patience is a virtue.

I thank the Chemistry Dpt., Emily and Jacy and the fellow TAs, where I had the *first* experience in teaching at a college level, IAB for summer funding on my *first* written research proposal and INBRE for two years of research assistantships. I thank BLaST and the people in the program for the opportunity to be a mentor with two years graduate mentoring research assistantships. BLaST had a *significant* impact on my development as a research mentor, providing resources and training.

I will be always grateful to my parents Claudio and Jacqueline who supported my choices, even when I told them I was moving to Alaska, to be fair I told them just for three years...They have always been there for me and they both still are. Thank you to “la famiglia” who has always a good story to share. I thank Ben, who supported and pushed me towards the finish line. He unexpectedly embraced this journey with me, three and a half years ago, and he will be my valuable companion in the next adventures. A sincere thanks to my friends, who have been there for me in the good times, but also when life was not so happy, E. Dinneen, C. Ebsen, M. Fant, A. Gädeke, C. Glassburn, J. Keeney, B. Laughlin, S. Luxton, S. Mitra, D. Ogata, J. Power, M. Reed, G. Rizzo, C. Schwartz, G. Smith. Thanks for being my best graduate school memories.

Last, I thank my squirrels and their contribution to science, without them, none of this work would have been possible.

Chapter 1: General introduction

1.1 The phenomenon of hibernation

Hibernation is an evolutionary strategy to conserve energy by entering a hypometabolic state, which results in a prolonged reduction in metabolism (Ruf and Geiser, 2015). This strategy is not only used in cold climates such as the Arctic, but also in the Tropics. As an example, in Madagascar, species like the tenrec and lemur hibernate to survive food scarcity, unexpected droughts or changes in microhabitat temperature (Blanco et al., 2018; Treat et al., 2018). The hypometabolic state can last from a few hours to several weeks, which distinguishes daily torpor from hibernation (Ruf and Geiser, 2015). Here, I will describe hibernation in ground squirrels, with a focus on the most northern species: the arctic ground squirrel (AGS, *Urocitellus parryii* renamed from *Spermophilus parryii* (Helgen et al., 2009)).

Hibernation is regulated by an endogenous circannual rhythm which persists under constant environmental conditions (Pengelley et al., 1978). Briefly, in the spring squirrels emerge from hibernation. Male AGS emerge a month before females to prepare for the brief mating season and feed on cache to restore their reproductive system (Williams et al., 2016). In summer, squirrels steadily increase their food intake by becoming hyperphagic (Carey et al., 2003) and their total body mass increases 50% in the pre-hibernation season, fall season (Sheriff et al., 2013; MacCannell et al., 2017). With the fat storage in place, AGS initiate hibernation that lasts seven to eight months (Williams et al., 2016) (Figure 1.1).

In the pre-hibernation season, after gaining the majority of the body mass, resting metabolic rate and energy expenditure decrease reducing euthermic body temperature (Sheriff et al., 2012, 2013) (Figure 1.2A) shifting to a positive energy balance. Squirrels stop eating and enter a hypophagic state that may be regulated by leptin, the satiety hormone, produced by the adipose tissue. Infusion of leptin during the hyperphagic phase decreases food intake in AGS (Ormseth et al., 1996) and evidence in other ground squirrels show high plasma levels of leptin and an increase in leptin receptors within the hypothalamus, the brain region controlling energy homeostasis, in hypophagic compared to hyperphagic animals (Schwartz et al., 2015). In addition, brown adipose tissue (BAT) undergoes substantial changes. BAT is a thermogenic tissue, characterized by a high density of mitochondria and blood vessels (Jastroch et al., 2018). Mitochondrial uncoupling protein 1 (UCP1) confers to the BAT the ability to produce heat, decreasing the metabolic efficiency producing heat instead of synthesizing ATP (Nedergaard et al., 2001). BAT thermogenesis is a mammalian adaption known as non-shivering

thermogenesis (NST). BAT is regulated by the sympathetic nervous system (SNS)(Morrison and Madden, 2014), which is critical during the hibernation season to initiate the regular arousal bouts (Ballinger and Andrews, 2018). Thus, BAT mass increases in volume enhancing the squirrel's ability to produce heat (i.e. thermogenic capacity)(Abbotts and Wang, 1980; Ballinger et al., 2016; MacCannell et al., 2017). As the hibernation season approaches, indicated by a slight ($\sim 2^{\circ}\text{C}$) decrease in euthermic body temperature, in the laboratory body temperature recordings show transient drops from 36°C to about 20°C , called test drops or test bouts (Ballinger et al., 2016)(Figure 1.2A). Interestingly, in the field AGS test drops are not observed with the same frequency as in captive AGS, 25% of free-living AGS show test drops compared to 66% of captive AGS (Sheriff et al., 2012). In the laboratory, the first torpor bout follows the test drops and the hibernation season begins. The hibernation season is composed of repeated torpor bouts, interrupted by arousal leading to regular interbout arousals (IBA) also known as interbout euthermia (IBE), a subsequent cooling phase precedes the next torpor bout (Figure 1.2B). The torpor bout length increases with the hibernation season. In mid-hibernation a torpor bout in AGS can last up to 20 consecutive days. Torpor is a hypothermic and hypometabolic state. The body temperature drops to a few degrees above ambient temperature and can reach a minimum of -2.9°C in free-living AGS (Barnes, 1989). Metabolic rate decreases to 1-2% of basal metabolic rate (Buck and Barnes, 2000), respiratory rate decreases to 1-2 breath/min (personal observations), heart rate decreases to 3- 5 beats/minute (personal observations consistent with marmots (Carey et al., 2003)). The arousal or rewarming phase lasts on average 5h (Karpovich et al., 2009) and in other species this has been shown to be initiated by BAT thermogenesis, followed by shivering once the body temperature increases up to around 16°C (Cannon and Nedergaard, 2004). During arousal, body temperature is restore to 36°C , metabolic rate restores to basal metabolic rate, respiratory rate levels off at 90-100 breath/minute and heart rate reaches 200-300 beats/min (personal observations consistent with published data in marmots (Carey et al., 2003)). These physiological parameters are maintained for about 15h in the IBA, until the start of the cooling phase (Karpovich et al., 2009). The onset of torpor is a regulated suppression of thermogenesis and metabolism. AGS housed at temperatures lower than -4°C , dramatically increase their metabolic rate maintaining a constant low body temperature (Buck and Barnes, 2000), highlighting the metabolic plasticity of the species.

1.2 Medical application

Thermoregulation is the ability to maintain body temperature and regulate energy balance (Lowell and Spiegelman, 2000). Metabolic reactions hydrolyzing ATP and catalyzed by the mitochondrial respiratory chain produce heat, i.e. thermogenesis. As an example, energy expenditure can be directly measured as thermogenesis or indirectly as the amount of oxygen consumed (Lowell and Spiegelman, 2000). Hence, interventions stimulating thermogenesis would stimulate metabolism, increasing energy expenditure and vice versa.

Plasticity in the thermoregulatory system and metabolism is key to hibernation. The understanding of the mechanisms used by hibernators to finely modulate their thermoregulatory system across seasons will advance thermal biology. With this new knowledge, we can develop clinical strategies to manipulate metabolic demand that is fundamental to conditions such as obesity, metabolic syndrome and therapeutic hypothermia.

1.2.1 Obesity

Obesity is a growing epidemic. The world health organization (WHO) reports that 39% of adults were overweight and 13% were obese in 2016, and current projections agree that the obesity rate will increase to 45% of the total population in 2035 (Revels et al., 2017). Obesity is associated with a significant decrease in life expectancy due to metabolic disorders such as diabetes, cardiovascular diseases and cognitive dysfunction (Lambert et al., 2013; Loh et al., 2017). Lifestyle interventions such as increasing physical activity and modifying diet are challenging strategies because they are followed by weight regain after weight-loss programs (Weiss et al., 2007). Thus, there is a need for novel approaches in developing treatment to minimize comorbidities.

The rediscovery of BAT in humans (Cypess et al., 2009; Zingaretti et al., 2009; Lee et al., 2010), has ignited research interest by the possibility to stimulate BAT thermogenesis to increase energy expenditure and potentially reverse obesity (Loh et al., 2017). Rodent studies show that cold-exposure and pharmacological stimulation of the β_3 -adrenoreceptors induce BAT thermogenesis (Srivastava and Veech, 2019). Similarly, cold-exposure increases BAT activation in healthy humans, but not in obese individuals (van Marken Lichtenbelt et al., 2009). BAT activation is controlled by the SNS (Morrison and Madden, 2014). Interestingly, studies show that SNS is impaired in obese individuals, who show an increase in resting sympathetic tone but a blunted sympathetic response to physiological stimuli (Lambert et al., 2013). Therefore, a deeper understanding of the mechanisms connecting the sympathetic regulation of BAT thermogenesis and energy balance in obesity is necessary to develop

novel therapies. The pre-hibernation fattening is a physiologically induced obesity that offers an ideal model to investigate the link between regulation of sympathetic activation of BAT thermogenesis and energy balance. As brown and white adipose tissue increase (MacCannell et al., 2017), thermogenesis gradually decreases (Sheriff et al., 2012) shifting the animals towards a positive energy balance, resembling human obesity, but without the associated comorbidities.

1.2.2 Therapeutic hypothermia

The benefits of induced hypothermia date back to the Egyptians, Greeks and Romans when hypothermia was recommended for battle-inflicted trauma and cerebral disturbances (Gunn et al., 2017). We have come a long way and currently therapeutic hypothermia or targeted temperature management (TTM) is a standard procedure for cardiac arrest and neonatal hypoxic-ischemic encephalopathy to prevent neurological damage (Song and Lyden, 2012; Krokhaleva and Vaseghi, 2018). Two randomized control trials show a better rate of good neurological outcome, 49% and 55% respectively, after cardiac arrest in patients treated with therapeutic hypothermia compared to the 26% and 39% with good neurological outcome in the normothermic group (Bernard et al., 2002; HACA, 2002). The neuroprotective benefits of TTM are multifactorial. They include a significant reduction in cerebral metabolism (for every degree of temperature reduction, cellular metabolism is reduced by 5%), and reduction of inflammation, oxygen free radical production and the accumulation of excitotoxic neurotransmitters (Delhayé et al., 2012; Song and Lyden, 2012; Taccone et al., 2014; Gunn et al., 2017).

TTM can be induced through endovascular cooling, infusion of cold fluids using catheters and through surface cooling as surface cooling pads (Deye et al., 2015); surface cooling has the advantage that it does not require expertise and advanced equipment compared to endovascular cooling, but it induces cooling at a slower rate (Song and Lyden, 2012). Nevertheless, both methods encounter the same side effects of shivering (Deye et al., 2015). Shivering is suppressed using paralytics, which prevent an accurate assessment of the neurological status due to the muscular blockade (Song and Lyden, 2012; Karcioğlu et al., 2018), highlighting the need to improve the current clinical protocols. This is challenging because shivering is a protective mechanism triggered by the thermoregulatory system to defend core body temperature in humans and other endothermic species.

Hibernators are heterothermic, they are able to defend their body temperature as endotherms but they also show poikilothermy-like characteristic during torpor, as their body temperature reaches the surrounding temperature. Hibernation is an *endogenous* hypometabolic state where the suppression of thermogenesis is controlled and regulated (Buck and Barnes, 2000; Richter et al., 2015). The

understanding of the thermoregulatory mechanisms promoting the onset of hibernation will provide novel approaches to induce a hypometabolic and hypothermic state avoiding the complication of shivering.

1.3 Adenosine, a potential mediator of hibernation

1.3.1 Adenosine biosynthesis in the brain

Within the central nervous system (CNS), astrocytes are the major source of adenosine. Adenosine is a neuromodulator and it affects neuronal activity presynaptically, controlling neurotransmitter release, postsynaptically, hyper or depolarizing neurons and non-synaptically regulating glial cells (Sachdeva and Gupta, 2013).

Adenosine is synthesized from ATP, the cellular "energy currency"(Figure 1.3). ATP is metabolized to ADP and subsequently to AMP. Cytosolic 5'-nucleotidase (c5'-NT) hydrolyzes AMP to adenosine. Adenosine accumulates in the cytosol and the equilibrative nucleoside transporters (ENTs) facilitate adenosine diffusion into the extracellular space. Thus, adenosine modulates neuronal activity through adenosine receptors (ARs) to restore energy balance (Masino and Boison, 2012). ARs are G-protein coupled receptors and they are categorized in four subtypes A₁AR, A_{2a}AR, A_{2b}AR and A₃AR (Masino and Boison, 2012). Activation of A₁AR, highly expressed in the CNS, and A₃AR inhibits neuronal activity, while activation of the A_{2a} AR and A_{2b}AR is stimulatory (Sachdeva and Gupta, 2013). Adenosine deaminase (ADA), which converts adenosine to inosine and adenosine kinase (ADK), which phosphorylates adenosine to AMP are responsible for decreasing adenosine concentration. ADK is located in astrocytes and is the primary regulator of extracellular adenosine. ADK activity lowers intracellular adenosine concentration. Therefore, ENT facilitates adenosine diffusion into the astrocytes, thus decreasing extracellular concentration, also shown by experimental manipulations of ADK. Pharmacological inhibition of ADK and genetic ADK knockout increase extracellular adenosine concentration, in contrast overexpression of ADK is associated with a decrease in extracellular adenosine (Boison et al., 2010; Park and Gupta, 2013).

1.3.2 Adenosine and energy metabolism

The increase in extracellular adenosine concentration reflects the increase in breakdown of cellular ATP, tying adenosine to cellular energy metabolism. Increases in neuronal activity, increases in energy consumption and increases in extracellular adenosine are directly related. Adenosine decreases energy demand inhibiting neuronal activity via the A₁AR (Porkka-Heiskanen and Kalinchuk, 2011). In addition, adenosine is the signaling molecule used by astrocytes in regulating energy homeostasis. The arcuate nucleus of the hypothalamus regulates metabolism and energy balance through orexigenic (i.e., promoting feeding) and anorexigenic (i.e., decreasing feeding) neurons. Astrocytes release adenosine and suppress orexigenic neuronal activity via A₁AR, reducing feeding and enhancing satiety (Yang et al., 2015; Sweeney et al., 2016). Thus, adenosine regulates brain energy metabolism through a general suppression in neuronal activity and modulates energy balance via a direct inhibition of orexigenic hypothalamic neurons.

1.3.3 Adenosine and sleep

Adenosine regulates sleep and wakefulness. Pharmacological studies in the past 50 years have shown that AR agonists increase sleep, while the antagonists disrupt sleep and increase wakefulness (Bjorness and Greene, 2009). These findings are also supported by the everyday used of caffeine, a non-selective adenosine antagonist, which affects sleep-wake behavior (Bjorness and Greene, 2009). Sleep is under homeostatic regulation, i.e., sleep pressure accumulates during the wake period and it dissipates during sleep (Porkka-Heiskanen and Kalinchuk, 2011). The homeostatic regulation is at its highest during sleep deprivation, which is associated with high adenosine levels in the basal forebrain (Porkka-Heiskanen and Kalinchuk, 2011; Donlea et al., 2017). Adenosine levels decrease in the following sleep recovery phase (Donlea et al., 2017). Thus, adenosine is recognized as the endogenous neuromodulator regulating the sleep homeostatic response.

The preoptic area of the hypothalamus regulates sleep through two brain nuclei: the ventrolateral preoptic area (VLPO) and median preoptic nucleus (MnPO) (Saper et al., 2005). The VLPO and the MnPO are characterized by sleep-active neurons and they promote sleep via inhibitory projections to the arousal systems within the hypothalamus and in the brainstem (Saper et al., 2005). Adenosine activates the inhibitory neurons in the MnPO and VLPO via the A_{2a}AR (Scammell et al., 2001; Kumar et al., 2013). The role of the A₁AR in the VLPO is more controversial. The tonic GABAergic inhibition of the VLPO was reduced by adenosine directly applied in brain slices, suggesting a dis-inhibition of the sleep active neurons through the A₁AR (Chamberlin et al., 2003; Morairty et al., 2004). However, in vivo studies show

that direct administration of the A₁AR agonists do not promote sleep (Methippara et al., 2005; Zhang et al., 2013). However, activation of the A₁AR induces sleep through a direct inhibition of the arousal centers, including the basal forebrain, the histaminergic neurons in the tuberomammillary nucleus and the hypocretin/orexin neurons in the lateral hypothalamus (Chen et al., 2016; Liu and Gao, 2007; Oishi et al., 2008; Rai et al., 2010; Yang et al., 2013). Hence, adenosine links together energy metabolism and sleep. Interestingly, sleep pressure increases during the hibernation season compared to summer (Walker et al., 1980), which is associated with reduced metabolic rate, highlighting similarity with the onset of sleep promoted by adenosine and the consequent decrease in metabolism.

1.3.4 Adenosine, hibernation and torpor

Pharmacological studies have shown that adenosine plays a role in the onset of hibernation and torpor, but the mechanisms and the brain regions associated with the phenomenon are still unclear. In the Syrian hamster, a hibernating species, intracerebroventricular (ICV) injection of adenosine induces hypothermia, which is attenuated when adenosine and 8-cyclopentyltheophylline (CPT), an adenosine A₁R antagonist, are delivered together. These results suggest that the A₁AR is the main mediator in inducing hibernation (Tamura et al., 2005). This finding was confirmed in other studies using ⁶N cyclohexyladenosine (CHA), an A₁AR agonist. CHA induces a decrease in body temperature and metabolic rate in hamster, AGS and in mice, that enters daily torpor after fasting (Shintani et al., 2005; Jinka et al., 2011; Iliff and Swoap, 2012). This was further validated by the lack of torpor onset in AGS treated with A₃AR agonist (Cl-IB-MECA) and the failure of A₂AR antagonists (MSX-2 and DMPX) to reverse torpor inducing arousal in AGS and hamsters (Tamura et al., 2005; Jinka et al., 2011). Moreover, CPT reversed torpor when delivered during the entrance-cooling phase in both the hamster and AGS (Tamura et al., 2005; Jinka et al., 2011). However, CPT was not effective when administered later in the torpor bout as shown in the hamster (Tamura et al., 2005), which is consistent with an earlier study in hippocampal brain slices showing a decrease in adenosine sensitivity in torpor compared to IBA, suggesting a downregulation of the adenosine receptors (Spangenberg et al., 1995). Thus, two different mechanisms control the onset of hibernation and the maintenance of torpor, and the A₁AR is critical in the onset of hibernation.

The hypometabolic state induced by CHA has been effective in rats, a non-hibernating species. CHA delivered ICV or within the nucleus tractus solitarius (NTS) in the brainstem produces a marked fall in body temperature due to an inhibition of BAT and shivering thermogenesis and other parasympathetic-like responses that resemble the onset of hibernation (Tupone et al., 2013). A₁AR-induced hibernation-

like effects in non-hibernating species shows biomedical potential to induce a controlled hypothermia; however, the mechanism is still unclear.

A₁AR-induced hibernation is a seasonal phenomenon in AGS. CHA promotes the onset of hibernation in AGS during the hibernation season, but not in euthermic-summer AGS where the response to CHA is transient (Jinka et al., 2011). Further experiments show a relation between a seasonal decrease in euthermic body temperature and the effectiveness of CHA-induced hibernation (Olson et al., 2013). CHA-induced hibernation in AGS may relate to a seasonal increase in sensitivity of A₁AR, regulated by a higher order process entrained by the circannual rhythm.

1.4 Research objectives

In the present study, I aim to characterize the neuronal pathways involved in CHA-induced hibernation in the AGS and how the endogenous circannual rhythm (i.e. seasons) affects the phenomenon and regulates the natural onset of hibernation. The research objectives included:

- 1- To assess the physiological characteristics that define each seasonal phenotype. I focused on changes in the thermoregulatory systems, in particular the hypothalamic-pituitary-thyroid axis, which regulates metabolism and thermogenesis. Thyroid hormones also regulate BAT thermogenesis synergistically with the SNS. Therefore, I investigated if the sympathetic premotor neurons in the raphe pallidus, which activate BAT thermogenesis, changed between seasons (Chapter 2).
- 2- Identify the neuronal pathways activated by CHA. In particular, to identify the seasonal differences in neuronal activation that may explain the seasonal difference in response to CHA (Chapter 3).
- 3- Identify whether changes in ADK expression are part of the mechanism underlying the seasonal increase in adenosine sensitivity leading to the onset of hibernation. I assessed changes in ADK in astrocytes and tanycytes, a type a glial cell involved in seasonal changes and part of the hypothalamic system regulating energy balance (Chapter 4).

Completion of these objectives is expected to lead to the understanding of the thermoregulatory mechanisms underlying the metabolic plasticity of hibernators. These mechanisms will provide novel targets to manipulate metabolic demand in clinical settings, such as obesity and therapeutic hypothermia.

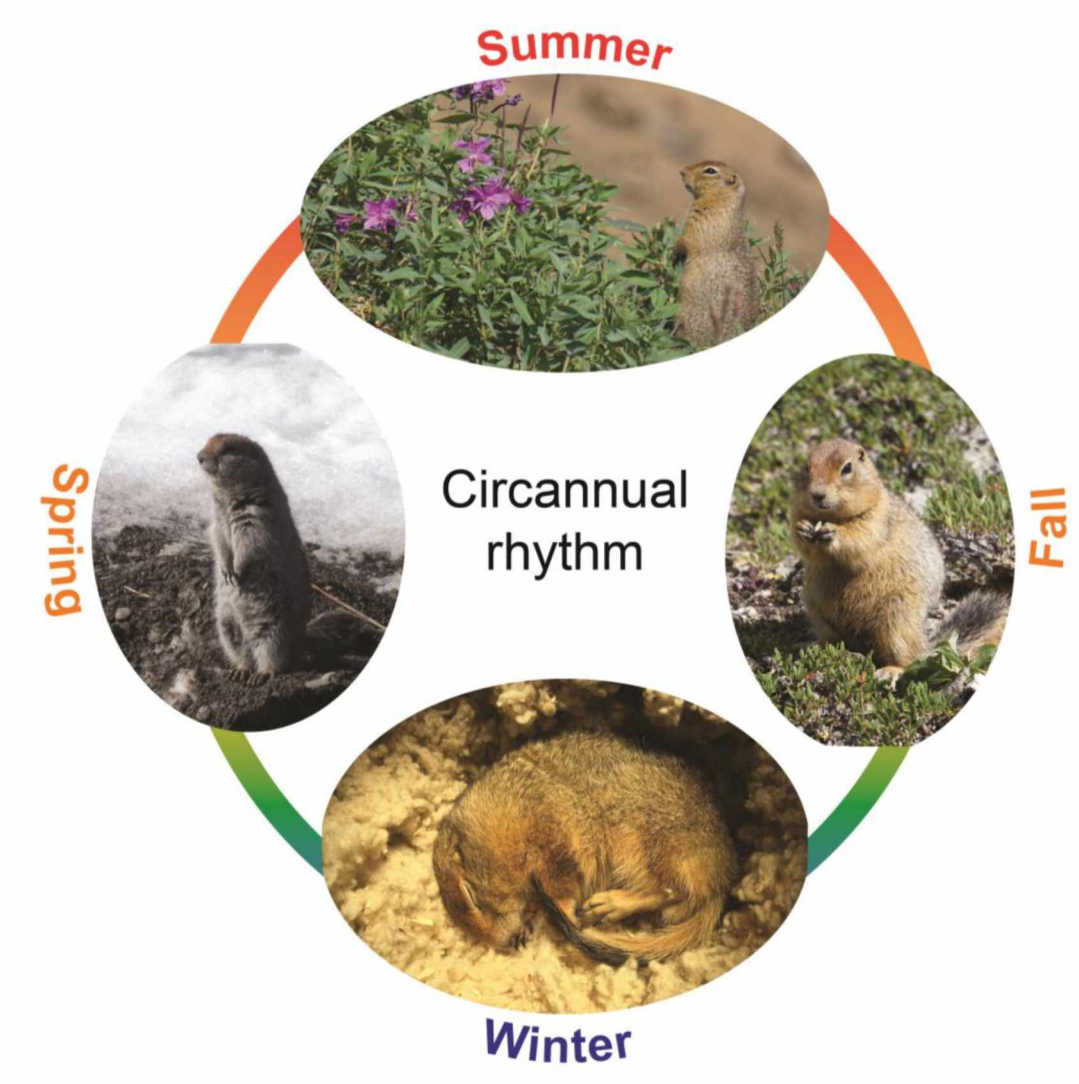


Figure 1.1: Circannual rhythm in the AGS.

The schematic shows AGS during different seasons, images taken by C. Frare.

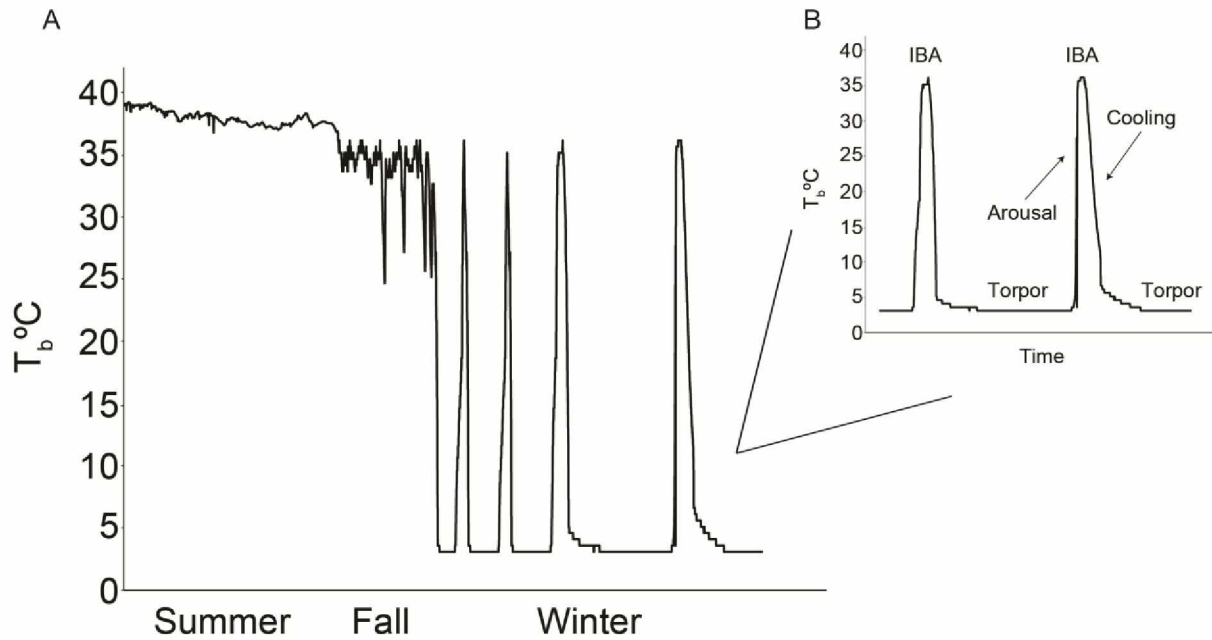


Figure 1.2: Seasonal change in T_b in the AGS.

A decrease in euthermic T_b defines the transition from Summer to Fall. Test drops in T_b occur in fall just prior to the onset of the hibernation season in winter (A). The hibernation season is characterized by Torpor bouts regularly interrupted by interbout arousals (IBA) (B).

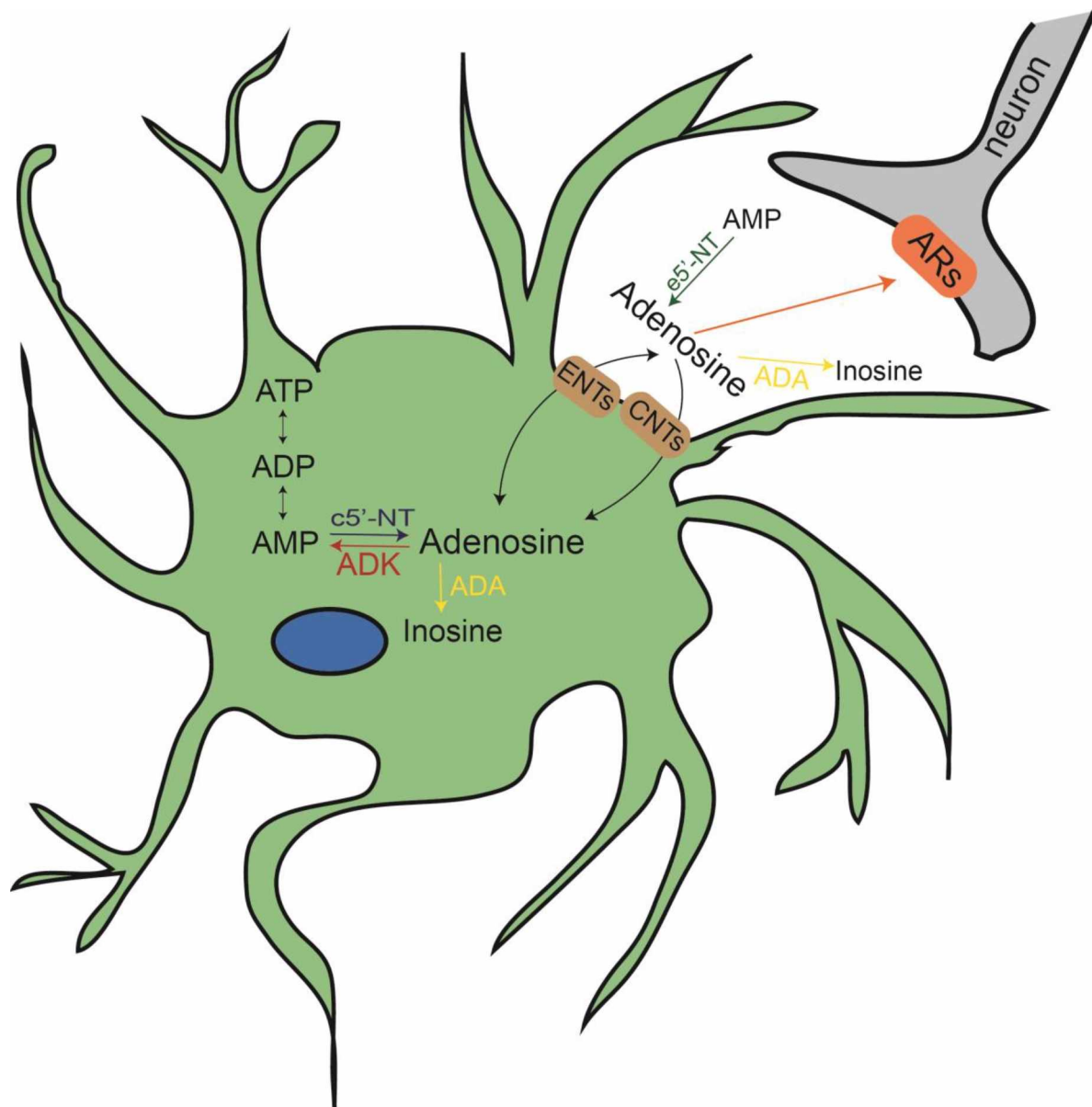


Figure 1.3: ATP-Adenosine formation and catabolism.

Breakdown of ATP increases adenosine concentration within the astrocytes. Adenosine diffuses to the extracellular space through the ENTs and modulates neuronal activity via adenosine receptors, here highlighted in the neurons, but widely distributed in the CNS. ADK and ADA regulates adenosine concentrations converting adenosine into AMP and inosine respectively. Extracellular AMP is converted back to ATP. ADA: adenosine deaminase, ADK: adenosine kinase, ARs: adenosine receptors, CNTs: concentrative nucleoside transporters, ENTs: equilibrative nucleoside transporters, c-5'-NT: cytosolic-5'-nucleotidase, e5'-NT: ecto-5'-nucleotidase.

1.5 References

- Abbotts, B., and Wang, L.C.H. (1980). Seasonal thermogenic capacity in a hibernator, *Spermophilus richardsonii*. *J. Comp. Physiol.* *140*, 235–240.
- Ballinger, M.A., and Andrews, M.T. (2018). Nature's fat-burning machine: brown adipose tissue in a hibernating mammal. *J. Exp. Biol.* *221*, jeb162586.
- Ballinger, M.A., Hess, C., Napolitano, M.W., Bjork, J.A., and Andrews, M.T. (2016). Seasonal changes in brown adipose tissue mitochondria in a mammalian hibernator: from gene expression to function. *Am. J. Physiol.-Regul. Integr. Comp. Physiol.* *311*, R325–R336.
- Barnes, B.M. (1989). Freeze avoidance in a mammal: body temperatures below 0 degree C in an Arctic hibernator. *Science* *244*, 1593–1595.
- Bernard, S.A., Gray, T.W., Buist, M.D., Jones, B.M., Silvester, W., Gutteridge, G., and Smith, K. (2002). Treatment of Comatose Survivors of Out-of-Hospital Cardiac Arrest with Induced Hypothermia. *N. Engl. J. Med.* *346*, 557–563.
- Bjorness, T.E., and Greene, R.W. (2009). Adenosine and Sleep. *Curr. Neuropharmacol.* *7*, 238–245.
- Blanco, M.B., Dausmann, K.H., Faherty, S.L., and Yoder, A.D. (2018). Tropical heterothermy is “cool”: The expression of daily torpor and hibernation in primates. *Evol. Anthropol. Issues News Rev.* *27*, 147–161.
- Boison, D., Chen, J.-F., and Fredholm, B.B. (2010). Adenosine Signalling and Function in Glial Cells. *Cell Death Differ.* *17*, 1071–1082.
- Buck, C.L., and Barnes, B.M. (2000). Effects of ambient temperature on metabolic rate, respiratory quotient, and torpor in an arctic hibernator. *Am. J. Physiol.-Regul. Integr. Comp. Physiol.* *279*, R255–R262.
- Cannon, B., and Nedergaard, J. (2004). Brown Adipose Tissue: Function and Physiological Significance. *Physiol. Rev.* *84*, 277–359.
- Carey, H.V., Andrews, M.T., and Martin, S.L. (2003). Mammalian Hibernation: Cellular and Molecular Responses to Depressed Metabolism and Low Temperature. *Physiol. Rev.* *83*, 1153–1181.
- Chamberlin, N.L., Arrigoni, E., Chou, T.C., Scammell, T.E., Greene, R.W., and Saper, C.B. (2003). Effects of adenosine on gabaergic synaptic inputs to identified ventrolateral preoptic neurons. *Neuroscience* *119*, 913–918.
- Chen, C.-R., Sun, Y., Luo, Y.-J., Zhao, X., Chen, J.-F., Yanagawa, Y., Qu, W.-M., and Huang, Z.-L. (2016). Paeoniflorin Promotes Non-rapid Eye Movement Sleep via Adenosine A1 Receptors. *J. Pharmacol. Exp. Ther.* *356*, 64–73.
- Cypess, A.M., Lehman, S., Williams, G., Tal, I., Rodman, D., Goldfine, A.B., Kuo, F.C., Palmer, E.L., Tseng, Y.-H., Doria, A., et al. (2009). Identification and Importance of Brown Adipose Tissue in Adult Humans. *N. Engl. J. Med.* *360*, 1509–1517.

- Delhaye, C., Mahmoudi, M., and Waksman, R. (2012). Hypothermia Therapy: Neurological and Cardiac Benefits. *J. Am. Coll. Cardiol.* *59*, 197–210.
- Deye N., Cariou A., Girardie P., Pichon N., Megarbane B., Midez P., Tonnelier J.-M., Boulain T., Outin H., Delahaye A., et al. (2015). Endovascular Versus External Targeted Temperature Management for Patients With Out-of-Hospital Cardiac Arrest. *Circulation* *132*, 182–193.
- Donlea, J.M., Alam, M.N., and Szymusiak, R. (2017). Neuronal substrates of sleep homeostasis; lessons from flies, rats and mice. *Curr. Opin. Neurobiol.* *44*, 228–235.
- Gunn, A.J., Laptook, A.R., Robertson, N.J., Barks, J.D., Thoresen, M., Wassink, G., and Bennet, L. (2017). Therapeutic hypothermia translates from ancient history in to practice. *Pediatr. Res.* *81*, 202–209.
- HACA (2002). Mild Therapeutic Hypothermia to Improve the Neurologic Outcome after Cardiac Arrest. *N. Engl. J. Med.* *346*, 549–556.
- Helgen, K.M., Cole, F.R., Helgen, L.E., and Wilson, D.E. (2009). Generic Revision in the Holarctic Ground Squirrel Genus *Spermophilus*. *J. Mammal.* *90*, 270–305.
- Iliff, B.W., and Swoap, S.J. (2012). Central adenosine receptor signaling is necessary for daily torpor in mice. *Am. J. Physiol.-Regul. Integr. Comp. Physiol.* *303*, R477–R484.
- Jastroch, M., Oelkrug, R., and Keipert, S. (2018). Insights into brown adipose tissue evolution and function from non-model organisms. *J. Exp. Biol.* *221*, jeb169425.
- Jinka, T.R., Tøien, Ø., and Drew, K.L. (2011). Season Primes the Brain in an Arctic Hibernator to Facilitate Entrance into Torpor Mediated by Adenosine A1 Receptors. *J. Neurosci.* *31*, 10752–10758.
- Karcioglu, O., Topacoglu, H., Dikme, O., and Dikme, O. (2018). A systematic review of safety and adverse effects in the practice of therapeutic hypothermia. *Am. J. Emerg. Med.* *36*, 1886–1894.
- Karpovich, S.A., Tøien, Ø., Buck, C.L., and Barnes, B.M. (2009). Energetics of arousal episodes in hibernating arctic ground squirrels. *J. Comp. Physiol. B* *179*, 691–700.
- Krokhaleva, Y., and Vaseghi, M. (2018). Update on prevention and treatment of sudden cardiac arrest. *Trends Cardiovasc. Med.*
- Kumar, S., Rai, S., Hsieh, K.-C., McGinty, D., Alam, M.N., and Szymusiak, R. (2013). Adenosine A2A receptors regulate the activity of sleep regulatory GABAergic neurons in the preoptic hypothalamus. *Am. J. Physiol. - Regul. Integr. Comp. Physiol.* *305*, R31–R41.
- Lambert, E.A., Straznicky, N.E., and Lambert, G.W. (2013). A sympathetic view of human obesity. *Clin. Auton. Res.* *23*, 9–14.
- Lee, P., Greenfield, J.R., Ho, K.K.Y., and Fulham, M.J. (2010). A critical appraisal of the prevalence and metabolic significance of brown adipose tissue in adult humans. *Am. J. Physiol.-Endocrinol. Metab.* *299*, E601–E606.

- Liu, Z.-W., and Gao, X.-B. (2007). Adenosine Inhibits Activity of Hypocretin/Orexin Neurons by the A1 Receptor in the Lateral Hypothalamus: A Possible Sleep-Promoting Effect. *J. Neurophysiol.* *97*, 837–848.
- Loh, R.K.C., Kingwell, B.A., and Carey, A.L. (2017). Human brown adipose tissue as a target for obesity management; beyond cold-induced thermogenesis. *Obes. Rev.* *18*, 1227–1242.
- Lowell, B.B., and Spiegelman, B.M. (2000). Towards a molecular understanding of adaptive thermogenesis. *Nature* *404*, 652–660.
- MacCannell, A., Sinclair, K., Friesen-Waldner, L., McKenzie, C.A., and Staples, J.F. (2017). Water–fat MRI in a hibernator reveals seasonal growth of white and brown adipose tissue without cold exposure. *J. Comp. Physiol. B* *187*, 759–767.
- van Marken Lichtenbelt, W.D., Vanhomerig, J.W., Smulders, N.M., Drossaerts, J.M.A.F.L., Kemerink, G.J., Bouvy, N.D., Schrauwen, P., and Teule, G.J.J. (2009). Cold-activated brown adipose tissue in healthy men. *N. Engl. J. Med.* *360*, 1500–1508.
- Masino, S., and Boison, D. (2012). *Adenosine: A Key Link between Metabolism and Brain Activity* (Springer Science & Business Media).
- Methippara, M.M., Kumar, S., Alam, M.N., Szymusiak, R., and McGinty, D. (2005). Effects on sleep of microdialysis of adenosine A1 and A2a receptor analogs into the lateral preoptic area of rats. *Am. J. Physiol.-Regul. Integr. Comp. Physiol.* *289*, R1715–R1723.
- Morairty, S., Rainnie, D., McCarley, R., and Greene, R. (2004). Disinhibition of ventrolateral preoptic area sleep-active neurons by adenosine: a new mechanism for sleep promotion. *Neuroscience* *123*, 451–457.
- Morrison, S.F., and Madden, C.J. (2014). Central Nervous System Regulation of Brown Adipose Tissue. *Compr. Physiol.* *4*, 1677–1713.
- Nedergaard, J., Golozoubova, V., Matthias, A., Asadi, A., Jacobsson, A., and Cannon, B. (2001). UCP1: the only protein able to mediate adaptive non-shivering thermogenesis and metabolic inefficiency. *Biochim. Biophys. Acta BBA - Bioenerg.* *1504*, 82–106.
- Oishi, Y., Huang, Z.-L., Fredholm, B.B., Urade, Y., and Hayaishi, O. (2008). Adenosine in the tuberomammillary nucleus inhibits the histaminergic system via A1 receptors and promotes non-rapid eye movement sleep. *Proc. Natl. Acad. Sci.* *105*, 19992–19997.
- Olson, J.M., Jinka, T.R., Larson, L.K., Danielson, J.J., Moore, J.T., Carpluck, J., and Drew, K.L. (2013). Circannual Rhythm in Body Temperature, Torpor, and Sensitivity to A1 Adenosine Receptor Agonist in Arctic Ground Squirrels. *J. Biol. Rhythms* *28*, 201–207.
- Ormseth, O.A., Nicolson, M., Pellemounter, M.A., and Boyer, B.B. (1996). Leptin inhibits prehibernation hyperphagia and reduces body weight in arctic ground squirrels. *Am. J. Physiol.-Regul. Integr. Comp. Physiol.* *271*, R1775–R1779.
- Park, J., and Gupta, R.S. (2013). Adenosine Metabolism, Adenosine Kinase, and Evolution. In *Adenosine: A Key Link between Metabolism and Brain Activity*, S. Masino, and D. Boison, eds. (New York, NY: Springer New York), pp. 23–54.

- Pengelley, E.T., Aloia, R.C., and Barnes, B.M. (1978). Circannual rhythmicity in the hibernating ground squirrel *Citellus lateralis* under constant light and hyperthermic ambient temperature. *Comp. Biochem. Physiol. A Physiol.* *61*, 599–603.
- Porkka-Heiskanen, T., and Kalinchuk, A.V. (2011). Adenosine, energy metabolism and sleep homeostasis. *Sleep Med. Rev.* *15*, 123–135.
- Rai, S., Kumar, S., Alam, M.A., Szymusiak, R., McGinty, D., and Alam, M.N. (2010). A1 receptor mediated adenosinergic regulation of perifornical-lateral hypothalamic area neurons in freely behaving rats. *Neuroscience* *167*, 40–48.
- Revels, S., Kumar, S.A.P., and Ben-Assuli, O. (2017). Predicting obesity rate and obesity-related healthcare costs using data analytics. *Health Policy Technol.* *6*, 198–207.
- Richter, M.M., Williams, C.T., Lee, T.N., Tøien, Ø., Florant, G.L., Barnes, B.M., and Buck, C.L. (2015). Thermogenic Capacity at Subzero Temperatures: How Low Can a Hibernator Go? *Physiol. Biochem. Zool.* *88*, 81–89.
- Ruf, T., and Geiser, F. (2015). Daily torpor and hibernation in birds and mammals. *Biol. Rev.* *90*, 891–926.
- Sachdeva, S., and Gupta, M. (2013). Adenosine and its receptors as therapeutic targets: An overview. *Saudi Pharm. J.* *21*, 245–253.
- Saper, C.B., Scammell, T.E., and Lu, J. (2005). Hypothalamic regulation of sleep and circadian rhythms. *Nature* *437*, 1257–1263.
- Scammell, T.E., Gerashchenko, D.Y., Mochizuki, T., McCarthy, M.T., Estabrooke, I.V., Sears, C.A., Saper, C.B., Urade, Y., and Hayaishi, O. (2001). An adenosine A2a agonist increases sleep and induces Fos in ventrolateral preoptic neurons. *Neuroscience* *107*, 653–663.
- Schwartz, C., Hampton, M., and Andrews, M.T. (2015). Hypothalamic gene expression underlying pre-hibernation satiety. *Genes Brain Behav.* *14*, 310–318.
- Sheriff, M.J., Williams, C.T., Kenagy, G.J., Buck, C.L., and Barnes, B.M. (2012). Thermoregulatory changes anticipate hibernation onset by 45 days: data from free-living arctic ground squirrels. *J. Comp. Physiol. B* *182*, 841–847.
- Sheriff, M.J., Fridinger, R.W., Tøien, Ø., Barnes, B.M., and Buck, C.L. (2013). Metabolic Rate and Prehibernation Fattening in Free-Living Arctic Ground Squirrels. *Physiol. Biochem. Zool.* *86*, 515–527.
- Shintani, M., Tamura, Y., Monden, M., and Shiomi, H. (2005). Characterization of N(6)-cyclohexyladenosine-induced hypothermia in Syrian hamsters. *J. Pharmacol. Sci.* *97*, 451–454.
- Song, S.S., and Lyden, P.D. (2012). Overview of Therapeutic Hypothermia. *Curr. Treat. Options Neurol.* *14*, 541–548.
- Spangenberg, H., Nikmanesh, F.G., and Igelmund, P. (1995). Effects of adenosine on synaptic transmission in hippocampal slices from hibernating and warm-acclimated Turkish hamsters and rats. *Neurosci. Lett.* *185*, 217–219.

- Srivastava, S., and Veech, R.L. (2019). Brown and Brite: The Fat Soldiers in the Anti-obesity Fight. *Front. Physiol.* *10*.
- Sweeney, P., Qi, Y., Xu, Z., and Yang, Y. (2016). Activation of hypothalamic astrocytes suppresses feeding without altering emotional states. *Glia* *64*, 2263–2273.
- Taccone, F.S., Cronberg, T., Friberg, H., Greer, D., Horn, J., Oddo, M., Scolletta, S., and Vincent, J.-L. (2014). How to assess prognosis after cardiac arrest and therapeutic hypothermia. *Crit. Care* *18*, 202.
- Tamura, Y., Shintani, M., Nakamura, A., Monden, M., and Shiomi, H. (2005). Phase-specific central regulatory systems of hibernation in Syrian hamsters. *Brain Res.* *1045*, 88–96.
- Treat, M.D., Scholer, L., Barrett, B., Khachatryan, A., McKenna, A.J., Reyes, T., Rezazadeh, A., Ronkon, C.F., Samora, D., Santamaria, J.F., et al. (2018). Extreme physiological plasticity in a hibernating basoendothermic mammal, *Tenrec ecaudatus*. *J. Exp. Biol.* *221*, jeb185900.
- Tupone, D., Madden, C.J., and Morrison, S.F. (2013). Central Activation of the A1 Adenosine Receptor (A1AR) Induces a Hypothermic, Torpor-Like State in the Rat. *J. Neurosci.* *33*, 14512–14525.
- Walker, J.M., Haskell, E.H., Berger, R.J., and Heller, H.C. (1980). Hibernation and Circannual Rhythms of Sleep. *Physiol. Zool.* *53*, 8–11.
- Weiss, E.C., Galuska, D.A., Kettel Khan, L., Gillespie, C., and Serdula, M.K. (2007). Weight Regain in U.S. Adults Who Experienced Substantial Weight Loss, 1999–2002. *Am. J. Prev. Med.* *33*, 34–40.
- Williams, C., Kathryn, W., Zhang Victor, Moore Jeanette, Barnes Brian M., and Buck C. Loren (2016). The secret life of ground squirrels: accelerometry reveals sex-dependent plasticity in above-ground activity. *R. Soc. Open Sci.* *3*, 160404.
- Yang, C., Franciosi, S., and Brown, R.E. (2013). Adenosine inhibits the excitatory synaptic inputs to Basal forebrain cholinergic, GABAergic, and parvalbumin neurons in mice. *Front. Neurol.* *4*, 77.
- Yang, L., Qi, Y., and Yang, Y. (2015). Astrocytes Control Food Intake by Inhibiting AGRP Neuron Activity via Adenosine A1 Receptors. *Cell Rep.* *11*, 798–807.
- Zhang, J., Yin, D., Wu, F., Zhang, G., Jiang, C., Li, Z., Wang, L., and Wang, K. (2013). Microinjection of adenosine into the hypothalamic ventrolateral preoptic area enhances wakefulness via the A1 receptor in rats. *Neurochem. Res.* *38*, 1616–1623.
- Zingaretti, M.C., Crosta, F., Vitali, A., Guerrieri, M., Frontini, A., Cannon, B., Nedergaard, J., and Cinti, S. (2009). The presence of UCP1 demonstrates that metabolically active adipose tissue in the neck of adult humans truly represents brown adipose tissue. *FASEB J.* *23*, 3113–3120.

Chapter 2: The raphe pallidus and the hypothalamic-pituitary-thyroid axis gate seasonal changes in thermoregulation in the hibernating Arctic Ground Squirrel (*Urocitellus Parryii*).¹

2.1 Abstract

Thermoregulation is necessary to maintain energy homeostasis. The novel discovery of brown adipose tissue (BAT) in humans has increased research interests in better understanding BAT thermogenesis to restore energy balance in metabolic disorders. The hibernating Arctic ground squirrel (AGS) offers a novel approach to investigate BAT thermogenesis. AGS seasonally increase their BAT mass to increase the ability to generate heat during interbout arousals. The mechanisms promoting the seasonal changes in BAT thermogenesis are not well understood. BAT thermogenesis is regulated by the raphe pallidus (rPA) and by thyroid hormones produced by the hypothalamic–pituitary–thyroid (HPT) axis. Here, we investigate if the HPT axis and the rPA undergo seasonal changes to modulate BAT thermogenesis in hibernation. We used histological analysis and tandem mass spectrometry to assess activation of the HPT axis and immunohistochemistry to measure neuronal activation. We found an increase in HPT axis activation in fall and in response to pharmacologically induced torpor when adenosine A₁ receptor agonist was administered in winter. By contrast, the rPA neuronal activation was lower in winter in response to pharmacologically induced torpor. Activation of the rPA was also lower in winter compared to the other seasons. Our results suggest that thermogenic capacity develops during fall as the HPT axis is activated to reach maximum capacity in winter seen by increased free thyroid hormones in response to cooling. However, thermogenesis is inhibited during torpor as sympathetic premotor neuronal activation is lower in winter, until arousal when inhibition of thermogenesis is relieved. These findings describe seasonal modulation of thermoregulation that conserves energy through attenuated sympathetic drive, but retains heat generating capacity through activation of the HPT axis.¹

¹ Published as Frare C, Jenkins ME, Soldin SJ and Drew KL (2018) The Raphe Pallidus and the Hypothalamic-Pituitary-Thyroid Axis Gate Seasonal Changes in Thermoregulation in the Hibernating Arctic Ground Squirrel (*Urocitellus parryii*). *Front. Physiol.* 9:1747. doi: 10.3389/fphys.2018.01747

2.2 Introduction

Thermoregulation is necessary to maintain energy homeostasis and when disrupted can lead to metabolic disorders. The novel discovery of brown adipose tissue (BAT) in humans (Betz and Enerbäck, 2015) has increased research interests in better understanding BAT thermogenesis to develop therapeutic approaches to increase energy expenditure activating BAT to treat obesity and diabetes (Betz and Enerbäck, 2015). The phenomenon of hibernation is an innovative model to investigate overall energy homeostasis and BAT thermogenesis, since this evolutionary adaptation is a model of physiological obesity (Cannon and Nedergaard, 2004) without any health consequences seen in humans such as type 2 diabetes and heart disease.

Hibernation is a seasonal phenomenon that is preceded by a fall transition phase where body weight increases by 40–60% (Sheriff et al., 2013; MacCannell et al., 2017) and body temperature (T_b) decreases 1–2°C from summer euthermic T_b (Russell et al., 2010; Sheriff et al., 2012). During hibernation, metabolic rate is suppressed to 1–2% of basal metabolic rate (BMR) and T_b approaches ambient temperature (Barnes, 1989; Buck and Barnes, 2000). The suppression in BMR and T_b characterize the torpid state, which is periodically interrupted by interbout arousals initiated by non-shivering thermogenesis (NST) via activation of BAT (Cannon and Nedergaard, 2004). While regulation of thermogenesis is important to sustain drastic changes in T_b and metabolic rate during the hibernation season, the seasonal regulation of thermogenesis is not fully understood. Previous work showed that AGS have a different seasonal response to pharmacologically induced torpor (Jinka et al., 2011). 6N -cyclohexyladenosine (CHA), an adenosine A_1 receptor agonist, induces similar decrease in T_b as seen in hibernation during winter, but not in summer underlining an endogenous seasonal modulation in thermogenesis independent of environmental factors such as light cycle and ambient temperature (Jinka et al., 2011). AGS are robust hibernators where the hibernation phenotype is strongly regulated by season. In hibernators, BAT is the main site of NST (Ballinger and Andrews, 2018). BAT thermogenesis is regulated synergistically by the sympathetic nervous system (SNS) and thyroid hormones (TH; Ortega-Carvalho et al., 2016). Hypothalamic–pituitary–thyroid (HPT) axis regulates TH production, increasing circulating TH to enhance thermogenic response when BAT is activated by the SNS (Silva and Larsen, 1983). Previous work in hibernation showed changes in circulating TH during torpor (Demeneix and Henderson, 1978; Nevretdinova and Shvareva, 1987; Magnus and Henderson, 1988) and thyroid morphology (Nunez and Becker, 1970; Krupp et al., 1977) in independent studies in different species. Here, we asked if seasonal modification of the HPT axis activation in AGS across season and in response to CHA-induced cooling could explain the seasonal response to CHA. As BAT thermogenesis is also

regulated by sympathetic premotor neurons in the raphe pallidus (rPA; Nakamura et al., 2004), we also describe the SNS through the rPA neuronal activity across season and in response to CHA.

2.3 Materials and Methods

All procedures were approved by Institutional Animal Care and Use Committee (IACUC) at the University of Alaska Fairbanks and conducted in accordance with the Guide for the Care and Use of Laboratory Animals (8th edition). The objective of this study was to define the role of the HPT axis in seasonal hibernation and in the seasonal modulation of CHA-induced cooling. We treated animals with CHA or vehicle in both summer and winter seasons. Because vehicle did not trigger changes in T_b in either winter or summer seasons, we included vehicle-treated animals in our analysis of seasonal changes. We used animals treated with vehicle in summer as Summer euthermic (Sum.VEH) and animals treated with vehicle in winter as interbout euthermic (ibe), also referred to as Winter euthermic (Win.VEH). For seasonal comparisons, we added samples from naïve animals at two additional time points, Fall (pre-hibernation) and Torpor.

2.3.1 Animals

Arctic Ground Squirrels (AGS, *Urocitellus parryii*) were captured in the Brooks Range (68°07'46"N 149°28'33"W) under permit by Alaska Department of Fish and Game. Beginning August 15th, the year of capture, we housed AGS, male and female, individually at constant environmental conditions at an ambient temperature (T_a) of 2°C and a photoperiod of 4L:20D until the end of the study to avoid any confounding results due to change in light cycle and T_a (Figure 2.1A). We provided approximately 47 g Mazuri rodent chow daily and water *ad libitum* although hibernating AGS do not drink or eat. Juveniles (one year old) were preferred for the study, adults were used when larger sample size was required.

2.3.2 Seasonal changes in the HPT-axis

To identify seasonal changes at the level of the HPT axis, we collected tissues at different time points defined as Fall, Winter euthermic (Win.VEH), Torpor, and Summer (Sum.VEH) (Figure 2.1B). Torpor was monitored daily using the shaving added technique (Jameson, 1964). The animal was defined torpid if wood shaving placed on the back remained undisturbed 1-day later. The presence of eight torpor bouts defined a winter phenotype that we referred to as a winter season. Summer phenotype (referred to as summer season) was characterized by at least 60 consecutive awake days following the end of the hibernation season. The fall transition state was characterized by a slight decrease in euthermic T_b .

Rectal T_b was measured in all animals before intracardial perfusion with a Digital Microprocessor Thermometer (model HH21 OMEGA Engineering, INC., Stamford, CT, United States). Table 2.1 reports details on each seasonal phenotype. We collected all the animals at the same time of day, 2 h into the dark cycle. Fall and torpid AGS were naïve and torpid AGS were collected between the first and fourth day of the torpor bout, consistent with the time of induced-arousal of winter AGS. Win.VEH and Sum.VEH were collected following the procedure illustrated in Figure 2.2A and described as follows. Brain, thyroid tissue, and blood samples were collected as described below.

2.3.3 Changes in the HPT-axis after CHA-induced cooling

AGS were implanted with iButton, (Maxim integrated, San Jose, CA, United States) abdominal temperature data loggers. Anesthesia was induced with 5% isoflurane and maintained at 3% mixed with 100% medical grade oxygen delivered at a flow rate of 1.5 L/min. During surgery T_b was maintained *via* a water circulating heating pad. Under aseptic conditions, the iButton was inserted intraperitoneally *via* a midline incision through linea alba and sealed with three layers of sutures. Buprenorphine (1.0 mg/kg, sc) slow release formulation was administered as analgesic and AGS were allowed at least 1 day of post-operative recovery in a warm room (17°C, 4L:20D) before being returned to home cage conditions (T_a of 2°C and 4L:20D). We induced arousal in winter AGS between the first and fourth day of the torpor bout and we moved the aroused animals to a warm room (17°C, 4L:20D) to maintain arousal state and to delay the occurrence of the following torpor bout. Animals displaying the summer phenotype were also moved to a warm room overnight (17°C, 4L:20D), for consistency in the procedure. During the overnight period, (approximately 12 h) food was withheld, and water was available *ad libitum*. In the morning of the experiment, AGS were moved to the environmental chamber (2°C, 4L:20D) 1 h before injection to acquire baseline data. Vehicle (2.5% hydroxypropyl- β -cyclodextrin) or CHA (0.5mg/kg, IP) were injected and animals were monitored for 3 h. At 3 h after injection, blood was collected *via* cardiac puncture and AGS were perfused intracardially prior to tissue collection. A schematic of the experimental designed is illustrated in Figure 2.2A and the related time points for tissue collection are shown in Figure 2.3A.

2.3.4 Drugs

A stock solution of CHA (10 mg/mL, Sigma-Aldrich, Saint Louis, MO, United States) was dissolved in 25% (w/v) hydroxypropyl- β -cyclodextrin (Tokyo Chemical Industry CO., Tokyo, Japan) in sterile water. On the week of the experiment, stock solution of CHA was diluted to 0.5 mg/mL in sterile normal saline (0.9%

NaCl). Diluted CHA was used within 1 month. Solutions for injection were sterilized by 0.2 µm filtration (Acrodisc syringe filter; Sigma-Aldrich, Saint Louis, MO, United States).

2.3.5 Brain tissue processing

At 3 h after injection, AGS were anesthetized with 5% isoflurane and maintained at 3% mixed with 100% medical grade oxygen delivered at a flow rate of 1.5 L/min. Blood was sampled by cardiac puncture and AGS were intracardially perfused first with 0.9% NaCl for 5 min and then with 4% PFA in 0.1 M PB buffer pH 7.4 at a flow rate of 79.5 mL/min with a 18 Ga needle through the left ventricle after the descending aorta was clamped to obtain a more efficient perfusion of the brain. Brains were removed and post fixed in 4% PFA overnight. Brains were blocked in 3 parts to allow better penetration of sucrose into the tissue. A gradient of sucrose solutions (5, 10, 15, 20, and 30 % w/v) was made in 0.1M PB buffer pH 7.4 to cryoprotect the tissue. Brains were maintained in each sucrose solution for up to 3 days and in 30% sucrose until brains sank. Brains covered with Tissue-Tek O.C.T. matrix (Electron Microscopy Sciences, Hatfield, PA, United States) were rapidly frozen in a bath of n-Hexane 95% cooled with dry ice to a temperature of -45°C. Coronal sections (40 µm) were cut with a cryostat (CM1850, Leica Biosystems, Buffalo Grove, IL, United States).

2.3.6 Immunohistochemistry

Free floating sections were washed using PBS pH 7.2, blocked with normal goat serum (Vector Laboratory, Burlingame, CA, United States) for 2 h at 4°C and labeled with mouse anti-cFos (1:20,000, Santa Cruz Biotechnology, Dallas, TX, United States) in PBS-0.2% TritonX-100 for 48 h, followed by incubation with biotinylated secondary goat anti-mouse antibody 1:600 (Vector Laboratory, Burlingame, CA, United States) in PBS-0.4% TritonX-100. After incubation in avidin-biotin-peroxidase (Vectastain ABC kit, Vector Laboratory, Burlingame, CA, United States), sections were treated with 0.05% DAB (3',3'-diaminobenzidine tetrahydrochloride, Sigma-Aldrich Corp. St. Louis, MO, United States) with 1% ammonium nickel sulfate in sodium acetate 0.175M and 0.1% H₂O₂. For double stain procedures, slices were then incubated with the second primary antibody, rabbit anti-TRH (1:10,000, gift from Eva Redei Northwestern University) or sheep anti-tryptophan hydroxylase (TPH) (1:2,000, AB1541, Millipore) in PBS-0.2% TritonX-100 overnight, followed by incubation with biotinylated secondary goat anti-rabbit or goat anti-sheep 1:600 (Vector Laboratory, Burlingame, CA, United States) in PBS-0.4% TritonX-100. After incubation with ABC, sections were treated with 0.05% DAB in PBS and 0.1% H₂O₂. Sections were mounted on Superfrost Plus slides (VWR, Radnor, PA, United States) with Cytoseal mounting media

(Thermo Fisher Scientific, Waltham, MA, United States) or PermOUNT (Thermo Fisher Scientific, Waltham, MA, United States). Control slices, in which primary antibody was omitted and replaced by PBS, were run in every experiment under the same conditions.

2.3.7 Image analysis

Images were analyzed using Metamorph software (version 7.8.8.0, Molecular Devices, San Jose, CA, United States) with a Nikon Eclipse TE2000-U inverted microscope equipped with a CCD camera (Cool Snap HQ2, Photometrics, Tucson, AZ, United States) for double stain analysis and with Nikon Eclipse 80i equipped with a digital camera (Micropublisher 3.3RTV, Qimaging, BC, Canada) for single stain analysis. A blind code was assigned to each animal to prevent any bias from the observer. For TRH analysis each hemisphere was counted individually in three consecutive slices for each AGS. The mean of six slices, three from each hemisphere per AGS, was used for subsequent statistical analysis. The count was done manually under a 20X objective using the manual count function in Metamorph to prevent double counting. Double stain was defined as brown DAB neurons with a distinct round dark black nucleus. All TRH positive neurons and the double stained neurons were counted in the paraventricular hypothalamic nucleus (PVN). The PVN was identified by reference to the Paxinos and Watson Rat Atlas Fourth Edition (bregma -1.40 to -1.60 mm). The percentage of activated TRH neurons was defined as the ratio between double stained neurons and the number of TRH positive neurons. We identified the rPA by Nissl stain with reference to the Paxinos and Watson Rat Atlas Fourth Edition (bregma -11.30 to -11.80 mm) and TPH staining. We defined a region of interest (ROI) of 0.05 mm² to include the entire rPA. cFos+ neurons were counted manually in the ROI in four consecutive slices under 10X objective in Metamorph.

2.3.8 Thyroid tissue processing and image analysis

After perfusion each thyroid lobe was isolated and stored in 70% ethanol until tissue processing. Paraffin sections (4 μm) were stained with hematoxylin and eosin (Carson, 1997). The first slice was collected when the tissue was exposed and the next four slices were collected at 50–80 μm intervals. Histological analyses were performed in bright field using the Nikon Eclipse 80i upright microscope under 40X objective. Stereological analyses were performed using the point-counting method. A grid of points was placed on top of the image at final magnification of 400X. A total of 15 randomly selected fields of view were analyzed per each section for a total of 4 sections per animal. A total of 60 fields of view per animal were used to calculate the thyroid activation index (TAI). First the volume of the colloid and follicular epithelium (V_{vph}) was calculated based on the following equation $V_{vph} = P_{ph}/P_{tot}$, where P_{ph} is

number of points on a particular phase (colloid or epithelium) and P_{tot} is the total number of points of the grid (Weibel et al., 1966), TAI was calculated based on the epithelial (V_{ve}) to colloid (V_{vc}) volume density ratio $\text{TAI} = V_{\text{ve}}/V_{\text{vc}}$ (Kalisnik, 1972).

2.3.9 TH analysis

Blood was collected *via* cardiac puncture using a heparinized syringe. Plasma was separated by centrifugation at 3,000 $\times g$ for 8 min at 4°C and then store at -80°C until use. TH were measured using micro high performance liquid chromatography-tandem mass spectrometry (LC-MS/MS) as previously described (Gu et al., 2007; Jonklaas et al., 2009; van Deventer et al., 2011; Masika et al., 2016).

For total thyroid hormones (TTH) analysis, 150 μL internal standards (IS) L-Thyroxine-[L-Tyr-d5] hydrochloride (T4-d₅) and 3,3',5-Triiodo-L-thyronine-¹³C₆ (T3-¹³C₆) were added to 200 μL plasma (thawed at RT) and mixed using a vortex for 30 s, then centrifuged for 10 min at 13,000 rpm. We added 500 μL 0.1M ammonium acetate in water to 200 μL supernatant and vortexed for 10 s before HPLC separation using a mobile phase A of 2% methanol with 0.01% formic acid and a mobile phase B of 98% methanol with 0.01% formic acid. For free thyroid hormones (FTH) analysis, 400 μL plasma was placed in a 30-kDa ultrafiltration device (Centrifree YM-30, Millipore) and centrifuged in an Eppendorf temperature-controlled centrifuge at 2,700 rpm for 40 min at 37°C. To 150 μL ultrafiltrate was added 250 μL IS. We added L-Thyroxine-¹³C₆ (T4-¹³C₆) and 3,3',5-Triiodo-L-thyronine-¹³C₆ (T3-¹³C₆) as IS to each aliquot and mixed using a vortex for 30 s, then centrifuged for 10 min at 13,000 rpm. The supernatant, diluted with water, was separated *via* HPLC using mobile phase A of 2% methanol with 0.01% acetic acid and mobile phase B of 100% methanol with 0.01% acetic acid.

Each sample, prepared as described, was then injected onto an Agilent SB C-18 (2.1 mm 50 mm, 3.5 m ID) chromatographic column (injection volume was 200 μL for TTH analysis and 400 μL for FTH analysis). The HPLC system consisted of 3 Shimadzu LC-20AD pumps, a Shimadzu SIL-HTA autosampler, and a Shimadzu DGU-20A5 degasser. The procedure involved an online extraction step followed by activation of a built-in Valco switching valve and subsequent sample introduction into the mass spectrometer. After a 3-min wash with 20% (vol/vol) methanol in 0.01% acetic acid at a flow rate of 1.0 mL/min, the switching valve was activated and the analytes of interest were eluted from the column and introduced into the mass spectrometer with a water/methanol gradient. We used an API-5000 tandem mass spectrometer (Applied Biosystems/MDS Sciex) equipped with TurbolonSpray source (ionspray voltage 4200V), operated in the negative ionization multiple reaction monitoring (MRM) mode. The MRM transitions monitored for T4-d₅, T3-¹³C₆, T4, and T3 were 783/135, 658/124, 778/150, and 652/150,

respectively in the TTH assay. The MRM transitions monitored for T4, T3, T4-¹³C₆, and T3-¹³C₆ were 776/127, 650/127, 782/127, and 656/127, respectively in the FTH assay. Data were acquired and processed by Analyst 1.4.1 software package. HPLC-grade methanol was from Fisher Scientific. The lower limits of detection were 0.55 ng/dL for Free T4 (FT4), 1.00 pg/mL for Free T3 (FT3), 0.25 µg/dL for T4, and 5.50 ng/dL for T3. Non-detectable values were assumed to be equal to the lower detection limit for statistical analysis. Intra assay variability reported as coefficient of variations ranged between 5.3 and 11.5% for FTH and 3.4–5.2% for TTH. The inter assay variability ranged between 9.4 and 12.6% for FTH and 4.8 and 6.2% for TTH.

2.3.10 Statistical analysis

Data are presented as mean ± SEM and a $p < 0.05$ was considered significant. Data analyses were performed using R (version 1.1.423). Groups with both season and treatment as independent variables were tested with a two-way ANOVA. To allow for a two-way ANOVA in the cell count analysis, data were normalized by transforming to the square root. ANOVA was followed by independent samples *t*-test. One-way ANOVA was used when season was the only independent variable and data were normally distributed. Kruskal Wallis and Wilcoxon signed-rank tests were used when data were not normally distributed. Groups were randomly matched by sex and age where indicated.

2.4 Results

Body weight and rectal T_b of animals collected in Fall, Winter, Torpor, and Summer were consistent with the seasonal phenotype of hibernation (Figure 2.1B and Table 2.1).

2.4.1 Seasonal changes in the HPT-axis

To assess seasonal changes in the HPT axis we defined HPT axis activation based on up-regulation at any point of the axis beginning with activation of TRH+ neurons in the PVN, and including TAI (Kalisnik, 1972) and circulating total and FTH. We found that TRH neurons were least active during Torpor [$F(3,16) = 11.13$, $p < 0.001$ one-way ANOVA, followed by *t*-test] compared to the three different euthermic states (Figures 2.1C,D). Suppressed activity in TRH neurons is consistent with reduced thermogenesis and metabolic rate during torpor. Surprisingly, TAI in Torpor was not lower compared to Summer or Winter euthermia. Moreover, TAI was significantly higher in Fall AGS compared to the other three states [$H(3) = 13.48$, $p < 0.01$, Kruskal Wallis test, followed by Wilcoxon's rank-sum test]. In fact, TAI trended toward higher activation in Torpor compared to Winter euthermic animals ($p = 0.051$, Wilcoxon's rank-sum test,

Figure 2.1E). Thus, thyroid activity is maintained between Summer, Winter, and Torpor and is significantly elevated in the Fall AGS.

Next, we measured the plasma levels of TH. Both total l-Thyroxine (TT4) and total 3,3',5-Triiodo-L-thyronine (TT3) are highest during torpor (Figures 2.1F,G). Plasma concentration of TT4 is significantly higher in Torpor compared to Summer euthermic and Fall [$F(3,18) = 3.74, p < 0.05$ one-way ANOVA, followed by t -test]. As with TAI, TT4 in torpor trends toward higher levels compared to Winter euthermic ($p = 0.07, t$ -test, Figure 2.1G). Likewise, plasma concentration of TT3 is significantly higher in Torpor compared to the three different euthermic states [$H(3) = 14.39, p < 0.01$ Kruskal Wallis test, followed by Wilcoxon's rank-sum test, Figure 2.1F]. Consistent with higher concentration of TTH in torpor, we found inverse correlations between TT3, TT4 and T_b (Supplementary Figures S2.3A,B). Neither FT3 nor FT4 changed significantly across season [$H(3) = 1.86, p\text{-value} > 0.05$ Kruskal Wallis test, FT3; [$F(3,18) = 0.85, p > 0.05$ one-way ANOVA, FT4; Figures 2. 1H,I]. [$H(3) = 1.86, p\text{-value} > 0.05$ Kruskal Wallis test, FT3; [$F(3,18) = 0.85, p > 0.05$ one-way ANOVA, FT4; Figures 2.1H,I].

We did not find any significant change in plasma levels of reverse triiodothyronine (rT3) the pharmacologically inactive hormone between seasons (Supplementary Figure S2.1A), however the ratio between rT3 and TT3 was significant lower in torpor compared to Summer and Winter euthermic animals, suggesting a downregulation of the HPT axis in torpor ($p < 0.05$, Supplementary Figure S2.2A).

2.4.2 CHA-induced cooling

Except for the fall transition period, our data support consistent HPT axis activation during euthermia across seasons. We next asked if HPT axis activation changes during onset of torpor mimicked by CHA-induced cooling. Consistent with previous observations, CHA administered to Winter AGS gradually decreased T_b to $26.0 \pm 0.9^\circ\text{C}$ after 3 h. By contrast, CHA in Summer AGS produced a rapid, but transient decrease in T_b that returned to euthermic values $36.9 \pm 1.9^\circ\text{C}$ within 3 h [$H(17) = 17.8, p < 0.001$, Kruskal Wallis test, Figure 2.2B]. Vehicle treatment did not change T_b [$H(16) = 8.4, p = 0.9$, Kruskal Wallis test, Figure 2.2C]. Also consistent with previous observations, resting T_b , reported as mean of T_b measured in the 1 h prior injection, was lower in Winter AGS ($36.4 \pm 0.3^\circ\text{C}$) compared to Summer AGS ($38.6 \pm 0.2^\circ\text{C}, p < 0.001, t$ -test). Such seasonal changes provide evidence of a seasonal decrease in thermogenesis as seen by significantly lowering euthermic T_b reported in Table 2.1.

2.4.3 Changes in the HPT-axis after CHA-induced cooling

At the level of TRH neuronal activation, CHA activated the HPT axis [percent of cFos+ and TRH+ over TRH+ after CHA ($79 \pm 3\%$) compared to vehicle ($69 \pm 3\%$), $F(1,17) = 5.562$, $p = 0.03$, two-way ANOVA, Figures 2.3B,C] but the interaction with season was not significant. After the two-way ANOVA failed to show an interaction with season we minimized inter-animal variation by matching pairs of animals by sex and age; sex and age are known to influence TH concentrations (Suzuki et al., 2012). In the analysis of TRH neuronal activation as the difference between matched pairs, we found a significant influence of season. Matched pairs showed that CHA activated more TRH neurons in Winter than in Summer (Figure 2.3D). Greater activation supports an increased thermogenic capacity in winter. Looking at the next level of HPT axis activation TAI was stable across CHA and vehicle treatment groups [$F(1,15) = 0.001$, $p = 0.98$, two-way ANOVA]. Although TAI did not change, TTH increased in parallel to TRH neuronal activation after CHA in Winter compared to CHA in Summer. Following CHA administration, both concentrations of TT4 and TT3 are higher in winter AGS compared to summer ($p < 0.05$, Wilcoxon's rank-sum test, Figures 2.3E,F). Consistent with increased HPT axis activation after CHA in Winter, we found greater increases in FT3 after CHA in Winter than after CHA in Summer [$F(1,15) = 5.34$, $p < 0.05$ two-way ANOVA, Figure 2.3G]. FT4, however, was not affected differently by CHA in Summer and Winter ($p > 0.05$ Wilcoxon's rank-sum test, Figure 2.3H). We did not find any significant change in the plasma levels of rT3 and in the ratio between rT3 and TT3 between the treatment groups (Supplementary Figures S2.1B, S2.2B). The greater HPT axis activation in response to CHA in Winter AGS compared to Summer is consistent with greater thermogenic capacity during the winter season.

2.4.4 Seasonal changes in the SNS and in CHA-induced cooling

In hibernating rodents, BAT activation is a significant source of thermogenesis, and BAT mass seasonally increases to sustain periodic arousals. Because BAT thermogenesis is regulated by the SNS *via* activation of sympathetic premotor neurons in the rPA, we next asked if changes in the rPA are associated with seasonal changes in thermogenesis. rPA activation, measured as the total number of cFos+ cells, decreases from Summer to Winter. Density plots visualize the distribution of the number of activated cells in the rPA; we chose a density plot, because it defines the distribution shape better than a frequency histogram (also shown) when the number of bins is small. Distribution of cFos+ cells in the rPA shows a transition between the highest activity in Summer (Figure 2.4A) to the lowest activity in Winter (Figure 2.4C) with a broader distribution of rPA neuronal activity during the Fall transition season (Figure 2.4B). The adjustment in rPA neuronal activity correlates positively with T_b ($r = 0.41$, $p < 0.05$,

Figure 2.4D). Due to the broader distribution of rPA activation in the fall, the fall group was omitted from the subsequent analysis and ANOVA was performed between Torpor, Winter, and Summer groups. We found significantly higher activation in Summer compared to Winter and Torpor [$F(2,22) = 4.16, p < 0.05$, one-way ANOVA, followed by t -test, Figure 2.4E]. Compared to Vehicle, CHA induced rPA activation in Summer, but not in Winter [$F(2,35) = 6.6, p < 0.01$, two-way ANOVA, followed by t -test, Figures 2.4F,G]. Although thermogenic capacity is increased in winter, these results suggest that a decrease in sympathetic premotor neuronal activity attenuates thermogenesis during the winter season (Figure 2.5).

2.5 Discussion

Here, we describe results that support a model in which thermogenic capacity increases in the hibernation season despite a decrease in sympathetic premotor neuronal activity and sympathetic response to cooling which is attenuated until interbout arousal. Thermogenesis is regulated within the rPA to gate SNS activation of shivering and NST (Tan and Knight, 2018). BAT thermogenesis, the primary form of NST in rodents, is regulated by both SNS and TH. Thermogenic capacity increases in winter as we find a greater response of HPT axis to CHA-induced cooling in winter compared to summer. HPT axis response is evident from higher TRH neuronal activation within the PVN and the increase in circulating FT3 and TTH during CHA-induced cooling. Although thermogenic capacity increases, overall sympathetic premotor neuronal activity needed to stimulate thermogenesis decreases during the winter season. We interpret the data as a decrease in sympathetic activity based on a lower euthermic T_b during winter compared to summer and on reduced activation of rPA neurons during winter compared to summer euthermia. We also see a decreased sympathetic response to cooling evident from lower rPA neuronal activation following CHA in winter compared to summer. Our data suggest that SNS activity changes during the fall season indicated by a wider distribution of the number of activated rPA neurons in fall compared to summer or winter. Increased TAI further supports modification of the HPT axis during the fall transition. Enhancement of HPT axis capacity during the fall transition establishes higher thermogenic capacity necessary to support periodic arousals. The higher thermogenic capacity is needed to rewarm from an average of 2.9–36°C in about 10 h during periodic arousal (Karpovich et al., 2009) as well as a protective mechanism to defend T_b when the thermal gradient between T_b and T_a increases (Richter et al., 2015). On the other hand, AGS suppress thermogenesis as seen in the rPA to allow the onset of hibernation, overwriting the thermogenic response at the level of the HPT axis in CHA-induced cooling. Our model describes how hibernators finely regulate thermogenesis across seasons. A lower

thermogenesis in winter allows the onset of hibernation and the parallel increase in thermogenic capacity is crucial to enhance thermogenesis when needed.

Other published literature supports our model. Thermogenic capacity measured as maximum NST in Richardson's ground squirrel is higher in winter animals (Abbotts and Wang, 1980). Seasonal changes in BAT also demonstrate increased thermogenic capacity in winter. BAT mass and BAT UCP1 mRNA increases in winter compared to summer hibernators (Kitao and Hashimoto, 2011; Ballinger and Andrews, 2018). Consistent with our model describing a period of fall transition in thermogenic capacity, a recent study showed that BAT mass increases during fall (Ballinger et al., 2016) and changes in thyroid morphology, similar to what we observed, occur in marmots and bats during the pre-hibernation season (Nunez and Becker, 1970; Krupp et al., 1977). Early thyroidectomy studies in hibernators underline the importance of this gland for hibernation and the role the thyroid plays to enhance thermogenic capacity to sustain periodic arousals. Thyroidectomy performed after cold exposure during the fall, does not affect hibernation as torpor bouts persist (Henderson et al., 1981), however, when thyroidectomy is performed in spring lethal hypothermia occurs (Canguilhem, 1972). Other studies in AGS and 13-lined ground squirrels illustrate a gradual decrease in T_b before the onset of hibernation (Barnes, 1989; Russell et al., 2010; Sheriff et al., 2012; Olson et al., 2013) consistent with our results. As thermogenic capacity increases in fall, basal thermogenesis decreases as seen by the modulation in T_b . In this study, we minimized the influence of feeding and gastric motility on rPA neuronal activity (Jacobs et al., 2002) by withholding food for approximately 12 h before the experiment. The positive association between T_b and the number of cFos+ cells within the rPA suggests that rPA neuronal activity is related to thermogenesis. Nonetheless, the influence of other autonomic nervous system responses on rPA cannot be ruled out and deserves further study.

The increase in TTH during torpor is also seen in 13-lined ground squirrel and hamster using RIA to detect TTH (Demeneix and Henderson, 1978; Nevretdinova and Shvareva, 1987; Magnus and Henderson, 1988). We also note that our TTH values, determined by LC-MS/MS are consistent with values measured by RIA in studies cited above. Increased TTH in torpor is consistent between species, however, changes in FTH values are not consistent. Our results are in agreement with previous study in Djungarian hamsters where FT4 and FT3 do not change during mid-winter torpor. Djungarian hamsters, however, do show an increase in FT3 during late season torpor in preparation for the reproductive phase (Seidel et al., 1987). In Richardson's ground squirrel results are contradictory. One study reports an increase in FT4 during torpor compared to arousal (Demeneix and Henderson, 1978) while another shows the opposite with FTH decreasing in torpor compared to arousal (Magnus and Henderson, 1988).

Differences in results may be due to species differences and to methods used to separate bound and free hormones. We used the ultrafiltration method instead of the classical equilibrium dialysis (ED) to separate FTH from bound TH. Ultrafiltration is becoming the preferred alternative method to ED in clinical settings (Soldin and Soldin, 2011). Clinical works show a better correlation with thyroid stimulating hormones when FTH are measured using MS instead of immunoassay, suggesting higher accuracy and precision of LC/MS-MS in quantifying FTH concentration compared to ED-RIA (van Deventer et al., 2011).

Our analysis of the HPT axis is limited by a lack of deiodinase levels in BAT. Deiodinase regulates intracellular TH levels, in particular type 2 iodothyronine deiodinase (Dio2) converts T4 to T3. Although we did not assess the Dio2 levels in AGS, previous studies in hamster reported seasonal changes in Dio2 levels in hypothalamus during short photoperiod (Herwig et al., 2009) and in BAT during torpor compared to normothermia (Bank et al., 2015). These studies suggest that a low level of T3, as a consequence of lower Dio2 expression, promotes torpor. Thus, while we show higher TTH and no change in FTH during torpor in AGS, the intercellular level of T3 may be decreased by lower Dio2 expression that we were unable to measure. Together, lower Dio2 expression and lower sympathetic premotor neuronal activity may contribute to decreased thermogenesis during torpor.

We are aware of technical limitations in our study such as the use of vehicle-treated animals for assessment of seasonal changes and the small sample size of some of the groups. It is unlikely that vehicle treatment confounds our interpretation since vehicle injection had no effect on T_b . Moreover, TTH concentration previously reported in AGS (Nevretdinova and Shvareva, 1987) was in the same range as values reported in vehicle-treated animals in our study, suggesting a minimal to null effect of handling on the parameters measured in the study. The sample size used depended on the availability of wild caught animals which is limited by the seasonal nature of hibernation and reproduction. Nonetheless, the sample size was sufficient to develop a model that can be further validated with future study. The use of cFos immunoreactivity to detect neuronal changes across season may be considered a methodological limitation as cFos expression is often used to investigate acute challenges. However, cFos is also expressed during spontaneous waking and under basal conditions (Cirelli and Tononi, 2000; Kovács, 2008), making cFos a reliable marker to investigate physiological states as sleep–wake cycle (Cirelli and Tononi, 2000), daily rhythm (Ikeno et al., 2017) hibernation (Bratincsak et al., 2007), and seasonal changes (Mishra et al., 2018). Our data does not show any change in cFos activation in the rPA between winter euthermic (Win.VEH) and torpor, which is consistent with previous work showing

constant cFos mRNA expression within the rPA during the hibernation season in 13-lined ground squirrels (Bratincsak et al., 2007).

In conclusion, we report changes in HPT axis activation that is associated with increased thermogenic capacity in winter. We also report lower rPA neuronal activity in the winter season and in response to CHA-induced cooling. We interpret these findings in the context of a model whereby increased thermogenic capacity in winter supports arousal. Meanwhile, attenuated sympathetic premotor neuronal activity promotes the onset of torpor.

This work is significant as an increase in thermogenic capacity in winter compared to summer also occurs in humans. In healthy subjects, higher thermogenic capacity is associated with higher BAT activation after cold exposure during winter season (Cohade et al., 2003; Saito et al., 2009; Ouellet et al., 2011; Senn et al., 2018) as well as an increase in BAT mass in winter (Ouellet et al., 2011). Furthermore, our results show a gradual decrease in thermogenesis from summer to winter during what is called physiological obesity in hibernation. The decrease in thermogenesis resembles human obesity. In obese individuals, BAT thermogenesis is impaired (Ooijen et al., 2006; Wijers et al., 2010; Orava et al., 2013; Loh et al., 2017) showing a blunted response to cold exposure compared to lean subjects. Our model combines a seasonal increase in thermogenic capacity (independent from photoperiod and T_a) with a decrease in thermogenesis and further study may lead to the understanding of endogenous thermoregulatory mechanisms to use as therapeutic targets.

2.6 Author contributions

CF and KD designed the study and interpreted the data. CF and MJ performed the experiments. SS performed the hormone analysis. CF analyzed the data. CF and KD wrote the paper. All authors contributed to the revision of the manuscript and approved the final draft.

2.7 Funding

Research reported in this publication was supported by NSF 10S-1258179; the National Institutes of Health under award number NS081637; the National Institute of General Medical Sciences of the National Institutes of Health under the award number TL4GM118992, UL1GM118991, and RL5GM118990; and Institutional Development Award (IDeA) from the National Institute of General Medical Sciences of the National Institutes of Health under grant number P20GM103395. The content is solely the responsibility of the authors and does not necessarily represent the official views of the National Institutes of Health.

2.8 Conflict of interest statement

KD has a financial interest in Be Cool Pharmaceuticals. The remaining authors declare that the research was conducted in the absence of any commercial or financial relationships that could be construed as a potential conflict of interest.

2.9 Acknowledgments

We thank E. E. Redei at the Northwestern University Chicago for the gift of the anti-TRH antibody and S. Rice, S. Bhowmick, and B. Laughlin for technical assistance.

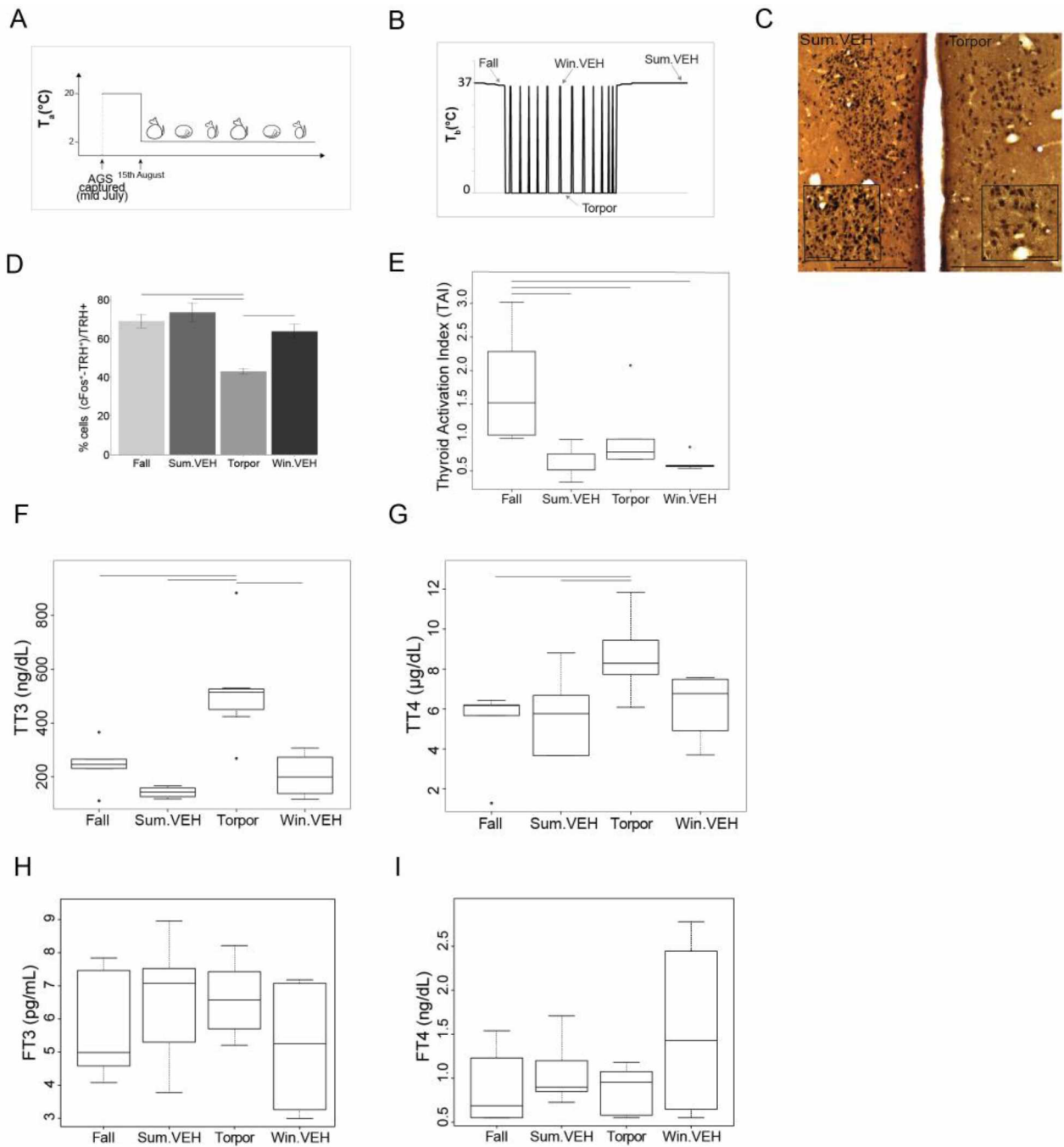


Figure 2.1: Caption on the following page.

Figure 2.1: HPT-axis is active in summer and winter euthermia, but not in torpor.

All AGS in the study were maintained under the constant environmental conditions (4L:20D and $T_a = 2^\circ\text{C}$) after capture as shown in (A), AGS maintain seasonal rhythm under the set constant environmental conditions. Results from samples collected at times shown in (B), illustrate that TRH activation in the PVN is lower in Torpor (D). Photomicrographs of double stained brain sections in (C), TRH neurons (brown) and cFos (black) in the PVN are shown in Sum.VEH, as representative of the higher activation group, and in torpor; the insert in PVN images show higher magnification area, scale bar 200 μm (lower magnification), scale bar 50 μm (higher magnification). Thyroid activity is significantly higher during the Fall (E) and concentration of TT3 and TT4 is higher in Torpor (F,G). No changes have been detected in FT3 or FT4 (H,I). Symbols in (E–G) represent outliers. Horizontal bars represent differences between groups, $p < 0.05$, t-test in (D,G) and Wilcoxon's rank-sum test in (E,F), $n = 4-7$.

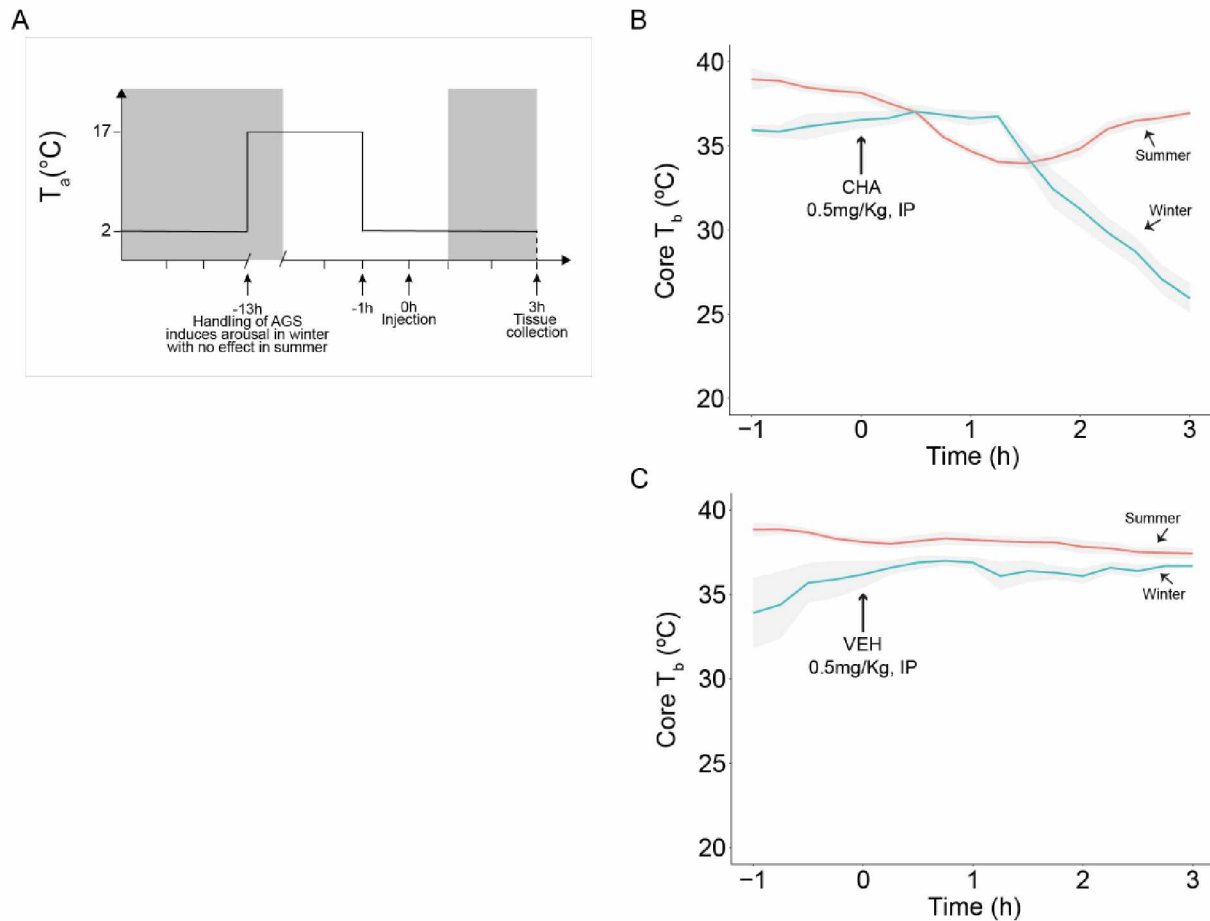


Figure 2.2: CHA, adenosine A1 receptor agonist, promotes onset of hibernation in a seasonally dependent manner.

Experimental design is illustrated in (A), treatment (CHA or VEH) was administered at time 0 and tissue collection was performed 3 h after injection, 2 h into the dark cycle (dark cycle is represented by gray area). CHA promotes the onset of hibernation in Winter AGS. Summer AGS respond to CHA briefly and restore the initial T_b value (B). Vehicle does not affect T_b (C). Data shown as mean \pm SEM, $n = 4-7$.

Arrow at 0 h indicates time of injection.

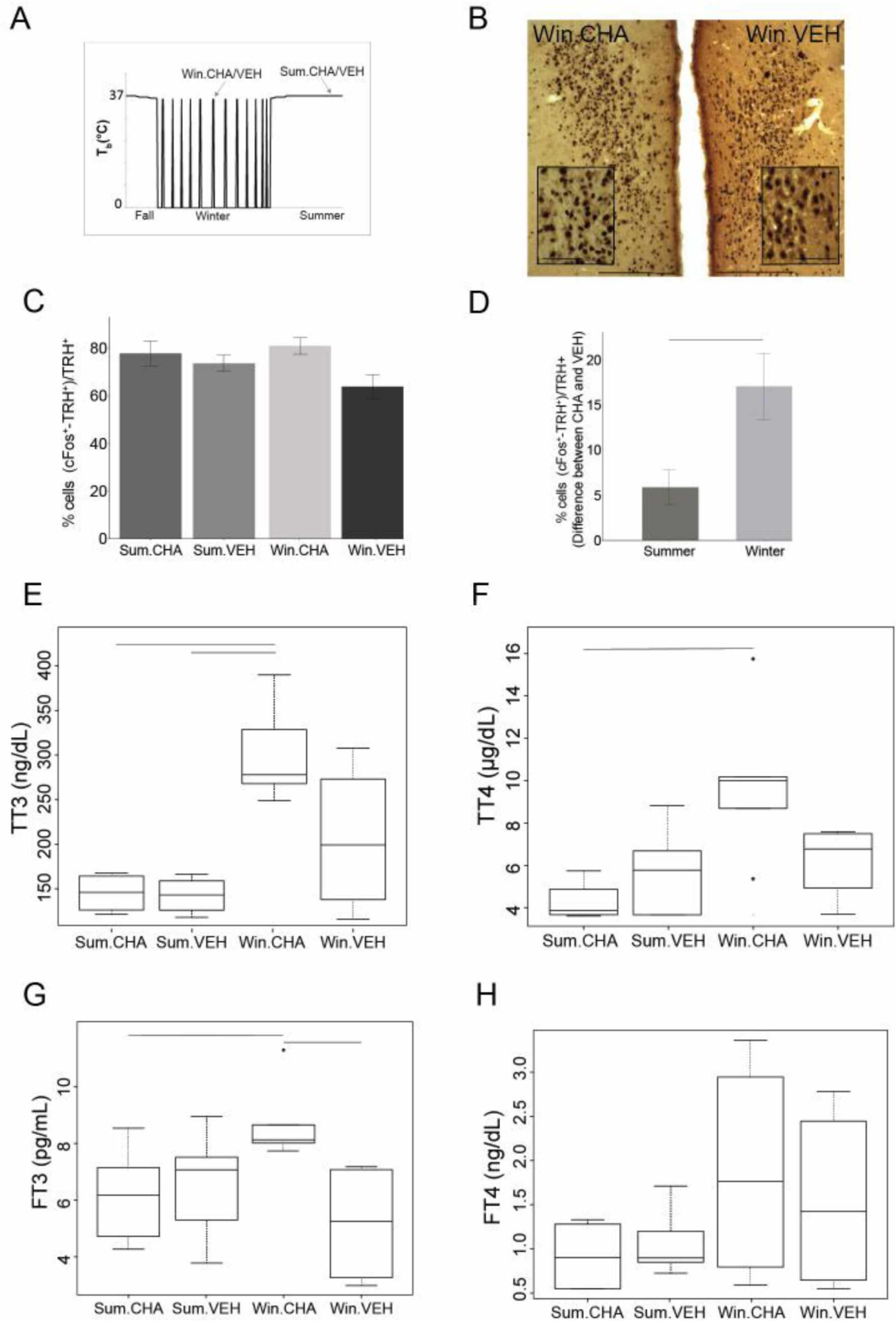


Figure 2.3: Caption on the following page.

Figure 2.3: CHA activates HPT axis more in winter than in summer.

Results from samples collected at times shown in (A). Photomicrographs of double stained brain sections in (B), TRH neurons (brown) and cFos (black) in the PVN are shown in VEH and CHA animal, the insert in PVN images show higher magnification area, scale bar 200 μm (lower magnification), scale bar 50 μm (higher magnification). TRH neurons are activated after CHA with no effect of season (C). Significantly higher activation of TRH neurons after CHA in Winter compared to Summer was evident when AGS were matched for age and gender. Data shown are mean \pm SEM of differences between CHA and vehicle-treated pairs matched for age and gender (D). CHA increases TT3 and TT4 more in Winter than in Summer (E,F), FT3 increases after CHA in Winter (G). FT4 does not change after CHA (H). Symbols in (F,G) represent outliers. Horizontal bars represent differences between groups, $p < 0.05$, Wilcoxon's rank-sum test in (E,F), t-test in (C,D,G), $n = 4-7$.

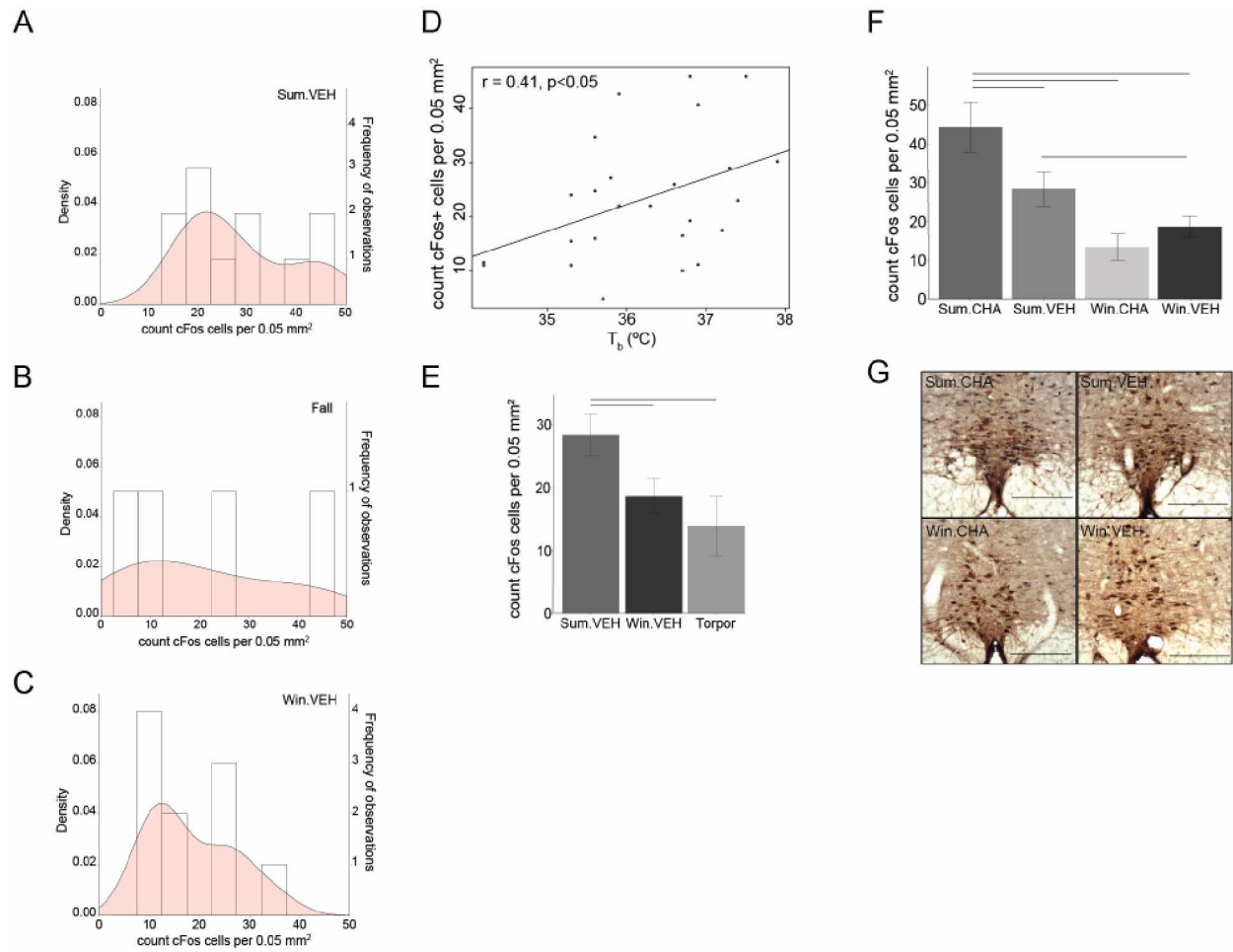


Figure 2.4: Sympathetic tone decreases in winter.

The density (probability distribution) of active neurons in the rPA is wider in Fall (B) compared to Summer (A) and Winter (C). A seasonal decrease in euthermic T_b correlates with a seasonal decrease in rPA neuronal activity (D). rPA activation is higher in Summer euthermia compared to Torpor and Winter euthermia (E) and significantly increases after CHA in Summer, but not in Winter (F). Photomicrographs of double stained brain sections in (G), TPH neurons (brown) used to identify the rPA and cFos (black) are shown in the 4 treatment groups (Sum.CHA, Sum.VEH, Win.CHA, and Win.VEH), scale bar 200 μm . Horizontal bars represent differences between groups, $p < 0.05$, t-test in (E,F), $n = 4-11$.

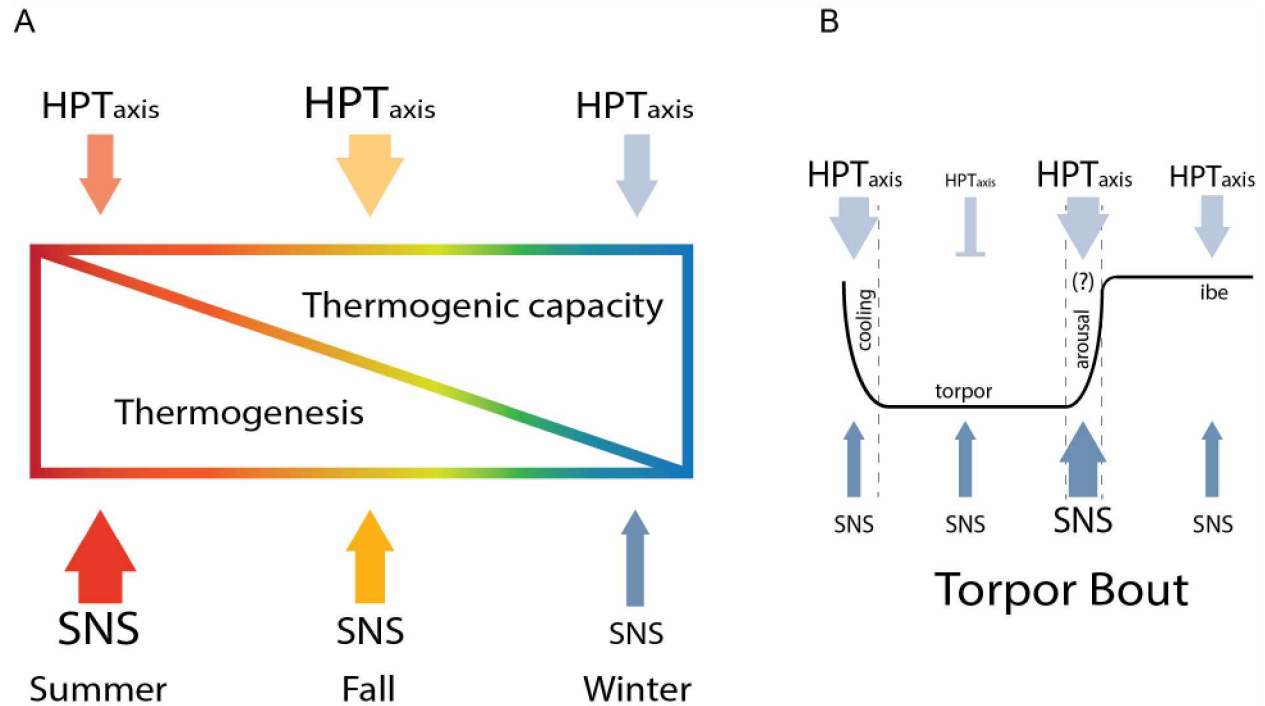


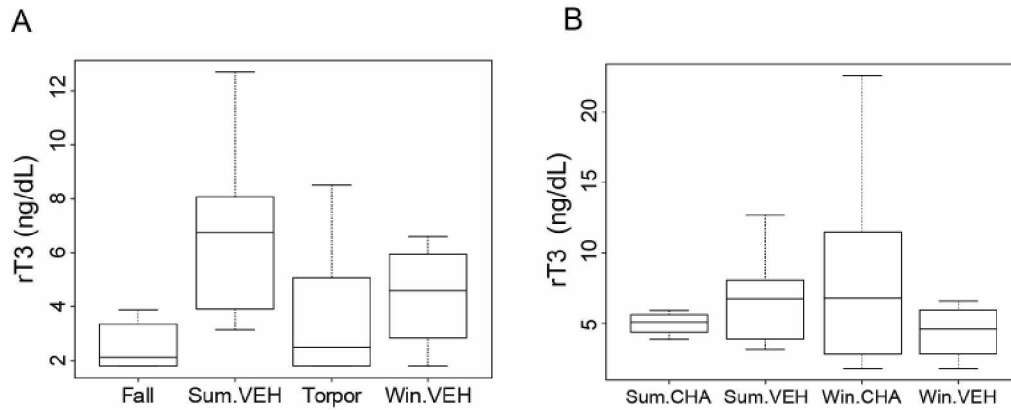
Figure 2.5: Seasonal modulation of thermoregulation in hibernation.

The HPT axis and SNS change across season to increase thermogenic capacity in winter and gradually reduce thermogenesis from summer to winter (A) until arousal, when the higher thermogenic capacity is critical to sustain thermogenesis needed to rewarm from torpor (B).

Table 2.1: Characteristics of each seasonal phenotype.

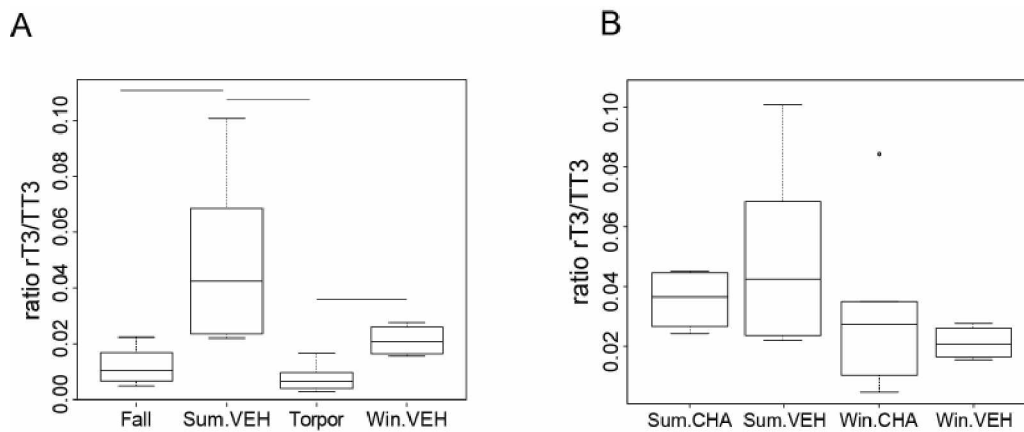
Seasonal phenotype	Sample size	Torpor Bouts	Body weight (g)	Rectal T_b ($^{\circ}\text{C}$)
Fall	7	0	$699 \pm 64^{b,c}$	35.4 ± 0.3^a
Torpor	4	≥ 8	594 ± 35^c	2.9 ± 0.3^c
Ibe (Winter Vehicle)	5	≥ 8	486 ± 28^a	36.1 ± 0.3^a
Summer (Summer Vehicle)	7	0	$584 \pm 33^{a,c}$	37.0 ± 0.2^b

Data shown \pm SEM, rectal T_b was measured prior to tissue collection. Different letters indicate significantly different values $p < 0.05$, Wilcoxon's rank-sum test.



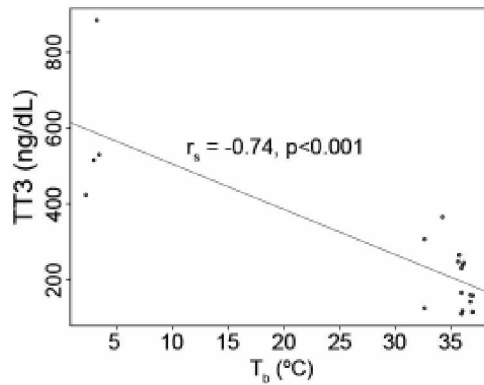
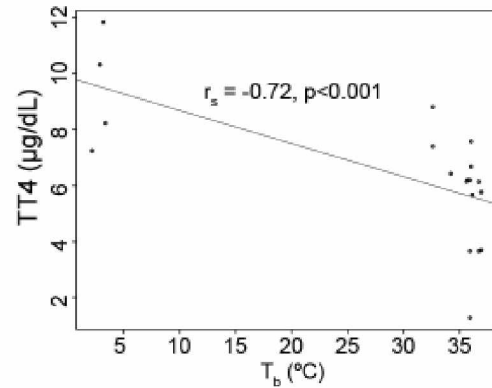
SI Figure 2.1: Level of reverse triiodothyronine (rT3) pharmacologically inactive hormone.

rT3 is considered a metabolically inactive thyroid hormone produced by the deiodination of T4 to rT3 catalyzed by type 3 iodothyronine deiodinase (Dio3), even though type 1 iodothyronine deiodinase (Dio1) can perform the conversion. The constant level across seasons (A) and between treatments (B) may be explained by a lack of significant alterations in the metabolism of circulating thyroid hormones. In eight of 31 AGS (26 %) the rT3 concentration was below the limit of detection. Wilcoxon’s rank-sum test in A and B, n=4 to 7.



SI Figure 2.2: During torpor HPT axis is downregulated.

The ratio between rT3 and TT3 is lower in torpor compared to winter euthermic and summer euthermic. In Fall the ratio is lower than summer euthermic but does not differ from winter euthermic, in agreement with Fall being a transition state where thermogenesis is modulated before hibernation starts (A). We did not detect any change in the ratio between treatments group (B). Horizontal bars represent differences between groups $p < 0.05$, Wilcoxon’s rank-sum test in A and B, n=4 to 7.

A**B**

SI Figure 2.3: Higher concentration of TT3 and TT4 are associated with low T_b consistent with higher circulating levels at minimum T_b during torpor.

We described an inverse correlations between TT3, TT4 and T_b using Pearson's correlation when data were normally distributed and Spearman's correlation when data were not normally distributed (for TT3, $r_s = -0.74, p < 0.001$, SI Fig. 3A, for TT4 $r_s = -0.72, p < 0.001$, SI Fig. 3B), $n = 4$ to 7 .

2.10 References

- Abbotts, B., and Wang, L.C.H. (1980). Seasonal thermogenic capacity in a hibernator, *Spermophilus richardsonii*. *J. Comp. Physiol.* *140*, 235–240.
- Ballinger, M.A., and Andrews, M.T. (2018). Nature's fat-burning machine: brown adipose tissue in a hibernating mammal. *J. Exp. Biol.* *221*, jeb162586.
- Ballinger, M.A., Hess, C., Napolitano, M.W., Bjork, J.A., and Andrews, M.T. (2016). Seasonal changes in brown adipose tissue mitochondria in a mammalian hibernator: from gene expression to function. *Am. J. Physiol.-Regul. Integr. Comp. Physiol.* *311*, R325–R336.
- Bank, J.H.H., Kemmling, J., Rijntjes, E., Wirth, E.K., and Herwig, A. (2015). Thyroid hormone status affects expression of daily torpor and gene transcription in Djungarian hamsters (*Phodopus sungorus*). *Horm. Behav.* *75*, 120–129.
- Barnes, B.M. (1989). Freeze avoidance in a mammal: body temperatures below 0 degree C in an Arctic hibernator. *Science* *244*, 1593–1595.
- Betz, M.J., and Enerbäck, S. (2015). Human Brown Adipose Tissue: What We Have Learned So Far. *Diabetes* *64*, 2352–2360.
- Bratincsak, A., McMullen, D., Miyake, S., Toth, Z.E., Hallenbeck, J.M., and Palkovits, M. (2007). Spatial and Temporal Activation of Brain Regions in Hibernation: c-fos Expression during the Hibernation Bout in Thirteen-Lined Ground Squirrel. *J. Comp. Neurol.* *505*, 443–458.
- Buck, C.L., and Barnes, B.M. (2000). Effects of ambient temperature on metabolic rate, respiratory quotient, and torpor in an arctic hibernator. *Am. J. Physiol.-Regul. Integr. Comp. Physiol.* *279*, R255–R262.
- Canguilhem, B. (1972). Role of thyroxine in the initiation of hibernation and resistance to cold in European hamsters (*Cricetus cricetus*) thyroidectomized in spring. *C. R. Seances Soc. Biol. Fil.* *166*, 688–692.
- Cannon, B., and Nedergaard, J. (2004). Brown Adipose Tissue: Function and Physiological Significance. *Physiol. Rev.* *84*, 277–359.
- Carson, F.L. (1997). *Histotechnology: A Self-Instructional Text* (Chicago: Amer Society of Clinical).
- Cirelli, C., and Tononi, G. (2000). On the functional significance of c-fos induction during the sleep-waking cycle. *Sleep* *23*, 453–469.
- Cohade, C., Mourtzikos, K.A., and Wahl, R.L. (2003). "USA-Fat": Prevalence Is Related to Ambient Outdoor Temperature—Evaluation with 18F-FDG PET/CT. *J. Nucl. Med.* *44*, 1267–1270.
- Demeneix, B.A., and Henderson, N.E. (1978). Thyroxine metabolism in active and torpid ground squirrels, *Spermophilus richardsoni*. *Gen. Comp. Endocrinol.* *35*, 86–92.

- Deventer, H.E. van, Mendu, D.R., Remaley, A.T., and Soldin, S.J. (2011). Inverse Log-Linear Relationship between Thyroid-Stimulating Hormone and Free Thyroxine Measured by Direct Analog Immunoassay and Tandem Mass Spectrometry. *Clin. Chem.* *57*, 122–127.
- Gu, J., Soldin, O.P., and Soldin, S.J. (2007). Simultaneous quantification of free triiodothyronine and free thyroxine by isotope dilution tandem mass spectrometry. *Clin. Biochem.* *40*, 1386–1391.
- Henderson, N.E., Demeneix, B.A., McGraw, K.I., and Meronek, R.P. (1981). Hibernation in thyroidectomized ground squirrels, *Spermophilus richardsoni*. *Gen. Comp. Endocrinol.* *43*, 543–548.
- Herwig, A., Wilson, D., Logie, T.J., Boelen, A., Morgan, P.J., Mercer, J.G., and Barrett, P. (2009). Photoperiod and acute energy deficits interact on components of the thyroid hormone system in hypothalamic tanycytes of the Siberian hamster. *Am. J. Physiol.-Regul. Integr. Comp. Physiol.* *296*, R1307–R1315.
- Ikeno, T., Williams, C.T., Buck, C.L., Barnes, B.M., and Yan, L. (2017). Clock Gene Expression in the Suprachiasmatic Nucleus of Hibernating Arctic Ground Squirrels. *J. Biol. Rhythms* *32*, 246–256.
- Jacobs, B.L., Martín-Cora, F.J., and Fornal, C.A. (2002). Activity of medullary serotonergic neurons in freely moving animals. *Brain Res. Rev.* *40*, 45–52.
- Jameson, E.W. (1964). Patterns of Hibernation of Captive *Citellus lateralis* and *Eutamias speciosus*. *J. Mammal.* *45*, 455–460.
- Jinka, T.R., Tøien, Ø., and Drew, K.L. (2011). Season Primes the Brain in an Arctic Hibernator to Facilitate Entrance into Torpor Mediated by Adenosine A1 Receptors. *J. Neurosci.* *31*, 10752–10758.
- Jonklaas, J., Kahric-Janjic, N., Soldin, O.P., and Soldin, S.J. (2009). Correlations of Free Thyroid Hormones Measured by Tandem Mass Spectrometry and Immunoassay with Thyroid-Stimulating Hormone across 4 Patient Populations. *Clin. Chem.* *55*, 1380–1388.
- Kalisnik, M. (1972). A histometric thyroid gland activation index (preliminary report). *J. Microsc.* *95*, 345–348.
- Karpovich, S.A., Tøien, Ø., Buck, C.L., and Barnes, B.M. (2009). Energetics of arousal episodes in hibernating arctic ground squirrels. *J. Comp. Physiol. B* *179*, 691–700.
- Kitao, N., and Hashimoto, M. (2011). Increased thermogenic capacity of brown adipose tissue under low temperature and its contribution to arousal from hibernation in Syrian hamsters. *Am. J. Physiol.-Regul. Integr. Comp. Physiol.* *302*, R118–R125.
- Kovács, K.J. (2008). Measurement of Immediate-Early Gene Activation- c-fos and Beyond. *J. Neuroendocrinol.* *20*, 665–672.
- Krupp, P.P., Young, R.A., and Frink, R. (1977). The thyroid gland of the woodchuck, *Marmota monax*: a morphological study of seasonal variations in the follicular cells. *Anat. Rec.* *187*, 495–514.
- Loh, R.K.C., Kingwell, B.A., and Carey, A.L. (2017). Human brown adipose tissue as a target for obesity management; beyond cold-induced thermogenesis. *Obes. Rev.* *18*, 1227–1242.

MacCannell, A., Sinclair, K., Friesen-Waldner, L., McKenzie, C.A., and Staples, J.F. (2017). Water–fat MRI in a hibernator reveals seasonal growth of white and brown adipose tissue without cold exposure. *J. Comp. Physiol. B* *187*, 759–767.

Magnus, T.H., and Henderson, N.E. (1988). Thyroid hormone resistance in hibernating ground squirrels, *Spermophilus richardsoni*. I. Increased binding of triiodo-L-thyronine and L-thyroxine by serum proteins. *Gen. Comp. Endocrinol.* *69*, 352–360.

Masika, L.S., Zhao, Z., and Soldin, S.J. (2016). Is measurement of TT3 by immunoassay reliable at low concentrations? A comparison of the Roche Cobas 6000 vs. LC–MSMS. *Clin. Biochem.* *49*, 846–849.

Mishra, I., Singh, D., and Kumar, V. (2018). Temporal Expression of c-fos and Genes Coding for Neuropeptides and Enzymes of Amino Acid and Amine Neurotransmitter Biosynthesis in Retina, Pineal and Hypothalamus of a Migratory Songbird: Evidence for Circadian Rhythm-Dependent Seasonal Responses. *Neuroscience* *371*, 309–324.

Nakamura, K., Matsumura, K., Hübschle, T., Nakamura, Y., Hioki, H., Fujiyama, F., Boldogkői, Z., König, M., Thiel, H.-J., Gerstberger, R., et al. (2004). Identification of Sympathetic Premotor Neurons in Medullary Raphe Regions Mediating Fever and Other Thermoregulatory Functions. *J. Neurosci.* *24*, 5370–5380.

Nevretdinova, Z.G., and Shvareva, N.V. (1987). Thyroid hormone levels in the peripheral blood of the ground squirrel *Citellus parryi* during winter hibernation. *Zh. Evol. Biokhim. Fiziol.* *23*, 42–47.

Nunez, E.A., and Becker, D.V. (1970). Secretory processes in follicular cells of the bat thyroid. I. Ultrastructural changes during the preearly and mid-hibernation periods with some comments on the origin of autophagic vacuoles. *Am. J. Anat.* *129*, 369–397.

Olson, J.M., Jinka, T.R., Larson, L.K., Danielson, J.J., Moore, J.T., Carpluck, J., and Drew, K.L. (2013). Circannual Rhythm in Body Temperature, Torpor, and Sensitivity to A1 Adenosine Receptor Agonist in Arctic Ground Squirrels. *J. Biol. Rhythms* *28*, 201–207.

Ooijen, A.M.J.C., Westerterp, K.R., Wouters, L., Schoffelen, P.F.M., Steenhoven, A.A. van, and Lichtenbelt, W.D.M. van (2006). Heat Production and Body Temperature During Cooling and Rewarming in Overweight and Lean Men. *Obesity* *14*, 1914–1920.

Orava, J., Nuutila, P., Nojonen, T., Parkkola, R., Viljanen, T., Enerbäck, S., Rissanen, A., Pietiläinen, K.H., and Virtanen, K.A. (2013). Blunted metabolic responses to cold and insulin stimulation in brown adipose tissue of obese humans. *Obesity* *21*, 2279–2287.

Ortiga-Carvalho, T.M., Chiamolera, M.I., Pazos-Moura, C.C., and Wondisford, F.E. (2016). Hypothalamus-Pituitary-Thyroid Axis. *Compr. Physiol.* *6*, 1387–1428.

Ouellet, V., Routhier-Labadie, A., Bellemare, W., Lakhil-Chaieb, L., Turcotte, E., Carpentier, A.C., and Richard, D. (2011). Outdoor Temperature, Age, Sex, Body Mass Index, and Diabetic Status Determine the Prevalence, Mass, and Glucose-Uptake Activity of 18F-FDG-Detected BAT in Humans. *J. Clin. Endocrinol. Metab.* *96*, 192–199.

- Richter, M.M., Williams, C.T., Lee, T.N., Tøien, Ø., Florant, G.L., Barnes, B.M., and Buck, C.L. (2015). Thermogenic Capacity at Subzero Temperatures: How Low Can a Hibernator Go? *Physiol. Biochem. Zool.* *88*, 81–89.
- Russell, R.L., O'Neill, P.H., Epperson, L.E., and Martin, S.L. (2010). Extensive use of torpor in 13-lined ground squirrels in the fall prior to cold exposure. *J. Comp. Physiol. [B]* *180*, 1165–1172.
- Saito, M., Okamatsu-Ogura, Y., Matsushita, M., Watanabe, K., Yoneshiro, T., Nio-Kobayashi, J., Iwanaga, T., Miyagawa, M., Kameya, T., Nakada, K., et al. (2009). High Incidence of Metabolically Active Brown Adipose Tissue in Healthy Adult Humans. *Diabetes* *58*, 1526–1531.
- Seidel, A., Heldmaier, G., and Schulz, F. (1987). Seasonal changes in circulating levels of thyroid hormones are not dependent on the age in Djungarian hamsters *Phodopus sungorus*. *Comp. Biochem. Physiol. A* *88*, 71–73.
- Senn, J.R., Maushart, C.I., Gashi, G., Michel, R., Lalive d'Epinay, M., Vogt, R., Becker, A.S., Müller, J., Baláz, M., Wolfrum, C., et al. (2018). Outdoor Temperature Influences Cold Induced Thermogenesis in Humans. *Front. Physiol.* *9*.
- Sheriff, M.J., Williams, C.T., Kenagy, G.J., Buck, C.L., and Barnes, B.M. (2012). Thermoregulatory changes anticipate hibernation onset by 45 days: data from free-living arctic ground squirrels. *J. Comp. Physiol. B* *182*, 841–847.
- Sheriff, M.J., Fridinger, R.W., Tøien, Øivind, Barnes, B.M., and Buck, C.L. (2013). Metabolic Rate and Prehibernation Fattening in Free-Living Arctic Ground Squirrels. *Physiol. Biochem. Zool.* *86*, 515–527.
- Silva, J.E., and Larsen, P.R. (1983). Adrenergic activation of triiodothyronine production in brown adipose tissue. *Nature* *305*, 712–713.
- Soldin, O.P., and Soldin, S.J. (2011). Thyroid hormone testing by tandem mass spectrometry. *Clin. Biochem.* *44*, 89–94.
- Suzuki, S., Nishio, S., Takeda, T., and Komatsu, M. (2012). Gender-specific regulation of response to thyroid hormone in aging. *Thyroid Res.* *5*, 1.
- Tan, C.L., and Knight, Z.A. (2018). Regulation of Body Temperature by the Nervous System. *Neuron* *98*, 31–48.
- Weibel, E.R., Kistler, G.S., and Scherle, W.F. (1966). Practical stereological methods for morphometric cytology. *J. Cell Biol.* *30*, 23–38.
- Wijers, S.L.J., Saris, W.H.M., and Lichtenbelt, W.D. van M. (2010). Cold-Induced Adaptive Thermogenesis in Lean and Obese. *Obesity* *18*, 1092–1099.

Chapter 3: Seasonal decrease in thermogenesis and increase in vasoconstriction explain seasonal response to N⁶-cyclohexyladenosine -induced hibernation in the Arctic Ground Squirrel (*Urocitellus parryii*).²

3.1 Abbreviations

A ₁ AR	A ₁ adenosine receptor
A ₂ AR	A ₂ adenosine receptor
ac	Anterior commissure
AGS	Arctic ground squirrel
AP	Area postrema
AVP	Arginine vasopressin
BAT	Brown adipose tissue
CHA	N ⁶ -Cyclohexyladenosine
DC	Dorsal cochlear
DMH	Dorsomedial hypothalamus
fx	Fornix
H ₃ R	Autoregulatory receptor
HIST	Histamine
LC	Locus coeruleus
LH	Lateral hypothalamus
ml	medial lemniscus
mt	mammillary tract
MnPO	Median preoptic nucleus
NTS	Nucleus tractus solitarius
ox	Optic chiasm
Opt	Optic tract

² Published as Frare C, Jenkins ME, McClure KM, Drew KL (2019). Seasonal decrease in thermogenesis and increase in vasoconstriction explain seasonal response to N⁶-cyclohexyladenosine-induced hibernation in the Arctic Ground Squirrel (*Urocitellus parryii*). J Neurochem.

PeF	Perifornical nucleus
POA	Preoptic area
PVN	Paraventricular nucleus of the hypothalamus
py	Pyramidal tract
ROI	Region of interest
rPA	Raphe pallidus
sm	Stria medullaris of the thalamus
SCN	Suprachiasmatic nucleus
SON	Supraoptic nucleus
SPZ	Subparaventricular zone
T _b	Body temperature
T _r	Rectal body temperature
T _{sc}	Subcutaneous body temperature
TH	Tyrosine hydroxylase
TMN	Tuberomammillary nucleus
TPH	Tryptophan hydroxylase
TRH	Thyrotropin- releasing hormone
VEH	Vehicle
VLPO	Ventrolateral preoptic nucleus

3.2 Abstract

Hibernation is a seasonal phenomenon characterized by a drop in metabolic rate and body temperature. Adenosine A₁ receptor agonists promote hibernation in different mammalian species, and the understanding of the mechanism inducing hibernation will inform clinical strategies to manipulate metabolic demand that are fundamental to conditions such as obesity, metabolic syndrome and therapeutic hypothermia. Adenosine A₁ receptor agonist-induced hibernation in Arctic ground squirrels is regulated by an endogenous circannual (seasonal) rhythm. This study aims to identify the neuronal mechanism underlying the seasonal difference in response to the adenosine A₁ receptor agonist. Arctic ground squirrels were implanted with body temperature transmitters and housed at constant ambient

temperature (2°C) and light cycle (4L:20D). We administered CHA (N⁶-cyclohexyladenosine), an adenosine A₁ receptor agonist in euthermic-summer phenotype and euthermic-winter phenotype and used cFos and phenotypic immunoreactivity to identify cell groups affected by season and treatment. We observed lower core and subcutaneous temperature in winter animals and CHA produced a hibernation-like response in winter, but not summer. cFos-ir was greater in the median preoptic nucleus and the raphe pallidus in summer after CHA. CHA administration also resulted in enhanced cFos-ir in the nucleus tractus solitarius and decreased cFos-ir in the tuberomammillary nucleus in both seasons. In winter, cFos-ir was greater in the supraoptic nucleus and lower in the raphe pallidus than in summer. The seasonal decrease in the thermogenic response to CHA and the seasonal increase in vasoconstriction, assessed by subcutaneous temperature, reflect the endogenous seasonal modulation of the thermoregulatory systems necessary for CHA-induced hibernation (Figure 3.1).

3.3 Introduction

Hibernation is a seasonal strategy to conserve energy and is characterized by a state of torpor, lasting up to 20 days in mid-winter in ground squirrels, interrupted by spontaneous regularly timed arousal called interbout arousal. In torpor, the body temperature (T_b) can reach a minimum of -2.9°C in the Arctic ground squirrel (AGS) (Barnes, 1989) and metabolism is suppressed to 1-2% of the basal metabolic rate (Buck and Barnes, 2000).

The ability to induce an *endogenous* hypometabolic state, like hibernation, will improve current therapeutic hypothermia protocols. Therapeutic hypothermia is a clinical approach proven to have neuroprotective benefits during ischemic trauma and to improve survival after cardiac arrest (Arrich et al., 2016; Song and Lyden, 2012), but artificial cooling shows side effects such as generation of thermogenesis through shivering (Song and Lyden, 2012). Obesity is a worldwide growing epidemic and is associated with increased morbidity and mortality (Mitchell et al., 2011; Lambert et al., 2013). Poor understanding of how metabolic rate and thermogenesis are regulated limits development of interventions aimed at manipulating metabolic rate for therapeutic benefit (Lambert et al., 2013; Schoeller, 2001).

The adenosine A₁ receptor (A₁AR) is a key target for inducing hibernation, torpor and hypothermia in non-hibernating species (Tamura et al., 2005; Jinka et al., 2011; Iliff and Swoap, 2012; Tupone et al., 2013). Previous work has shown that in AGS, which are obligate (seasonal) hibernators, N⁶-cyclohexyladenosine (CHA), an A₁AR agonist, induces a decrease in T_b and metabolic rate similar to the endogenous onset of torpor only in winter (the hibernation season) (Jinka et al., 2011). The same AGS

treated in summer show a brief and slight response to CHA, which does not lead to hibernation even if the environmental conditions are kept constant (Jinka et al., 2011). The response to CHA is mediated by the central nervous system, *but the mechanism underlying the seasonal difference in response is still unclear.*

A seasonal decrease in euthermic T_b followed by a decrease in thermogenesis precedes the onset the hibernation season (Sheriff et al., 2012; Frare et al., 2018), which coincides with a circannual increase in sleep in euthermic ground squirrels (Walker et al., 1980) and an increase in vasoconstriction (Karooon et al., 1998; Swoap and Gutilla, 2009). Vasoconstriction, sleep and the decrease in thermogenesis are seasonal strategies employed to achieve energy conservation during hibernation. However, we do not know if the seasonal phenotypes are expressed independent of environmental conditions or their role in the seasonal response to CHA. Recently, we found that the winter decrease in neuronal activity of the sympathetic premotor neurons in the raphe pallidus (rPA), decreasing thermogenesis, is associated with the different seasonal response to CHA (Frare et al., 2018). Here, we investigate if the other energy saving strategies, sleep and vasoconstriction, and the brain regions regulating these physiological functions may also explain the seasonal response to CHA. In particular, we hypothesized that brain nuclei in thermoregulatory pathways upstream of the rPA may show similar changes in neuronal activity associated with the seasonal response to CHA and that CHA inhibits brain regions controlling arousal, as adenosine is known to promote sleep through the A_1AR (Bjorness and Greene, 2009).

3.4 Materials and Methods

All procedures were approved by the Institutional Animal Care and Use Committee (IACUC) at the University of Alaska Fairbanks (assurance number D16-00482) and were conducted in accordance with the Guide for the Care and Use of Laboratory Animals (8th edition). *The objective of this study was to identify neuronal activity after CHA administration underlying the seasonal difference in the physiological response to the drug.* The study was not pre-registered.

3.4.1 Animals

Arctic ground squirrels (AGS, *Urocitellus parryii*) were captured in the Brooks Range (68°07'46"N 149°28'33"W) under permit by Alaska Department of Fish and Game. AGS are available to investigators upon request. Beginning August 15th of the year of capture, AGS were housed at constant environmental conditions at an ambient temperature (T_a) of 2°C and a photoperiod of 4L:20D until the end of the

experiment (Figure 3.2a). AGS, male and female, were housed individually in stainless steel ¼" wire mesh cages (dimensions 12"X19"X12") and provided with approximately 47 g Mazuri rodent chow and water ad libitum, even though AGS do not eat or drink during the hibernation season. Juveniles (one year old) were preferred for the study to minimize age as a biological variable, but when juveniles were limited at time of capture, adults were used to increase the sample size (Table 3.1).

We excluded 11 of 52 animals who met any or all of these exclusion criteria. We excluded five animals tested during the winter season for failure to hibernate. We excluded an additional six animals during the winter season because they did not display the characteristic response to CHA. Three of these six animals had displayed irregular hibernation bouts, characterized by frequent two-day long torpor bouts interrupted by unusually long interbout arousals lasting two or more days. In two of these six AGS, we administered CHA after only 7 bouts of hibernation. For subsequent tests, we administered CHA after at least 8 bouts of hibernation, since responsiveness to CHA increases as the hibernation season increases (Jinka et al., 2011). One animal tested during the summer season was excluded because it responded like a winter phenotype. This animal had displayed three spontaneous test drops prior to testing, which indicated an advanced circannual rhythm approaching the winter phenotype. Of the 52 animals we used a final number of 41 for the study.

Two groups of AGS were used for the study. Group 1 was implanted with IPTT -300 transponders (Bio Medic Data Systems) subcutaneously between the scapulae and subcutaneous temperature (T_{sc}) was recorded every 30 min throughout the experiment. Group 2 was surgically implanted with an iButton (Maxim integrated, San Jose, CA) abdominal data logger and T_b was recorded every 15 min. In group 2, we implanted the iButtons in all AGS in August. We programmed the data logger to record T_b from mid-November to mid-March in Winter AGS, and to record data from mid-May to mid-July in Summer AGS. Additionally, as standard laboratory procedure, we measured rectal T_b (T_r) just prior to intracardial perfusion with a digital microprocessor thermometer (model HH21 OMEGA Engineering, INC., Stamford, CT).

3.4.2 Surgery

AGS were implanted with iButton using sterile technique. Anesthesia was induced with 5% isoflurane and maintained at 3% mixed with 100% medical grade oxygen delivered at a flow rate of 1.5 L/min. During surgery, T_b was maintained via a water circulating heating pad. The iButton was inserted intraperitoneally via a midline incision through the linea alba, and the abdomen was sutured closed in three layers. We administered buprenorphine (1.0 mg/kg, subcutaneously) slow release formulation for

analgesia, and AGS were allowed at least one day of postoperative recovery in a warm room (17°C, 4L:20D) before being returned to home cage conditions (2°C, 4L:20D). Surgery occurred at least one month before the onset of hibernation.

3.4.3 Oxygen consumption

O₂ consumption was monitored as described previously (Tøien, 2013). Briefly, we used a Plexiglas cylinder as a metabolic chamber (diameter 28 cm, height 23 cm). The air drawn from the chamber was filtered and passed through a mass flow controller at 3 L/min (Model 840, 0–5 L/min, Sierra Instruments). An air subsample was passed through a multiplexing valve system and dried by a Nafion drier (model PD-50T-24-PP, Perma Pure) before passing through the O₂ and CO₂ analyzers (Model FC-1B and CA-2A, Sable Systems International). The software LabGraph (Tøien, 2013) was used for automated data acquisition and analysis. We tested the accuracy and precision of the system before and during the study period by burning a measured amount (grams) of 100% ethanol in a small lamp (a glass vial with a wick). Measured O₂ consumption was within 3% of O₂ consumption calculated from the stoichiometric loss of ethanol from the lamp.

3.4.4 Experimental procedure

We arbitrarily assigned AGS to each experimental group before the surgical procedure. Based on the list of animals provided by the animal facility, we assigned every other AGS to a season (Summer or Winter); for each season, we assigned each treatment to every other AGS, starting with CHA. We attempted to balance the number of female and male AGS within each experimental group, although the availability of the sexes depended on the availability at the time of capture.

As previously described (Frare et al., 2018), *winter phenotype* (referred to as Winter AGS) was defined by at least eight torpor bouts. Torpor was monitored by the shavings added technique (Jameson, 1964); when the wood shaving placed on the animal's back remained undisturbed the following day, the animal was considered torpid. *Summer phenotype* (referred to as Summer AGS) was characterized by at least 60 consecutive awake days following the end of the hibernation season. Physiological characteristics of summer and winter phenotypes are described in Table 3.1. All AGS were housed in an environmental chamber (2°C, 4L:20D).

In Winter AGS, arousal was induced within the fourth day of the torpor bout by handling the AGS the night before the day of the experiment. After handling, the AGS was placed overnight in a warm room (17°C, 4L:20D) to delay onset of the following torpor bout. To be consistent with Winter AGS,

Summer AGS were also moved to a warm room (17°C, 4L:20D) the night before the experiment. We withheld food during the overnight period (approximately 12 hours) and throughout the experiment, but water was available ad libitum. All animals used in the experiment were food deprived in the same manner. If hunger activated cFos, the same cFos expression would be measured in both VEH-treated and in the CHA-treated groups. Therefore, the VEH group is not only a control for the drug effect, but also for food deprivation.

On the day of the experiment, the AGS were moved back into the environmental chamber (2°C, 4L:20D) one hour before the drug injection. Group 1 AGS, implanted with IPTT, were moved back into their home cage and T_{sc} recorded every 30 min. Group 2 AGS were placed in the metabolic chamber and O_2 consumption was acquired for one hour as baseline. We handled and restrained the animals for two minutes to perform the intraperitoneal (IP) injection; as USDA Pain and Distress classifies this procedure a category C, there was no requirement for any medication to reduce pain. Vehicle (2.5% hydroxypropyl- β -cyclodextrin, 0.5mg/kg, IP) or CHA (0.5mg/kg, IP) was administered by a researcher who was aware of the treatment. AGS were returned to the cage and monitored for the following three hours. We alternated VEH and CHA treatment every other test. At the time of injection, the metabolic chamber was opened to handle AGS in group 2. At three hours after injection, AGS were perfused intracardially prior to tissue collection (Figure 3.2a).

We choose three hours after injection based on the time required to express the cFos protein. We are interested in the seasonal difference in response to CHA, which is evident at one hour after injection. cFos protein is an immediate early gene induced by a stimulus. The highest level of cFos protein expression occurs two hours after the applied stimulus (Chaudhuri, 1997; Cirelli and Tononi, 2000). To detect the neuronal activity associated with the seasonal difference in response to CHA (one hour after injection), we collected the brains at the time when cFos expression was presumed to be at the highest (three hours after injection). cFos can also be expressed in astrocytes associated with differentiation and proliferation (Hisanaga et al., 1990) or in reactive astrocytes associated with neuroinflammation and pathological conditions (Groves et al., 2018). We do not expect CHA to promote proliferation or differentiation of astrocytes or to induce neuroinflammation; therefore, we interpret cFos+ cells as cFos+ neurons, but we cannot rule out involvement of astrocytes.

3.4.5 Drugs

A stock solution of CHA (10 mg/mL, Sigma Aldrich, Saint Louis, MO) was dissolved in 25% (w/v) hydroxypropyl- β -cyclodextrin (Tokyo Chemical Industry CO., Tokyo, Japan) in sterile water. On the week

of the experiment, the stock solution of CHA was diluted to 0.5mg/mL in sterile normal saline (0.9% NaCl). Diluted CHA was used within one month. Solutions for injection were sterilized by 0.2 µm filtration (Acrodisc syringe filter; Sigma-Aldrich, Saint Louis).

3.4.6 Brain tissue processing

Three hours post injection, AGS were anesthetized via chamber induction with 5% isoflurane and maintained via facemask at 3% mixed with 100% medical grade oxygen delivered at a flow rate of 1.5 L/min. AGS were intracardially perfused, first with 0.9% NaCl for 5 minutes, and then with 4% PFA in 0.1M PB buffer pH 7.4 at a flow rate of 79.5mL/min with an 18Ga needle, through the left ventricle, after the descending aorta was clamped, to obtain a more efficient perfusion of the brain. Brains were removed and post fixed in 4% PFA overnight.

Group 1 brains were cryoprotected in 30% w/v sucrose solution made in milliQ water, until brains sank. Brains were blocked in two parts rostral and caudal to the cerebellum and rapidly frozen in a bath of n-Hexane 95% cooled with dry ice to a temperature of -45°C. Frozen blocks were covered with Shandon™ M-1 Embedding Matrix (Thermo Fisher Scientific, Waltham, MA) and placed in -20°C freezer until frozen. This procedure caused some freezer artifacts in the tissue that disrupted appearance of the plasma membrane and cytoplasm; therefore, we used these brains for nuclear cFos-ir. We next optimized the procedure as follows for double staining immunohistochemistry. Group 2 brains were blocked in three parts to allow for better penetration of sucrose into the tissue. A gradient of sucrose solutions (5,10,15, 20 and 30% w/v) was made in 0.1M PB buffer pH 7.4 to cryoprotect the tissue. Brains were maintained in each sucrose solution for up to 3 days and in 30% sucrose until brains sank. Brains covered with Tissue-Tek O.C.T. Matrix (Electron Microscopy Sciences, Hatfield, PA) were rapidly frozen in a bath of n-Hexane 95% cooled with dry ice to a temperature of -45°C. Coronal sections (40µm) from all brains were cut with a cryostat (CM1850, Leica Biosystems, Buffalo Grove, IL).

3.4.7 Immunohistochemistry

Free floating sections were washed using PBS pH 7.2, blocked with normal goat serum (NGS) (Vector Laboratory, Burlingame, CA) for 2 hours at 4°C and labeled with monoclonal mouse anti-cFos (1:20,000, Santa Cruz Biotechnology, Dallas, TX, CAT# sc271243, RRID:AB_10610067) in PBS-0.2% TritonX-100 for 48 hours, followed by incubation with biotinylated secondary goat anti-mouse antibody (1:600, Vector Laboratory, Burlingame, CA, CAT# BA9200, RRID: AB_2336171) in PBS-0.4% TritonX-100. After incubation in avidin-biotin-peroxidase (Vectastain ABC kit, Vector Laboratory, Burlingame, CA, CAT#

PK6100, RRID:AB_2336819), sections were treated with 0.05% DAB (3',3-diaminobenzidine tetrahydrochloride, Sigma–Aldrich Corp. St. Louis, MO) with 1% ammonium nickel sulfate in sodium acetate 0.175M and 0.1% H₂O₂. Sections were mounted on Superfrost Plus slides (VWR, Radnor, PA) with Cytoseal mounting media (Thermo Fisher Scientific, Waltham, MA) or Permount (Thermo Fisher Scientific, Waltham, MA). Control slices, in which primary antibody was omitted and replaced by PBS, were run in every experiment under the same conditions.

3.4.8 Double-labeled immunohistochemistry

Free floating sections were washed using PBS pH 7.2, blocked with NGS for 2 hours at 4°C and labeled with monoclonal mouse anti-cFos as the first, primary antibody in PBS-0.2% TritonX-100 for 48 hours, followed by incubation with biotinylated secondary goat anti-mouse antibody in PBS-0.4% TritonX-100. After incubation with ABC, sections were treated with 0.05% DAB with 1% ammonium nickel sulfate in sodium acetate 0.175M and 0.1% H₂O₂. The sections were then washed before incubation with the second, primary antibody prepared in PBS-0.2% TritonX-100 to double-label the cFos+ cells. Table 3.2 shows the list of all the primary antibodies used. Slices were then incubated with biotinylated secondary goat anti-rabbit (1:600, Vector Laboratory, Burlingame, CA, CAT# BA1000, RRID: AB_2313606) or rabbit anti-sheep (1:600, Vector Laboratory, Burlingame, CA, CAT# BA 6000, RRID: AB_2336217) in PBS-0.4% TritonX-100. After incubation with ABC, sections were treated with 0.05% DAB in PBS and 0.1% H₂O₂. Sections were mounted on Superfrost Plus slides with Cytoseal mounting media or Permount. Control slices, in which primary antibody was omitted and replaced by PBS, were run in every experiment under the same conditions.

Before the NGS blocking step, we performed an antigen retrieval step (adapting one of the protocols provided by the website www.ihcworld.com) with the polyclonal rabbit anti-histamine antibody (1:1000, ImmunoStar, Hudson, WI, CAT#22939, RRID: AB_572245). Slices were incubated in hot 10mM Sodium Citrate with 0.05% Tween 20 at pH 6.0 (pre heated up to 80°C) for 30 min. Slices were then washed for 15 min in PBS and blocked with NGS as described above.

3.4.9 Antibody characterization

We used brain tissue collected from animals that were not part of the study to optimize and assess antibody specificity. We performed immunohistochemistry in brain slices at different distances from bregma. For each antibody, we assessed specificity from presence of immunoreactivity in the region where antigen is known to be expressed, and absence of immunoreactivity in other regions. Specificity

of immunoreactivity was also assessed on the basis of neuronal morphology, evident in the stained sections. We found that the number of immunoreactive neurons gradually increased as the sections approached the brain region known to express the antigen within defined cell group. The pattern of phenotypic-ir in the AGS brain regions was similar to the neuroanatomical pattern described previously in rat.

We used pro-TRH antibody to label TRH neurons in the paraventricular nucleus of the hypothalamus (PVN) (bregma -1.8). In brain sections of the hypothalamus, the TRH-ir gradually increased at the level of the PVN; few TRH+ neurons were detected in box2 (SI Figure 3.1a) compared to a larger number of TRH+ neurons in the PVN (box1 SI Figure 3.1b). The pro-TRH-ir is identical to immunoreactivity in rat brain at bregma -1.8 using the same rabbit anti-pro TRH donated by Eva Redei (Al-Noori et al., 2008; Fekete et al., 2000). In addition, TRH-ir was detected only in the PVN region, as seen by the lack of TRH-ir in box1 (SI Figure 3.1a) and box2 (SI Figure 3.1b). We used a similar approach to characterize the other antibodies. AVP-ir was absent in the frontal region of the hypothalamus (box1, SI Figure 3.1c) and in the cortex (box3, SI Figure 3.1d). A dense AVP-ir was detected in the PVN (box1, SI Figure 3.1d), and throughout the supraoptic nucleus (SON) (box3, SI Figure 3.1c and box2, SI Figure 3.1d) as expected. Using a different AVP antibody (guinea pig anti-AVP) together with AVP mRNA expression, AVP-ir was previously shown in the PVN of AGS, but not in the suprachiasmatic nucleus (SCN), which is in contrast to other species (Williams et al., 2017). We detected the same pattern of AVP-ir in the PVN and the lack of AVP+ cells in the SCN in AGS (box2, SI Figure 3.1c) consistent with Williams et al. Moreover, the rabbit anti-AVP antibody used in our study (RRID: AB_90782, AB_11212336, AB_90772) shows an identical AVP-ir pattern in the PVN in rats (Das et al., 2007; Parker et al., 2017). Orexin A+ neurons are detected in the perifornical nucleus of the hypothalamus (PeF), on top of the fornix (box2, SI Figure 3.1e). Orexin fibers are also visible in the ventral part of the hypothalamus (box3, SI Figure 3.1e), but we did not detect any immunoreactivity in the area above the mammillary tract (box1, SI Figure 3.1e). The same orexin-ir pattern is detected in rats using the same rabbit anti-orexin A (RRID: AB_91545)(Zhao et al., 2012), which specificity has been previously shown in preadsorption experiments in rats (Nambu et al., 1999). The histamine-ir was visible in PFA perfused tissue after antibody penetration was enhanced with the antigen retrieval step. Histamine+ neurons were detected in the ventral location of the brain slice, identified as the tuberomammillary nucleus (TMN) (box3, SI Figure 3.1f), but not in other areas of the same coronal section (box1, box2, SI Figure 3.1f). The histamine-ir pattern in AGS is identical to the pattern seen in rats stained with the same rabbit anti-histamine (RRID: AB_572245) after 4% 1-ethyl-3-[3-dimethylaminopropyl] carbodiimide perfusion (Ellender et al., 2011; Nosedá et al., 2014), and to the

histaminergic neurons at bregma -3.80 identified by adenosine deaminase-ir (Parks et al., 2016). TH-ir was detected in the catecholaminergic neurons in the locus coeruleus (LC) (box1, SI Figure 3.2a) and nucleus tractus solitarius (NTS) (box1, SI Figure 3.2b). Ventral immunoreactivity was associated with the A5 noradrenaline cells (box3, SI Figure 3.2a). We did not detect other clusters of TH+ neurons in the same coronal section (box2, SI Figure 3.2a and box2, SI Figure 3.2b). The neuroanatomical distribution of TH+ neurons in AGS is the same as the distribution reported in rats using the same antibody (RRID: AB_390204) in both the NTS (García-Pérez et al., 2012) and LC, where specificity was confirmed by TH downregulation experiments (Khanday et al., 2016). TPH-ir was detected in the rPA (box3, SI Figure 3.2c) and in the midline corresponding to the raphe magnus. We did not detect TPH-ir in other areas of the section (box1-2, SI Figure 3.2c). The anatomical distribution of TPH+ neurons in AGS is identical to TPH+ neurons distribution in rats using the same sheep-anti TPH (RRID: AB_90754) (Oliveira et al., 2018) or using a different antibody (Hale et al., 2011).

3.4.10 Cell counting procedures

We assigned a blind code to each animal to prevent any bias from the observer. Images were analyzed using Metamorph software (version 7.8.8.0, Molecular Devices, San Jose, CA) with a Nikon Eclipse TE2000-U inverted microscope equipped with a CCD camera (Cool Snap HQ2, Photometrics, Tucson, AZ) or with Nikon Eclipse 80i equipped with a digital camera (Micropublisher 3.3RTV, Qimaging, BC, Canada). When tissue sections were symmetrical in each brain hemisphere (i.e. PVN, SON, SCN, NTS, LC, TMN), each hemisphere was counted individually in at least two consecutive slices for each AGS. The mean of at least four slices, two from each hemisphere per AGS, was used for subsequent statistical analysis. The mean of at least three slices was used in non-symmetrical sections such as the median preoptic nucleus (MnPO) and rPA. The count was done manually under a 20X objective using the manual count function in Metamorph to prevent double counting. Double stain was defined as brown DAB neurons with a distinct round dark black nucleus. In double stained analysis, the percentage of activated neurons was defined as the ratio between double stained neurons and the number of neurons positive for the phenotypic marker used. As an example, percent activation of AVP neurons was calculated as the ratio between AVP+cFos+ neurons and total AVP+ neurons.

The region of interest (ROI) included each brain region identified by Nissl stain (0.1% w/v Cresyl Violet) or positive phenotypic-ir (SI Figure 3.1-2) and anatomical landmarks (i.e. the anterior commissure, the optic chiasm, the mammillary tract, the fornix), by reference to the Paxinos and Watson Rat Atlas Fourth Edition (Paxinos and Watson, 1998) (Figure 3.3). We counted all cFos-ir cells

within the ROI borders in the MnPO, SON, VLPO, SCN, PVN and dorsal medial hypothalamus (DMH). We counted all cFos-ir cells and double labeled neurons within the ROI borders in the PeF/lateral hypothalamus (LH), TMN, LC, rPA, NTS.

MnPO: The ROI was identified by the presence of the anterior commissure and the fornix, corresponding to bregma -0.30 in the rat atlas (all the references to bregma refer to the rat brain). The bottom border of the ROI (1000 μ m by 350 μ m) was placed on top of the third ventricle.

The cFos-ir in the SON and VLPO were counted in the same coronal section corresponding to bregma -0.80. SON: The shorter edge of the ROI (400 μ m by 650 μ m) was placed on the edge of the optic chiasm and the bottom aligned with the ventral edge of the slice. VLPO: The ROI (200 μ m by 650 μ m) was placed along the top border of the SON ROI.

SCN: The ROI was identified in the brain section corresponding to bregma -0.92 in the rat atlas. The size of the ROI was defined by the area that included the entire SCN identified in nissl stained sections from three animals not included in the study. The bottom border of the ROI (400 μ m by 225 μ m) was placed on the dorsal edge of the optic chiasm. The medial border was aligned with the third ventricle.

PVN: We defined the ROI by proximity to regionally specific anatomic landmarks; these included the shape of the optic chiasm and the presence of the fornix and the mammillary tract, corresponding to bregma -1.88. The ROI box (650 μ m by 400 μ m) was placed next to the ventricle and the shorter edge aligned with the top of the ventricle.

We counted cells in the DMH and PeF/LH in the same coronal section corresponding to bregma -3.14. LH/PeF: We identified the ROI by orexin-ir and anatomical landmarks including the ventricle shape, the median eminence and the location of the mammillary tract. The ROI box (650 μ m by 540 μ m) was placed with the longer edge just on top of the fornix, and the middle of the box was aligned with the middle of the fornix.

DMH: The ROI box (689 μ m by 519 μ m) was placed with the longer edge next to the third ventricle wall and the bottom of the box aligned with the ventral extent of the fornix.

TMN: The ROI was identified by histamine-ir and by landmarks including the caudal extent of the third ventricle, the mammillary tract shape and the presence of the medial lemniscus. This corresponded to the plane defined by bregma -3.80 in the rat atlas. The longest edge of the box (688 μ m by 374 μ m) was placed on the ventral edge of the brain slice and the box was aligned with the middle of the fornix.

LC: The ROI was identified by the distinct shape of the fourth ventricle at bregma -10.04 and by TH-ir. The shorter edge of the box (1035 μ m by 517 μ m) was aligned with the top of the fourth ventricle.

rPA: The ROI was identified by TPH-ir and the “protrusion” of the pyramidal tract and the dorsal cochlear nucleus at bregma -11.60. The box (311 μ m by 173 μ m) was placed with the middle part aligned with the medial longitudinal fasciculus and the bottom part of the box (the smaller edge) on the ventral edge of the slice between the pyramidal tracts.

NTS: We identified the ROI by the area postrema and the central canal at bregma -13.68 and TH-ir. The shorter edge of the box (302 μ m by 647 μ m) was aligned with the middle of the central canal and the bottom part of the box was placed on top of the central canal.

The AVP and TRH neurons were identified by immunoreactivity. We counted all the TRH-ir neurons and all the cFos-TRH-ir neurons in the slice in the PVN at bregma -1.88, and all the AVP-ir neurons and all the cFos-AVP-ir neurons in the slice in the PVN at bregma -1.40.

3.4.11 Statistical analysis

A statistical a priori power analysis (G*Power software version 3.1.9.4), using the statistical test ANOVA: Fixed effects, special, main effects and interactions in the F tests family, was performed for sample size estimation based on published data on cFos count in the MnPO during sleep and wakefulness (Gong et al., 2000). With the effect size=3.1, alpha=0.05, power=0.8, numerator df=1 and number of groups=4, the estimated sample size is approximately n=6 to detect a significant interaction between season and treatment (Faul et al., 2007). All outliers were included in the data analyses performed using R (version 1.1.423). Data are presented as mean \pm SEM and a $p < 0.05$ was considered significant. We tested the normality assumptions on the data using Shapiro test, when the assumption was not met, the data were normalized by transforming to the square root. Before combining data from group 1 and group 2, we ran a three way ANOVA to test for effects of season, treatment and group. Groups 1 and 2 were combined when no significant interactions with group were noted and we excluded group 1 from the analysis when interactions with group were statistically significant. Next, we used two way ANOVA to test for effects of season and treatment. When the interaction between the independent variables was significant and one mean tended to be different from the three other means, we used the Dunnett test. When the two way ANOVA showed only a significant ($p < 0.05$) main effect of season or treatment and did not show any significant interaction, we reported data collapsed across variables that were not statistically different from one another, and we performed a single post-hoc t test. We report results grouped by effect of season, effect of treatment and effect of an interaction between season and treatment. If data, after transformation, failed the assumption of normality, we used the nonparametric

Kruskal Wallis test for multiple comparisons and the Wilcoxon signed-rank test for comparison between groups.

3.5 Results

CHA induced-hibernation promotes a delayed and persistent decrease in metabolic rate and T_b in Winter AGS, but not in Summer AGS under constant environmental conditions (Figure 3.2). Our results show the time course of this response for three hours, at which time we collected the brain tissues for immunohistochemical analysis.

3.5.1 Effect of handling on torpor bout in Winter AGS

As shown in Figure 3.2a, we handled the torpid AGS the night before the experiment to induce arousal in Winter AGS. We then moved the Winter AGS to a warm room (17°C, 4L:20D) to delay the natural onset of the next torpor bout. In 94.4% of AGS the torpor bout was successfully delayed, but the procedure was not effective in one AGS, assigned to the Winter VEH group. Four hours prior to drug administration, we found the AGS in a curled position, re-entering torpor. We handled the AGS a second time to restore the arousal state. At the time of injection, the T_b reached the euthermic temperature of 35.1°C. This animal contributed to the large variation in the T_b data between time -1 and time 0 in the Winter VEH group (Figure 3.2c).

3.5.2 Seasonal changes in euthermic T_b

Hibernation is a seasonal phenomenon characterized by physiological changes between summer and winter, which led us to ask if the euthermic T_b changes between seasons under constant environmental conditions. We found a significantly lower core T_b and T_{sc} in Winter AGS compared to Summer AGS ($t(17)=6.57$, $p<0.001$ t test in T_b ; $t(16)=5.90$, $p<0.001$ t test in T_{sc} ; Table 3.1). VEH-treated AGS also showed a significantly lower T_r in Winter AGS compared to Summer AGS, measured just prior to perfusion ($t(19)=4.08$, $p<0.001$ t test in T_r ; Table 3.1). We also observed in VEH-treated AGS a significantly lower core T_b in winter compared to summer when core T_b was monitored over the VEH treatment period, beginning one hour before VEH administration to the time of tissue collection for a total of 4 hours ($F(1,156)=4.45$, $p<0.05$ Season by time, two way ANOVA, Figure 3.2c-2e).

3.5.3 Effect of treatments on T_b and metabolic rate

CHA significantly decreases metabolic rate, measured as the rate of O_2 consumption, and T_b from time of injection (time zero) to the time of tissue collection. In Winter AGS, the effect of CHA on metabolic rate and T_b leads to the onset of hibernation ($H(192)=479.3$, $p < 0.001$, for O_2 consumption; $H(12)=50.567$, $p < 0.001$ for T_b ; Kruskal Wallis test; Figure 3.2b). Summer AGS show a transient decrease in metabolic rate and T_b ; metabolic rate and T_b return to the initial values within one hour from CHA administration ($H(182)=396.78$, $p < 0.001$, Kruskal Wallis test for O_2 consumption; $F(11,36)=13.16$, $p < 0.001$ one way ANOVA for T_b ; Figure 3.2d). Interestingly, in Winter AGS metabolic rate decreases immediately at time zero, while the decrease in T_b is delayed by one hour (Figure 3.2b). By contrast, both the metabolic rate and T_b decrease at the same time in Summer AGS (Figure 3.2d). In the control groups, Winter and Summer AGS treated with VEH, metabolic rate and T_b showed no change after injection (Winter AGS: $H(181)=84.77$, $p=1$, Kruskal Wallis test for O_2 consumption; $F(11,48)=0.468$, $p=0.9$ one way ANOVA for T_b ; Figure 3.2c. Summer AGS: $H(182)=148.4$, $p=1.0$, Kruskal Wallis test for O_2 consumption, $F(11,60)=0.877$, $p=0.6$ one way ANOVA for T_b ; Figure 3.2e). We found that the seasonally dependent effect of CHA was the same whether we monitored core T_b or T_{sc} (SI Figure 3.3a-b).

3.5.4 Effect of season on sleep-wake and thermoregulatory pathways

Summer and Winter AGS are characterized by seasonal changes in physiology. First, we asked if neuronal activity within sleep-wake and thermoregulatory pathways changes with season. We identified seasonal differences in neuronal activity in the SON, the SCN and in the rPA. Table 3.3 shows a significant increase in cFos activation in the SON ($t(16)=-2.1676$ $p < 0.05$ two sample t test) and a significant decrease in the SCN ($t(9.49)=4.01$, $p < 0.01$ two sample t test) in Winter compared to Summer AGS, also shown by photomicrographs (SI Figure 3.4a-b). In the rPA, two way ANOVA analysis showed a significant interaction, so data were not collapsed and we performed a post hoc t test between the two VEH groups to assess the effect of season. We found significantly higher cFos activation in the Summer VEH compared to the Winter VEH ($t(18.9)=2.35$, $p < 0.05$ two sample t test, Table 3.2 and SI Figure 3.4c). These results suggest that a seasonal modulation of neuronal activity in the SCN, the SON and the rPA is associated with the AGS seasonal phenotype.

3.5.5 Effect of CHA on sleep-wake pathways

We next asked how CHA affects the sleep-wake pathways (Schwartz and Roth, 2008; Saper and Fuller, 2017) illustrated in Figure 3.4a. We identified the ventrolateral preoptic nucleus (VLPO) a known sleep-

active region, based on anatomical landmarks within the hypothalamus; this region did not show any change in cFos expression after CHA (SI Table 3.1). Unfortunately, we were not able to confirm the identity of the region because the antibodies used as phenotypic markers were not effective in AGS brain (SI Table 3.2). Next, we looked at the brain nuclei within the arousal pathways. cFos-ir cells were counted in the TMN, but we excluded group 1 AGS from the analysis because of a significant interaction with group ($F(1,31)=8.06$, $p<0.05$, interaction treatment by group three way ANOVA). The TMN (Figure 3.4b) shows a decrease in cFos expression after CHA compared to VEH ($t(19)=-3.5184$ $p<0.01$ two sample t test, Figure 3.4d). When we double stained the TMN for cFos+ and histamine (HIST)+ neurons (Figure 3.4c), the percent activation of HIST+ neurons was significantly lower in the CHA-treated compared to the VEH-treated group ($t(19)=-3.6208$ $p<0.01$ two sample t test, Figure 3.4e). Group 1 and 2 data were combined in the LH ($F(1,31)=0.066$, $p=0.8$, interaction season by treatment by group three way ANOVA). Although we saw a tendency towards lower cFos expression in the LH in Winter AGS compared to Summer AGS ($t(37)=1.9168$ $p=0.06$ two sample t test, Table 3.3), after double staining the LH for cFos+ and orexin+ neurons, we did not find any change in percent activation of orexin+ neurons (SI Table 3.1). Moreover, we did not find any difference in activation of TH+ neurons in the LC (SI Table 3.1). The TMN is the main nucleus in the sleep-wake pathways significantly inhibited by CHA, independent of season.

3.5.6 Effect of CHA on thermoregulatory pathways

As CHA lowers T_b and metabolic rate, we asked if brain regions regulating thermogenesis are affected by CHA. First, we looked at the PVN, as a main regulator of energy homeostasis. We did not find any significant difference in the number of cFos+ neurons in the PVN between CHA and VEH-treated AGS (Table 3.4). However, we found a significant increase in percent activation in AVP+ neurons ($t(18)=4.0517$, $p<0.001$ two sample t test, Table 3.4, SI Figure 3.5a) as well as in percent activation of TRH+ neurons in CHA-treated AGS compared to VEH ($t(19)=2.2838$, $p<0.05$ two sample t test, Table 3.4, SI Figure 3.5b). We found higher numbers of TRH+ neurons in Winter AGS compared to Summer (131 ± 11 Summer, 83 ± 7 Winter, $t(19)=-3.8$ $p<0.01$, $n=10-11$ animals per group); and no difference in AVP+ neurons (103 ± 4 Summer, 114 ± 8 Winter, $p>0.05$, $n=10$ animals per group). Although an increase in TRH+ neurons suggests plasticity and increased thermogenic capacity consistent with prior findings (Frare et al., 2018), we cannot conclude that TRH+ neurons proliferate in the PVN without counting neurons within the full extent of the nucleus and this was beyond the scope of this study.

Next, we looked at the brain regions known to regulate thermogenesis reported in Figure 3.5a. The DMH, showed an increased neuronal activity in the CHA-treated group compared to VEH ($t(18)=3.5153$ $p<0.01$ two sample t test, Figure 3.5d-e). We also found changes in cFos activation in the NTS, a nucleus located in the brainstem. cFos-ir cells were counted in the NTS, but we excluded group 1 AGS from the analysis because of a significant interaction with group ($F(1,31)=8.12$, $p<0.05$, interaction season by group three way ANOVA). The NTS showed an increase in neuronal activation in CHA-treated AGS compared to VEH-treated AGS ($t(10.92)=3.27$ $p<0.01$ two sample t test, Table 3.5). We double stained the NTS for cFos+ and TH+ neurons. We expressed the number of double-labeled neurons as a percentage of total TH+ neurons. Using this approach, we found an increase in percent activation of TH+ neurons within the NTS in the CHA-treated AGS compared to VEH-treated AGS ($t(18)=2.1763$, $p<0.05$, Table 3.5 and SI Figure 3.5c). We saw no difference between absolute numbers of neurons double stained for cFos and TH ($F(1,16)=1.57$, $p=0.23$, interaction season by treatment, two way ANOVA).

3.5.7 Interaction of CHA and season on sleep-wake and thermoregulatory pathways

Finally, because the metabolic and thermoregulatory response to CHA is different with seasons, we asked in which brain regions CHA induces a different neuronal activation between summer and winter. The MnPO and rPA show seasonal differences in cFos expression in response to CHA. Neuronal activation is significantly higher in the MnPO in the Summer CHA group compared to Summer VEH, Winter CHA and Winter VEH ($F(1,16)=4.862$ $p<0.05$ interaction season by treatment two way ANOVA, followed by Dunnett test; Figure 3.5b-c). cFos+ cells counted in group1 and 2 in the rPA were combined ($F(1,31)=0.2$, $p=0.6$, interaction season by treatment by group three way ANOVA). The rPA shows a higher number of cFos+ cells in the Summer CHA compared to Summer VEH, Winter CHA and Winter VEH ($F(1,35)=6.605$ $p<0.05$ interaction season by treatment two way ANOVA, followed by Dunnett test; Figure 3.5f-g). We did not observe any changes in the percent activation of TPH+ neurons in the rPA (SI Table 3.1). The changes in neuronal activation in the MnPO and the rPA explain the seasonal difference in response to CHA.

3.6 Discussion

3.6.1 Seasonal modulation of thermoregulatory response to CHA underlies onset of hibernation

Consistent with our previous findings (Frare et al., 2018; Jinka et al., 2011), we report the different seasonal response to CHA in Winter and Summer AGS, maintained under constant environmental conditions (2°C, 4L:20D). Here we show that the MnPO and the rPA, two brain nuclei that are part of the

thermoregulatory pathways (Morrison and Madden, 2014), are associated with the seasonal response to CHA. We define for the first time the MnPO as another seasonal component of CHA-induced hibernation, together with the previously described premotor neurons in the rPA (Frare et al., 2018), which regulate both shivering and non-shivering thermogenesis (Tan and Knight, 2018). The direct inhibition of the rostral ventromedial medulla including the rPA by the GABA_A agonist muscimol induces a torpor-like state in rats (Cerri et al., 2013), therefore, it is likely that the suppressed activation of the rPA should promote the onset of hibernation. However, the direct inhibition of the rPA in rats produced massive cutaneous vasodilation that worked in concert with suppressed thermogenesis to lower T_b (Cerri et al., 2013). By contrast, vasoconstriction predominates during hibernation shown by T_{sc} measurements. The seasonal increase in neuronal activation of the MnPO and the rPA after CHA in Summer reflects activation of the thermogenic pathway. Previous evidence suggests that when T_b decreases, the GABAergic neurons in the MnPO disinhibit the DMH allowing activation of the premotor neurons in the rPA which in turn activates sympathetic innervation of brown adipose tissue (BAT) and increases thermogenesis (Nakamura et al., 2004; Morrison and Madden, 2014). However, this response is blunted after CHA in Winter so T_b decreases. Where CHA acts to blunt the thermogenic response remains unknown.

The MnPO is part of the preoptic area (POA) of the hypothalamus that integrates thermogenic stimuli and other physiological states (McKinley et al., 2015). We focused our interpretation on the role of the MnPO in the thermoregulatory and sleep pathways as the most likely physiological functions affected by CHA (Bjorness and Greene, 2009; Tupone et al., 2013), but acknowledge that the function of the MnPO is diverse (McKinley et al., 2015) and we cannot rule out activation of the MnPO related to other functions without further study. The GABAergic neurons in the MnPO not only regulate thermoregulatory function, as described above, but also promote sleep through direct inhibition of the arousal centers and dis-inhibition of the VLPO (Uschakov et al., 2007). The MnPO, a sleep active region, is most likely a major component in the cross-talk between thermoregulation and sleep (Gong et al., 2004; Dentico et al., 2009; Harding et al., 2018). Currently published data suggest that different GABAergic populations within the MnPO may control the two physiological processes (Dentico et al., 2009; Harding et al., 2018). Unfortunately, we were not able to perform a comprehensive characterization of the cFos+ neurons in the MnPO using phenotypic markers for GABA neurons, due to limited cross-species reactivity of commercially available antibodies. Inability to label GABAergic neurons within the POA, also limited our analysis in this region with dispersed cell groups that Nissl stain cannot define. However, the distinctly higher cFos expression in the MnPO in our data and the well

described activation of the MnPO and the rPA associated with thermogenesis (Nakamura et al., 2004; Nakamura and Morrison, 2008) are consistent with our interpretation that the thermogenic response after CHA in Summer AGS is suppressed after CHA in Winter. Thus, our data suggest the MnPO and rPA as the likely regulators of the seasonal response to CHA.

Nonetheless, as sleep increases in euthermic (not hibernating) squirrels during the hibernation season compared to summer (Walker et al., 1981), we cannot exclude possible seasonal changes in subpopulations of GABAergic neurons in the MnPO promoting sleep and also regulating the seasonal response to CHA. Although we found no evidence of a change in seasonal sensitivity to CHA in sleep active neurons in the VLPO, CHA inhibited the arousal promoting neurons in the TMN (discussed below) regardless of seasonal phenotypes.

3.6.2 Thermolytic and somnogenic effects of CHA promote the onset of hibernation

Brain nuclei within the thermoregulatory pathways are activated in response to CHA. The thermolytic effect of CHA is evident from the decrease in metabolic rate followed by a decrease in T_b after drug administration. Our data suggest that the NTS is the brain region mediating the thermolytic effect of CHA. The role of the NTS in suppression of thermogenesis has been previously suggested via indirect projections to the rPA (Cao et al., 2010), but the mechanism is still poorly understood. However, the NTS is characterized by a large number of A_1AR (Pickel et al., 2006), making this area a likely site of action of CHA. Our result in AGS are consistent with previous findings also showing a higher cFos activation in the NTS in CHA-induced hypometabolic state in rats (Tupone et al., 2013), and supported by the direct effect of CHA administration in the NTS in suppressing T_b (Tupone et al., 2013), thus metabolism. Within the NTS, we saw no difference between absolute numbers of neurons double stained for cFos+ and TH+, consistent with prior work in rat (Tupone et al., 2013). However, we expressed the number of double-labeled neurons as a percentage of total TH+ neurons, and we found a significant effect of CHA on the activation of TH+ neurons in the NTS. An alternative interpretation as to why we saw TH+ neurons activated is that our observations may reflect hypotension caused by systemic administration of CHA. Hypotension activates the barosensitive TH+ neurons in the NTS (Daubert et al., 2012; Li and Dampney, 1994) to adjust arterial pressure through the baroreceptor reflex control system. The neuronal activity of TH+ neurons in the NTS increases after CHA administration as a negative feedback mechanism to the direct peripheral effect of CHA on decreasing heart rate with subsequent decrease in blood pressure (Tupone et al., 2013; Vicent et al., 2017; Laughlin et al., 2018).

Interestingly, AGS maintain their cold-defense response despite CHA-induced inhibition of thermogenesis. TRH neurons and AVP neurons within the PVN, known to stimulate thermogenesis (Angulo et al., 1991; Jasnic et al., 2015; Küchler et al., 2010), are activated after CHA in Summer and Winter but these cold defense responses are attenuated at the level of the MnPO and rPA in Winter to allow the onset of hibernation, but not in Summer. The ability of AGS to maintain a cold-defense mechanism is especially important during the hibernation season when the stimulation of thermogenesis is necessary to rewarm from torpor during interbout arousals, and in extreme ambient cold when torpid AGS increase their metabolic rate (Buck and Barnes, 2000; Richter et al., 2015). The thermogenic brain nuclei (AVP and TRH) activated in response to CHA-induced cooling are most likely the nuclei activated during rewarming from torpor. It has been shown that both AVP injection in the lateral septum (Hermes et al., 1993) and intracerebroventricular injection of TRH (Tamura et al., 2005) interrupt torpor and induce arousal. In addition, TRH receptor quantification in ground squirrel shows seasonal variations (Stanton et al., 1992). TRH receptor density decreases in torpor compared to the euthermia in the PVN and in the medial preoptic area of the POA, both thermoregulatory regions (Stanton et al., 1992). As TRH is linked to metabolic state, we can speculate that a metabolic clue may trigger thermogenesis, however the signaling mechanisms initiating rewarming are still unknown (Drew et al., 2017).

DMH is the intermediary nucleus between the MnPO and the rPA (Zhang et al., 2011; Morrison and Madden, 2014) so it is unclear why we did not observe any winter seasonal blunting of activation of DMH neurons as seen in the rPA and the MnPO. In Summer, the increase in cFos expression in the DMH after CHA may be associated with the activation of thermogenesis through the MnPO-rPA pathway. In Winter, activation of cold-defense mechanisms may also activate neurons within the DMH which are blunted downstream at the level of the sympathetic premotor neurons in the rPA.

Adenosine is a well-known endogenous sleep promoting neurotransmitter (Bjorness and Greene, 2009) and the role of the A₁AR in hibernation and torpor has been shown in AGS, hamsters and mice (Drew et al., 2017). We identify the TMN, within the sleep-wake pathway as the major nuclei mediating the somnogenic effect of CHA. We discussed above a possible effect of CHA in the disinhibition of the sleep active neurons (i.e. the MnPO and VLPO) that suppress arousal, but CHA may also inhibit the TMN directly. A previous study supports a direct effect of A₁AR agonist on the histaminergic neurons to promote sleep in rats (Oishi et al., 2008).

The significant effect of CHA on HIST+ neurons could be explained by the larger extent of the histaminergic system in the ground squirrel compared to rat (Sallmen et al., 1999). The extensive

histaminergic system in ground squirrel could place the histamine signaling as the major wakefulness nucleus within the arousal pathways in hibernators. Moreover, the histamine signaling has been proposed as the mechanism triggering arousal from torpor as the histaminergic fibers increased during the hibernation season (Sallmen et al., 1999; Panula et al., 2000). Therefore a direct inhibition through A_1AR and the increase in autoregulatory receptor (H_3R) in hypothalamic regions seen in torpor (Sallmen et al., 2003a; Herwig et al., 2007) may act together to suppress wakefulness and to promote torpor. However, the role of histaminergic signaling in hibernation is controversial. One study showed increased torpor bout length by intrahippocampal histamine administration (Sallmen et al., 2003b), which is surprising, but the possibility that histamine lengthened torpor through H_3R , has not been excluded. CHA suppresses thermogenesis and promotes sleep, but a seasonal clock controls both the onset of natural and CHA-induced hibernation.

3.6.3 Seasonal decrease in thermogenesis is required for the onset of hibernation

Here we show that a seasonal decrease in thermogenesis involves attenuated activation of thermogenesis as well as a seasonal increase in vasoconstriction, both of which occur without changes in environmental conditions and contribute to energy conservation. T_{sc} is an indirect, but valid measure of vasoconstriction. The seminal core-shell model of thermoregulation defines T_{sc} and skin temperature as the component of the outer shell (Webb, 1992) whereby a decrease in T_{sc} and skin temperature is secondary to a decrease in vasoconstriction (Barcroft and Edholm, 1946). The lack of thermogenic response, likely attenuated at the level of the MnPO and the rPA after CHA administration in Winter, reflects a seasonal decrease in sensitivity of thermoregulatory pathways as described in our previous model of seasonal modulation of thermogenesis (Frare et al., 2018).

Increased vasoconstriction described here and by others during fasting-induced torpor in mice and hibernation in ground squirrels and hamsters (Lyman and O'Brien, 1961; Lyman and O'Brien, 1963; Karoon et al., 1998; Swoap and Gutilla, 2009) decreases conductive heat loss in Winter AGS after CHA treatment. CHA induces an immediate drop in O_2 consumption, followed by a delayed decrease in T_b in Winter AGS. The delayed decrease in T_b is due to the seasonal increase in vasoconstriction.

In hibernation, the seasonal modulation of thermogenesis occurs despite of external stimuli, challenging the classic view of warm- and cold-activated pathways where a stimulus activates a suite of coordinated responses that together promote an increase or decrease in T_b . Here we show *for the first time* that vasoconstriction in hibernation is seasonally modulated to conserve energy regardless of

environmental cues. Challenging the current compartmentalization of neuronal pathways, hibernation shows that neuronal circuits can be individually used to conserve heat and energy.

We identify the SON, characterized by vasopressinergic neurons, as the brain area most likely to mediate the increase in vasoconstriction as AVP is known to be a strong vasoconstrictor (Ohbuchi et al., 2015). We were not able to quantify activated AVP+ neurons in the SON because the high density of AVP+ neurons prevented the accurate count of the individual neurons and densitometry was not feasible in double stained slices. Even though we had these technical issues, we speculate that the cFos+ neurons are vasopressinergic neurons as the majority of cells in the SON are AVP+ (Zhao and Ai, 2011; Otero-García et al., 2016) and the oxytocin neurons in the SON mediate behaviors and functions (Althammer and Grinevich, 2018), which do not occur during the hibernation season.

CHA-induced hibernation highlights the similarity between hibernation and sleep, in particular the relation between sleep and thermoregulation. The physiological onset of sleep follows the circadian decrease in core T_b (Szymusiak, 2018; Te Lindert and Van Someren, 2018) just as the seasonal onset of hibernation is facilitated by a seasonal decrease in core T_b . While in sleep, the decrease in T_b is obtained through vasodilation, in hibernation it is not. In hibernation, the decrease in T_b is reached through the seasonal increase in vasoconstriction and decrease in thermogenesis, which are intended to conserve energy. Thus, the idea that hibernation is an extension of sleep (Walker et al., 1981) is in part supported by our data as the seasonal decrease in thermogenesis is needed for adenosine mediated hibernation.

3.6.4 Seasonal differences in neuronal activation within the SCN unrelated to CHA

Modulation in thermoregulatory pathways is necessary for the onset of hibernation; however, the mechanism underlying the circannual clock is still unknown. The SCN controls the circadian rhythm and plays a role in the timing of daily torpor (Ruby, 2003), however its function in hibernation is still debated. During the hibernation season, the SCN is arrested as cFos expression is significantly reduced in Winter compared to Summer AGS. Our results are consistent with previous work in AGS that found the periodicity of the SCN to be absent during hibernation (Ikeno et al., 2017). Moreover, we found similar levels of cFos measured here under a 4L:20D cycle as levels of cFos measured by others under constant darkness (Ikeno et al., 2017). A study in 13-lined ground squirrels also excludes the role of the SCN in regulating hibernation as the level of cFos mRNA is constant throughout the torpor bout (Bratincsak et al., 2007). By contrast to reports of cFos protein expression in AGS, cFos mRNA levels are higher in hibernating 13-lined ground squirrels compared to the euthermic control group (Bratincsak et al., 2007).

Notably, the control group was not well characterized with regard to season and may have included both summer and winter phenotypes, and mRNA and protein expression may differ.

Even if we suggest that activity of the SCN is attenuated during the hibernation season, some baseline neuronal activity is still present, consistent with a reduced but persistent SCN metabolic activity in hibernating golden-mantled ground squirrels (Kilduff et al., 1989). Moreover, cFos protein expression in AGS and cFos mRNA in golden-mantled ground squirrels are both higher during arousal at 20°C T_b compared to torpor and interbout arousal (Bitting et al., 1994; Ikeno et al., 2017). It is tempting to speculate that the SCN activity during rewarming is required to produce melatonin, also known to be a potent neuroprotectant. A surge in melatonin production is detected in early arousal in Siberian hamsters (Larkin et al., 2003) and melatonin signaling pathway is critical for neuroprotection during arousal at 20°C T_b 13-lined ground squirrels (Schwartz et al., 2015).

In conclusion, the seasonal decrease in T_b achieved through a decrease in thermogenesis and an increase in vasoconstriction contributes to CHA-induced hibernation in the winter season. A circannual rhythm modulates thermogenesis and vasoconstriction independent of environmental temperature and day length. The MnPO and the rPA stand out as key sites of circannual modulation of thermogenesis and the SON stands out as a site of circannual modulation of vasoconstriction. Understanding thermoregulatory mechanisms in hibernation will expand our fundamental understanding of T_b and metabolic regulation and will develop novel strategies to regulate metabolic demand.

3.7 Acknowledgments and conflict of interest

We thank J. Moore, L. Bogren, S. Rice, B. Laughlin for technical assistance. Research reported in this publication was supported by NSF I0S-1258179; the National Institutes of Health under Award Numbers NS081637; the National Institute Of General Medical Sciences of the National Institutes of Health under the Award Number TL4GM118992; Institutional Development Award (IDeA) from the National Institute of General Medical Sciences of the National Institutes of Health under grant number P20GM103395. The content is solely the responsibility of the authors and does not necessarily represent the official views of the National Institutes of Health. KD has a financial interest in Be Cool Pharmaceuticals.

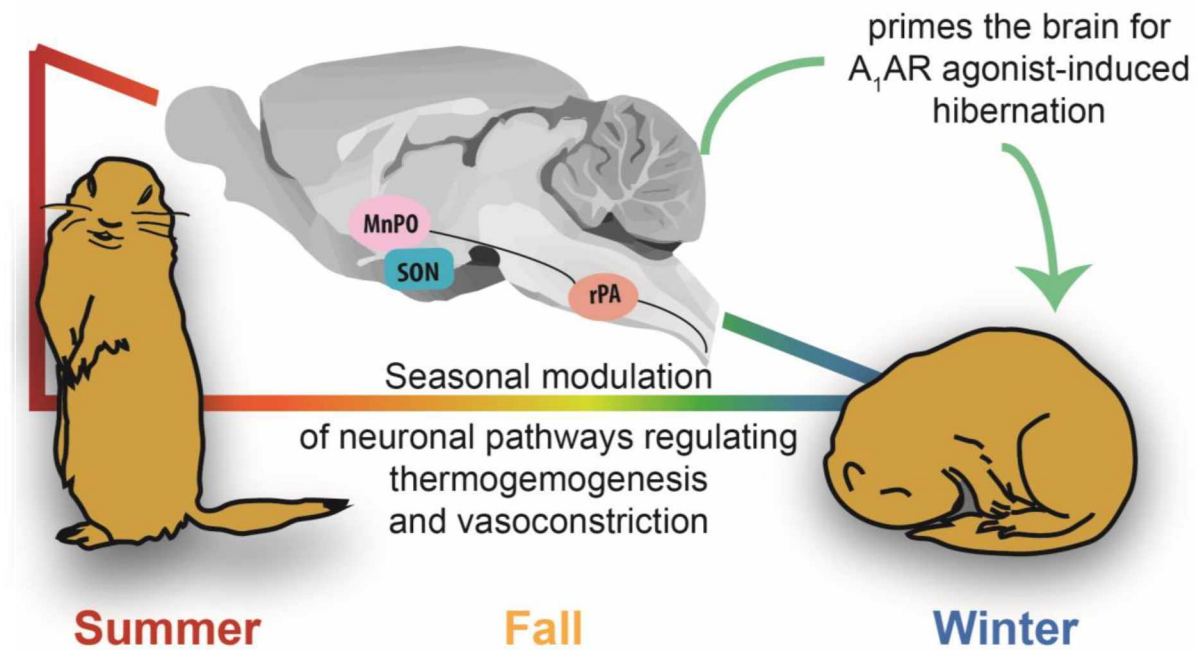


Figure 3.1: Graphical abstract

Adenosine promotes hibernation and torpor through the A₁ receptor. However, an endogenous seasonal rhythm regulates the response to adenosine A₁ receptor agonist-induced hibernation in arctic ground squirrels. We hypothesized that thermoregulation is seasonally modulated. Using immunohistochemical analyses in brain tissue of arctic ground squirrels, we identify the median preoptic area (MnPO) and raphe pallidus (rPA) as the main brain nuclei regulating the seasonal difference in response to CHA, an adenosine A₁ receptor agonist. The seasonal increase in vasoconstriction, measured by subcutaneous body temperature and associated with higher cFos expression in the supraoptic nucleus (SON) explains the delayed fall in T_b observed in winter ground squirrels after CHA.

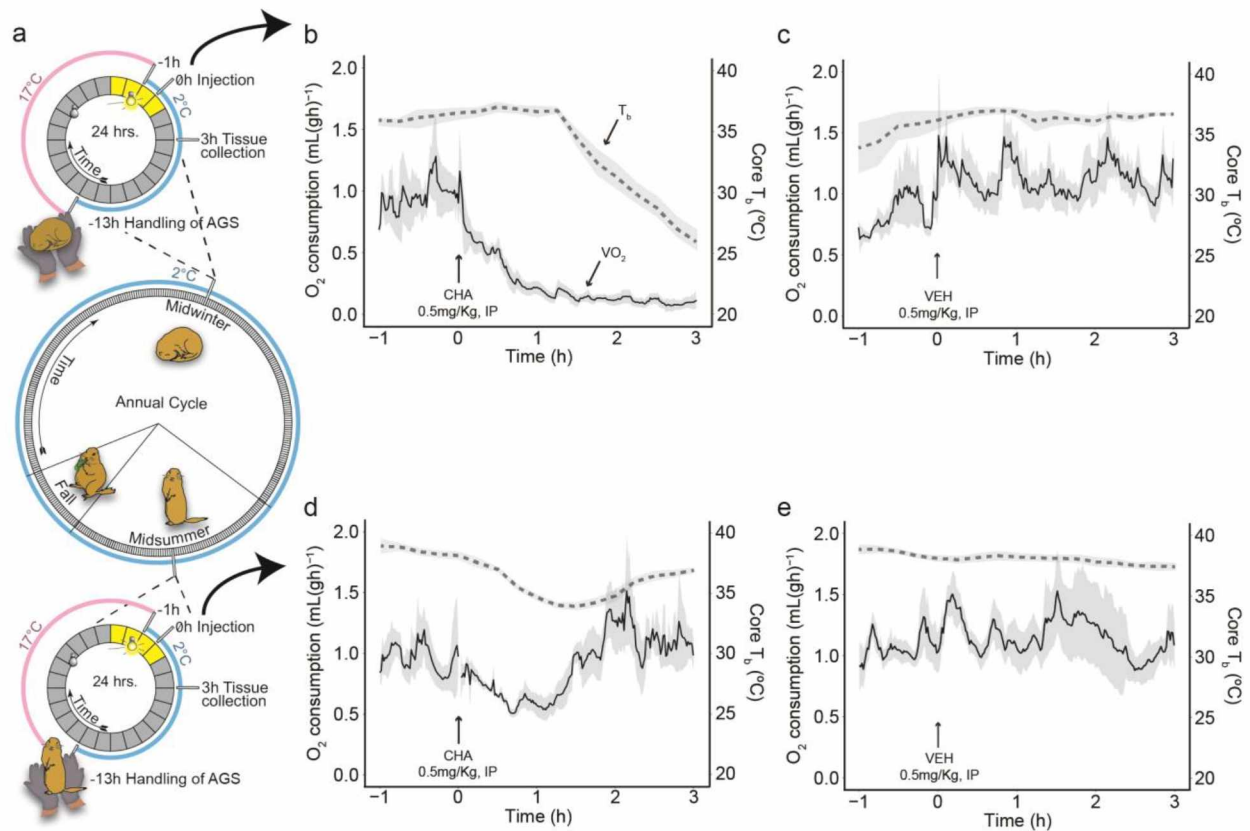


Figure 3.2: CHA promotes the onset of hibernation in a seasonally dependent manner.

(a) After capture, AGS were kept in constant environmental conditions (2°C, 4L:20D) year-round. The night before the experiment, both Summer and Winter AGS were handled and moved into a warm room (17°C, 4L:20D). An hour before injection we moved the AGS back to the environmental chamber (2°C, 4L:20D). Collected one hour of baseline measurements, then administered CHA or VEH at time 0, and we collected the tissue after three hours. (b) Winter AGS treated with CHA, decreased O₂ consumption followed by T_b leading to the onset of hibernation. (d) Summer AGS treated with CHA showed a transient and gradual decrease in O₂ consumption and T_b. (c and e) VEH produced no change in T_b or O₂ consumption in either Winter AGS or Summer AGS. Dotted line represents T_b, solid line represents O₂ consumption. Data are shown as mean ± SEM. SEM are represented as shaded area, number of animals per group n= 4 to 7. Arrow at 0h indicates injection time.

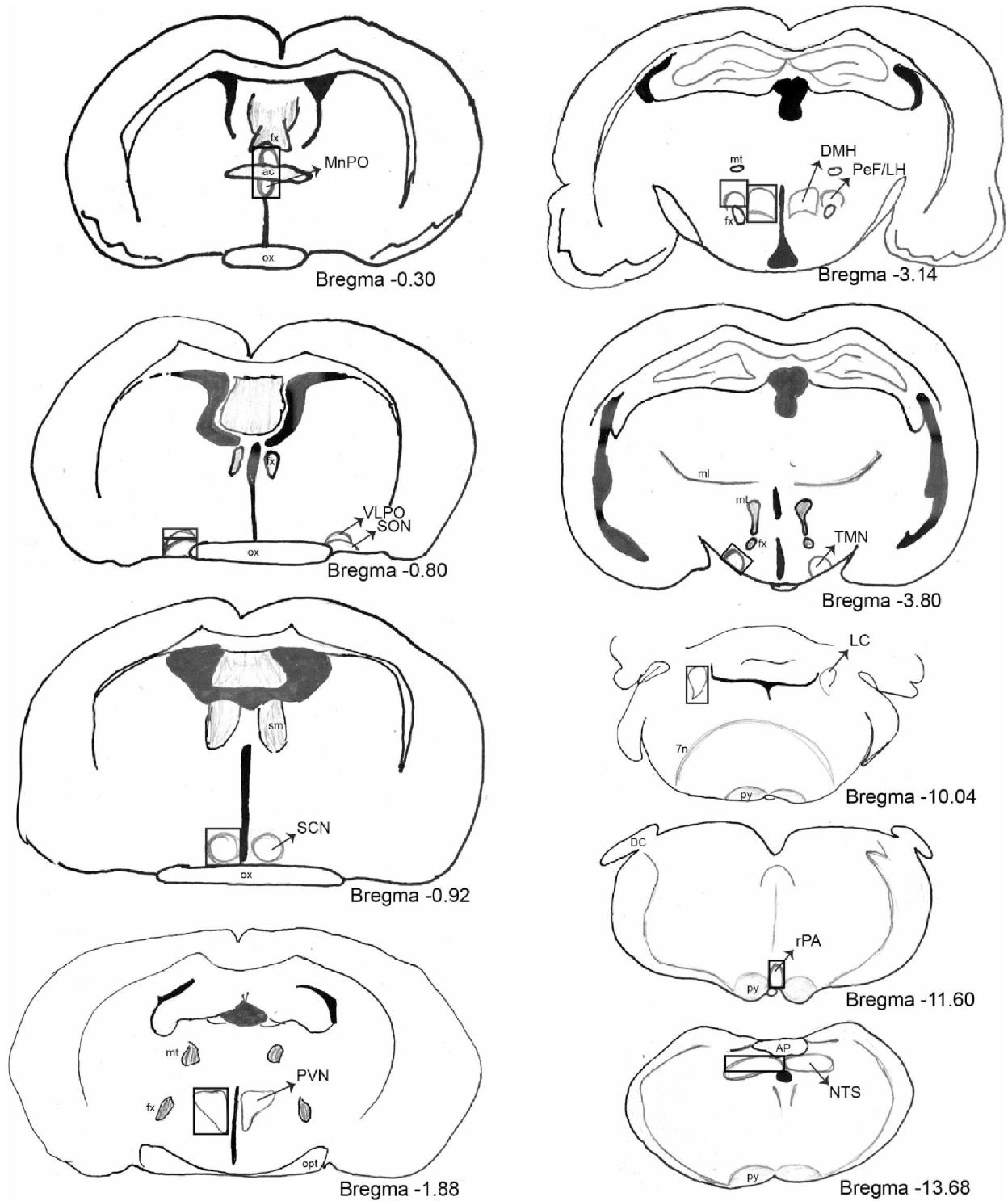


Figure 3.3: Caption on the following page.

Figure 3.3: Regions of interests investigated in this study.

The coronal plane and bregma are based on the Paxinos and Watson Rat Brain Atlas. For bilateral ROI, labels are positioned on the side opposite the box defining the ROI. See methods section for a detailed description of each ROI. MnPO: median preoptic nucleus, VLPO: ventrolateral preoptic nucleus, SON: supraoptic nucleus, SCN: suprachiasmatic nucleus, PVN: paraventricular nucleus of the hypothalamus, LH: lateral hypothalamus, PeF: perifornical nucleus, DMH: dorsal medial hypothalamus, TMN: tuberomammillary nucleus, LC: locus coeruleus, rPA: raphe pallidus, NTS: nucleus tractus solitarius, fx: fornix, ac: anterior commissure, ox: optic chiasm, sm: stria medullaris of the thalamus, opt: optic tract, mt: mammillary tract, ml: medial lemniscus, 7n: facial nerve, py: pyramidal tract, DC: dorsal cochlear nucleus, AP: area postrema.

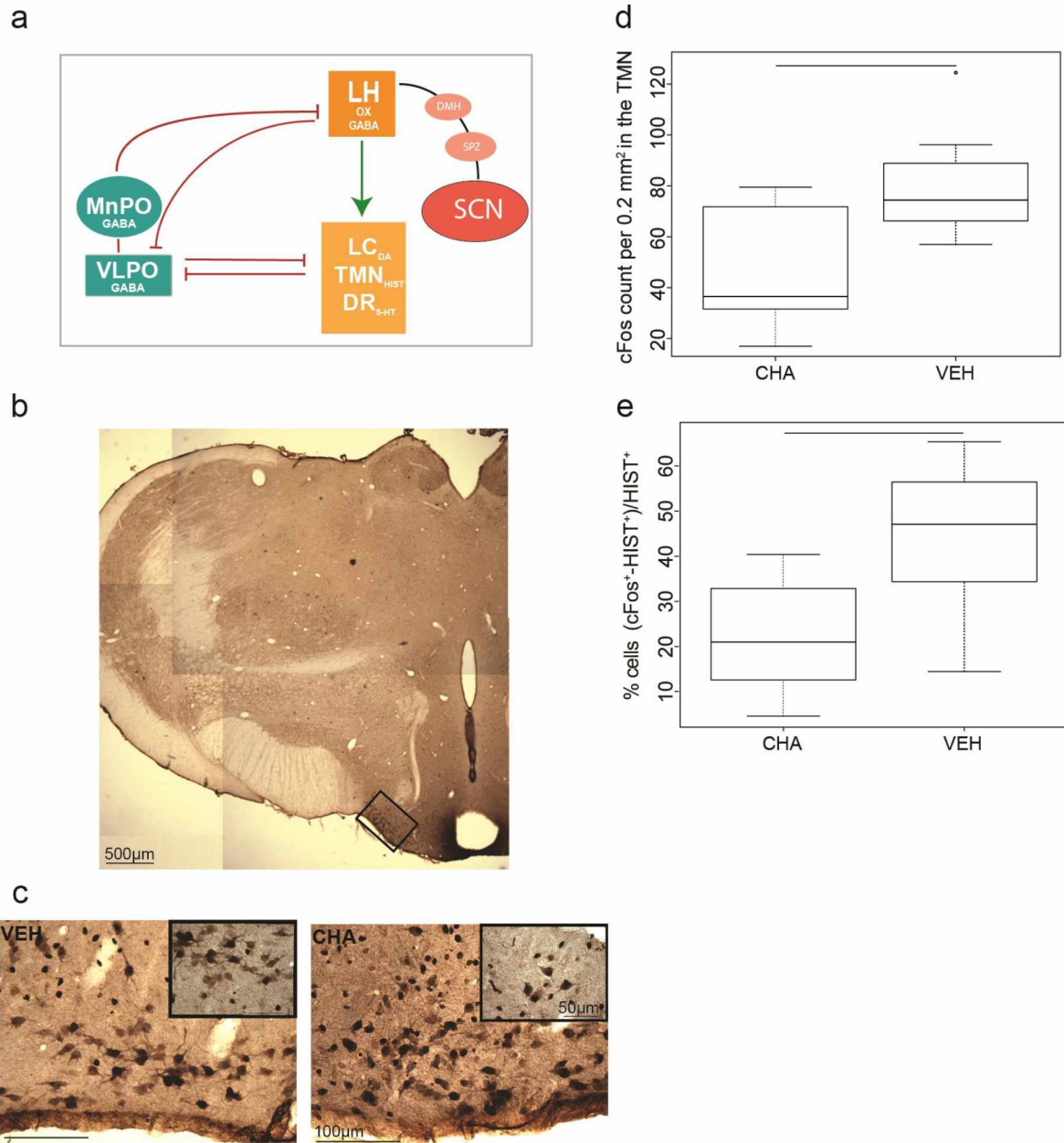


Figure 3.4: CHA reduces neuronal activity in the histaminergic neurons of the TMN.

The classical sleep-arousal pathways are illustrated in (a), green arrows represent excitatory connections, red arrows represent inhibitory connections, in addition the circadian regulation of sleep is illustrated by the black line from the SCN to the LH. (b) Representative photomicrograph of the TMN at low magnification (for better resolution, the image was constructed from images taken under 2X magnification). (c) Photomicrographs of double stained brain sections, histamine (HIST) neurons (brown) and cFos (black) in the TMN. The inserts in the TMN image show an area at higher magnification. (d) The TMN shows a decrease in cFos expression, in the CHA group compared to VEH group. (e) CHA

significantly inhibits histaminergic neurons compared to VEH, measured as the percent activation of HIST+cFos+/HIST+ in the TMN. Data are shown as mean \pm SEM, solid line represents $p < 0.05$, t test. Number of animals $n = 10$ to 11 per each treatment group. Cell count represents the mean of three slices per animal (d, e); symbols represent outliers (d). MnPO: median preoptic nucleus, VLPO: ventrolateral preoptic nucleus, LH: lateral hypothalamus, LC: locus coeruleus, TMN: tuberomammillary nucleus, DR: dorsal raphe nucleus, SCN: suprachiasmatic nucleus, DMH: dorsomedial hypothalamus, SPZ: subparaventricular zone, 5-HT: serotonin, DA: dopamine, OX: orexin, HIST: histamine.

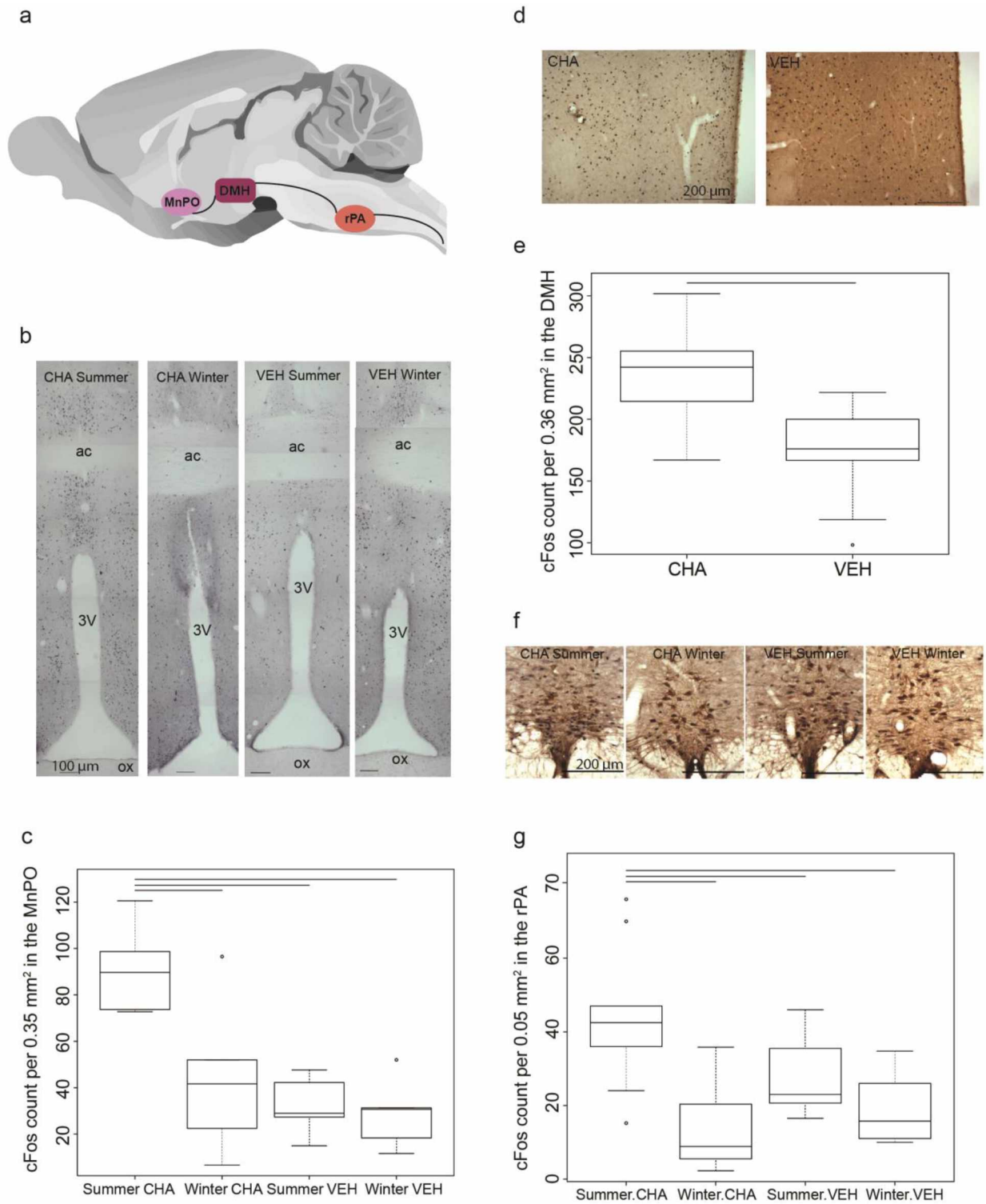


Figure 3.5: Caption on the following page.

Figure 3.5: Regions in the thermoregulatory pathway show differential activation in CHA groups compared to VEH.

(a) Schematic of the pathway known to regulate brown adipose tissue (BAT) thermogenesis showing the brain regions analyzed. (b) Representative images showing cFos expression in the MnPO (for better resolution the image was constructed from five images taken under 10X magnification). (c) The MnPO shows higher cFos expression after CHA in summer compared with Summer VEH, Winter CHA and Winter VEH. (d) Photomicrographs of cFos stained brain sections in the DMH. (e) DMH shows increased cFos expression in the CHA-treated group compared to the VEH-treated group independent of season. (f) Photomicrographs of cFos stained brain sections in the rPA. (g) The rPA shows higher cFos expression in Summer CHA compared with Summer VEH, Winter CHA and Winter VEH. Data shown as mean \pm SEM, number of animals per groups n=5 to 11. Cell count represents the mean of three slices per animal. Symbols represent outliers (c, g). Solid line indicates $p < 0.05$, Dunnett test (c, g), t test (e). MnPO: median preoptic nucleus, DMH: dorsomedial hypothalamus, rPA: raphe pallidus nucleus, 3V: third ventricle, ac: anterior commissure, ox: optic chiasm.

Table 3.1: Physiological parameters of Summer and Winter euthermic AGS.

	Summer AGS (Summer Phenotype)		Winter AGS (Winter Phenotype)	
Number of torpor bouts	0		>8	
Body Weight (g) all AGS	573 ±2	n=22	489 ±3*	n=18
Body Weight (g) Adult Female	628 ±3	n=6	n/a	n/a
Body Weight (g) Adult Male	594	n=1	665	n=1
Body Weight (g) Juvenile Female	547 ±4	n=8	421 ±2	n=8
Body Weight (g) Juvenile Male	553 ±4	n=7	515 ±4	n=9
Euthermic respiratory rate (breath/min)	139 ±8	n=22	91 ±8*	n=18
Euthermic Core T_b (T_b, °C) ^{a,b}	38.6 ±0.2	n=10	36.4 ±0.3*	n=9
Euthermic Subcutaneous T_b (T_{sc}, °C) ^a	37.4 ±0.3	n=10	33.7 ±0.6*	n=8
Euthermic Rectal T_b (T_r, °C)	37.0 ±0.2	n=11	35.7 ±0.3*	n=10

Data are shown as mean ±SEM, number of animals per each phenotype (n), * $p < 0.05$ t test. In the Juvenile AGS, we found a significant lower body weight in the Winter AGS compared to the Summer AGS ($F(1,27)=5.5$, $p < 0.05$, main effect of season, two way ANOVA with sex and season as variables) and no sexual differences. ^aData represent the mean of the average T_b in the hour before the injection. ^bWe excluded the animal re-entering torpor from the mean and statistical analysis.

Table 3.2: List of primary antibodies used to identify cFos and phenotypic markers, Research Resource Identifier (RRID).

Primary antibody	Dilution	Incubation	CAT#	Company	RRID
Mouse anti-cFos	1:20,000	48 hours, 4°C	SC271243	Santa Cruz Biotech, TX	AB_10610067
					Monoclonal; Immunogen: amino acids 120-155 within an internal region of c-Fos of human origin.
Rabbit anti-tyrosine hydroxylase (TH)	1:8,000	Overnight, 4°C	AB152	Millipore, CA	AB_390204
					Polyclonal; Immunogen: denatured tyrosine hydroxylase from rat pheochromocytoma.
Sheep anti-tryptophan hydroxylase (TPH)	1:2,000	Overnight, 4°C	AB1541	Millipore, CA	AB_90754
					Polyclonal; Immunogen: recombinant rabbit tryptophan hydroxylase.
Rabbit anti-orexin A	1:5,000	48 hours, 4°C	AB3704	Millipore, MA	AB_91545
					Polyclonal; Immunogen: synthetic peptide corresponding to the C-terminal portion of the bovine Orexin-A peptide.
Rabbit anti-histamine	1:1,000	Overnight, 4°C	22939	ImmunoStar, WI	AB_572245
					Polyclonal; Immunogen: Synthetic histamine coupled to succinylated keyhole limpet hemocyanin (KLH) with carbodiimide (CDI) linker.
Rabbit anti-pro thyrotropin releasing hormones (TRH)	1:10,000	Overnight, 4°C	N/A	Gift from Eva Redei, Northwestern University	N/A
					Polyclonal; Immunogen: amino acids 178-199 pro-TRH.
Rabbit anti-vasopressin (AVP)	1:20,000	Overnight, 4°C	AB1565	Millipore, MA	AB_90782 AB_11212336 AB_90772
					Polyclonal; Immunogen: Arginine vasopressin conjugated to thyroglobulin.

Table 3.3: Seasonal changes in cFos expression.

ROI	Number of cFos+ neurons				Percent change
	Summer		Winter		
Lateral hypothalamus (LH) (ROI= 0.4 mm ²)	88± 6	n=21	72± 7 [#]	n=18	18%
Supraoptic nucleus (SON) (ROI= 0.3 mm ²)	199± 14	n=10	244± 15 [*]	n=8	23%
Suprachiasmatic nucleus (SCN) (ROI= 0.09 mm ²)	196± 39	n=10	36± 7 [*]	n=9	82%
Raphe pallidus (rPA) (ROI= 0.05 mm²)	28± 3	n=11	19± 3 [*]	n=10	32%

The mean number of cFos+ neurons in three to four brain slices per each animal was used to calculate the mean ±SEM. n indicates the number of animals, *p<0.05, # p=0.06, t test. Percent change indicates the magnitude of the changes observed from Summer to Winter. The rPA data are not collapsed as the two way ANOVA showed a significant interactions between season and treatment; thus the rPA Summer and Winter data in the table includes only the Summer VEH and the Winter VEH groups.

Table 3.4: Treatment induced changes in neuronal activation, measured as cFos activation, in the paraventricular nucleus of the hypothalamus (PVN).

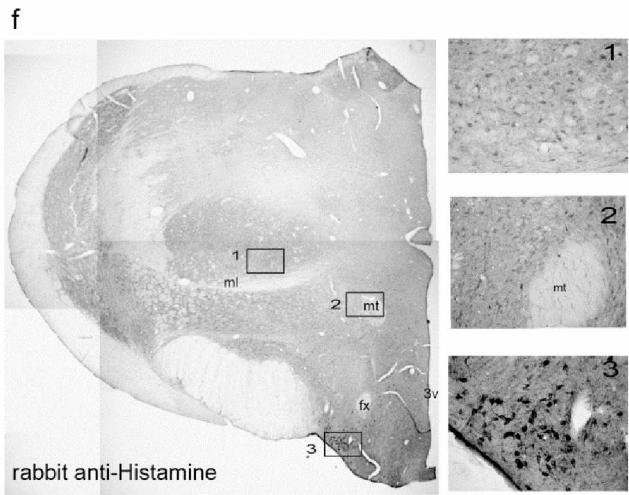
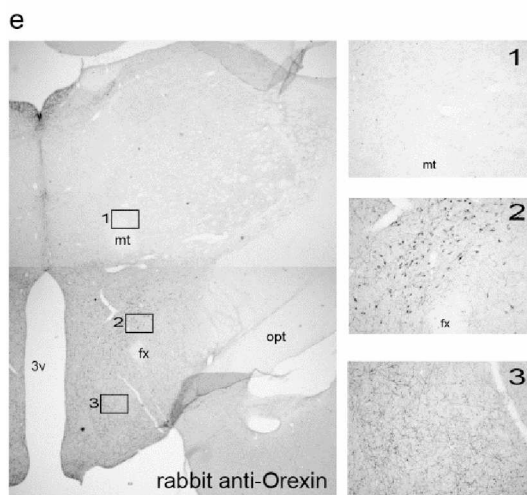
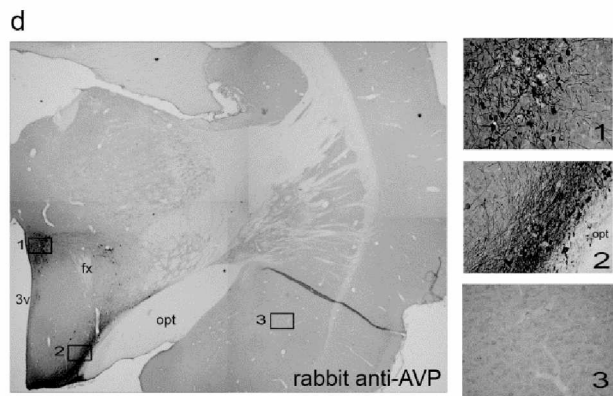
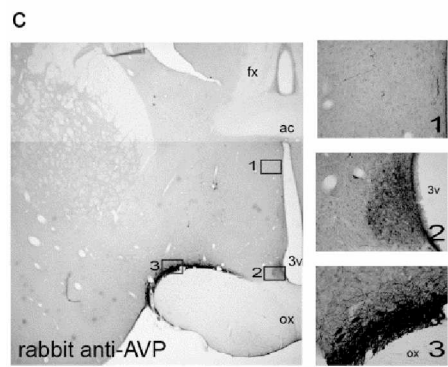
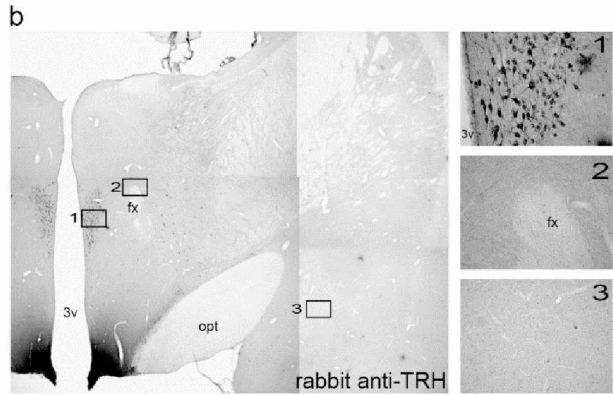
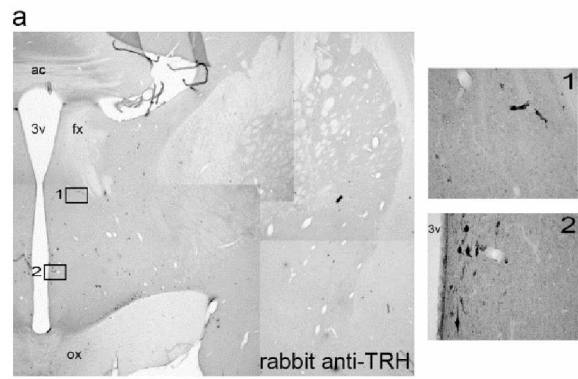
	CHA		VEH	
Number of cFos+ neurons (ROI=in 0.3 mm²)	445 ± 56	n=11	386 ± 54	n=9
Percent activation of TRH+ neurons (%)	79.4 ± 2.8	n=9	69.4 ± 3.1*	n=12
Percent activation of AVP+ neurons (%)	73.5 ± 3.1	n=10	54.2 ± 3.6*	n=10

Data are shown as mean ±SEM, number of animals per each treatment group (n). Cell count represents the mean of three to two brain slices per animal, *p<0.05 t test. The percentage of activated neurons was defined as the ratio between double stained neurons and the number of neurons positive for the phenotypic marker used.

Table 3.5: Treatment induced changes in neuronal activation, measured as cFos activation, in the nucleus tractus solitarius (NTS).

	CHA		VEH	
Number of cFos+ neurons (ROI=in 0.2 mm²)	70 ± 8	n=17	42 ± 3*	n=20
Percent activation of TH+ neurons (%)	58.3 ± 4.7	n=9	45.9 ± 3.4*	n=11

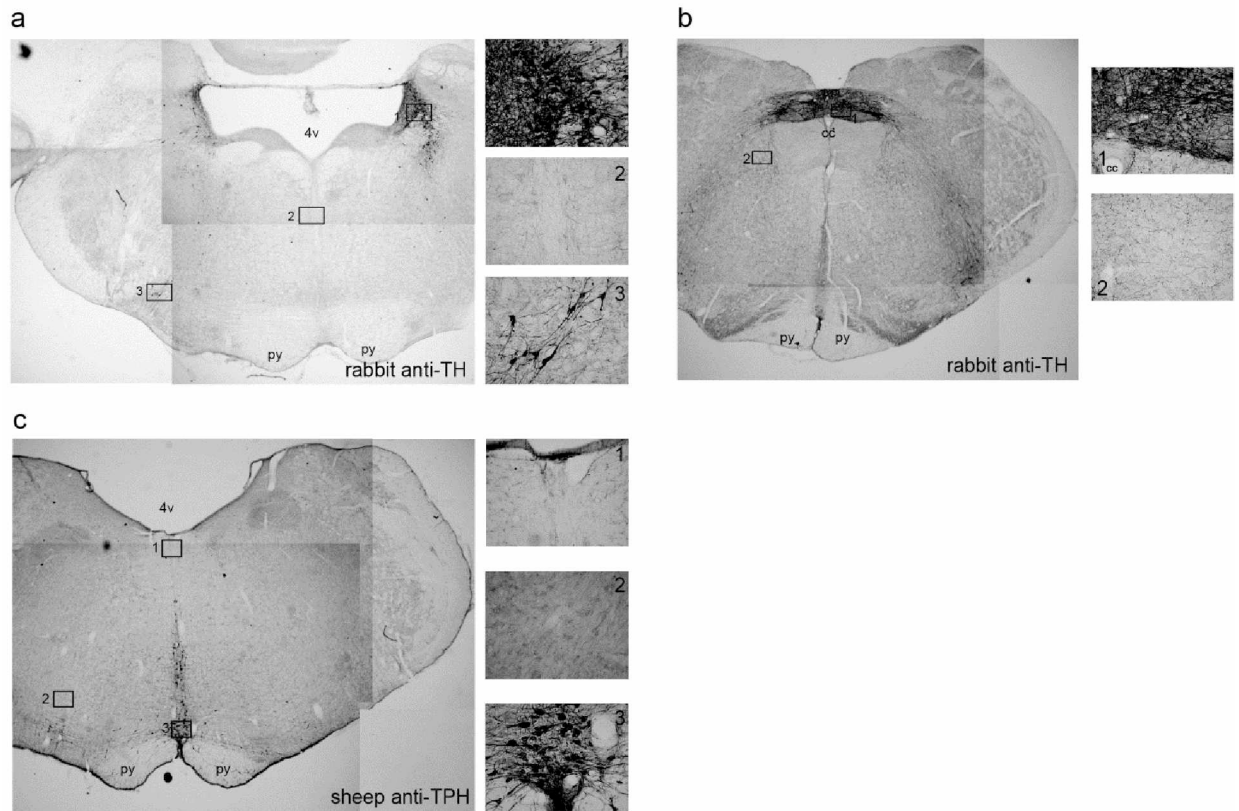
Data are shown as mean ±SEM, number of animals per treatment group (n), Cell count represents the mean of three slices per animal, *p<0.05 t test. The percent activation of TH+ neurons was calculated as the ratio between TH+cFos+ neurons and total TH+ neurons.



SI Figure 3.1: Caption on the following page.

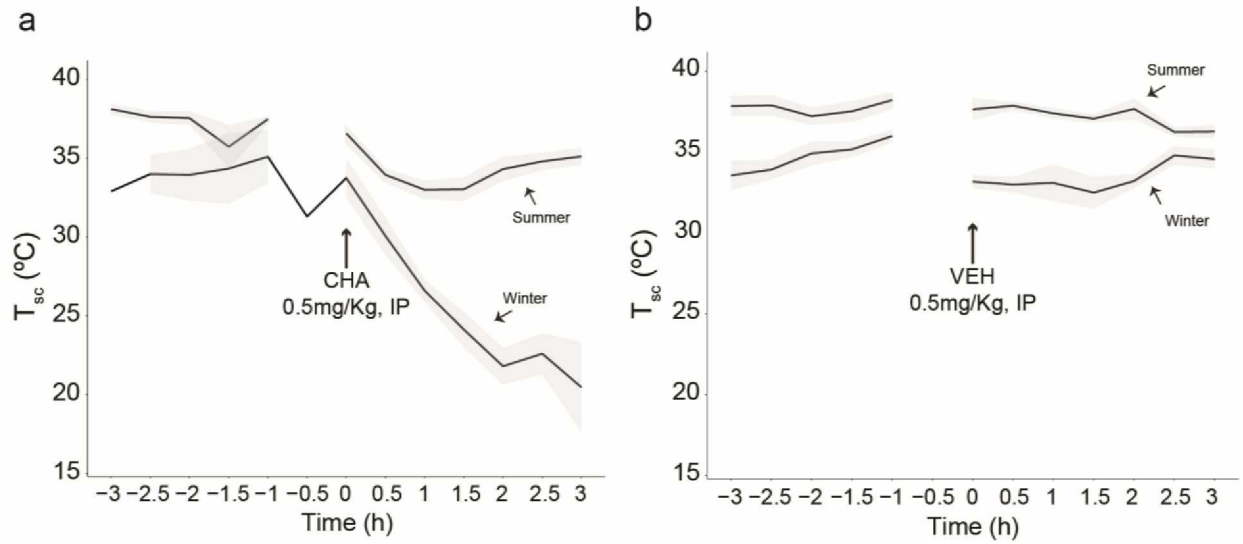
SI Figure 3.1: Characterization of the antibodies used in the hypothalamus.

Antibodies have been characterized in brain tissue from AGS, which were not part of the study. Antibody immunoreactivity is present in the brain regions expected to show positive immunoreactivity. An initial thyrotropin-releasing hormones (TRH)-ir is visible in the frontal hypothalamic region (a-2) and the number of TRH+ neurons increase moving towards to mid part of the hypothalamus (b-1); TRH-ir is specific for the area of interest as the lack of immunoreactivity is visible in other hypothalamic regions (a-1, b-2) and in the cortex (b-3). Arginine vasopressin (AVP)-ir is expected in the SON, SCN and in the PVN. AVP-ir is visible in the SON (c-3), but not in the SCN (c-2) and the frontal hypothalamic area (c-1), AVP-ir increases in the hypothalamus moving towards to mid part of the forebrain (d-1), AVP+ neurons are still present in the SON (d-2), but not in the cortex (d-3). Orexin-ir is present in the area above the fornix as expected (e-2), and orexin fibers not neurons are visible in the ventral area of the hypothalamus (e-3). Orexin-ir is absent in other hypothalamic areas (e-1). Histamine-ir is present in the region identified as the TMN (f-3). Histamine+ neurons are not detected in the other hypothalamic area (f-2, f-1)). For better resolution, each image was constructed from images taken under 2X magnification. SON: supraoptic nucleus, SCN: suprachiasmatic nucleus, PVN: paraventricular nucleus of the hypothalamus, TMN: tuberomammillary nucleus, 3v: third ventricle, fx: fornix, ac: anterior commissure, ox: optic chiasm, opt: optic tract, mt: mammillary tract, ml: medial lemniscus.



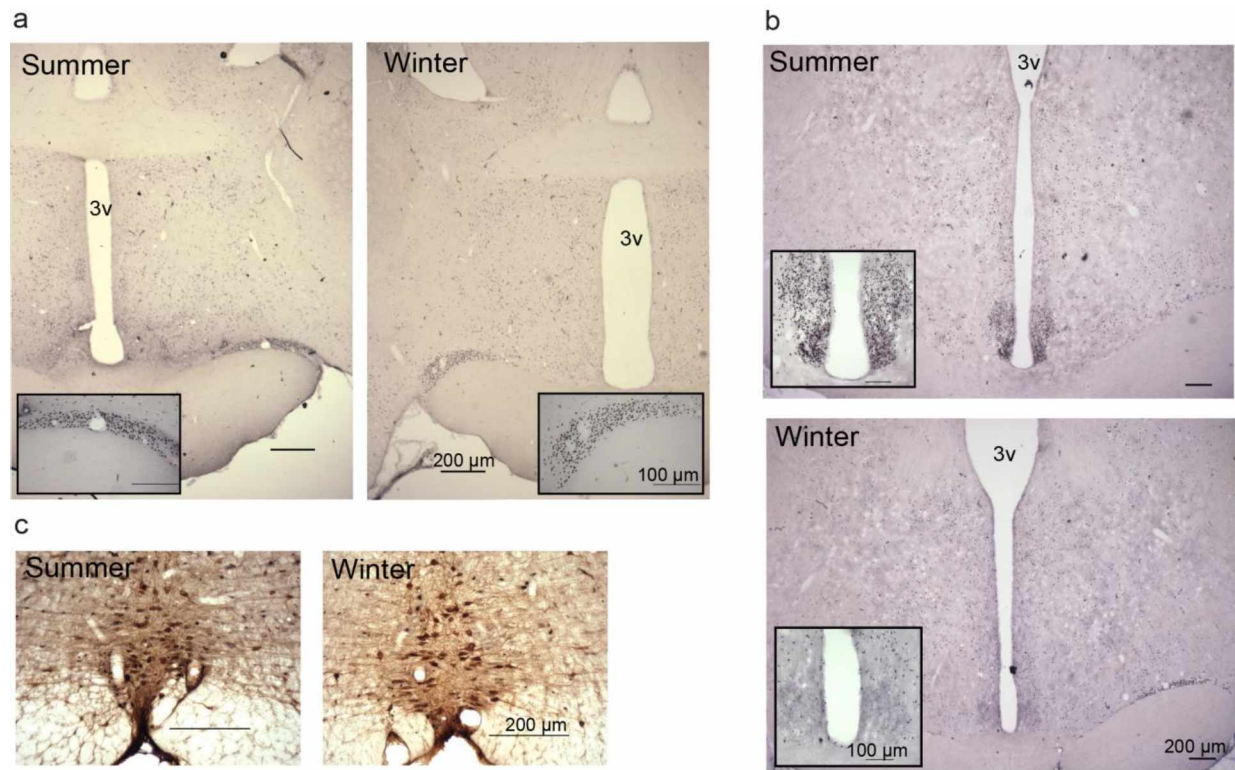
SI Figure 3.2: Characterization of the antibodies used in the brainstem.

Antibodies have been characterized in brain tissue from AGS, which were not part of the study. Antibody immunoreactivity is present in the brain regions expected to show positive immunoreactivity. Tyrosine hydroxylase (TH)-ir is visible in the LC (a-1), the noradrenaline cells A5 (a-3) and in the NTS (b-1) as expected, TH+ neurons are not detected in mid region of the slice (a-2, b-2). Thryptophan hydroxylase (TPH)-ir is detected in the raphe region as the rPA (c-3), but not in the mid region of the slice (c-1, c-2). For better resolution, each image was constructed from images taken under 2X magnification. LC: locus coeruleus, rPA: raphe pallidus, NTS: nucleus tractus solitarius, 4v: fourth ventricle, py: pyramidal tract, cc: central canal, AP: area postrema.



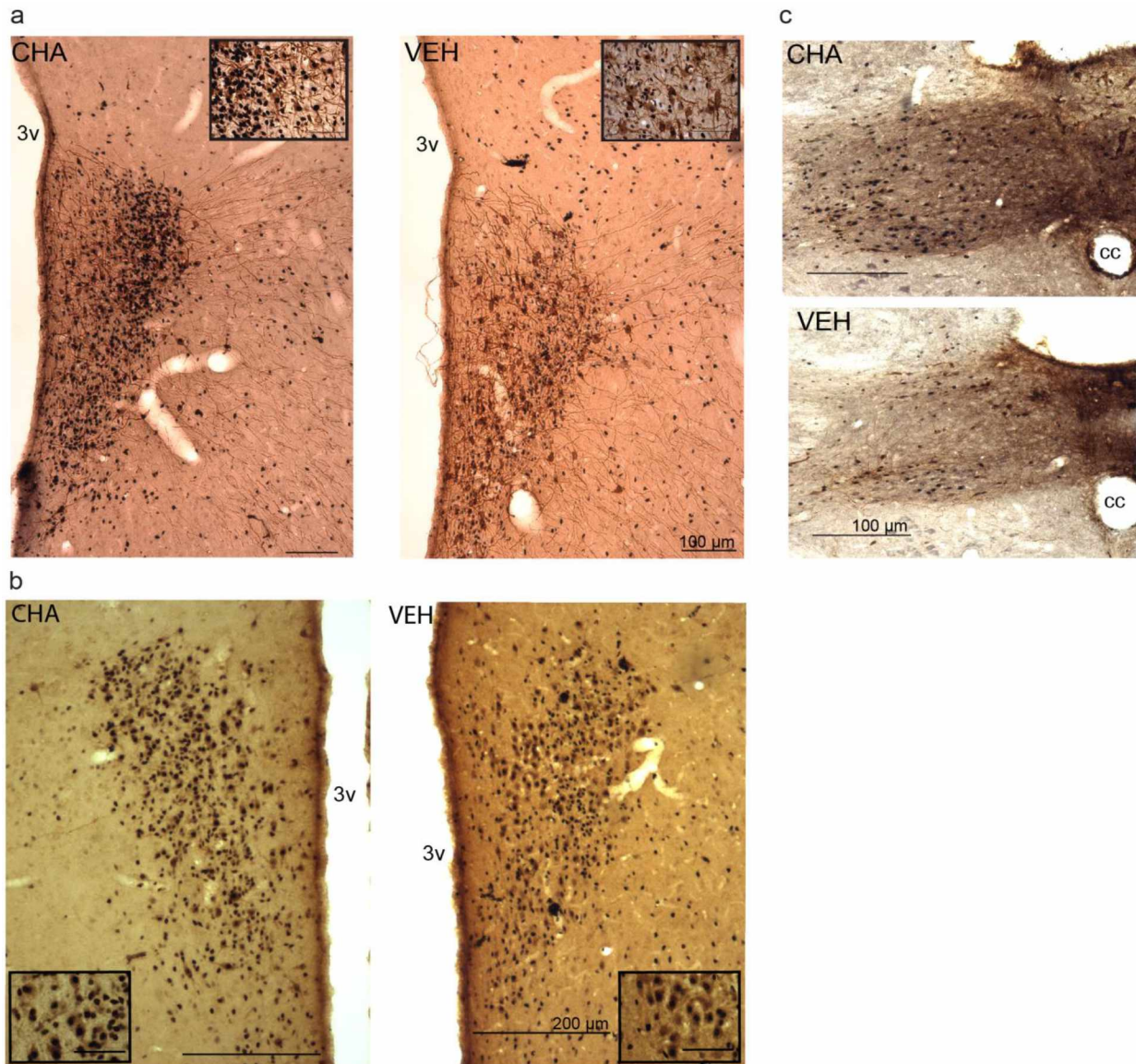
SI Figure 3.3: CHA induces a decrease in subcutaneous T_b (T_{sc}) that resembles the effect of CHA on core T_b .

In Winter AGS, CHA decreases T_{sc} leading to the onset of hibernation. On the contrary, in Summer AGS CHA has a transient effect on T_{sc} (a). Vehicle does not show changes in T_{sc} in both Winter and Summer animals. A greater vasoconstriction characterized the winter season, indicated by the lower T_{sc} in euthermic Winter AGS compared to euthermic Summer AGS, both phenotypes housed at 2°C and 4L:20D(b). Breaks in the lines represent missing data points in T_{sc} . Data are shown as mean \pm SEM, represented as shaded area. Where shaded area is missing only one data point is plotted. Number of animals per group $n=3$ to 6. Arrow at 0h indicates the time of injection.



SI Figure 3.4: Representative images showing the seasonal changes in cFos expression.

Photomicrographs show cFos expression in the SON (a). The inserts show an area of higher magnification (a). Photomicrographs show cFos expression in the SCN (b). The inserts show an area at higher magnification (b). Photomicrographs show cFos expression in the rPA (c). SON: supraoptic nucleus, SCN: suprachiasmatic nucleus, rPA: raphe pallidus, 3v: third ventricle.



SI Figure 3.5: Representative images showing changes in neuronal activation in the CHA and VEH groups. Vasopressinergic (AVP) neurons (brown) and cFos (black) are stained in the paraventricular nucleus of the hypothalamus (a). The inserts show an area of higher magnification scale bar 50μm (a). Thyrotropin-releasing hormone (TRH) (brown) and cFos (black) are stained in the paraventricular nucleus of the hypothalamus (b). The inserts show an area of higher magnification area, scale bar 50μm (b). Tyrosine hydroxylase neurons (TH) (brown) and cFos (black) are stained in the nucleus tractus solitarius (c). 3v: third ventricle, cc: central canal.

SI Table 3.1: Brain regions in the AGS that do not show any differences between groups.

	Summer CHA	Summer VEH	Winter CHA	Winter VEH
Number of cFos+ neurons in the ventrolateral preoptic nucleus (VLPO) (ROI= 0.3mm²)	45 ± 6 n=6	38 ± 3 n=4	42 ± 7 n=4	40 ± 9 n=4
Percent activation of orexin+ neurons in the LH (%)	25 ± 5 n=5	26 ± 4 n=6	43 ± 11 n=5	31 ± 8 n=5
Percent activation of TPH+ neurons in the rPA (%)	24.3 ± 7.0 n=3	18.9 ± 3.1 n=7	12.8 ± 3.9 n=5	17.7 ± 4.5 n=5
Percent activation of TH+ neurons in the LC (%)	19.0 ± 4.0 n=5	16.4 ± 4.6 n=7	24.6 ± 10.8 n=4	20.6 ± 5.1 n=5

Data are shown as mean ± SEM, animal number per group (n), represents the mean of three slices per animal. The percentage of activated neurons was defined as the ratio between double stained neurons and the number of neurons positive for the phenotypic marker used.

SI Table 3.2: List of primary antibody not showing immunoreactivity in AGS brain tissue.

Primary antibody	Cat #	Company	RRID
Rabbit anti-HDC, polyclonal	Ab37291	Abcam, Cambridge, MA	AB_732789
Rabbit anti-cFos Ab-2, polyclonal	PC38	Calbiochem, Millipore, Temecula, CA	AB_2106755
Rabbit anti-galanin, polyclonal	Ab5909	Millipore, Temecula, CA	AB_2108517
Rabbit anti-galanin H-80, polyclonal	Sc25446	Santa Cruz Biotechnology, Dallas TX	AB_2108391
Mouse anti-galanin H-11, polyclonal	Sc166431	Santa Cruz Biotechnology, Dallas TX	AB_2232144
Rabbit anti-vGAT, polyclonal	Ab5062P	Millipore, Temecula, CA	AB_2301998
Rabbit anti-GAD67, polyclonal	Ab97739	Abcam, Cambridge, MA	AB_10681171
Mouse anti-GAD67, monoclonal	MAB5406 B	Millipore, Temecula, CA	AB_2278725
Mouse anti-GAD67, monoclonal	MAB5406 (-ir in Cortex only)	Millipore, Temecula, CA	AB_2278725

3.8 References

- Al-Noori, S., Sanders, N.M., Taborsky, G.J., Wilkinson, C.W., Zavosh, A., West, C., Sanders, C.M., and Figlewicz, D.P. (2008). Recurrent hypoglycemia alters hypothalamic expression of the regulatory proteins FosB and synaptophysin. *Am. J. Physiol. Regul. Integr. Comp. Physiol.* *295*, R1446-1454.
- Althammer, F., and Grinevich, V. (2018). Diversity of oxytocin neurones: Beyond magno- and parvocellular cell types? *J. Neuroendocrinol.* *30*, e12549.
- Angulo, J.A., Ledoux, M., and McEwen, B.S. (1991). Genomic Effects of Cold and Isolation Stress on Magnocellular Vasopressin mRNA-Containing Cells in the Hypothalamus of the Rat. *J. Neurochem.* *56*, 2033–2038.
- Arrich, J., Holzer, M., Havel, C., Müllner, M., and Herkner, H. (2016). Hypothermia for neuroprotection in adults after cardiopulmonary resuscitation. *Cochrane Database Syst. Rev.*
- Barcroft, H., and Edholm, O.G. (1946). Temperature and blood flow in the human forearm. *J. Physiol.* *104*, 366–376.
- Barnes, B.M. (1989). Freeze avoidance in a mammal: body temperatures below 0 degree C in an Arctic hibernator. *Science* *244*, 1593–1595.
- Bitting, L., Sutin, E.L., Watson, F.L., Leard, L.E., O'Hara, B.F., Craig Heller, H., and Kilduff, T.S. (1994). C-fos mRNA increases in the ground squirrel suprachiasmatic nucleus during arousal from hibernation. *Neurosci. Lett.* *165*, 117–121.
- Bjorness, T.E., and Greene, R.W. (2009). Adenosine and Sleep. *Curr. Neuropharmacol.* *7*, 238–245.
- Bratincsak, A., McMullen, D., Miyake, S., Toth, Z.E., Hallenbeck, J.M., and Palkovits, M. (2007). Spatial and Temporal Activation of Brain Regions in Hibernation: c-fos Expression during the Hibernation Bout in Thirteen-Lined Ground Squirrel. *J. Comp. Neurol.* *505*, 443–458.
- Buck, C.L., and Barnes, B.M. (2000). Effects of ambient temperature on metabolic rate, respiratory quotient, and torpor in an arctic hibernator. *Am. J. Physiol.-Regul. Integr. Comp. Physiol.* *279*, R255–R262.
- Cao, W.-H., Madden, C.J., and Morrison, S.F. (2010). Inhibition of brown adipose tissue thermogenesis by neurons in the ventrolateral medulla and in the nucleus tractus solitarius. *Am. J. Physiol.-Regul. Integr. Comp. Physiol.* *299*, R277–R290.
- Cerri, M., Mastrotto, M., Tupone, D., Martelli, D., Luppi, M., Perez, E., Zamboni, G., and Amici, R. (2013). The Inhibition of Neurons in the Central Nervous Pathways for Thermoregulatory Cold Defense Induces a Suspended Animation State in the Rat. *J. Neurosci.* *33*, 2984–2993.
- Chaudhuri, A. (1997). Neural activity mapping with inducible transcription factors. *Neuroreport* *8*, iii–vii.
- Cirelli, C., and Tononi, G. (2000). On the functional significance of c-fos induction during the sleep-waking cycle. *Sleep* *23*, 453–469.

Das, M., Vihlen, C.S., and Legradi, G. (2007). Hypothalamic and Brainstem Sources of Pituitary Adenylate Cyclase-Activating Polypeptide Nerve Fibers Innervating the Hypothalamic Paraventricular Nucleus in the Rat. *J. Comp. Neurol.* *500*, 761–776.

Daubert, D.L., McCowan, M., Erdos, B., and Scheuer, D.A. (2012). Nucleus of the solitary tract catecholaminergic neurons modulate the cardiovascular response to psychological stress in rats. *J. Physiol.* *590*, 4881–4895.

Dentico, D., Amici, R., Baracchi, F., Cerri, M., Sindaco, E.D., Luppi, M., Martelli, D., Perez, E., and Zamboni, G. (2009). c-Fos expression in preoptic nuclei as a marker of sleep rebound in the rat. *Eur. J. Neurosci.* *30*, 651–661.

Drew, K.L., Frare, C., and Rice, S.A. (2017). Neural signaling metabolites may modulate energy use in hibernation. *Neurochem. Res.* *42*, 141–150.

Ellender, T.J., Huerta-Ocampo, I., Deisseroth, K., Capogna, M., and Bolam, J.P. (2011). Differential Modulation of Excitatory and Inhibitory Striatal Synaptic Transmission by Histamine. *J. Neurosci.* *31*, 15340–15351.

Faul, F., Erdfelder, E., Lang, A.-G., and Buchner, A. (2007). G*Power 3: A flexible statistical power analysis program for the social, behavioral, and biomedical sciences. *Behav. Res. Methods* *39*, 175–191.

Fekete, C., Mihály, E., Luo, L.G., Kelly, J., Clausen, J.T., Mao, Q., Rand, W.M., Moss, L.G., Kuhar, M., Emerson, C.H., et al. (2000). Association of cocaine- and amphetamine-regulated transcript-immunoreactive elements with thyrotropin-releasing hormone-synthesizing neurons in the hypothalamic paraventricular nucleus and its role in the regulation of the hypothalamic-pituitary-thyroid axis during fasting. *J. Neurosci. Off. J. Soc. Neurosci.* *20*, 9224–9234.

Frare, C., Jenkins, M., Soldin, S., and Drew, K. (2018). The raphe pallidus and the hypothalamic-pituitary-thyroid axis gate seasonal changes in thermoregulation in the hibernating Arctic Ground Squirrel (*Urociltellus parryii*). *Front. Physiol.* *9*.

García-Pérez, D., Laorden, M.L., Milanés, M.V., and Núñez, C. (2012). Glucocorticoids Regulation of FosB/ Δ FosB Expression Induced by Chronic Opiate Exposure in the Brain Stress System. *PLOS ONE* *7*, e50264.

Gong, H., Szymusiak, R., King, J., Steininger, T., and McGinty, D. (2000). Sleep-related c-Fos protein expression in the preoptic hypothalamus: effects of ambient warming. *Am. J. Physiol.-Regul. Integr. Comp. Physiol.* *279*, R2079–R2088.

Gong, H., McGinty, D., Guzman-Marin, R., Chew, K.-T., Stewart, D., and Szymusiak, R. (2004). Activation of c-fos in GABAergic neurones in the preoptic area during sleep and in response to sleep deprivation. *J. Physiol.* *556*, 935–946.

Groves, A., Kihara, Y., Jonnalagadda, D., Rivera, R., Kennedy, G., Mayford, M., and Chun, J. (2018). A Functionally Defined In Vivo Astrocyte Population Identified by c-Fos Activation in a Mouse Model of Multiple Sclerosis Modulated by S1P Signaling: Immediate-Early Astrocytes (ieAstrocytes). *ENeuro* *5*, ENEURO.0239-18.2018.

- Hale, M.W., Dady, K.F., Evans, A.K., and Lowry, C.A. (2011). Evidence for in vivo thermosensitivity of serotonergic neurons in the rat dorsal raphe nucleus and raphe pallidus nucleus implicated in thermoregulatory cooling. *Exp. Neurol.* 227, 264–278.
- Harding, E.C., Yu, X., Miao, A., Andrews, N., Ma, Y., Ye, Z., Lignos, L., Miracca, G., Ba, W., Yustos, R., et al. (2018). A Neuronal Hub Binding Sleep Initiation and Body Cooling in Response to a Warm External Stimulus. *Curr. Biol.* 28, 2263–2273.e4.
- Hermes, M.L.H.J., Kalsbeek, A., Kirsch, R., Buijs, R.M., and Pe'vet, P. (1993). Induction of arousal in hibernating European hamsters (*Cricetus cricetus* L.) by vasopressin infusion in the lateral septum. *Brain Res.* 631, 313–316.
- Herwig, A., Ivanova, E.A., Lydon, H., Barrett, P., Steinlechner, S., and Loudon, A.S. (2007). Histamine H3 receptor and orexin A expression during daily torpor in the Djungarian hamster (*Phodopus sungorus*). *J. Neuroendocrinol.* 19, 1001–1007.
- Hisanaga, K., Sagar, S.M., Hicks, K.J., Swanson, R.A., and Sharp, F.R. (1990). c-fos proto-oncogene expression in astrocytes associated with differentiation or proliferation but not depolarization. *Mol. Brain Res.* 8, 69–75.
- Ikeno, T., Williams, C.T., Buck, C.L., Barnes, B.M., and Yan, L. (2017). Clock Gene Expression in the Suprachiasmatic Nucleus of Hibernating Arctic Ground Squirrels. *J. Biol. Rhythms* 32, 246–256.
- Iliff, B.W., and Swoap, S.J. (2012). Central adenosine receptor signaling is necessary for daily torpor in mice. *Am. J. Physiol.-Regul. Integr. Comp. Physiol.* 303, R477–R484.
- Jameson, E.W. (1964). Patterns of Hibernation of Captive *Citellus lateralis* and *Eutamias speciosus*. *J. Mammal.* 45, 455–460.
- Jasnic, N., Dakic, T., Bataveljic, D., Vujovic, P., Lakic, I., Jevdjovic, T., Djurasevic, S., and Djordjevic, J. (2015). Distinct vasopressin content in the hypothalamic supraoptic and paraventricular nucleus of rats exposed to low and high ambient temperature. *J. Therm. Biol.* 52, 1–7.
- Jinka, T.R., Tøien, Ø., and Drew, K.L. (2011). Season Primes the Brain in an Arctic Hibernator to Facilitate Entrance into Torpor Mediated by Adenosine A1 Receptors. *J. Neurosci.* 31, 10752–10758.
- Karoon, P., Knight, G., and Burnstock, G. (1998). Enhanced vasoconstrictor responses in renal and femoral arteries of the golden hamster during hibernation. *J. Physiol.* 512, 927–938.
- Khanday, M.A., Somarajan, B.I., Mehta, R., and Mallick, B.N. (2016). Noradrenaline from Locus Coeruleus Neurons Acts on Pedunculo-Pontine Neurons to Prevent REM Sleep and Induces Its Loss-Associated Effects in Rats. *ENeuro* 3.
- Kilduff, T.S., Radeke, C.M., Randall, T.L., Sharp, F.R., and Heller, H.C. (1989). Suprachiasmatic nucleus: phase-dependent activation during the hibernation cycle. *Am. J. Physiol.-Regul. Integr. Comp. Physiol.* 257, R605–R612.

- Küchler, S., Perwitz, N., Schick, R.R., Klein, J., and Westphal, S. (2010). Arginine–vasopressin directly promotes a thermogenic and pro-inflammatory adipokine expression profile in brown adipocytes. *Regul. Pept.* *164*, 126–132.
- Lambert, E.A., Straznicky, N.E., and Lambert, G.W. (2013). A sympathetic view of human obesity. *Clin. Auton. Res.* *23*, 9–14.
- Larkin, J.E., Yellon, S.M., and Zucker, I. (2003). Melatonin Production Accompanies Arousal from Daily Torpor in Siberian Hamsters. *Physiol. Biochem. Zool.* *76*, 577–585.
- Laughlin, B.W., Bailey, I.R., Rice, S.A., Barati, Z., Bogren, L.K., and Drew, K.L. (2018). Precise Control of Target Temperature Using N6-Cyclohexyladenosine and Real-Time Control of Surface Temperature. *Ther. Hypothermia Temp. Manag.* *8*, 108–116.
- Li, Y.-W., and Dampney, R.A.L. (1994). Expression of fos-like protein in brain following sustained hypertension and hypotension in conscious rabbits. *Neuroscience* *61*, 613–634.
- Lyman, C.P., and O'Brien, R.C. (1961). Circulatory changes in the 13-lined ground squirrel during the hibernating cycle. *Tech. Rep. TR Arct. Aeromed. Lab. US* *60*, 1–18.
- Lyman, C.P., and O'Brien, R.C. (1963). Autonomic control of circulation during the hibernating cycle in ground squirrels. *J. Physiol.* *168*, 477–499.
- McKinley, M.J., Yao, S.T., Uschakov, A., McAllen, R.M., Rundgren, M., and Martelli, D. (2015). The median preoptic nucleus: front and centre for the regulation of body fluid, sodium, temperature, sleep and cardiovascular homeostasis. *Acta Physiol.* *214*, 8–32.
- Mitchell, N., Catenacci, V., Wyatt, H.R., and Hill, J.O. (2011). OBESITY: OVERVIEW OF AN EPIDEMIC. *Psychiatr. Clin. North Am.* *34*, 717–732.
- Morrison, S.F., and Madden, C.J. (2014). Central Nervous System Regulation of Brown Adipose Tissue. *Compr. Physiol.* *4*, 1677–1713.
- Nakamura, K., and Morrison, S.F. (2008). Preoptic mechanism for cold-defensive responses to skin cooling. *J. Physiol.* *586*, 2611–2620.
- Nakamura, K., Matsumura, K., Hübschle, T., Nakamura, Y., Hioki, H., Fujiyama, F., Boldogkői, Z., König, M., Thiel, H.-J., Gerstberger, R., et al. (2004). Identification of Sympathetic Premotor Neurons in Medullary Raphe Regions Mediating Fever and Other Thermoregulatory Functions. *J. Neurosci.* *24*, 5370–5380.
- Nambu, T., Sakurai, T., Mizukami, K., Hosoya, Y., Yanagisawa, M., and Goto, K. (1999). Distribution of orexin neurons in the adult rat brain. *Brain Res.* *827*, 243–260.
- Nosedá, R., Kainz, V., Borsook, D., and Burstein, R. (2014). Neurochemical Pathways That Converge on Thalamic Trigeminovascular Neurons: Potential Substrate for Modulation of Migraine by Sleep, Food Intake, Stress and Anxiety. *PLoS ONE* *9*.

- Ohbuchi, T., Haam, J., and Tasker, J.G. (2015). Regulation of Neuronal Activity in Hypothalamic Vasopressin Neurons. *Interdiscip. Inf. Sci.* *21*, 225–234.
- Oishi, Y., Huang, Z.-L., Fredholm, B.B., Urade, Y., and Hayaishi, O. (2008). Adenosine in the tuberomammillary nucleus inhibits the histaminergic system via A1 receptors and promotes non-rapid eye movement sleep. *Proc. Natl. Acad. Sci.* *105*, 19992–19997.
- Oliveira, L.M., Moreira, T.S., and Takakura, A.C. (2018). Raphe Pallidus is Not Important to Central Chemoreception in a Rat Model of Parkinson's Disease. *Neuroscience* *369*, 350–362.
- Otero-García, M., Agustín-Pavón, C., Lanuza, E., and Martínez-García, F. (2016). Distribution of oxytocin and co-localization with arginine vasopressin in the brain of mice. *Brain Struct. Funct.* *221*, 3445–3473.
- Panula, P., Karlstedt, K., Sallmen, T., Peitsaro, N., Kaslin, J., Michelsen, K.A., Anichtchik, O., Kukko-Lukjanov, T., and Lintunen, M. (2000). The histaminergic system in the brain: structural characteristics and changes in hibernation. *J. Chem. Neuroanat.* *18*, 65–74.
- Parker, L.M., Le, S., Wearne, T.A., Hardwick, K., Kumar, N.N., Robinson, K.J., McMullan, S., and Goodchild, A.K. (2017). Neurochemistry of neurons in the ventrolateral medulla activated by hypotension: Are the same neurons activated by glucoprivation? *J. Comp. Neurol.* *525*, 2249–2264.
- Parks, G.S., Warriar, D.R., Dittrich, L., Schwartz, M.D., Palmerston, J.B., Neylan, T.C., Morairty, S.R., and Kilduff, T.S. (2016). The Dual Hypocretin Receptor Antagonist Almorexant is Permissive for Activation of Wake-Promoting Systems. *Neuropsychopharmacology* *41*, 1144–1155.
- Paxinos, G., and Watson, C. (1998). *The Rat Brain: In Stereotaxic Coordinates* (Academic Press).
- Pickel, V.M., Chan, J., Linden, J., and Rosin, D.L. (2006). Subcellular distributions of adenosine A1 and A2A receptors in the rat dorsomedial nucleus of the solitary tract at the level of the area postrema. *Synapse* *60*, 496–509.
- Richter, M.M., Williams, C.T., Lee, T.N., Tøien, Ø., Florant, G.L., Barnes, B.M., and Buck, C.L. (2015). Thermogenic Capacity at Subzero Temperatures: How Low Can a Hibernator Go? *Physiol. Biochem. Zool.* *88*, 81–89.
- Ruby, N.F. (2003). Hibernation: When Good Clocks Go Cold. *J. Biol. Rhythms* *18*, 275–286.
- Sallmen, T., Beckman, A.L., Stanton, T.L., Eriksson, K.S., Tarhanen, J., Tuomisto, L., and Panula, P. (1999). Major Changes in the Brain Histamine System of the Ground Squirrel *Citellus lateralis* during Hibernation. *J. Neurosci.* *19*, 1824–1835.
- Sallmen, T., Lozada, A.F., Anichtchik, O.V., Beckman, A.L., and Panula, P. (2003a). Increased brain histamine H3 receptor expression during hibernation in golden-mantled ground squirrels. *BMC Neurosci.* *4*, 24.
- Sallmen, T., Lozada, A.F., Beckman, A.L., and Panula, P. (2003b). Intrahippocampal histamine delays arousal from hibernation. *Brain Res.* *966*, 317–320.

- Saper, C.B., and Fuller, P.M. (2017). Wake-sleep circuitry: an overview. *Curr. Opin. Neurobiol.* *44*, 186–192.
- Schoeller, D.A. (2001). The importance of clinical research: the role of thermogenesis in human obesity. *Am. J. Clin. Nutr.* *73*, 511–516.
- Schwartz, J.R., and Roth, T. (2008). Neurophysiology of Sleep and Wakefulness: Basic Science and Clinical Implications. *Curr. Neuropharmacol.* *6*, 367–378.
- Schwartz, C., Ballinger, M.A., and Andrews, M.T. (2015). Melatonin receptor signaling contributes to neuroprotection upon arousal from torpor in thirteen-lined ground squirrels. *Am. J. Physiol. Regul. Integr. Comp. Physiol.* *309*, R1292-1300.
- Sheriff, M.J., Williams, C.T., Kenagy, G.J., Buck, C.L., and Barnes, B.M. (2012). Thermoregulatory changes anticipate hibernation onset by 45 days: data from free-living arctic ground squirrels. *J. Comp. Physiol. B* *182*, 841–847.
- Song, S.S., and Lyden, P.D. (2012). Overview of Therapeutic Hypothermia. *Curr. Treat. Options Neurol.* *14*, 541–548.
- Stanton, T.L., Caine, S.B., and Winokur, A. (1992). Seasonal and state-dependent changes in brain TRH receptors in hibernating ground squirrels. *Brain Res. Bull.* *28*, 877–886.
- Swoap, S.J., and Gutilla, M.J. (2009). Cardiovascular changes during daily torpor in the laboratory mouse. *Am. J. Physiol.-Regul. Integr. Comp. Physiol.* *297*, R769–R774.
- Szymusiak, R. (2018). Body temperature and sleep. *Handb. Clin. Neurol.* *156*, 341–351.
- Tamura, Y., Shintani, M., Nakamura, A., Monden, M., and Shiomi, H. (2005). Phase-specific central regulatory systems of hibernation in Syrian hamsters. *Brain Res.* *1045*, 88–96.
- Tan, C.L., and Knight, Z.A. (2018). Regulation of Body Temperature by the Nervous System. *Neuron* *98*, 31–48.
- Te Lindert, B.H.W., and Van Someren, E.J.W. (2018). Skin temperature, sleep, and vigilance. *Handb. Clin. Neurol.* *156*, 353–365.
- Tøien, Ø. (2013). Automated open flow respirometry in continuous and long-term measurements: design and principles. *J. Appl. Physiol.* *114*, 1094–1107.
- Tupone, D., Madden, C.J., and Morrison, S.F. (2013). Central Activation of the A1 Adenosine Receptor (A1AR) Induces a Hypothermic, Torpor-Like State in the Rat. *J. Neurosci.* *33*, 14512–14525.
- Uschakov, A., Gong, H., McGinty, D., and Szymusiak, R. (2007). Efferent Projections From the Median Preoptic Nucleus to Sleep- and Arousal Regulatory Nuclei in the Rat Brain. *Neuroscience* *150*, 104–120.
- Vicent, M.A., Borre, E.D., and Swoap, S.J. (2017). Central activation of the A1 adenosine receptor in fed mice recapitulates only some of the attributes of daily torpor. *J. Comp. Physiol. [B]* *187*, 835–845.

Walker, J.M., Haskell, E.H., Berger, R.J., and Heller, H.C. (1980). Hibernation and Circannual Rhythms of Sleep. *Physiol. Zool.* 53, 8–11.

Walker, J.M., Haskell, E.H., Berger, R.J., and Heller, H.C. (1981). Hibernation at moderate temperatures: a continuation of slow wave sleep. *Experientia* 37, 726–728.

Webb, P. (1992). Temperatures of skin, subcutaneous tissue, muscle and core in resting men in cold, comfortable and hot conditions. *Eur. J. Appl. Physiol.* 64, 471–476.

Williams, C.T., Barnes, B.M., Yan, L., and Buck, C.L. (2017). Entraining to the polar day: circadian rhythms in arctic ground squirrels. *J. Exp. Biol.* 220, 3095–3102.

Zhang, Y., Kerman, I.A., Laque, A., Nguyen, P., Faouzi, M., Louis, G.W., Jones, J.C., Rhodes, C., and Münzberg, H. (2011). Leptin-Receptor-Expressing Neurons in the Dorsomedial Hypothalamus and Median Preoptic Area Regulate Sympathetic Brown Adipose Tissue Circuits. *J. Neurosci.* 31, 1873–1884.

Zhao, D.-Q., and Ai, H.-B. (2011). Oxytocin and Vasopressin Involved in Restraint Water-Immersion Stress Mediated by Oxytocin Receptor and Vasopressin 1b Receptor in Rat Brain. *PLoS ONE* 6.

Zhao, P., Shao, Y.F., Zhang, M., Fan, K., Kong, X.P., Wang, R., and Hou, Y.P. (2012). Neuropeptide S promotes wakefulness through activation of the posterior hypothalamic histaminergic and orexinergic neurons. *Neuroscience* 207, 218–226.

Chapter 4: Seasonal changes in adenosine kinase in tanycytes underlie the possible mechanism of adenosine-induced hibernation in the Arctic Ground Squirrel (*Urocitellus parryii*).

4.1 Abstract

Hibernation is a seasonal strategy to conserve energy, characterized by modified thermoregulation, an increase in sleep pressure and drastic metabolic changes. The mechanisms controlling hibernation are still undefined, but adenosine plays a significant role through the activation of the adenosine A₁ receptor (A₁AR). In Arctic ground squirrels, hibernation, induced by activating A₁AR, occurs during the hibernating season, but not in summer. This suggests that a higher order process entrained to an endogenous circannual rhythm controls adenosine-induced hibernation. Seasonal changes in brain tissue levels of adenosine may contribute to seasonal sensitivity to A₁AR agonist. Adenosine kinase, located in astrocytes, is a primary regulator of extracellular adenosine concentration. Astrocytes and tanycytes are brain metabolic sensors, and tanycytes regulate seasonal changes in phenotypes, but it remains unknown if either cell type contributes to seasonal expression of hibernation. This study aims to characterize changes in adenosine kinase expression and tanycyte morphology during the seasonal modulation of adenosine signaling, as potential contributors to the higher order process regulating hibernation. We collected brain tissue from Arctic ground squirrels in different seasons. We performed immunohistochemical analysis to identify changes in tanycytes morphology and in adenosine kinase expression within the hypothalamus and the area postrema, two regions characterized by tanycytes and involved in energy homeostasis. We found seasonal changes in tanycyte morphology in the hypothalamus. Next, we observed for the first time the presence of adenosine kinase in tanycyte cell bodies, and we found a seasonal change in adenosine kinase levels in tanycytes, but not in astrocytes. We suggest that tanycytes may regulate adenosine signaling through the presence of ADK.

4.2 Introduction

Hibernation is a seasonal strategy of energy conservation (Carey et al., 2003). In obligate hibernators like the Arctic ground squirrel (AGS), a circannual rhythm regulates the onset of the hibernation season (Pengelley et al., 1978). A fall transition phase, characterized by a seasonal modulation in thermogenesis leading to a decrease in euthermic body temperature (T_b), precedes the onset of hibernation (Sheriff et al., 2012; Frare et al., 2018, 2019). The mechanisms that control hibernation are poorly understood. However, the activation of central nervous system (CNS) adenosine A_1 receptors (A_1AR) promotes the onset of hibernation and torpor in different species (Drew et al., 2017), suggesting a possible common mechanism that is conserved between species. A_1AR agonist-induced hibernation in AGS is controlled by processes affecting A_1AR signaling that are entrained to an endogenous circannual rhythm (Jinka et al., 2011; Frare et al., 2019). The nature of these processes are unknown, but are expected to include modulation of extracellular concentrations of adenosine in the CNS or the efficacy of A_1AR agonist signaling.

Adenosine kinase (ADK) is the primary enzyme regulating extracellular levels of adenosine in the CNS. In adult brain ADK is expressed in astrocytes and not neurons (Boison, 2013), but expression in tanycytes has not been defined. The role of adenosine in sleep is well established and ADK may modulate sleep drive by affecting extracellular levels of adenosine highlighting the connection between sleep and energy metabolism (Bjorness et al., 2016). In addition, adenosine release from astrocytes inhibits orexigenic hypothalamic neurons via A_1AR , and consequently feeding (Yang et al., 2015). Although the hibernation season is characterized by an increase in sleep pressure compared to summer (Walker et al., 1980) and a suppression in metabolism and feeding (Carey et al., 2003), it is unknown if ADK expression changes seasonally.

Tanycytes, ependymal glial cells with a distinct morphology, line the floor of the third ventricle (3V) and function as a barrier regulating the transport of substances from the vasculature to the brain parenchyma (Rodríguez et al., 2005; Ebling and Lewis, 2018). Tanycytes are characterized by long processes originating from the cell body and extending to the median eminence and to the nearby parenchyma (Rodríguez et al., 2005). The plasticity of the tanycytes' endfeet regulates the release of hormones in the fenestrated blood vessels of the median eminence in seasonal reproductive species (Prevot et al., 2010), and a seasonal "plasticity in gene expression" also regulates seasonal changes in body weight and energy homeostasis (Bolborea and Dale, 2013; Herwig et al., 2013; Ebling, 2014). Tanycytes are also metabolic sensors and deliver metabolic information from the periphery directly to the hypothalamic neurons regulating energy homeostasis (Frayling et al., 2011; Balland et al., 2014).

Tanycyte-like cells are present in the floor of the fourth ventricle (4V) and in the area postrema (AP) functioning as a barrier between the periphery and the CNS (Felten et al., 1981; Langlet et al., 2013a), but not enough work has been done to fully assess the function of tanycytes of the 4V. Although tanycytes share features with astrocytes, it is unknown if tanycytes express ADK or if tanycyte or astrocyte plasticity and ADK expression is associated with seasonal expression of hibernation. Here we test the hypothesis that seasonal changes in tanycytes morphology and ADK levels are phenotypic markers of the hibernation season.

4.3 Materials and Methods

All procedures were approved by the Institutional Animal Care and Use Committee (IACUC) at the University of Alaska Fairbanks and conducted in accordance with the Guide for the Care and Use of Laboratory Animals (8th edition). The objective of this study was to identify seasonal changes in tanycyte morphology and ADK expression.

4.3.1 Animals

Arctic Ground Squirrels (AGS, *Urocitellus Parryii*) were captured in the Brooks Range (68°07'46"N 149°28'33"W) under permit by Alaska Department of Fish and Game. After capture, AGS were housed in an environmental chamber at constant conditions at an ambient temperature (T_a) of 2°C and a photoperiod of 4L:20D until the end of all experiments. The hibernation cycle persists under constant environmental conditions that are needed to investigate the endogenous circannual rhythm without confounding variables such as T_a and photoperiod. We housed AGS individually and fed the animals approximately 47 g Mazuri rodent chow, daily, and provided water ad libitum. Food and water were provided even though AGS do not eat or drink during the hibernation season. We included both juvenile and adult animals of both sexes in the study as the age and sex of the animals depended on the availability at the time of capture. We collected euthermic animals in Summer, defined as two months after the last day of hibernation, and Fall. Fall AGS were identified by the lower euthermic T_b that precedes the beginning of the hibernation season (Sheriff et al., 2012). During the hibernation season we monitored torpor by the shavings added technique (Jameson, 1964); when the wood shavings placed on the animal's back remained undisturbed the following day, the animal was considered to be hibernating (i.e., torpid). We collected AGS during deep torpor (Torpor AGS) and we induced arousal within the third day of the torpor bout. Tissue from the induced-aroused AGS were then collected during the interbout arousal (IBA) phase, here referred to as Winter AGS. All AGS collected during the

hibernation season had at least eight torpor bouts. We measured rectal T_b in all AGS just prior to intracardial perfusion with a Digital Microprocessor Thermometer (model HH21 OMEGA Engineering, INC., Stamford, CT). Physiological characteristics of each seasonal phenotype are described in Table 4.1.

4.3.2 Brain tissue processing

AGS were anesthetized via chamber induction with 5% isoflurane and maintained via facemask at 3% mixed with 100% medical grade oxygen delivered at a flow rate of 1.5 L/min. AGS were intracardially perfused first with 0.9% NaCl for 5 min and then with 4% PFA in 0.1M PB buffer pH 7.4 at a flow rate of 79.5mL/min with a 18Ga needle through the left ventricle after the descending aorta was clamped to obtain a more efficient perfusion of the brain. Brains were removed and post fixed in 4%PFA overnight. Brains were blocked in three parts to allow better penetration of sucrose into the tissue. A gradient of sucrose solutions (5,10,15, 20 and 30 % w/v) was made in 0.1M phosphate buffer (PB) pH 7.4 to cryoprotect the tissue. Brains were maintained in each sucrose solution for up to 3 days and in 30% sucrose until brains sank. Brains covered with Tissue-Tek O.C.T. matrix (Electron Microscopy Sciences, Hatfield, PA) were rapidly frozen in a bath of n-Hexane 95% cooled with dry ice to a temperature of -45°C . Coronal sections ($40\mu\text{m}$) were cut with a cryostat (CM1850, Leica Biosystems, Buffalo Grove, IL). Slices were then stored until used at -20°C in cryo-protective (antifreeze) solution made in 0.1 M PB pH 7.4 with 60%w/v sucrose, 2%w/v polyvinylpyrrolidone (PVP-40, Sigma, St. Louis, MO) and 60%v/v ethylene glycol (VWR, Radnor, PA).

4.3.3 Immunohistochemistry

We used five animals per group from the brain tissue bank. Upon tissue availability, we used two tissue slices per animal at Bregma -2.80 to -3.14 based on the Paxinos and Watson Rat Atlas Fourth Edition. Free floating sections were washed using PBS pH 7.2, treated with 0.5% Triton X-100 for 20 min at RT, then blocked with 10% normal goat serum (NGS) (Vector Laboratory, Burlingame, CA) in PBS for 30min at room temperature (RT). After a second wash in PBS, the sections were incubated in a humidified chamber for 48hours at 2°C with a cocktail of antibodies including mouse anti-vimentin (1:1000, Millipore, MA) and rabbit anti-adenosine kinase (ADK, 1:4000, Bethyl Laboratories, TX) diluted in PBS with 1% NGS and 0.1% TritonX-100. Slices were washed in PBS and incubated with a mixture of goat anti-mouse Alexa 488 (1:500, Invitrogen, NY) and goat anti-rabbit Alexa 456 (1:750, Invitrogen, NY) in PBS containing 1% NGS in a dark room for 2hours at RT. Brain slices were mounted on Superfrost Plus slides (VWR, Radnor, PA) with Vectashield mounting media (Vector Laboratories, CA).

4.3.4 Image analysis

Images were collected with Slidebook 6 software using the Olympus IX81 inverted confocal microscope (objective LUCPlanFLN 40X, NA 0.60), equipped with a CCD camera (Hamamtsu ORCA-ER, 6.45 μm x 6.45 μm pixel size, Japan). To minimize exposure time, first we captured images for ADK analysis (exposure time 3000ms, Gain150); next we collected images as a Z-stack over 10 μm with a step of 0.5 μm (exposure time 400ms, Gain255) for tanycyte analysis. Images were analyzed using ImageJ software (version 1.52a, National Institute of Health, USA).

We stained two consecutive brain slices per animal. In the hypothalamus, we analyzed six to eight fields of view per each brain slice, for a total of 12 to 16 fields of view per animal. In the AP we analyzed five to six fields of view, for a total of 10 to 12 fields of view per animal.

To measure the length of the tanycyte processes, we overlapped a grid on top of the image. The grid number zero was assigned to the grid containing the cell body, and then we traced the processes emanating from the cell body. We counted the number of grid lines crossed by each process. We set the number of processes crossing the first line of the grid (grid_1) as 100% of the processes present in the field of view. We then calculated the percent of processes crossing the other lines of the grid as follow:
 $\% \text{ processes in grid}_n = (\text{number of processes in grid}_n * 100\%) / (\text{number of processes in grid}_1)$.

To measure the width of the tanycyte processes, we traced a vertical line parallel to the 3V, across the tanycytes' processes. We used the function "plot profile" in ImageJ, which displays the intensity peak for each process along the traced line. Then, we set the threshold to 500 grey value and we manually measured the process's width at the base of each peak. We averaged 12 to 16 plots for each AGS. We displayed the data as the percentage of tanycytes with processes' width smaller than 5 μm and greater than 5 μm .

We measured ADK intensity in the layer of the 3V, tracing the region of interest (ROI) around the tanycyte cell bodies. For the remainder of the hypothalamus we traced the ROI excluding the ventricle layer ROI. In the AP and 4V, we applied the same technique. Since the ROI were different within fields of view, we used the image J measure of the mean grey value that allows comparison of different size ROI. The mean grey value measures the average of grey value within the ROI (the sum of all the grey value of all the ROI pixels divided by the total number of pixels in the ROI).

4.3.5 Statistical analysis

Data are presented as mean \pm SEM and a $p \leq 0.05$ was considered significant. Data analyses were performed using R (version 1.1.423). First, we tested the data for the assumption of normality using

Shapiro test and the assumption of homogeneity of variance using the Bartlett test. If these assumptions were met, we compared the groups using a one way ANOVA followed by Tukey's honestly significant difference (HSD) test. When the data did not meet the assumption of homogeneity of variance, even after being transformed to the square root, we performed a Welch's ANOVA test followed by multiple comparison t tests with the Bonferroni's correction. We performed a linear regression analysis using the relative intensity of ADK as a predictor of T_b . Our preliminary data was used to perform a priori linear regression power analysis using G*Power software (version 3.1.9.4) to calculate the optimal sample size to detect a significant difference in the regression model, which details are reported under the result section "4.4.2 Tanycytes express ADK".

4.4 Results

4.4.1 Seasonal changes alter tanycytes process width, but not length in the 3V.

Qualitative observations, showed a difference in tanycyte morphology between the Summer and the Winter groups. The Winter group was characterized by tanycytes with consistently thinner processes compared to the Summer group, which had wider processes (Figure 4.1A). The two morphologies were not as distinct in the Torpor and Fall groups, which included both thin and wide processes (SI Figure 4.1-4.2). We followed this qualitative assessment with a measure of the processes' width in the 3V. We found that Winter AGS showed a significantly higher number of thin tanycytes compared to Summer, reported as percentage of tanycytes with processes' width less than 5 μm ($F(3,7.08)=12.386$, $p<0.01$ Welch's ANOVA, followed by t tests with Bonferroni's correction, Figure 4.1B). This quantitative analysis supports our qualitative observation of thinner tanycyte processes in Winter AGS. Data show a significant decrease in the number of tanycytes wider than 5 μm in Winter compared to the other seasons ($F(3,16)=9.055$, $p<0.001$ one way ANOVA, followed by Tukey HSD test, SI Figure 4.3). We next asked if tanycyte process length changes across seasons. We did not find any difference in process length between seasons in the tanycytes of the 3V (Figure 4.1C). We next examined the morphology of tanycyte-like cells around the central canal compared to the tanycytes lining the 3V: the cell body is cubical with short processes converging towards the ventral part of the brain (Figure 4.1D). The lack of long processes in 4V tanycyte-like cells prevented us from quantifying process width and length like we did for 3V.

4.4.2 Tanycytes express ADK

ADK is the primary regulator of extracellular adenosine concentration in the brain prompting us to ask if ADK is present in tanycytes. We identify ADK within the cell bodies of the tanycytes lining the 3V (Figure 4.2). We next measured ADK intensity in the tanycytes. ADK intensity showed a high variation in the torpor group (Figure 4.3A), and for this reason, we excluded the torpor group from the following statistical analysis. ADK intensity in the tanycyte cell bodies changed between seasons ($F(2,6.52)=12.287$, $p<0.01$ Welch's ANOVA); ADK intensity significantly decreased in the Winter group compared to the Summer ($p<0.01$ t test with Bonferroni's correction, Figure 4.3B). A multiple linear regression was calculated to predict T_b based on ADK levels (Figure 4.3C). A regression equation was found with a tendency towards significance ($F(1,8)=4.25$, $p=0.07$), with an R^2 of 0.35. As ADK tended towards significance as a predictor of T_b , we performed an a priori power analysis to estimate the sample size needed based on the data we collected. We used the statistical test 'Linear bivariate regression: One group, size of slope' in the t tests family with two tails. We performed the analysis using the experimental standard deviation for ADK intensity=75.60 and $T_b=0.78$, and the correlation coefficient $\rho=0.59$ to calculate the Slope H1. With $H1=0.006087$, $\alpha=0.05$ and $\text{power}=0.8$ the estimated sample size of 17 animals is needed to detect a significant regression analysis between ADK and T_b .

We next asked if ADK levels in the hypothalamic astrocytes show a similar tendency. We observed similar variation in ADK levels in the torpor group as seen in tanycytes (Figure 4.3E). We then excluded the torpor group for the statistical analysis, but we did not detect any significant difference between groups in ADK intensity in the ventral hypothalamic astrocytes ($F(2,12)=1.456$, $p=0.27$ one way ANOVA, Figure 4.3F).

4.4.3 ADK expression in the tanycyte-like cells in the AP and 4V

Next, we looked at the tanycyte-like cells in the AP and the ADK intensity in astrocytes and tanycyte-like cells. We observed ADK immunoreactivity in the AP and in the cell bodies of tanycyte-like cells lining the 4V (Figure 4.4A). We did not find a significant difference in ADK intensity between the groups in the tanycyte-like cells ($F(3,16)=1.3$, $p=0.30$ one way ANOVA, Figure 4.4B). Similar to the hypothalamic data, we observed a high variation in ADK levels in the AP of the torpor group and we excluded the torpor group from the following statistical analysis. We did not find a significant difference in ADK levels between groups in the AP ($F(3,16)=1.53$ $p=0.24$ one way ANOVA, Figure 4.4C).

4.5 Discussion

In this study, for the first time we identify the presence of ADK in the cell bodies of tanycytes lining the 3V and tanycyte-like cells lining the 4V. Adenosine kinase (AdK; EC 2.7.1.20) is an enzyme that phosphorylates adenosine to AMP. ADK determines the availability of adenosine and thereby controls adenosine receptor activation (Etherington et al., 2009). The presence of ADK in tanycytes has not been characterized before this study, although the use of ATP, as a signaling molecule, by tanycytes was previously described. ATP is released from tanycytes in the parenchyma by metabolic clues, such as glucose and amino acids and it activates the nearby neurons (Frayling et al., 2011; Lazutkaite et al., 2017). The presence of purinergic receptors in the cell membrane and the expression of the enzyme hydrolyzing ATP, suggest that tanycytes also metabolize ATP (Braun et al., 2003; Dale, 2011; Prevot et al., 2018). Through this work, we show that tanycytes could be an additional cell type for ATP-adenosine metabolism. As tanycytes and astrocytes already share some functions such as being glucose responsive and releasing ATP (García-Cáceres et al., 2019), it is not surprising that tanycytes may contribute in regulating extracellular adenosine levels.

ADK is the main regulator of extracellular adenosine, a neuromodulator known to play a role in sleep and in energy metabolism (Boison et al., 2010). Interestingly, the role of ADK is emerging as a component in the somnogenic properties of adenosine. Overexpression of astrocytic ADK suppresses sleep (Palchykova et al., 2010; Diógenes et al., 2014), while the ablation of ADK increases homeostatic sleep drive highlighting the connection between sleep and energy metabolism (Bjorness et al., 2016).

In addition, adenosine promotes the onset of hibernation through stimulation of A₁AR, but in a seasonally dependent manner (Jinka et al., 2011; Frare et al., 2018). A₁AR-induced hibernation is effective after the seasonal modulation of thermogenesis occurs, indicated by an increase in vasoconstriction and a decrease in euthermic T_b (Frare et al., 2019). We previously reported a seasonal adjustment in the neuronal pathways during the fall season, in particular a progressive decrease in neuronal activity of the premotor neurons in the raphe pallidus leading to a decrease in euthermic T_b (Frare et al., 2018). Here, we observed a similar phenomenon. In the Fall group, tanycyte morphology shares characteristics of both the Summer and Winter morphologies suggesting a transition from thick processes in summer to thinner processes in Winter. Furthermore, the ADK levels in the Fall group are not different from Summer or Winter groups, suggesting a progressive seasonal modulation of extracellular adenosine during the fall transition. The lower levels of ADK in Winter compared to Summer is expected to increase extracellular adenosine in winter. Intracellular ADK activity decreases intracellular adenosine and thus clears adenosine from the extracellular space via equilibrative

nucleoside transporters (Boison, 2013). Overexpression of ADK in the brain leads to a decrease in extracellular ADK and to sleep disruption (Palchykova et al., 2010; Diógenes et al., 2014). If the ADK levels change between seasons in the AGS, adenosine metabolism and the rate of adenosine clearance would change accordingly. During arousal metabolic activity increases significantly (Karpovich et al., 2009) and adenosine, as a byproduct of ATP, increases in plasma in 13-lined ground squirrel (Epperson et al., 2011). Similarly, adenosine may increase in the extracellular space as neuronal activity is restored during arousal from torpor (Ohe et al., 2007) or directly through the plasma via adenosine transporters in the blood brain barrier (Isakovic et al., 2004). Lower ADK levels in Winter compared to Summer, would reduce the rate of adenosine clearance and adenosine persisting in the extracellular milieu would promote the onset of hibernation through A₁AR.

Interestingly, we do not observe a similar change in ADK levels in the AP. The AP is a circumventricular organ that conveys the peripheral information through the dense population of fenestrated capillaries to the CNS (Price et al., 2008). In particular the AP regulates autonomic pathways controlling food intake, fluid homeostasis and the cardiovascular system (Price et al., 2008). In hibernation, the cardiovascular system undergoes significant changes between torpor and IBA; heart rate can drop from 300 to 10 beats/min during entrance into torpor and it is reversed during arousal (Milsom et al., 1999). The AP regulating cardiovascular output, may need to maintain its integrity throughout the seasons avoiding additional changes in adenosine metabolism, that could augment the sensitivity of AP neurons to adenosine (Chen and He, 1999).

We did not expect to observe such a large variation in ADK expression during torpor. However, torpor is characterized by a significant decrease in T_b and the neuronal network changes dramatically with a 50-60% loss in synapses and retraction of neuronal cell bodies and dendrites, which are restored during IBA (Ohe et al., 2006, 2007). A high variability may derive from the small sample size or by the state of torpor *per se* that may affect ADK expression, through an unknown mechanism.

In AGS, the tanycyte-like cells in the AP and the central canal showed a different morphology from the tanycytes in the 3V. The central canal was characterized by a honeycomb structure with polygonal and cuboidal shape, with processes that did not extend as far as the one in the 3V. Interestingly the processes merged towards the midline and the ventral part of the brain. These morphological assessments are similar to previous work describing the tanycytes of the 4V floor in rabbit, showing similar polygonal shape and the tendency of the processes to cluster in the midline (Felten et al., 1981). We also observed some differences between the tanycyte-like cells in the AP and in the central canal. We could not identify any distinct process within the AP, and even if there was a honeycomb structure

similar to the central canal, the shape of the cell bodies was round; a shape that resembled the shape of tanycyte cell bodies in the 3V. The lack of processes within the AP in the AGS is consistent with previous work showing the processes emanating from the edge of the AP, not within the AP (Guillebaud et al., 2017). Another study describes the processes within the AP to elongate in several directions (Langlet et al., 2013a), if the processes of the tanycyte-like cells “tangle” in a complex 3D structure, a coronal cut would truncate the processes limiting visualization to short segments. Tanycyte-like cells in the 4V are suggested to be a barrier within the CSF and the periphery (Langlet et al., 2013a), however this group of ependymal cells requires further anatomical and functional characterization.

A well know feature of tanycytes is their ability to change morphology depending on the physiological state of the animals such as reproductive state (Prevot et al., 2010; Pouchain Ribeiro Neto et al., 2017) and diet (Langlet et al., 2013b; Ramalho et al., 2018). Hibernation is characterized by seasonal changes in the reproduction system (Barnes et al., 1986; Darrow et al., 1988; Barnes and York, 1990) and by drastic changes in metabolism (Andrews et al., 2009). We were able to asses changes in the processes’ width between the Summer and the Winter groups, which is consistent with previous data showing a decrease in vimentin gene expression in winter compared to summer in hamsters (Herwig et al., 2013; Petri et al., 2014). Even if we did not find difference in process length, we cannot exclude a change in the tanycytes’ endfeet as seen in rats during the reproductive cycle (Prevot et al., 2010). Further work is required to identify if endfeet morphology undergoes similar changes between seasons, and during hibernation (Torpor and IBA) via higher resolution microscopy. Tanycytes also play a role in seasonal changes in phenotype modulating availability of thyroid hormones in hamster (Herwig et al., 2013). Here we propose that tanycytes serve as seasonal modulators of adenosine signaling through changes in ADK expression.

In conclusion, tanycytes likely play a role in adenosine signaling through expression of ADK. An expected increase in extracellular adenosine during the hibernation season may explain part of the seasonal phenotype and the seasonal response to A_1 AR agonist-induced hibernation.

4.6 Conflict of Interest

KD has a financial interest in Be Cool Pharmaceuticals.

4.7 Funding

Research reported in this publication was supported by NSF 10S-1258179; the National Institutes of Health under Award Numbers NS081637; the National Institute Of General Medical Sciences of the National Institutes of Health under the Award Number TL4GM118992; Institutional Development Award (IDeA) from the National Institute of General Medical Sciences of the National Institutes of Health under grant number P20GM103395. The content is solely the responsibility of the authors and does not necessarily represent the official views of the National Institutes of Health.

4.8 Acknowledgments

We thank L. Smith, K. Hueffer for the use of the confocal microscope, T. Kuhn for technical help in the images analysis methods and D. Boison for his ADK expertise.

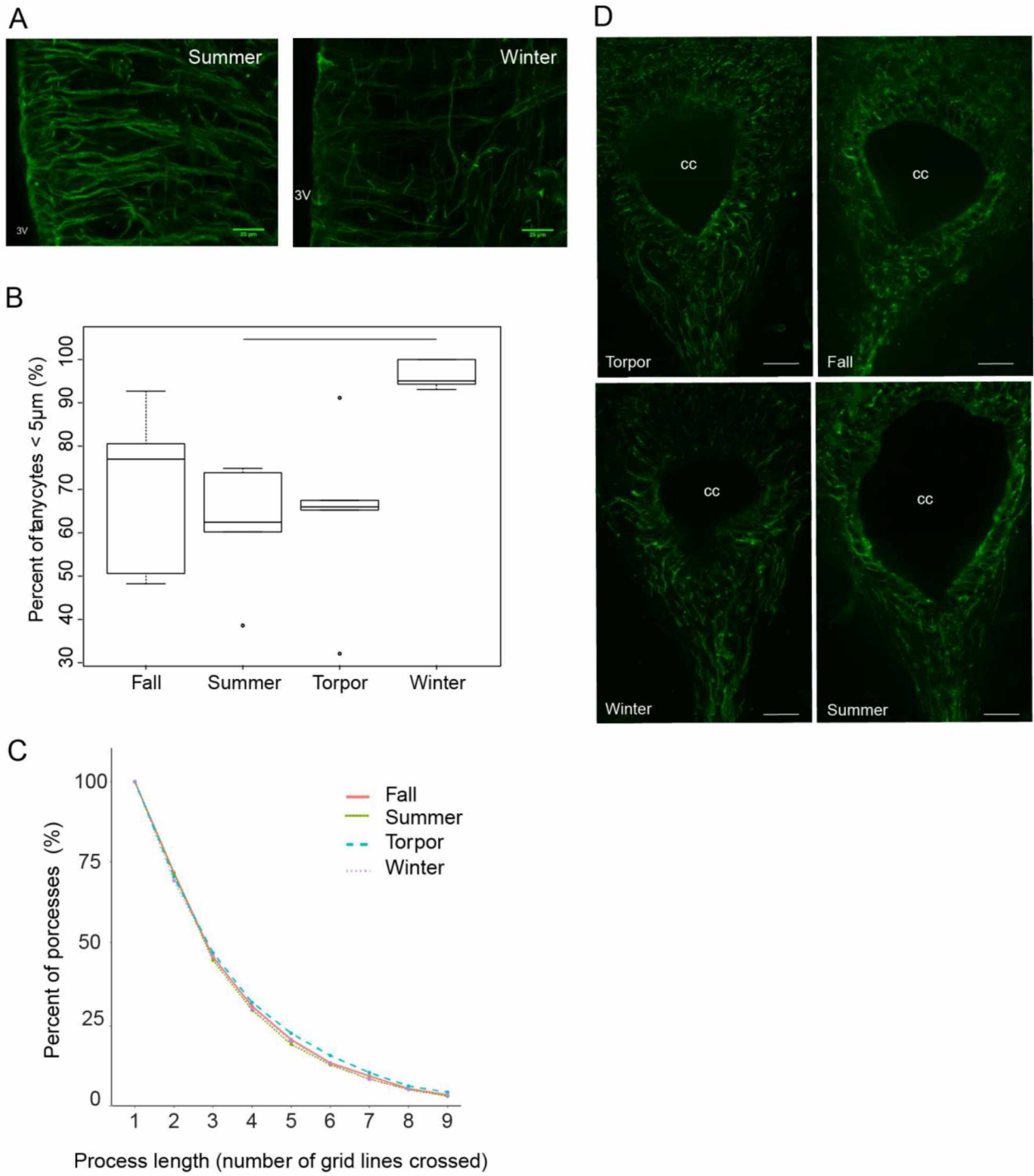


Figure 4.1: Caption on the following page.

Figure 4.1: Tanycytes process' width does change between seasons, but not tanycytes length.

Qualitative observations showed a difference in morphology between Summer and Winter tanycytes as visible by the photomicrographs of tanycytes stained with vimentin (green) taken from an AGS in the Summer and Winter seasons (A). Consistent with our observations, we measured a significant higher number of tanycytes with a width smaller than 5 μm in Winter AGS compared to Summer; percent of processes represent the ration between the thinner processes over the total number of processes measured, solid line rapresent $p < 0.05$, t test with Bonferroni's correction, and symbols rapresent outliers (B). The process length did not change between seasons; percent of processes refers to the percent of processes that reach the grid line indicated on the x-axis (C). The central canal is characterized by tanycyte-like cells with very short processes and a cubical cell body (for better resolution the image was constructed from two images taken under 40X magnification) (C). Scale bar 25 μm . Sample size $n=5$ animals per season, values in the y-axis are the average of 12 to 16 fields of view analyzed in two consecutive brain slices per each animal. 3V: third ventricle, 4V: fourth ventricle, cc: central canal.

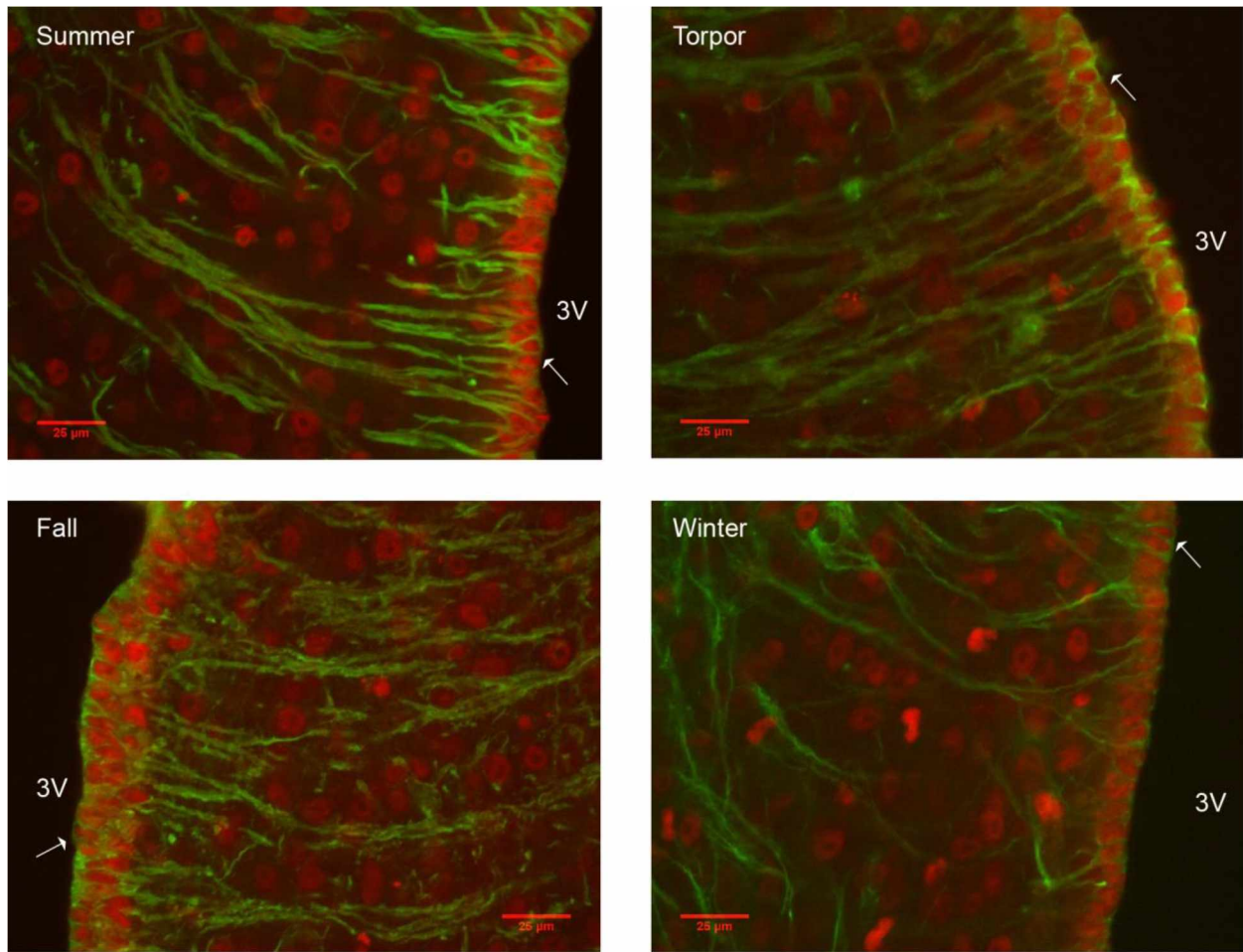


Figure 4.2: ADK is present in the cell body of the tanycytes.

Photomicrographs show ADK (red) present in the cell body of the tanycytes (green) in endothelium of the 3V (white arrow) in all four groups. ADK in astrocytes is visible in the ventral hypothalamus. Scale bar 25μm. 3V: third ventricle.

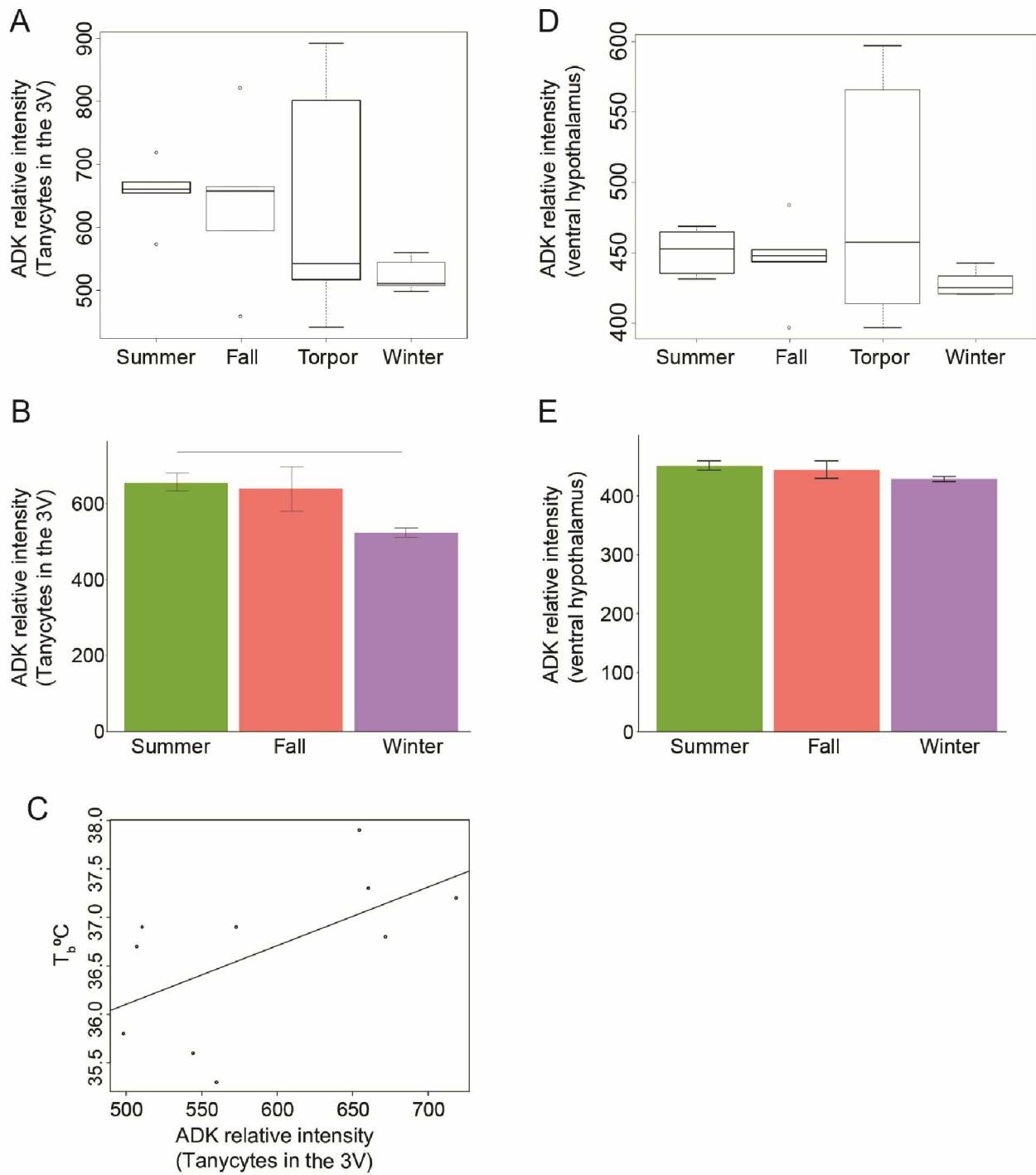


Figure 4.3: Caption on the following page.

Figure 4.3: ADK levels are lower in Winter compared to Summer in the tanycytes cell bodies. Relative intensity of ADK was measured within the cell bodies of tanycytes in the 3V, Torpor shows a high variability compared to the other groups (A), similar variability in Torpor was present in the relative intensity of ADK in the astrocytes in the ventral hypothalamus (D). Relative intensity of ADK is higher in Summer compared to Winter in the cell bodies of the tanycytes in the 3V; solid line represents $p < 0.01$, t test with bonferroni's correction (B). Relative intensity does not change in the astrocytes in the ventral hypothalamus (E). A linear regression analysis shows a tendency for ADK levels to predict T_b ($p = 0.07$) (C). Sample size $n = 5$ animals per season, values in the y-axis are the average of 12 to 16 fields of view analyzed in two consecutive brain slices per each animal; symbols represent outliers (A-D).

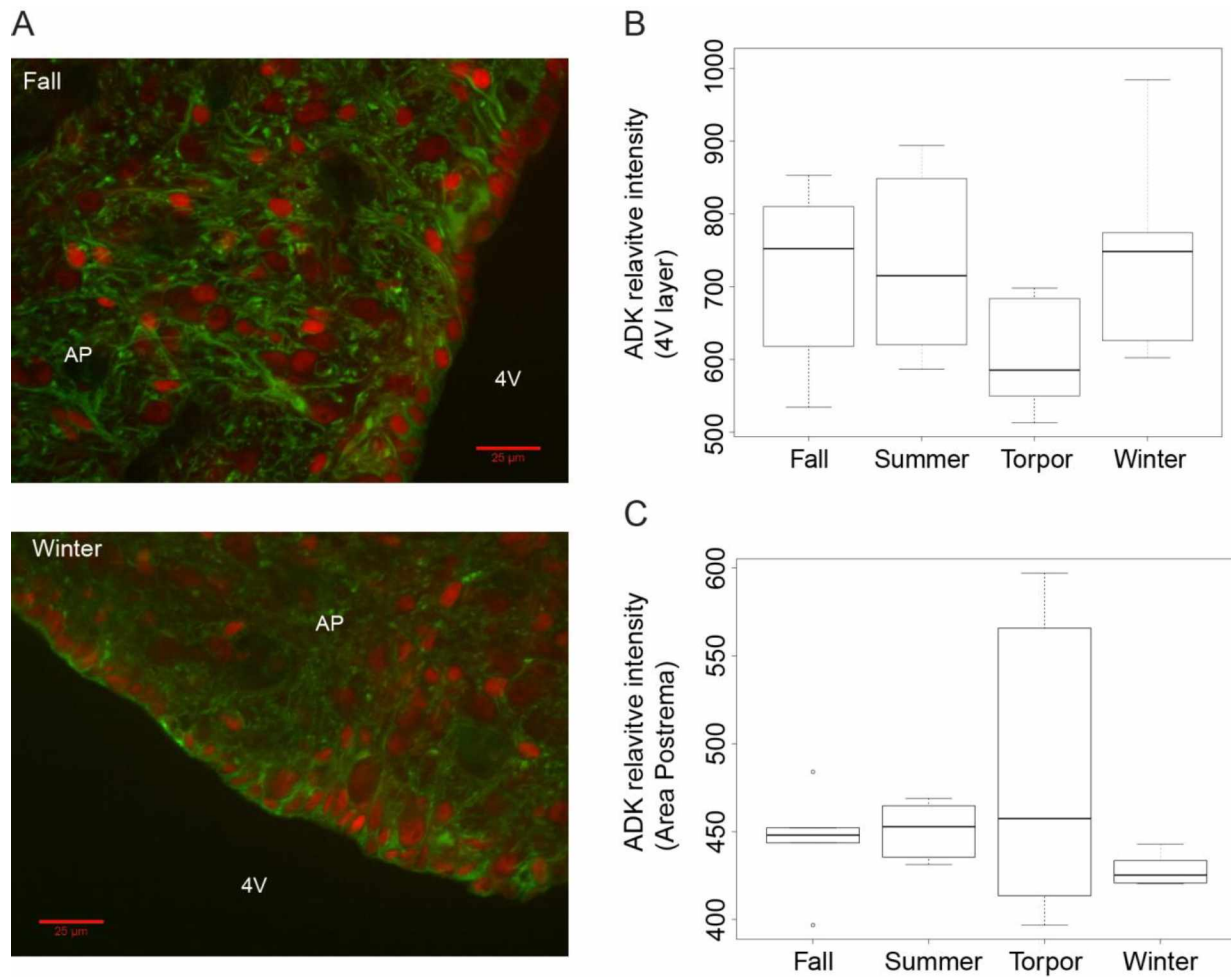
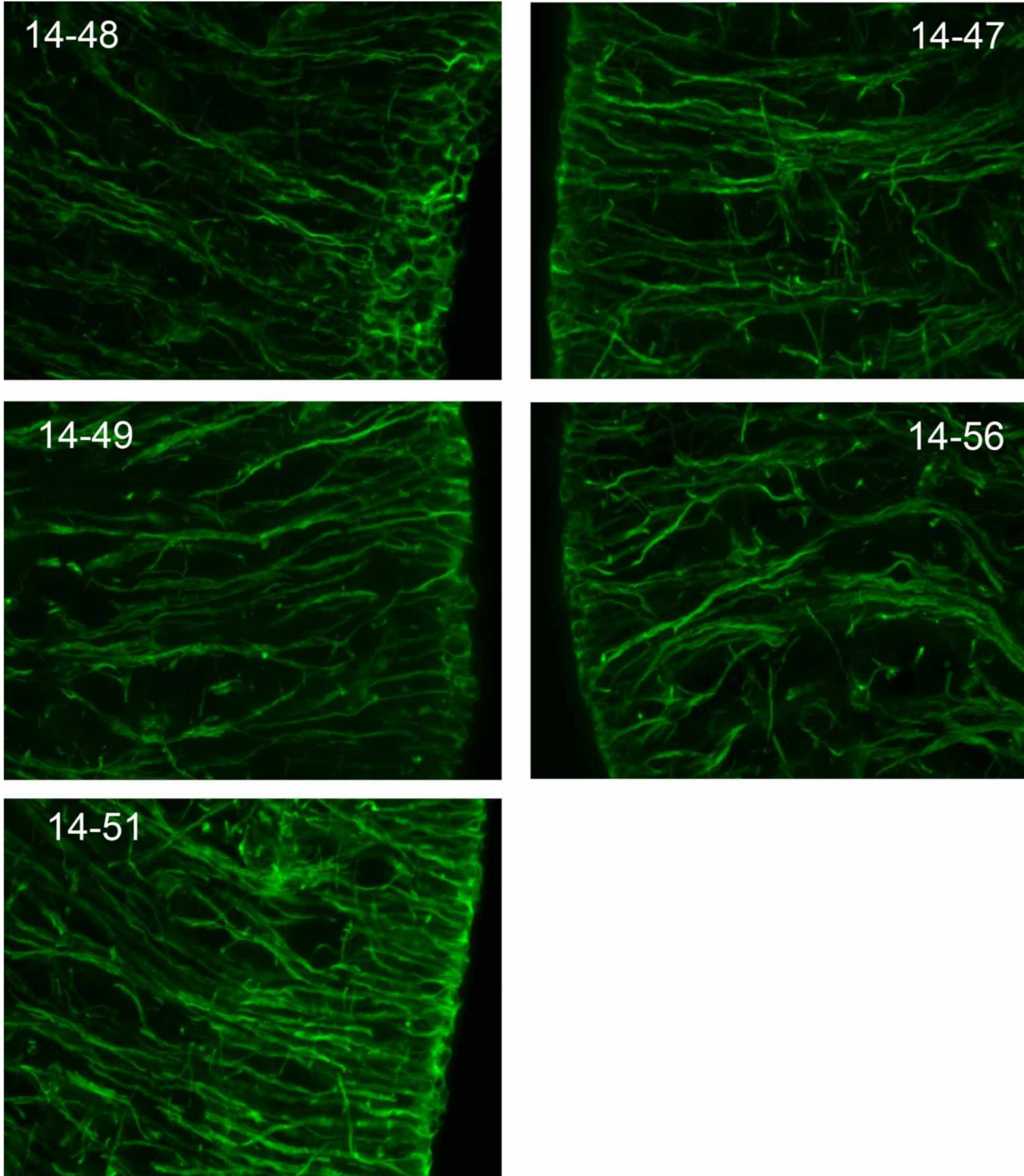


Figure 4.4: Tanycyte-like cells and ADK are present in the AP. Vimentin (green) stained tanycyte-like cells in the AP and in the area contacting the 4V. ADK (red) is visible within the tanycyte cell bodies lining the 4V and in the astrocytes present in the AP, representative photomicrographs taken from a Fall and a Winter AGS (A). Relative intensity of ADK did not change between seasons within the cell body of tanycyte-like cells in the 4V (B), and in the astrocytes within the AP (C). Scale bar 25 μ m. 4V: fourth ventricle, cc: central canal, AP: area postrema. Sample size n=5 animals per season, values in the y-axis are the average of 10 to 12 fields of view analyzed in two consecutive brain slices per each animal, symbol represents outliers (C).

Table 4.1: Physiological characteristics of the animals.

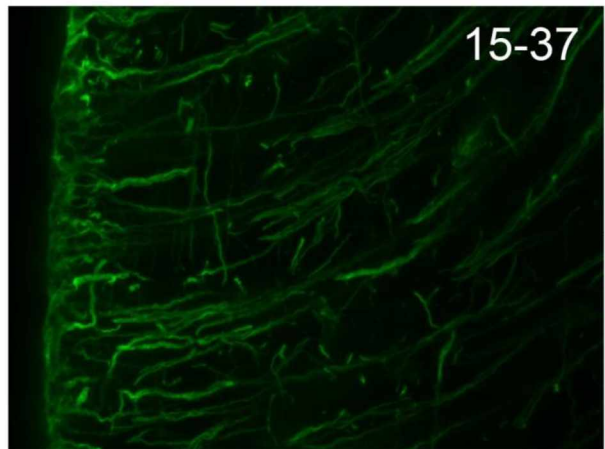
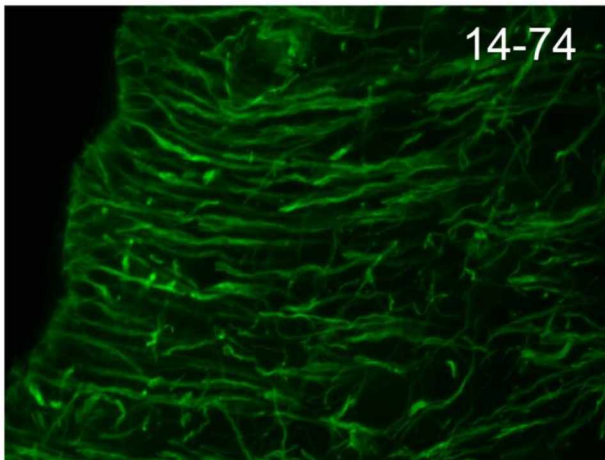
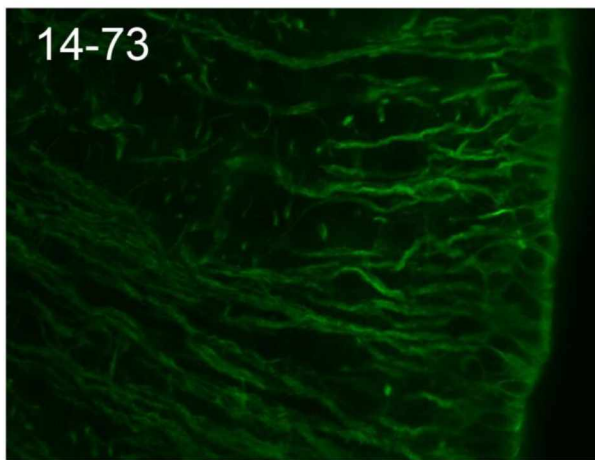
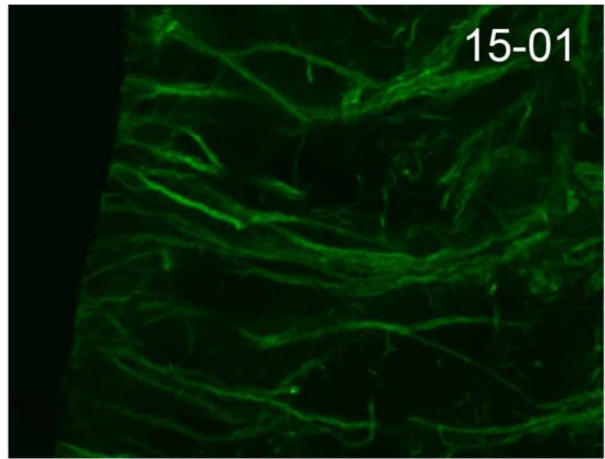
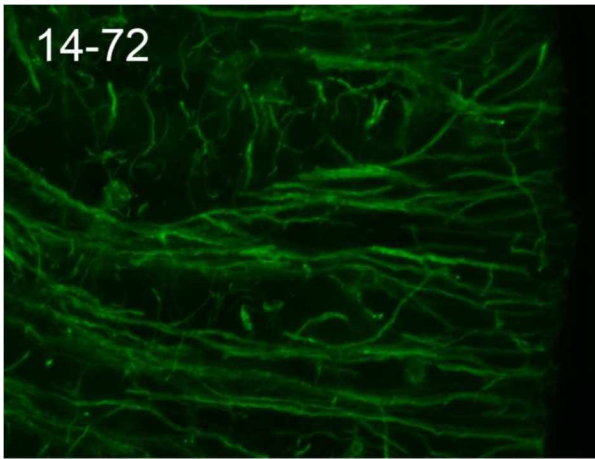
	Weight (g)	T _b (°C)	Torpor Bout
Summer	564± 18	37.22± 0.2 ^{a,c}	0
Fall	645± 78	35.46± 0.3 ^{b,d}	0
Winter (IBA)	486± 28	36.06± 0.3 ^{c,d}	≤8
Torpor	546± 55	2.62± 0.4 ^e	≤8

Data are presented as mean ± SEM. Values with different letters are statistically different from each other (p<0.05, Tukey HSD test). Sample size n=5 animal per season.



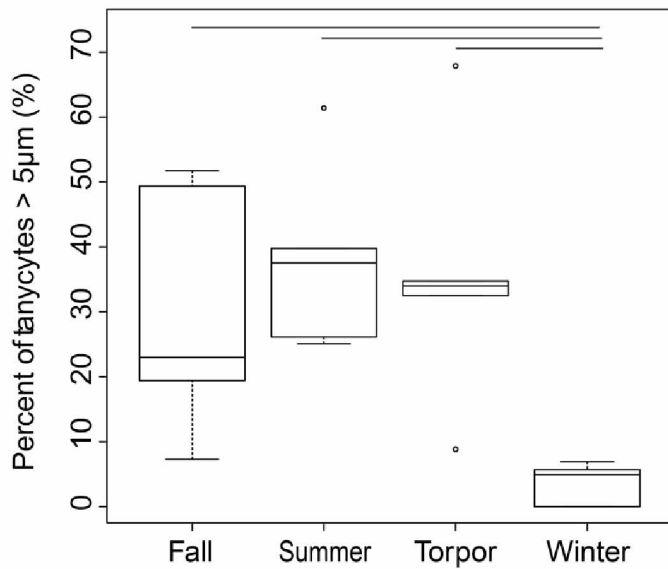
SI Figure 4.1: Tanyocytes morphology in the Torpor group.

Qualitative observations show that tanyocytes stained with vimentin (green) presented morphology inclusive of thin and wide processes within the Torpor group. The majority of tanyocytes are thin in AGS 14-48, while 14-51 shows wider tanyocytes. A combination of both wide and thin processes is visible in AGS 14-49.



SI Figure 4.2: Tanycytes morphology in the Fall group.

Qualitative observations show that tanycytes stained with vimentin (green) presented morphology inclusive of thin and wide processes within the Fall group. As an example AGS 15-37 is characterized by thin processes, while AGS 14-73 shows wider processes.



SI Figure 4.3: Tanycytes width decreased in Winter IBA.

Winter euthermic AGS showed a significant lower number of tanycytes wider of 5 μm compared to the other seasons. Solid line indicates $p < 0.05$, Tuckey HSD test, symbols rapresent outliers. Sample size $n=5$ animals per season, values in the y-axis are the average of 12 to 16 fields of view analyzed in two consecutive brain slices per each animal.

4.9 References

Andrews, M.T., Russeth, K.P., Drewes, L.R., and Henry, P.-G. (2009). Adaptive mechanisms regulate preferred utilization of ketones in the heart and brain of a hibernating mammal during arousal from torpor. *Am. J. Physiol. - Regul. Integr. Comp. Physiol.* 296, R383–R393.

Balland, E., Dam, J., Langlet, F., Caron, E., Steculorum, S., Messina, A., Rasika, S., Falluel-Morel, A., Anouar, Y., Dehouck, B., et al. (2014). Hypothalamic Tanycytes Are an ERK-Gated Conduit for Leptin into the Brain. *Cell Metab.* 19, 293–301.

Barnes, B.M., and York, A.D. (1990). Effect of Winter High Temperatures on Reproduction and Circannual Rhythms in Hibernating Ground Squirrels. *J. Biol. Rhythms* 5, 119–130.

Barnes, B.M., Kretzmann, M., Licht, P., and Zucker, I. (1986). The influence of hibernation on testis growth and spermatogenesis in the golden-mantled ground squirrel, *Spermophilus lateralis*. *Biol. Reprod.* 35, 1289–1297.

Bjorness, T.E., Dale, N., Mettlach, G., Sonneborn, A., Sahin, B., Fienberg, A.A., Yanagisawa, M., Bibb, J.A., and Greene, R.W. (2016). An Adenosine-Mediated Glial-Neuronal Circuit for Homeostatic Sleep. *J. Neurosci.* 36, 3709–3721.

Boison, D. (2013). Adenosine Kinase: Exploitation for Therapeutic Gain. *Pharmacol. Rev.* 65, 906–943.

Boison, D., Chen, J.-F., and Fredholm, B.B. (2010). Adenosine Signalling and Function in Glial Cells. *Cell Death Differ.* *17*, 1071–1082.

Bolborea, M., and Dale, N. (2013). Hypothalamic tanycytes: potential roles in the control of feeding and energy balance. *Trends Neurosci.* *36*, 91–100.

Braun, N., Sévigny, J., Mishra, S.K., Robson, S.C., Barth, S.W., Gerstberger, R., Hammer, K., and Zimmermann, H. (2003). Expression of the ecto-ATPase NTPDase2 in the germinal zones of the developing and adult rat brain. *Eur. J. Neurosci.* *17*, 1355–1364.

Carey, H.V., Andrews, M.T., and Martin, S.L. (2003). Mammalian Hibernation: Cellular and Molecular Responses to Depressed Metabolism and Low Temperature. *Physiol. Rev.* *83*, 1153–1181.

Chen, S., and He, R.R. (1999). Effect of intracarotid administration of adenosine on the activity of area postrema neurons in barodenervated rats. *Sheng Li Xue Bao* *51*, 667–674.

Dale, N. (2011). Purinergic signaling in hypothalamic tanycytes: Potential roles in chemosensing. *Semin. Cell Dev. Biol.* *22*, 237–244.

Darrow, J.M., Duncan, M.J., Bartke, A., Bona-Gallo, A., and Goldman, B.D. (1988). Influence of photoperiod and gonadal steroids on hibernation in the European hamster. *J. Comp. Physiol. [A]* *163*, 339–348.

Diógenes, M.J., Neves-Tomé, R., Fucile, S., Martinello, K., Scianni, M., Theofilas, P., Lopatář, J., Ribeiro, J.A., Maggi, L., Frenguelli, B.G., et al. (2014). Homeostatic Control of Synaptic Activity by Endogenous Adenosine is Mediated by Adenosine Kinase. *Cereb. Cortex N. Y. NY* *24*, 67–80.

Drew, K.L., Frare, C., and Rice, S.A. (2017). Neural signaling metabolites may modulate energy use in hibernation. *Neurochem. Res.* *42*, 141–150.

Ebling, F.J.P. (2014). On the value of seasonal mammals for identifying mechanisms underlying the control of food intake and body weight. *Horm. Behav.* *66*, 56–65.

Ebling, F.J.P., and Lewis, J.E. (2018). Tanycytes and hypothalamic control of energy metabolism. *Glia* *66*, 1176–1184.

Epperson, L.E., Karimpour-Fard, A., Hunter, L.E., and Martin, S.L. (2011). Metabolic cycles in a circannual hibernator. *Physiol. Genomics* *43*, 799–807.

Etherington, L.A., Patterson, G.E., Meechan, L., Boison, D., Irving, A.J., Dale, N., and Frenguelli, B.G. (2009). Astrocytic adenosine kinase regulates basal synaptic adenosine levels and seizure activity but not activity-dependent adenosine release in the hippocampus. *Neuropharmacology* *56*, 429–437.

Felten, D.L., Harrigan, P., Burnett, B.T., and Cummings, J.P. (1981). Fourth ventricular tanycytes: A possible relationship with monoaminergic nuclei. *Brain Res. Bull.* *6*, 427–436.

Frare, C., Jenkins, M., Soldin, S., and Drew, K. (2018). The raphe pallidus and the hypothalamic-pituitary-thyroid axis gate seasonal changes in thermoregulation in the hibernating Arctic Ground Squirrel (*Urociltellus parryii*). *Front. Physiol.* *9*, 1747.

- Frare, C., Jenkins, M.E., McClure, K.M., and Drew, K.L. (2019). Seasonal decrease in thermogenesis and increase in vasoconstriction explain seasonal response to 6 N-cyclohexyladenosine-induced hibernation in the Arctic Ground Squirrel (*Urocitellus parryii*). *J. Neurochem.*
- Frayling, C., Britton, R., and Dale, N. (2011). ATP-mediated glucosensing by hypothalamic tanycytes. *J. Physiol.* *589*, 2275–2286.
- García-Cáceres, C., Balland, E., Prevot, V., Luquet, S., Woods, S.C., Koch, M., Horvath, T.L., Yi, C.-X., Chowen, J.A., Verkhatsky, A., et al. (2019). Role of astrocytes, microglia, and tanycytes in brain control of systemic metabolism. *Nat. Neurosci.* *22*, 7.
- Guillebaud, F., Girardet, C., Abysique, A., Gaigé, S., Barbouche, R., Verneuil, J., Jean, A., Leprince, J., Tonon, M.-C., Dallaporta, M., et al. (2017). Glial Endozepines Inhibit Feeding-Related Autonomic Functions by Acting at the Brainstem Level. *Front. Neurosci.* *11*.
- Herwig, A., de Vries, E.M., Bolborea, M., Wilson, D., Mercer, J.G., Ebling, F.J.P., Morgan, P.J., and Barrett, P. (2013). Hypothalamic Ventricular Ependymal Thyroid Hormone Deiodinases Are an Important Element of Circannual Timing in the Siberian Hamster (*Phodopus sungorus*). *PLoS ONE* *8*.
- Isakovic, A.J., Abbott, N.J., and Redzic, Z.B. (2004). Brain to blood efflux transport of adenosine: blood–brain barrier studies in the rat. *J. Neurochem.* *90*, 272–286.
- Jameson, E.W. (1964). Patterns of Hibernation of Captive *Citellus lateralis* and *Eutamias speciosus*. *J. Mammal.* *45*, 455–460.
- Jinka, T.R., Tøien, Ø., and Drew, K.L. (2011). Season Primes the Brain in an Arctic Hibernator to Facilitate Entrance into Torpor Mediated by Adenosine A1 Receptors. *J. Neurosci.* *31*, 10752–10758.
- Karpovich, S.A., Tøien, Ø., Buck, C.L., and Barnes, B.M. (2009). Energetics of arousal episodes in hibernating arctic ground squirrels. *J. Comp. Physiol. B* *179*, 691–700.
- Langlet, F., Mullier, A., Bouret, S.G., Prevot, V., and Dehouck, B. (2013a). Tanycyte-Like Cells Form a Blood–Cerebrospinal Fluid Barrier in the Circumventricular Organs of the Mouse Brain. *J. Comp. Neurol.* *521*, 3389–3405.
- Langlet, F., Levin, B.E., Luquet, S., Mazzone, M., Messina, A., Dunn-Meynell, A.A., Balland, E., Lacombe, A., Mazur, D., Carmeliet, P., et al. (2013b). Tanycytic VEGF-A Boosts Blood-Hypothalamus Barrier Plasticity and Access of Metabolic Signals to the Arcuate Nucleus in Response to Fasting. *Cell Metab.* *17*, 607–617.
- Lazutkaite, G., Soldà, A., Lossow, K., Meyerhof, W., and Dale, N. (2017). Amino acid sensing in hypothalamic tanycytes via umami taste receptors. *Mol. Metab.* *6*, 1480–1492.
- Milsom, W.K., Zimmer, M.B., and Harris, M.B. (1999). Regulation of cardiac rhythm in hibernating mammals. *Comp. Biochem. Physiol. A. Mol. Integr. Physiol.* *124*, 383–391.
- Ohe, C.G. von der, Darian-Smith, C., Garner, C.C., and Heller, H.C. (2006). Ubiquitous and Temperature-Dependent Neural Plasticity in Hibernators. *J. Neurosci.* *26*, 10590–10598.

- Ohe, C.G. von der, Garner, C.C., Darian-Smith, C., and Heller, H.C. (2007). Synaptic Protein Dynamics in Hibernation. *J. Neurosci.* *27*, 84–92.
- Palchykova, S., Winsky-Sommerer, R., Shen, H.-Y., Boison, D., Gerling, A., and Tobler, I. (2010). Manipulation of adenosine kinase affects sleep regulation in mice. *J. Neurosci. Off. J. Soc. Neurosci.* *30*, 13157–13165.
- Pengelley, E.T., Aloia, R.C., and Barnes, B.M. (1978). Circannual rhythmicity in the hibernating ground squirrel *Citellus lateralis* under constant light and hyperthermic ambient temperature. *Comp. Biochem. Physiol. A Physiol.* *61*, 599–603.
- Petri, I., Dumbell, R., Scherbarth, F., Steinlechner, S., and Barrett, P. (2014). Effect of Exercise on Photoperiod-Regulated Hypothalamic Gene Expression and Peripheral Hormones in the Seasonal Dwarf Hamster *Phodopus sungorus*. *PLoS ONE* *9*.
- Pouchain Ribeiro Neto, R., Clarke, I.J., and Conductier, G. (2017). Alteration in the relationship between tanycytes and gonadotropin releasing hormone (GnRH) neurosecretory terminals following long-term metabolic manipulation in the sheep. *J. Neuroendocrinol.*
- Prevot, V., Bellefontaine, N., Baroncini, M., Sharif, A., Hanchate, N.K., Parkash, J., Campagne, C., and Seranno, S.D. (2010). Gonadotrophin-Releasing Hormone Nerve Terminals, Tanycytes and Neurohaemal Junction Remodelling in the Adult Median Eminence: Functional Consequences for Reproduction and Dynamic Role of Vascular Endothelial Cells. *J. Neuroendocrinol.* *22*, 639–649.
- Prevot, V., Dehouck, B., Sharif, A., Ciofi, P., Giacobini, P., and Clasadonte, J. (2018). The Versatile Tanycyte: A Hypothalamic Integrator of Reproduction and Energy Metabolism. *Endocr. Rev.* *39*, 333–368.
- Price, C.J., Hoyda, T.D., and Ferguson, A.V. (2008). The Area Postrema: A Brain Monitor and Integrator of Systemic Autonomic State. *The Neuroscientist* *14*, 182–194.
- Ramalho, A.F., Bombassaro, B., Dragano, N.R., Solon, C., Morari, J., Fioravante, M., Barbizan, R., Velloso, L.A., and Araujo, E.P. (2018). Dietary fats promote functional and structural changes in the median eminence blood/spinal fluid interface—the protective role for BDNF. *J. Neuroinflammation* *15*.
- Rodríguez, E.M., Blázquez, J.L., Pastor, F.E., Peláez, B., Peña, P., Peruzzo, B., and Amat, P. (2005). Hypothalamic Tanycytes: A Key Component of Brain–Endocrine Interaction. In *International Review of Cytology*, (Academic Press), pp. 89–164.
- Sheriff, M.J., Williams, C.T., Kenagy, G.J., Buck, C.L., and Barnes, B.M. (2012). Thermoregulatory changes anticipate hibernation onset by 45 days: data from free-living arctic ground squirrels. *J. Comp. Physiol. B* *182*, 841–847.
- Walker, J.M., Haskell, E.H., Berger, R.J., and Heller, H.C. (1980). Hibernation and Circannual Rhythms of Sleep. *Physiol. Zool.* *53*, 8–11.
- Yang, L., Qi, Y., and Yang, Y. (2015). Astrocytes Control Food Intake by Inhibiting AGRP Neuron Activity via Adenosine A1 Receptors. *Cell Rep.* *11*, 798–807.

Chapter 5: General conclusions

In the present work, I used CHA, the adenosine A₁ receptor agonist, to promote hibernation in Arctic ground squirrels (AGS) housed under constant ambient temperature (2°C) and light cycle (4L:20D). AGS maintained their circannual rhythm as previously shown (Pengelley et al., 1978) and the seasonal manipulation allowed for the investigation of the endogenous circannual rhythm, without confounding factors such as photoperiod and temperature. AGS showing at least eight torpor bouts were referred to as Winter AGS (i.e. Winter phenotype), and AGS that did not show any torpor for at least two months, since their last day of hibernation, were defined as Summer AGS (i.e. Summer phenotype). I confirmed the seasonal difference in CHA-induced hibernation. CHA triggered the onset of hibernation in Winter AGS shown by a decrease in metabolic rate and body temperature (T_b). On the contrary, CHA provoked a slight and transient decrease in metabolic rate and T_b in Summer AGS. These findings highlight that the seasonal difference in response to CHA is regulated by an endogenous circannual rhythm, which is independent from photoperiod and ambient temperature.

The seasonal changes in AGS phenotypes mirror the endogenous circannual rhythm. The pre-hibernation season, i.e. fall, is critical to prepare hibernating mammals, for instance by increasing brown adipose tissue (BAT) mass and adjusting feeding behavior (Schwartz et al., 2015; Ballinger et al., 2016; MacCannell et al., 2017). Thus, Fall is when the transition from Summer to Winter phenotype occurs. A gradual decrease in euthermic T_b during the Fall season has been previously reported in AGS and 13-lined squirrels (Russell et al., 2010; Sheriff et al., 2012). However, I found that the decrease in T_b correlated with a decrease in sympathetic activity in the raphe pallidus (rPA). The gradual decrease in the sympathetic tone in Fall led to lower thermogenesis in Winter compared to Summer (Chapter 2). However, the thermogenic capacity, the ability to produce heat and rewarm, increased as seen by the higher response of the hypothalamic-pituitary-thyroid axis to CHA-induced cooling in Winter AGS compared to Summer AGS (Chapter 2), also shown in Richardson's ground squirrels (Abbotts and Wang, 1980). Thermogenic capacity is fundamental to the hibernation season as the T_b is restored from 2-3°C to 36°C in 5 hours during arousal (Karpovich et al., 2009), but also to defend T_b when the ambient temperature drops below -4°C (Buck and Barnes, 2000). The seasonal modulation of the thermoregulatory system is also supported by the observed increase in vasoconstriction in Winter AGS compared to Summer AGS (Chapter 3). After I assessed the seasonal changes in thermoregulation associated with seasonal phenotypes, I identified the neuronal pathways of CHA-induced hibernation. A dis-inhibition of the nucleus tractus solitarius (NTS) and an inhibition of the tuberomammillary nucleus (TMN) occurred in both Summer AGS and Winter AGS in response to CHA. The same effect of CHA in

both Summer and Winter phenotypes underlined a higher order process entrained to the endogenous circannual rhythm that regulated CHA-induced hibernation.

The seasonal difference in response to CHA resided in the thermoregulatory system, highlighting a connection between thermoregulation and the higher order process. I primarily investigated the rPA and median preoptic area (MnPO), two brain nuclei associated with the BAT thermogenesis (Morrison and Madden, 2014). The thermogenic response was suppressed in winter CHA-induced hibernation as shown by the significant decreased in neuronal activity in the rPA and MnPO in Winter AGS compared to Summer AGS. These results reflected the seasonal physiological response to CHA seen by the drop in metabolic rate and T_b in Winter AGS. A seasonal decrease in thermogenesis was a prerequisite for CHA-induced hibernation (Chapter 3).

Preliminary data also showed a possible circannual modulation of adenosine signaling within the tanycytes. I described the tanycytes as an alternative location of adenosine signaling in the brain, as shown by the presence of adenosine kinase (ADK). The preliminary results showed a decreased of ADK in Winter compared to Summer, leading to a likely seasonal increase in extracellular adenosine (Chapter 4). The high level of extracellular adenosine would explain the seasonal increase in sleep pressure seen in euthermic ground squirrels (Walker et al., 1980). In sleep-awake studies, an increase in adenosine, reflecting ATP breakdown, indicates activity-dependent neuronal energy use and is associated with increase sleep (Bjorness and Greene, 2009; Holst and Landolt, 2015). Similarly, ATP breakdown may occur in arousal from torpor as metabolic rate increases and neuronal activity is restored (Ohe et al., 2006; Karpovich et al., 2009), likely increasing adenosine levels. In addition, the decrease in ADK activity in Winter may have reduced the clearance rate of adenosine from the extracellular space. Thus, adenosine may trigger the onset of hibernation via A_1AR dis-inhibiting the NTS, further suppressing thermogenesis and inhibiting the TMN, promoting sleep.

In conclusion, a circannual decrease in euthermic T_b achieved by attenuating sympathetic tone and increasing vasoconstriction, and a circannual increase in thermogenic capacity are mechanisms underlying the higher order process that regulates the onset of the hibernation season.

These findings are a significant contribution to the field of thermo-biology. It is well established that cold exposure activates BAT thermogenesis to generate heat and that vasoconstriction, another cold-defense strategy, prevents heat loss in rats and mice (Tan and Knight, 2018), but I showed that hibernation challenges these mechanisms. Hibernators employ vasoconstriction to conserve energy reducing heat loss, but vasoconstriction is not associated with an increased in BAT thermogenesis. On the contrary, I showed that the sympathetic tone is attenuated. Thus, in hibernation the

thermoregulatory mechanisms, present in homeothermic species, are individually used to maintain the seasonal energy homeostasis required.

In addition, seasonal suppression in thermogenesis is required for adenosine-induced hibernation reaffirming the similarity between hibernation and sleep. The onset of sleep is characterized by a decrease in core T_b , which is obtained by increasing heat loss through vasodilation (Szymusiak, 2018) and it is regulated by adenosine, an endogenous neuromodulator (Bjorness and Greene, 2009). Here, I confirmed that adenosine via the A_1AR extends sleep into the onset of hibernation, that is preceded by a seasonal decrease in core T_b . This illustrates another parallel with sleep as a decrease in core T_b precedes sleep onset. This is consistent with previous work in AGS maintained at 12L:12L and ambient temperature of 18°C, showing that CHA is more effective in decreasing T_b when administered at the seasonal minimal T_b (Olson et al., 2013). However, the decrease in T_b is facilitated by vasodilation in sleep, while in hibernation vasoconstriction occurs. Interestingly, even if sleep is associated with vasodilation, thus heat loss, sleep-related behaviors prevent heat loss by creating microclimates using bedding and curled positions (Van Someren, 2006; Okamoto-Mizuno and Mizuno, 2012). In addition, a mild increase in skin temperature, without an effect on core T_b , increases sleep and suppresses nocturnal wakefulness (Van Someren, 2006; Okamoto-Mizuno and Mizuno, 2012). Therefore, sleep may minimize heat loss through behavioral adaptations while autonomic adaptations prevail in hibernation. The understanding of hibernation and its thermoregulatory system may help us understand the complex relation between sleep and thermoregulation.

Further studies are needed to confirm these findings using a direct manipulation of the brain regions here identified through optogenetic or chemogenetic techniques (Park and Carmel, 2016). To validate the role of the autonomic nervous system in the cooling phase, I would expect that a stimulation of the rPA or the MnPO in Winter AGS after CHA would prevent the onset of hibernation. I would also assess changes in adenosine receptor sensitivity. First, I would test if a higher dose of CHA may overwrite the thermogenic response seen in Summer AGS with a dose response study; next, I would manipulate the adenosine signaling pathway. A chronic inhibition of ADK, mimicking the ADK levels seen in Winter phenotype, would affect sensitivity to adenosine, thus CHA-induced hibernation. Finally, to fully reverse a Summer phenotype into a Winter phenotype the chronic inhibition of ADK would be combined to the optogenetic suppression of the rPA. The attenuated sympathetic drive and the increase in adenosine accumulation would provide the AGS with the optimal conditions for CHA-induced hibernation.

5.1 References

- Abbotts, B., and Wang, L.C.H. (1980). Seasonal thermogenic capacity in a hibernator, *Spermophilus richardsonii*. *J. Comp. Physiol.* *140*, 235–240.
- Ballinger, M.A., Hess, C., Napolitano, M.W., Bjork, J.A., and Andrews, M.T. (2016). Seasonal changes in brown adipose tissue mitochondria in a mammalian hibernator: from gene expression to function. *Am. J. Physiol.-Regul. Integr. Comp. Physiol.* *311*, R325–R336.
- Bjorness, T.E., and Greene, R.W. (2009). Adenosine and Sleep. *Curr. Neuropharmacol.* *7*, 238–245.
- Buck, C.L., and Barnes, B.M. (2000). Effects of ambient temperature on metabolic rate, respiratory quotient, and torpor in an arctic hibernator. *Am. J. Physiol.-Regul. Integr. Comp. Physiol.* *279*, R255–R262.
- Holst, S.C., and Landolt, H.-P. (2015). Sleep Homeostasis, Metabolism, and Adenosine. *Curr. Sleep Med. Rep.* *1*, 27–37.
- Karpovich, S.A., Tøien, Ø., Buck, C.L., and Barnes, B.M. (2009). Energetics of arousal episodes in hibernating arctic ground squirrels. *J. Comp. Physiol. B* *179*, 691–700.
- MacCannell, A., Sinclair, K., Friesen-Waldner, L., McKenzie, C.A., and Staples, J.F. (2017). Water–fat MRI in a hibernator reveals seasonal growth of white and brown adipose tissue without cold exposure. *J. Comp. Physiol. B* *187*, 759–767.
- Morrison, S.F., and Madden, C.J. (2014). Central Nervous System Regulation of Brown Adipose Tissue. *Compr. Physiol.* *4*, 1677–1713.
- Ohe, C.G. von der, Darian-Smith, C., Garner, C.C., and Heller, H.C. (2006). Ubiquitous and Temperature-Dependent Neural Plasticity in Hibernators. *J. Neurosci.* *26*, 10590–10598.
- Okamoto-Mizuno, K., and Mizuno, K. (2012). Effects of thermal environment on sleep and circadian rhythm. *J. Physiol. Anthropol.* *31*, 14.
- Olson, J.M., Jinka, T.R., Larson, L.K., Danielson, J.J., Moore, J.T., Carpluck, J., and Drew, K.L. (2013). Circannual Rhythm in Body Temperature, Torpor, and Sensitivity to A1 Adenosine Receptor Agonist in Arctic Ground Squirrels. *J. Biol. Rhythms* *28*, 201–207.
- Park, H.G., and Carmel, J.B. (2016). Selective Manipulation of Neural Circuits. *Neurotherapeutics* *13*, 311–324.
- Pengelly, E.T., Aloia, R.C., and Barnes, B.M. (1978). Circannual rhythmicity in the hibernating ground squirrel *Citellus lateralis* under constant light and hyperthermic ambient temperature. *Comp. Biochem. Physiol. A Physiol.* *61*, 599–603.
- Russell, R.L., O’Neill, P.H., Epperson, L.E., and Martin, S.L. (2010). Extensive use of torpor in 13-lined ground squirrels in the fall prior to cold exposure. *J. Comp. Physiol. [B]* *180*, 1165–1172.

Schwartz, C., Hampton, M., and Andrews, M.T. (2015). Hypothalamic gene expression underlying pre-
hibernation satiety. *Genes Brain Behav.* *14*, 310–318.

Sheriff, M.J., Williams, C.T., Kenagy, G.J., Buck, C.L., and Barnes, B.M. (2012). Thermoregulatory changes
anticipate hibernation onset by 45 days: data from free-living arctic ground squirrels. *J. Comp. Physiol. B*
182, 841–847.

Szymusiak, R. (2018). Body temperature and sleep. *Handb. Clin. Neurol.* *156*, 341–351.

Tan, C.L., and Knight, Z.A. (2018). Regulation of Body Temperature by the Nervous System. *Neuron* *98*,
31–48.

Van Someren, E.J.W. (2006). Mechanisms and functions of coupling between sleep and temperature
rhythms. In *Progress in Brain Research*, A. Kalsbeek, E. Fliers, M.A. Hofman, D.F. Swaab, E.J.W. van
Someren, and R.M. Buijs, eds. (Elsevier), pp. 309–324.

Walker, J.M., Haskell, E.H., Berger, R.J., and Heller, H.C. (1980). Hibernation and Circannual Rhythms of
Sleep. *Physiol. Zool.* *53*, 8–11.

Appendices

Appendix A: Protocols

Appendix A 1: IACUC Approval Letter for Research Protocol



(907) 474-780

(907) 474-5993 fax

uaf-iacuc@alaska.edu www.uaf.edu/iacuc

Institutional Animal Care and Use Committee

909 N Koyukuk Dr. Suite 212, P.O. Box 757270, Fairbanks, Alaska 99775-7270

May 22, 2018

To: Kelly Drew
Principal Investigator

From: University of Alaska Fairbanks IACUC

Re: [467983-45] Brain regions involved in seasonally dependent A1AR agonist-induced torpor

The IACUC has reviewed the Progress Report by Designated Member Review and the Protocol has been approved for an additional year.

Received:	May 21, 2018
Initial Approval Date:	June 20, 2013
Effective Date:	May 22, 2018
Expiration Date:	June 20, 2019

This action is included on the June 14, 2018 IACUC Agenda.

PI responsibilities:

- *Acquire and maintain all necessary permits and permissions prior to beginning work on this protocol. Failure to obtain or maintain valid permits is considered a violation of an IACUC protocol and could result in revocation of IACUC approval.*
- *Ensure the protocol is up-to-date and submit modifications to the IACUC when necessary (see form 006 "Significant changes requiring IACUC review" in the IRBNet Forms and Templates)*
- *Inform research personnel that only activities described in the approved IACUC protocol can be performed. Ensure personnel have been appropriately trained to perform their duties.*
- *Be aware of status of other packages in IRBNet; this approval only applies to this package and the documents it contains; it does not imply approval for other revisions or renewals you may have submitted to the IACUC previously.*
- *Ensure animal research personnel are aware of the reporting procedures detailed in the form 005 "Reporting Concerns".*

**Standard Operating Procedures
Drew Lab**

IACUC#: **Date Approved:** **Last Revised:**

TITLE: **Arctic Ground Squirrel Husbandry (non-breeders)**

PURPOSE: Daily care for non-breeding Arctic Ground Squirrels

- **Person(s) Responsible for Daily Care and Welfare:** Drew lab personnel
- **Required permits:**
- **Seasons**
 - o Summer months = May 15 – August 15 (or AGS which do not show torpor bout for at least 30 consecutive days)
 - o Winter months = August 15 – May 15 (or AGS which show signs of torpor bouts)
- **Animal Room 39 B (recovery room)**
 - o **Lighting:**
 - ☒ **Intensity (Range):** 10-20
ft. candles ☒
 - Photoperiod:**
 - Summer: May 15th Fast switch to 16L:8D, 7am to 11pm
 - Winter: beginning August 1, 16L:8D transitioning to D:D by reducing lighting 30 minutes a day (split am and pm) when animals first brought into the facility. Following years fast switch on August 15th to 4L:20D
 - o **Temperature:**
 - Warm Room 39 B 16-18°C
- **Animal Room 39 C1 and C2 (cold chambers)**
 - o **Lighting:**
 - ☒ **Intensity (Range):** 10-20
ft. candles

☐ **Photoperiod:**

- Summer: May 15th Fast switch to 16L:8D, 7am to 11pm
- Winter: beginning August 1, 16L:8D transitioning to D:D by reducing lighting 30 minutes a day (split am and pm) when animals first brought into the facility. Following years fast switch on August 15th to 4L:20D

o **Temperature**

- Chamber 39 C2 2°C year-round
- Chamber 39 C1 16-18°C Summer, 2°C Winter

• **Housing**

o **Primary containment:**

- **Non-hibernators** When animals are not hibernating, stainless steel ¼" wire mesh hanging cages, dimensions 12"X19"X12". Cages hang over trays of ammonia absorbing corn cob litter.
- **Hibernators** Hibernating animals will be housed in polycarbonate cages (8.5"x17"x8.5") with stainless steel top or micro insulation top

o **Bedding:**

- **Non-hibernators** All cages with wire mesh floors require cotton batting equal to two times the animal's body size.
- **Hibernators** Cotton batting equal to two times the animals body size on a bed of shavings, 1"deep

o **Density:**

- One animal per cage

o **Enrichment:**

- **Non-hibernators**
 - 8" length of 4" PVC tube
 - Containment plate under the cotton nest to prevent the loss of cache through the wire.
- **Hibernators**
 - None

• **Diet**

o **Feed:**

- **Non-hibernators** Mazuri Rodent Chow, minimum of 10 pellets per day

- **Hibernators** none
 - o **Water:**
 - **Non-hibernators** One 8 or 16 ounce bottle with stainless steel sipper tube, ad lib
 - **Hibernators** One water gel pack, ad lib, replace if less than 2 ounces or soiled
- **Animal Marking or Identification:**
 - Type of Mark or Identification: Cage cards
 - Age and sex: Marked upon arrival at animal facility.
 - Person(s) Responsible for Applying Identification, age and sex: ARC staff
- **Veterinary Care:**
 - Person(s) Responsible for Veterinary Care: ARC Veterinary Staff
- **Euthanasia & Disposal**
 - Disposition of Non-Usable or Surplus Animals: euthanasia or hold until moved to an IACUC approved protocol
 - Euthanasia Method to be used for emergencies or routine culling:
 - Routine procedure is overdose of isoflurane using isoflurane vaporizer in a suitable induction chamber.
 - Alternative methods may only be used on order by Attending Veterinarian or designee.
- **Daily care of non-hibernators**
 - Fill out Animal Room Activity sheet
 - Scrape feces from inside of cage. Decontaminate tool with GS Neutral solution between cages.
 - dilution instructions; ½ ounce GS Neutral per gallon of water
 - Ad lib feeding till August 15th
 - Fill the water bottle if ½ full or below
 - Remove any soiled bedding & replace with new, making sure cotton batting is at least 2x the size of the animal.
 - Twice a week, replace trays under wire mesh hanging cages and line trays with fresh cobs. Provide clean wire cages only if excessively dirty.
 - Record the animals status (Awake = A, Hibernating Shavings Added = HSA, or Hibernating = H) on the room hibernation sheet

- Record maximum & minimum temperature from thermometer in room.
 - Check all animals for any abnormalities; behavioral, illness or injuries.
 - Note any abnormalities on disposition records and notify ARC staff
 - Any deaths should be reported to ARC staff - refer to SOP ARC-5454
 - Clean up cart or countertop
 - Fill feed and water containers if getting low - making sure lids are on the feed and water containers once done
 - Sweep the floor and mop if necessary
- **Transition into hibernation**
 - 24 hours after the first day of torpor, AGS are moved into the plastic tub for the hibernation season.
 - When AGS is moved into the plastic tub, food will not be moved, a gel pack for water will be provided.
- **Daily care of hibernators**
 - Fill out Animal Room Activity sheet
 - Record the animals status (Awake = A, Hibernating Shavings Added = HSA, or Hibernating = H) on the room hibernation sheet
 - **If animal is hibernating and bin/cage appears clean, cage will not be disturbed. Animal must be aroused/awake when moved to a new bin/cage.**
 - Spot remove feces from corner of cage.
 - Remove any soiled bedding & replace with new, making sure cotton batting is at least 2x the size of the animal.
 - Record maximum & minimum temperature from thermometer in room.
 - Check all animals for any abnormalities; behavioral, illness or injuries.
 - Note any abnormalities on disposition records and notify ARC staff

- Any deaths should be reported to ARC staff - refer to SOP ARC-XXXX
- When arousal is longer than 3 days, AGS is moved to a separate location in chamber and food is returned to the animal. If AGS is awake for other 7 days it will be moved out of the experimental chamber.
- Clean up cart or countertop
 - Fill feed and water containers if getting low - making sure lids are on the feed and water containers once done
- Sweep the floor and mop if necessary

Winter AGS EXPERIMENT DESIGN:

“Mid-season” AGS needs to be at least in the 8th torpor bout of the season.
AGS needs to be within day 1 to day 4 of the torpor bout

1. At the second hour of the light cycle starts experiment (if the light cycle is from 12pm to 4pm, the experiment will start at 2pm).
2. Collect respiratory rate (count the number of breath per min). Move the shaving from the AGS and move a little the cotton to expose the AGS so you can well see the belly. When you are ready start the timer (noise doesn't bother the AGS) and count the movements of the belly. Do it at least couple of times (usually the first try helps you to find the point in the belly where to look at).
3. In the meantime leave the thermometer on so you can monitor the Chamber temperature.
4. Take the AGS with the nest outside of the cage (usually on the top of the racket). Record core body temperature with rectal thermometer (use large amount of lubricant, they are really dry and slowly insert the thermometer).
5. Put the AGS back in the cage with the nest.
6. Move the cage outside to weight the AGS
7. Take the AGS without nest and put in the balance right outside of the Chamber
8. Bring the AGS (with the cage) to the warm room ($T_a=20^{\circ}\text{C}$) light cycle 4:20 L:D room B12 (the light cycle has to match the one in the cold chamber)
9. With a little shaver, shave the AGS above the shoulder
10. Test the IPTT with the wound, it must read!!
11. Implant IPTT transponders subcutaneous: Take the shaved skin within your finger, make a little tent

Inject the IPPT
Feel the transponder pushed out
Slowly roll your finger around it
Put some surgical glue on the hole of the injection (vectabond) with 25g needle and 1mL syringe.
12. Handle the animal to make sure it is going to wake up
13. Check the transponder getting few reads.
14. Fast OV in the warm room MARK “do not feed”
15. The morning after check that the animal is awake
16. In the two hours before the animal is moved back in the cold room, record the T_b (every half an hour if you can)
17. Move the animal back in the cold room exactly at the same time you took it off the day before (two hour in the light cycle)
18. Leave the animal there for 1 hour to acquire baseline
19. At the 3rd hour in the light cycle do the **injection** with CHA (0.5 mg/kg IP) or Vehicle using 25G 1 ½ inches (blue needle). The injection is i.p., two people one handles the AGS and the other give the injection in the belly (make sure the needle goes under the large amount of fat they have)
20. When you handle the animal read the T_b and start the timer because every 30 min the T_b needs to be recorded
21. After 3 hours move the AGS in the jar and start the perfusion.

DAY 1	DAY 2
Steps 1 to 14	Steps 15 to 21
Perfusion protocol Day 1	Perfusion protocol Day 2

Summer AGS EXPERIMENT DESIGN:

“Off season” AGS needs to be awake for at least one month (no showing torpor consecutively for a month).

If the IPTT has not been implanted while the animal was torpid, it’s necessary to anesthetize the AGS with isoflurane.

1. Put the animal in the jar
2. Weight the animal and record the weight in your note book
3. Turn on the anesthetic and oxygen tank
4. When the animal is down, take it off of the jar and keep it down with the mask (isoflurane at 3).
5. With a little shaver, shave the AGS above the shoulder
6. Test the IPTT with the wound, it must read!!
7. Implant IPTT transponders subcutaneous: Take the shaved skin within your finger, make a little tent
8. Inject the IPPT
9. Feel the transponder pushed out
10. Slowly roll your finger around it
11. Put some surgical glue on the hole of the injection (vectabond) with 25g needle and 1mL syringe.
12. Put the animal back to its cage in the cold chamber.
13. Wait one week before the experiment.

Day before the experiment

1. At the second hour of the light cycle starts experiment (if the light cycle is from 12pm to 4pm, the experiment will start at 2pm).
2. Collect respiratory rate (count the number of breath per min) with the timer.
3. Collect body temperature reading the IPTT
4. Have the thermometer to monitor the Chamber temperature.
5. Put the AGS in the jar
6. Record weight on the balance outside the Chamber
7. Bring the AGS (with the cage) to the warm room ($T_a=20^{\circ}\text{C}$) light cycle 4:20 L:D room B12 (the light cycle has to match the one in the cold chamber)
8. Fast OV in the warm room MARK “do not feed”

Day of the experiment

1. In the two hours before the animal is moved back in the cold room, record the T_b (every half an hour if you can)
2. Move the animal back in the cold room exactly at the same time you took it off the day before (two hour in the light cycle)
3. Leave the animal there for 1 hour to acquire baseline
4. At the 3rd hour in the light cycle do the **injection** with CHA (0.5 mg/kg IP) or Vehicle using 25G 1 ½ inches (blue needle). The injection is i.p., two people one handles the AGS and the other give the injection in the belly (make sure the needle goes under the large amount of fat they have)
5. When you handle the animal read the T_b and start the timer because every 30 min the T_b needs to be recorded
6. After 3 hours move the AGS in the jar and start the perfusion.

PERFUSION PROTOCOL (updated Carla Frare 2016)

JOVE video – Whole Animal Perfusion Fixation for Rodents - <http://library.uaf.edu/dbnews-jove>

1. Prepare 4%PFA and stored in a 4C (in a sealed container is good for one month- usually stored in a 4 L empty methanol bottle)
2. Day before prep:
 - Make 0.9% saline solution, stored in 4C until perfusion (possible to make it the day of perfusion, but it needs to be cold at time of perfusion).
 - Print data sheets
 - Label tube for brains and spinal cords with Date, Animal #, Tissue (Brain or Spinal Column), Treatment (eg. CHA), and 4% PFA. Fill with ~20 ml PFA (or fill it the day of perfusion)
 - Check O2 tank and isoflurane levels
 - Weigh scavenger
 - Weigh animals
 - Check for all material needed (mask for rat/needles with sleeves (*usually the needle is inserted in a plastic tube 1 cm shorter than the needle, so the needle does not go too further into the heart*) /syringes/timer/light/PFA funnel)
3. Day of prep:
4. Saline and PFA are used cold, moved them from the fridge into an ice bucket
5. Turn on pump (setting 1 for rat, 2 for squirrel) and run saline through line to work out all air and prime the pump, get ready instruments (little scissors to cut right atrium, curved hemostat to clamp the aorta, big scissor to cut abdomen, big hemostat to grab bib cage and expose to heart)
6. Get the animal and anesthetize it with isoflurane starting at 5
7. Move animal to perfusion tray in hood, put the mask and maintain anesthesia level at 3 for squirrels and 2 for rats. Check for surgical plane of anesthesia with toe pinch method.
8. Open abdomen and thorax, exposing heart: cut across abdomen just beneath rib cage, cut diaphragm, lift away sternum with the long hemostat and cut away connective tissue
9. Move the heart and clamp descending aorta behind it with hemostat.
10. Make small incision in left ventricle and insert 18 gauge olive-tipped or blunted perfusion needle through left ventricle into ascending aorta (Usually the needle is inserted in the apex proximity and does not necessary reach the aorta). Tip should be visible through wall of aorta, shouldn't reach aortic arch, and should be at correct angle to facilitate max flow rate. If you can, clamp the heart and aorta with 2 hemostats to keep needle in place (sometimes it is not feasible and you have to hold the needle in place by yourself). Clip right atrium to release fluids.
11. Start the pump: perfuse with 0.9% saline ~5 minutes, pump setting 1 (34 ml/min) or 2 (62mL/min) until fluid from right atrium runs clear (~300 ml total, depends on animal size). Note end time of saline wash.
12. Turn pump off. Move uptake tubing to 4% PFA (to avoid air bubbles, squeeze tube or clamp it so that drop of saline protrudes from end). Restart pump, making sure it is on correct setting (sometimes moving the tube may touch the setting knob).
13. Perfuse with 4% PFA for ~10-15 min or until end of 'formalin dance' (~500 ml, 1L for squirrel). Note time of fixation (time that fixation tremors are seen)
14. At completion of perfusion, rinse tubing with clean water and replace needle/sleeve.

15. Remove head with blade or guillotine. Carefully expose and remove brain, making sure to cut optic chiasm without damage. Place brain in 4%PFA for 24 hours at 4C. *Best to do it in the fume hood.*
16. Remove whole spinal column, mark rostral end with marker for reference, and place in 4% PFA. *Best to do it in the fume hood.*
17. Clean up perfusion area and tools.
18. Return unused solutions to refrigeration and other support tools to proper storage.
19. Empty the tray with used solutions mixed to blood into the blue waste container with the proper PFA funnel (in the flammable cabinet), Do not Spill! when containers are full, tell Vet Services and they will dispose it.
20. Place carcass in refrigerator (pit tag disposed of with body- no need to remove) if it's after 8pm, otherwise bring carcass upstairs in the incinerator fridge, tag the bag with the yellow "pathological waste" and fill the log (with weight, the animal and your name). If you leave the carcass in room 20, make sure to bring it upstairs the morning after, or we get in troubles!!!!
21. Fill out disposition form in animal Suite, include IACUC protocol #

SOLUTIONS:

0.9% Saline total volume 1 L (make it fresh the day of experiment and keep it at 4°C):

9 g NaCl dissolved in 1L milliQ water, make up in 1L designated flask (in the fume hood)

4% PFA make up 2 L (good for one month at 4°C):

Sodium phosphate dibasic Na_2HPO_4 SIGMA S9763 FM 141.96

Sodium phosphate monobasic $\text{NaH}_2\text{PO}_4 \cdot \text{H}_2\text{O}$ SIGMA S9638 FM 138.0

Paraformaldehyde prilled, 95% 1 Kg cat#441244 SIGMA

1. Dissolve 21.87 g Dibasic Na_2HPO_4 (sodium phosphate) in ~1050 ml milliQ water. Make up in designated 2L flask in hood and put heat setting on 2-3 to help dissolve
2. Dissolve 6.35 g Monobasic $\text{NaH}_2\text{PO}_4 \cdot \text{H}_2\text{O}$ (sodium dihydrogen phosphate) in ~270 ml milliQ water in 500 ml flask
3. When dibasic dissolved, add 80g PFA prills (rinse PFA tray with milliQ):
 - a. Weigh out PFA in hood (move scale to hood)
 - b. Use designated weigh tray
 - c. Put designated thermometer in PFA while it dissolves, do not let heat rise above 60 deg C
4. When everything is dissolved, add monobasic to dibasic container (~ 2-3 hr)
5. Filter and measure volume as it filters
6. Finally bring to volume (2000 ml) with milliQ water
7. Do not rinse out flasks: cover with paraffin and store in hood
8. Dispose of all PFA waste in designated containers

BRAIN TISSUE PREPARATION:

5% Sucrose	w/V = g/100 ml	5g in 100mL PB
10% Sucrose	w/V = g/100 ml	10g in 100mL PB
15% Sucrose	w/V = g/100 ml	15g in 100mL PB
20% Sucrose	w/V = g/100 ml	20g in 100mL PB
30% Sucrose	w/V = g/100 ml	30g in 100mL PB

0.1M Phosphate Buffer (PB): 3.2g $\text{NaH}_2\text{PO}_4 \cdot \text{H}_2\text{O}$, 10.9g Na_2HPO_4 reach final volume of 1L, adjust pH to 7.4,

Antifreeze: 500 ml 0.1 M phosphate buffer pH 7.4, 300g sucrose, 10g polyvinylpyrrolidone (PVP-40), 300ml ethylene glycol. Let it dissolved overnight and adjust to final volume 1L with PB. Store at -20°C . *Before use it, test it overnight at -20°C : it should be liquid.*

24 hours after perfusion

Move brain to sucrose at 4°C . Follow sucrose gradient from 5%, 10%, 15% to 20% let the brain for two days in each gradient. Last move it in 30% sucrose and leave it until it sank or until you are ready to freeze it and cut it (it's better to leave it in sucrose than in -80°C , usually I leave it in 30% sucrose for 10 days).

Before moving the brain in 10% sucrose, it is necessary to block it for optimal penetration (cryoprotection):

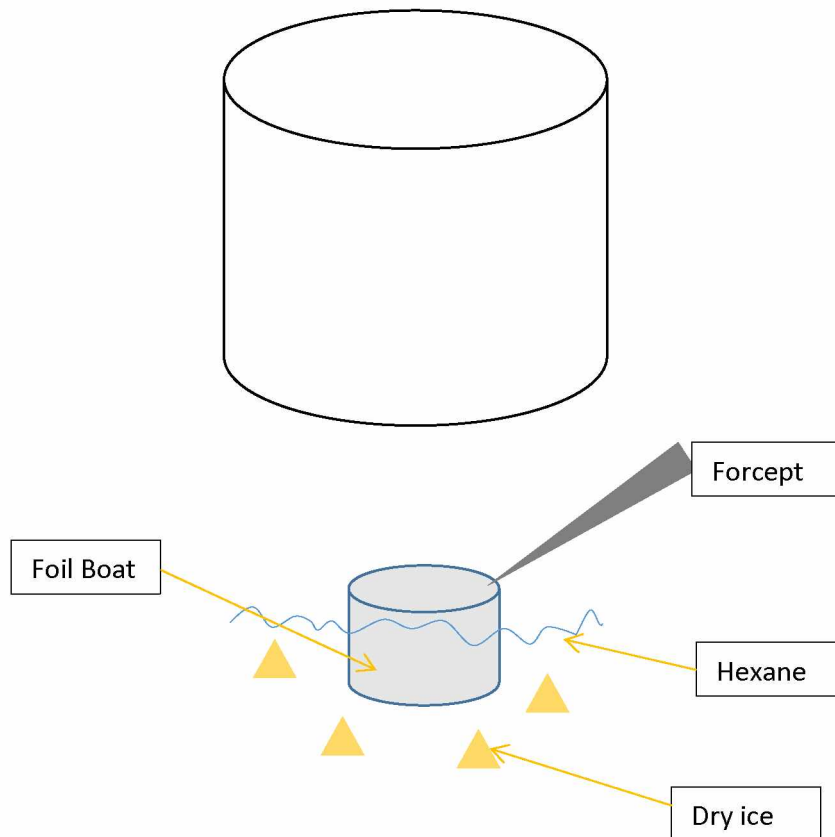
I cut the brain in 3 parts, at the cerebellum level and the rostral part. In theory the volume of sucrose solution should be at least 4 times the volume of your sample. (I used 50mL falcon tube). (DO NOT STORE IN ANTIFREEZE if you want to use cryostat!)

Flash Freezing procedure:



- Foil boat/ or plastic container
 - Dewar (store it at -20°C , so it is cold when you are ready to use it)
 - Forceps
 - n-Hexane, 95%
 - OCT
 - Thermometer – Omega thermocouple
 - Dry ice
 - Styrofoam box with lid
1. Prepare little boat with aluminum foil (I use a little glass vial and shaped around with foil) or if you have something like “dixie cup”, label it with animal ID.
 2. Get the Hexane solution cold, fill the dewar with hexane and start adding pieces of dry ice, until you reach temperature -45° to -50°C (control it with the thermocouple). If a little dewar is not available I have used a styrofoam coffee cup.
 3. Get the brain out of 30% sucrose, “rinse” it in OCT using a dixie cup (flip the brain around gentle to get rid of sucrose and have a first layer of OCT around)

4. Place the brain into the foil boat and add OCT to completely submerge the tissue (watch for bubbles)
5. Hold the boat with forceps and place it in the cold hexane in the dewar. The boat should be surrounded by liquid, you might need to add dry ice pieces (temperature gets warmer, you want to keep it as stable as possible).



6. Once OCT is becoming white, you can drop the boat to the bottom and let it there for 2minutes.
7. Then move the brain in a styrofoam container with dry ice until you freeze all the brains you need, then store the brains at -80°C not for a long time (max 2 weeks). *Even small oscillations in temperature can damage the tissue.*

Cutting the brain with the cryostat:

- Set cryostat temperature to -20°C
- Bring the brain to the cryostat in a styrofoam box with dry ice and leave it to equilibrate for at least 1 hour
- Label your 6-wells plate with animal ID, treatment, both on the lid and on the side of the plate
- Place OCT on the chuck and position the brain on it when the OCT is still liquid/non frozen
- Start cutting (follow the rat brain atlas, looking for symmetry between left and right hemisphere and similarity to the atlas at the top and bottom of the brain)
- Store the slices in 6-well plates with antifreeze in it. Place each slice in a consecutive well using all 6-well plate. For the squirrel forebrain use 5 6-wells plates, label each single well 1 to 30.
- At the end store the 6-well plate in the fridge 4°C overnight
- The day after change antifreeze solution by drawing off and adding fresh antifreeze with a transfer pipette (pay attention not to lose any brain slice) and store the plate at -20°C

Appendix A 6: General Immunohistochemistry Protocol

Day One

1. 6x10 min wash PBS
2. Incubate sections with 0.52% H₂O₂: 175 µl 30% H₂O₂ in 10 ml PBS for 30 min at room temperature (263 µl H₂O₂ in 15 ml PBS – 420 µl H₂O₂ in 24 mL PBS)
3. Rinse sections 6 x 5 min in PBS
4. Incubate in blocking (4% NGS normal goat serum + 0.2% Triton X-100 in PBS) for 2 h at 4°C with gentle agitation (10 ml blocking solution: 400 µl NGS + 200 µl Triton X-100 10% + 9400 µl PBS – 960 µl NGS + 480 µl Triton X-100 10% + 22560 ml PBS)
5. Incubate sections in *Primary Antibody (Ab)* diluted in PBS + 0.4% Triton X-100 24 or 48 hours at 4°C with gentle agitation (Time depends on Ab and Dilution)

Day Two

6. Rinse sections 6 x 10 min with PBS
7. Incubate sections in biotinylated *Secondary Antibody* (Vector labs BA-1000), diluted 1:600 in PBS + 0.4% Triton X-100 for 1 h at RT (or diluted 1:1000 in blocking solution, for 2 h at 4°C)
 - Make 12 ml: 480 µl Triton X-100 10% + 11.520 ml PBS + 20 µl antibody
 - Make 24 ml: 960 µl Triton X-100 10% + 23000 ml PBS + 40 µl antibody
8. Rinse sections 5 x 10 min in PBS
9. During rinse, prepare ABC kit (Vectastain ABC kit PK-6100). Let stand >30 minutes before use. To 10 ml PBS or PBS and 0.4% Triton X-100 (400 µl Triton X-100 10% and 9.6 ml PBS), add 45 µl Solution A then B (24 ml: 960 µl Triton X-100 10% + 22824 ml PBS + 108 µl A + 108 µl B)
10. Incubate sections with the A/B (Elite) solution 1 hour at room temperature
11. Rinse sections 6 x 5 min: 6 x 5 min in PBS if doing Brown DAB
3 x 5 min in PBS and 3 x 5 min in Sodium Acetate if doing Ni-DAB
12. Pre-incubate sections in DAB solution (suggested: 3 ml to large wells and 1 ml to control)**** for 15 min at room temperature then add 30% H₂O₂ (1 µl per 1 ml DAB) directly to plate for 1-5 min (or less depending: just until properly stained) and note time you allowed it to incubate (50 seconds/ 1 min) **CHECK at the end of the protocol for DAB waste disposal.**
13. Rinse 3 x 5 minutes in Sodium Acetate (0.175M 5.74g Sodium Acetate per 400mL MilliQ H₂O)
14. Rinse 3 x 5 minutes in PBS

Nickel DAB:

20mL Sodium Acetate add 0.5gr Nickel Sulfate and let it mix. Add 1 tabled DAB let it dissolve. pH solution to 7.2/7.3 and filter.

Add 1ul H₂O₂ 30% for each 1mL of DAB solution used

Brown DAB:

20mL PBS add 1 tabled DAB let it dissolve; pH solution to 7.2/7.3 and filter.

Add 1ul H₂O₂ 30% for each 1mL of DAB solution used

If Primary Ab is mouse, Secondary Ab has to be goat anti-mouse

If Primary Ab is rabbit, Secondary Ab has to be goat anti-rabbit

Immunohistochemistry Reagents:

PBS (0.01 M/ 10 mM Phosphate Buffered Saline – pH ~7.2)

PBS Stock Solution 10X:

- 12.0 g Na₂HPO₄ (anhydrous) (*Sodium Phosphate Dibasic SIGMA product # S9763, CAS# 7558-79-4*)
- 2.2 g NaH₂PO₄ · H₂O (*Sodium Phosphate Monobasic Monohydrate SIGMA product # S9638, CAS# 10049-21-5*)
- 85 g NaCl (*Sodium Chloride SIGMA product # S7653, CAS #7647-14-5*)

Add 900 mL MilliQ H₂O.

Mix well until all reagents are dissolved.

Reach final volume of 1 L with MilliQ H₂O.

Immuno reagents

PBS final solution 1X:

100mL PBS 10X, Stock Solution and 900 mL MilliQ H₂O.

Adjust pH to **7.2** with 0.1 N HCl or 1N NaOH.

Triton X-100 10% w/v

- In a small beaker weight 10 grams of Triton X-100 (*C34H62O11 VWR product #3929-2, CAS# 9002-93-1*)
- Add around 60 mL of MilliQ H₂O
- Let it on the stirring plane to dissolve (usually overnight), reach final volume 100 mL

Sodium Acetate 0.175 M

Sodium Acetate (*C2H3NaO3 Na acetate anhydrous Fluka product #71179, CAS# 127-09-3*)

2.87 g Sodium Acetate in 160 mL MilliQ H₂O

Let dissolve and reach final volume of 200mL.

0.3% H₂O₂

100uL of 30%H₂O₂ in 10 mL MilliQ H₂O

Keep it at 4C in a dark container(cover it with aluminum foil)

DAB (*C12H14N4. 4HCl SIGMA product # D5905*)

Tablet 10mg substrate per tablet store at -20C

1%DAB -10mg per 1mL MilliQ H₂O -

Add 5tablets (50 mg) and 5 mL MilliQ H₂O in the designated container (conical tube with magnetic stirring bar already contaminated) let mix and add 3 to 5 drops HCl 10N until the solution change colour to a clear brown/red.

Vectastain **ABC Kit elite** (*Vector Laboratories product# PK-6100*)

Ammonium Nickel II Sulfate hexahydrate (*SIGMA product # A1827, CAS # 7785-20-8*)

0.1 g Ammonium Nickel II Sulfate in 10 mL MilliQ H₂O

Monoclonal mouse anti cFos (c-Fos Antibody (C-10): sc-271243 Santa Cruz Biotech.)

Polyclonal rabbit anti histamine (Immunostar catalog number 22939 – required antigen retrieval step or perfusion with no PFA)

FOS Day One

15. 6x10 min wash PBS
 16. Warm the sodium citrate buffer in a water bath up to 80C
 17. Incubate sections with 175 ul 30% H₂O₂ in 10 ml PBS for 30 min at room temperature (263 ul H₂O₂ in 15 ml PBS, 420 uL in 24 mL PBS)
 18. Rinse sections 6 x 5 min in PBS
 19. Incubate slices in hot sodium citrate buffer and let it sit for 30 min (it should be cooling down by then)
 20. Rinse section 3 x 5 min in PBS
 21. Incubate in in blocking (4% NGS normal goat serum + 0.2% Triton X-100 in PBS) for 2 h at 4°C with gentle agitation (10 ml blocking solution: 400 µl NGS + 200 µl Triton X-100 10% + 9400 µl PBS; 24 mL blocking solution: 960 µl NGS + 480 µl Triton X-100 10% + 22560 µl PBS)
 22. Incubate sections in **mouse anti-cFos** primary antibody diluted 1:20,000 in PBS + 0.4% Triton X-100. Do not add to control well.
- Make 20 ml: 800 µl Triton X-100 + 19200 µl PBS + 1 µl cFos + then 48 hours at 4°C with gentle agitation
 - Make 24 mL: 960 µl Triton X-100 + 23040 µl PBS + 1.2 µl cFos + then 48 hours at 4°C with gentle agitation

FOS Day Two (48 hours later)

23. Rinse sections 6 × 10 min with PBS (*begin dissolving Ni in sodium acetate, but don't add H₂O₂ yet*)
 24. Incubate sections in biotinylated **goat anti-mouse** secondary antibody (Vector labs BA-1000), diluted 1:600 in PBS + 0.4% Triton X-100 for 1 h at RT (or diluted 1:1000 in blocking solution, for 2 h at 4°C)
- Make 12 ml: 480 µl Triton X-100 + 11.520 ml PBS + 20 µl antibody
 - Make 24 ml: 960 µl Triton X-100 + 23 ml PBS + 40 µl antibody
25. Rinse sections 5 × 10 min in PBS
 26. During rinse, prepare ABC kit (Vectastain ABC kit PK-6100). Let stand >30 minutes before use. To 10 ml PBS (or 400 µl Triton X-100 and 9.6 ml PBS), add 45 ul Solution A then B (24mL: 960 µl Triton X-100 + 108 µl A+ 108 µl B)
(add the DAB tablet to the Ni-Na Acetate solution and let it dissolve)
 27. Incubate sections with the A/B (Elite) solution 1 hour at room temperature
 28. Rinse sections 3 x 5 min in PBS
 29. Rinse sections 3 x 5 min in Sodium Acetate

30. Pre-incubate sections in **Ni sulfate-DAB solution** (suggested: 3 ml to large wells and 1 ml to control)**** for 15 min at room temperature then add H₂O₂ (1 ul per 1 ml Ni sulfate-DAB) directly to plate for 5-10 min (or less depending: just until properly stained) and note time you allowed it to incubate (cFos 1 min to 1 min and 30 sec)
31. Rinse 3 x 5 minutes in Sodium Acetate
32. Rinse 3 x 5 minutes in PBS
33. Incubate sections in **rabbit anti-Histamine** primary antibody 1:1,000 in PBS + 0.4% Triton X-100 over night at 4°C. Do not add to control well.

Day three (24 hours later)

34. Rinse sections 6 x 10 min with PBS (Dissolve 1 DAB tablet into 20mL PBS)
35. Incubate sections in biotinylated **goat anti-rabbit** secondary antibody (Vector labs BA-1000), diluted 1:600 in PBS + 0.4% Triton X-100 for 1 h at RT
- Make 12 ml: 480 µl Triton X-100 + 11.520 ml PBS + 20 µl antibody
36. Rinse sections 5 x 10 min in PBS
37. During rinse, prepare ABC kit (Vectastain ABC kit PK-6100). Let stand >30 minutes before use, 10 ml PBS (400 ul Triton X-100 and 9.6 ml PBS), add 45 ul Solution A then B
38. Incubate sections with the A/B (Elite) solution 1 hour at room temperature
39. Rinse sections 6 x 5 min in PBS
40. Pre-incubate sections in **DAB solution** (suggested: 3 ml to large wells and 1 ml to control)**** for 15 min at room temperature then add H₂O₂ (1 ul per 1 ml DAB) directly to plate for 5-10 min (or less depending: just until properly stained) and note time you allowed it to incubate (2 min)
41. Rinse 3 x 5 minutes in Sodium Acetate
42. Rinse 3 x 5 minutes in PBS
43. RECORD IN LOG

Nickel DAB:

20mL Sodium Acetate add 0.5gr Nickel Sulfate and let it mix. Add 1 tabled DAB let it dissolve. pH solution to 7.2/7.3 and filter.

Add 1ul H₂O₂ 30% for each 1mL of DAB solution used

Brown DAB:

20mL PBS add 1 tabled DAB let it dissolve; pH solution to 7.2/7.3 and filter.

Add 1ul H₂O₂ 30% for each 1mL of DAB solution used

Double staining Tanycytes and ADK (adenosine kinase) in the hypothalamus.

Protocol adapted from:

Sánchez E, Vargas MA, Singru PS, Pascual I, Romero F, Fekete C, Charli JL, Lechan RM. Tanycyte pyroglutamyl peptidase II contributes to regulation of the hypothalamic-pituitary-thyroid axis through glial-axonal associations in the median eminence. *Endocrinology*. 2009 May;150(5):2283-91

Mouse anti-vimentin Millipore # MAB3400 and **rabbit anti-ADK** Bethyl Lab #A304-280A

Humid chamber: Tupperware with a good sealed lid, inside few millimeters of water and a piece of nitrocellulose membrane (for Western blot) covering the bottom of the Tupperware. Place the 6-wells plate in the Tupperware. The 6-wells plate should be without lid, so make sure you mark the plate and its own lid (mark the lid and the plate with the same tape color) if you are using more than one 6-well plates at the time.

- Wash sections in PBS 6x10 min at RT
- Treat sections with 0.5% Triton X-100 in PBS for 20 min RT
- Treat sections with 10% Normal goat serum (original used horse serum) for 30 min in PBS
- Wash with PBS 3x10 min at RT
- The sections were then incubated in a humid chamber for 2 days at 4 C in a mixture of mouse anti vimentin (Millipore) diluted 1:1000 and rabbit polyclonal anti-ADK (Bethyl) at 1:4000 dilution in PBS, 1% BSA, 0.1% triton X-100 on a shaker
- Wash with PBS 3x10 min at RT

From now on work in a DARK ROOM!!!!

- Incubate the slices in a mixture of goat anti-mouse Alexa 488 (1:500, Invitrogen, NY) and goat anti-rabbit Alexa 456 (1:750, Invitrogen, NY) in PBS, 1% NGS in a dark room for 2 hours at RT on a shaker.
- Wash with PBS 3x10 min at RT in the dark room.
- In the dark, mount the slice on the glass slide leave them to dry for about 30 min (not too long), then apply the mounting media Vectashield and cover with a coverslip, seal with nail polish the edges. Let the slides dry for another 30 min before storing them in a dark box at 4°C.

Appendix A 9: Abdominal Transmitter Protocol

- Weight the animal (you might want to cover the jar so the AGS does not freak out)
- Start anesthesia in the jar (induced at 4-5%; maintained at 2-3%, delivered at 1.5L/min mixed with medical grade O₂)
- Implant the IPTT-300 (following the protocol # 467983: *The site may be shaved with a small shaver if necessary to locate the insertion site and the working area will be disinfected before starting on implantation. The skin will be lifted in a tent-shape and the trocar will be fully inserted underneath the skin, dispensing plunger will be pushed forward to release the transponder in the subcutaneous region, and the trocar will be removed. With finger roll the transponder to make sure it won't come out of the hole. The hole is plugged with a single drop of surgical glue applied using 25g needle and tuberculin syringe.*)
- Give the animal Buprenorphine-SR administrated SQ - it is very thick so it is necessary to use 20G needle , the drug is locked in room 005 (authorization needed to use it) –
- Sx prep of the animal: *Abdomen area will be shaved and washed 3 times with betadine (or generic equivalent). Prepare some wet gauze with tap water, use them for the wash with iodine/water/iodine/water/iodine/final wash 70& isopropyl alcohol rinse. Once the alcohol is dry the final prep is to apply full strength betadine solution by painting it on with a cotton tip swab. This is applied using a circling motion starting at the center of the shaved site and end at the shaved margin.*
- Move the Animal on the sx table on the heating blanket and add the eye lubricant.
- Open the sx pack
- Wear sx gloves and create the sterile area where you are performing the sx
- Put the drape on the AGS (*make a hole if it has not one to expose only the abdomen area and cover the rest of the body*)
- Make the skin incision with the scalpel blade #10 on the abdominal midline
- Using the hemostat retract the skin and the fat
- Make an incision along the linea alba with the scalpel blade, hold the blade up side down (the non-sharp edge is parallel/in contact with the rat abdomen)
- Using the hemostat open the muscle sheet along the linea alba
- Wet the ibutton with saline and insert it into the abdomen
- Start closing the incision (*the linea alba is sutured closed using a simple interrupted pattern with 3-0 chromic gut (absorbable) taper, RB-1, ~17mm needle (or equivalent). Drip 0.25% bupivacaine (2 drops) onto suture site from 1mL sterile syringe and 26ga needle. Sub-cutaneous tissue is gently approximated with a simple continuous pattern using 3-0 absorbable suture (Dexon or PDS) with an RB-1, ~17mm needle (or equivalent). The skin is then sutured with 3-0 Prolene/Surgilene (non absorbable), FS-2 or FS-1 (or equivalent) with cutting needle using a simple interrupted pattern. Finally, the closed skin incision may be sealed where needed with tissue adhesive (Vetbond) administered from a 1mL sterile syringe, 25ga needle.*)
- During skin closure the anesthesia can be gradually lowered to 0%
- Prepare a new cage to house the animal after sx

SX PACK:

- Scalpel blade holder
- Tooth forceps 2by1
- Non tooth forceps
- Small pair of scissor
- Small needle driver
- Hemostat 2 (just in case)
- Gauze (in case there is a bleeding)
- Drape for cover the animal

List Equipment:

- SX Gloves size 6 ½
- Transmitter gas-sterilized
- Mask/head cover/lab coat
- Isoflurane
- Water/heat blanket
- Eye lubricant
- Scalpel blade #10
- Chromic gut 3-0/PDS monosorb 3-0/Prolene 3-0
- Vetbond
- Needle 26G and 20G
- 10mL and 1 mL syringes
- Drapes
- Gauze
- IPTT-300
- Chlorexine to clean

Appendix B: Syllabi

Appendix B 1: Biology of Torpor Syllabus

Course information:

INDS XXX Biology of Torpor

Individual study 1 credit, 16 hours

Spring 2019

Instructor:

Course reading materials:

ARRIVE guidelines <https://www.nc3rs.org.uk/arrive-guidelines>

The instructor will assign current research papers relevant to the phenomenon of torpor.

Course description:

Torpor is an energy saving strategy widely used within species. This class is a 1 credit class that will expand the student knowledge of hibernation and torpor. The course will provide the student with well-known and novel information about torpor within different phylum (i.e. Arthropoda, Chordata), different class (i.e. Mammalia, Aves) and in different habitat (i.e. the Arctic, Madagascar).

A focus of the individual study will be also teaching how to perform a literature search, to be exposed to different journals and to present the information learnt during the class.

Course Goals:

The specific goals of the course are:

- to learn about torpor in different species
- to be able to perform a literature search
- become familiar with peer-reviewed journals

Student Learning Outcomes:

At the end of the course:

1. The student will perform literature searches by using specific keywords and search engines as PubMed and Google Scholar providing a list with paper title, keywords and the search engine used, twice during the course.
2. The student will describe what is an impact factor
3. The student will recognize different article structures
4. The student will recognize when an article follows the ARRIVE guidelines
5. The student will relate the article with the journal mission (demonstrate if the journal and the article are a good fit)

6. The student will critique the fit between the article and the journal, using the table provided.
7. The student will be able to outline some of the article qualities for a high impact factor journal
8. The student will describe the difference between Torpor and Hibernation
9. The student will describe and compare Torpor in difference species
10. The student will compare torpor in different climate and habitat.
11. The student will be able to combine the knowledge in an oral presentation
12. The student will be able to communicate his/her results to peers.

Course Calendar:

6 hours per week will be scheduled in line with the student's class schedule, the 6 hours will be broken down in 2.5 hours reading of the assigned paper, 2.5 hour for journal analysis and/or literature review and 1 hour per week will be used for paper discussion and review the journal format.

			Learning objectives	Due
Week 1	Different type of Torpor	PMID: 25123049 (Torpor) PMID: 8728854 (Estivation)	Definition of torpor and hibernation and discussion Paper-Journal Fit Form	
Week 2	Birds	PMID: 19929636 (Owl) PMID: 11285367 (Hummingbird)	Paper discussion Literature Search Process	• Paper-Journal Fit Form
Week 3	Mammals	PMID: 17919955 (Armadillo) PMID: 30158129 (Tenrec)	Paper discussion	• Paper-Journal Fit Form • Literature search (2 articles and keywords)
Week 4	Insect	PMID: 29356405 (Butterfly) PMID: 27853281 (Mosquito)	Paper discussion	• Paper-Journal Fit Form
Week 5	Reptiles Amphibia	PMID: 27424164 (Frog) PMID: 11919272 (Lizard)	Paper discussion	• Paper-Journal Fit Form • Literature search (2 articles and keywords)
Week 6	Primates	PMID: 15215852 (Lemur) PMID: 20520735 (non-Lemur)	Paper discussion	• Paper-Journal Fit Form
Week 7	Oral presentation			

Instructional methods:

This is an individual study course primarily based on independent reading of the material followed by an active discussion with the instructor summarizing the paper findings and the quality of the study.

Evaluation:

The overall grade will be based on the total score in the following categories:

Time management (Completing tasks, following deadline, organizing the presentation) 10%

Comprehension skills (summarizing and giving definitions) 15%

Critical thinking (the use of literature to interpret the results) 25%

Communication (content of presentation) 30%

Communication (mechanics of the presentation) 20%

98% - 100%	A+
93% - 97%	A
90% - 92%	A-
88% - 89%	B+
83% - 87%	B
80% - 82%	B-
78% - 79%	C+
73% - 77%	C
70% - 72%	C-
60% - 69%	D
below 60%	F

Category		1 Did not meet the expectations	2 fairly satisfactory	3 satisfactory	4 good	5 excellent
Time management	1. The student provides a list with paper title, keywords and search engine twice during the course.					
Time management	2. The student follows the schedule and she/he is on time					
Comprehension skills	3. The student summarizes the article findings					
Comprehension skills	4. The student is able to describe what is an impact factor					
Comprehension skills	5. The student is able to explain the ARRIVE guidelines					
Critical Thinking	6. The student is able to relate the article structure to the quality of the journal					
Critical Thinking	7. The student identifies the limitation of the study					
Critical Thinking	8. The student recognizes different article structures (review, research, report) and give examples during the discussion					
Critical Thinking	9. The student relates the article with the journal mission. During discussion the student is able to demonstrate if the article is/is not a good fit for the journal					
Critical Thinking	10. The student critiques the fit between the article and the journal filling up the evaluation					
Communication	11. The student describes the difference between Torpor and Hibernation					
Communication	12. The student describes and compares Torpor in difference species					

Communication	13. The student compares Torpor in different climate and habitat.					
Communication	14. The student uses appropriate graphics to present the information					
Communication	15. The student answers the questions with explanations and elaboration					
Communication	16. The student is overall prepared and knowledgeable					
	TOT					

Rubric to evaluate the mechanic of the presentation taken from:

Points	1	2	3	4	Total
Organization	There is no sequence of information and/or so much is missing that the presentation makes little sense.	Information is inconsistently organized (i.e. the visual information may be in order but the student jumps around).	Student presents information in logical sequence. More or less information would have been helpful.	Student presents adequate information in logical sequence.	
Graphics	Presentation includes no graphics or graphics are unrelated to the subject or distract from the message.	Presentation includes graphics that rarely support text and presentation. Graphics are too "busy".	Student's graphics relate to text and presentation.	Student's graphics explain and reinforce screen text and presentation.	
Mechanics	Presentation has four or more spelling errors and/or grammatical errors.	Presentation has three misspellings and/or grammatical errors.	Presentation has no more than two misspellings and/or grammatical errors.	Presentation has no misspellings or grammatical errors.	
Eye Contact	Student reads all of report with no eye contact.	Student occasionally uses eye contact, but still reads most of report.	Student maintains eye contact most of the time but frequently returns to notes.	Student maintains eye contact with audience, seldom returning to notes.	
Elocution	Student mumbles, incorrectly pronounces terms, and speaks too quietly for students in the back of class to hear.	Student's voice is low. Student incorrectly pronounces terms. Audience members have difficulty hearing presentation.	Student's voice is clear. Student pronounces most words correctly. Most audience members can hear presentation.	Student uses a clear voice and correct, precise pronunciation of terms so that all audience members can hear presentation.	
				Total Points:	/20

https://uni.edu/ietti/impact/experiences_in_inquiry_secondary/evaluation.html

Course policies:

Be punctual and communicate in advance any changes in schedule so we can locate a substitute assistant.

Support services:

Other reading materials will be available when necessary as well as longer discussion time if concepts have not been understood.

Disabilities services:

The instructor will work with the Office of Disabilities Services (208 WHITAKER BLDG, 474-5655) to provide reasonable accommodation to students with disabilities.

Student Material:

Journal Description				
Journal Name	Is it a Peer review Journal?	Impact factor	Does the Journal comply with the ARRIVE guidelines?	Mission statement

Paper-Journal Fit Evaluation Form				
Paper PMID:			Journal:	
	1	2	3	4
Original findings	Research confirm previous finding	Research confirm previous finding and add somehow new information	Research confirm previous finding and add novel information	Original and novel findings are presented
Journal topic of interests	The paper does not really fit in any categories/topics listed in the mission	Match at least one of the categories/topics listed in the mission	Match at least two of the categories/topics listed in the mission	Match more than two the categories/topics listed in the mission
ARRIVE guidelines	The paper does not follow the ARRIVE guidelines	Comply with the ARRIVE guidelines In only one the major sections (Methods/Results/Discussion)	Comply with the ARRIVE guidelines In two of the major sections (Methods/Results/Discussion)	Comply with the ARRIVE guidelines In all the major sections (Methods/Results/Discussion)
Methods	Only one lab technique is used	More than one lab technique are used but are similar (i.e. immunohistochemistry and histology)	More than one lab technique are used and are not similar (i.e. immunohistochemistry and PCR)	More than one lab technique are used and complement each other (i.e. immunohistochemistry, Western Blot, PCR and behavioral test)

Attending a conference

Instructor: Carla Frare

Course description:

Attending a conference is a fundamental step for your professional development; it combines both the professional and social aspects of your work, during this experience you will develop a professional network that will be essential along your career.

Preparation for a conference consists of three main sections: Before (what to do and how to prepare for it) During (how to handle the busy schedule) After (how to complete the travel, how to consolidate new connections).

Before the Conference:

- Identify personal goals: The student will answer the questions: Why do you want to attend the conference? What do you want to gain from this experience?
- Planning: The student will need to plan ahead. The student will notify as soon as possible the class instructors about the intention to attend the conference. Note the main deadline: as submission deadline, registration deadline and travel grant submission. The student will apply for travel grant and plan the trip with the travel office. When available the student will apply for the student award or poster competition.
- Schedule: Once the conference program is released the student will make a schedule with the different talks and event to attend. When attending talks of major interest in the student project, the student will read relevant papers to prepare. The student will make a list of people that she/he wants to meet.
- Presentation: Prepare poster and practice the presentation several times before leaving.

During the Conference:

- Take a picture with your poster, it is important to document your presentation, usually a picture is requested in the travel report
- Build your network: Don't hesitate to introduce yourself: "Hi I am Carla, grad student at UAF, are you enjoying the conference?/ what do you think about this talk?/ is this your first time at this conference?" , meet people from different institutions and industry. Connect over meals and after conference events. If you are part of the hosting society attend the society reception.
- Don't overbook yourself, schedule break and downtime. Take some time to look over your notes and to think how they may apply to your research project.

After the Conference:

- If you are interested in some of the institutions, plan a visit in the local labs or facilities.
- Fill the travel report and submit the receipts.

- Stay in touch with the new contacts; send a personal email after the conference or a follow up questions.
- Share the new acquired information at the next meeting with your peers.

Learning outcome:

The student will learn how to effectively attend a conference. The student will be able to use his/hers time to attend talks and poster sessions as well as networking.

Learning goals:

- The student will identify the criteria of a good talk after attending oral sessions.
- The student will learn how to formulate good questions. The student will listen to other people's questions – what makes a good or a bad question? What types of question stimulate discussions? What language people are using that makes a clear, concise question?
- The student will identify the good poster. First the student will identify personal preference in a poster layout. Then the student will evaluate the overall poster quality using the following questions: Does the poster tell a story? Can you read the figure legend and the text from a distance? Is there a "hero image"? Does it stimulate your curiosity?
- The student will learn how to introduce herself/himself: who you are, your institution, what you study, and why it is important. If possible, tailor the importance statement to each person so they immediately know why they should be interested in meeting you.
- The student will be able to explain her/his research in 1 minute/elevator speech
- The student will make at least one new connection, to start developing her/his networking skills.
- The student will learn about career options attending career development workshop or talk.

Course requirement:

Download the conference program and notes from the instructor.

Appendix B 3: Neurochemistry Research Syllabus

Course information:

INDS F497 Neurochemistry research

Individual study 4 credits

Instructor:

Course reading materials:

Immunohistochemistry technical notes and primary immunohistochemistry literature:

- Morgan JI, Curran T. Stimulus-transcription coupling in neurons: role of cellular immediate-early genes. *Trends Neurosci.* 1989 Nov;12(11):459-62.
- Hoffman GE, Smith MS, Verbalis JG. c-Fos and related immediate early gene products as markers of activity in neuroendocrine systems. *Front Neuroendocrinol.* 1993 Jul;14(3):173-213.

Papers relevant to the research topic.

Course description:

Neurochemistry research will teach basic laboratory practice, microscopy and immunohistochemistry, a specific laboratory technique widely used in Neuroscience. A focus of the individual study will be teaching brain pathways, brain anatomy and the physiological functions associated with each brain region as well as good laboratory technique.

Course Goals:

The specific goals of the course are:

- to be able to perform immunohistochemistry and microscopy
- to understand and apply good laboratory practice
- to learn the hibernation phenomenon
- to understand brain pathways related to the sleep-wake cycle, thermogenesis and energy balance.
- to learn hypothesis driven research
- become familiar with current peer-reviewed literature related to the specific research topic

Student Learning Outcome:

At the end of the course:

- 1- The student will perform immunohistochemistry independently.
- 2- The student will apply good laboratory technique.
- 3- The student will be able to describe the hibernation phenomenon.
- 4- The student will identify the brain regions in the arctic ground squirrel using a brain rat atlas.
- 5- The students will be able to describe the physiological functions of each investigated brain regions.
- 6- The student will be able to sketch the investigated neuronal pathways.
- 7- The student will apply literature-based knowledge to develop a research hypothesis and test it.

- 8- The student will collect and analyze data.
- 9- The student will compare the results with the initial hypothesis to proof or disproof it
- 10- The student will be able to connect the results with the current scientific models of sleep-wake cycle and thermoregulation.
- 11- The student will be able to communicate his/her results to peers.

Course Calendar:

12 hours per week will be scheduled in line with the student's class schedule. 9 hours will be assigned for laboratory experiments, data collection and analysis. 2 hours will be used for literature reviews and discussion and hypothesis development. 1 hour per week will be used for data discussion and updates to lab meeting.

Instructional methods:

This is an individual study course primarily based on hands on laboratory experience and literature review.

Evaluation:

1. Test of competence

The instructor will assign a brain region based on the rat atlas and ask to perform a full stain with assigned antibody (as cFos or GAD) and mount slides.

Referring to the Rat Brain Atlas, the student will choose the assigned slice from the wells where the brain is stored. He/She will perform immunohistochemistry without supervision. The student will deliver a mounted glass slides as a final product for the test together with the notebook pages of the procedure.

2. The evaluation of lab performance will be based on attention to details (as bubble on the mounted slides, if any slice have been lost during the procedure, if slices have been dried for too long etc...), completion of assigned tasks on time, notebook keeping and basic lab techniques as solutions making, use of the pipette, pH meter and chemical handles (location and storage of chemicals/reagents and waste disposal)
3. Cell count skill will be evaluated on count reproducibility between two different people on the same slides.
4. Hypothesis development. The student will start reading paper with the instructor and discuss them; we will formulate a hypothesis based on the paper. Afterwards the student will received a set of results which may prove or not the initial hypothesis. This will train the student to independently think of hypothesis while reading current literature
5. Intellectual engagement will be evaluated on the ability to contextualize the results with current literature. The student will perform literature review related to the background knowledge to be used for data interpretation.
6. Communication skills will be evaluated by poster organization/structure as well as poster presentation at local events as UAF Research Day and University of Alaska Biomedical Conference 2018.

Points	1	2	3	4	Total
Organization	There is no sequence of information and/or so much is missing that the presentation makes little sense.	Information is inconsistently organized (i.e. the visual information may be in order but the student jumps around).	Student presents information in logical sequence. More or less information would have been helpful.	Student presents adequate information in logical sequence.	
Graphics	Presentation includes no graphics or graphics are unrelated to the subject or distract from the message.	Presentation includes graphics that rarely support text and presentation. Graphics are too 'busy'.	Student's graphics relate to text and presentation.	Student's graphics explain and reinforce screen text and presentation.	
Mechanics	Presentation has four or more spelling errors and/or grammatical errors.	Presentation has three misspellings and/or grammatical errors.	Presentation has no more than two misspellings and/or grammatical errors.	Presentation has no misspellings or grammatical errors.	
Eye Contact	Student reads all of report with no eye contact.	Student occasionally uses eye contact, but still reads most of report.	Student maintains eye contact most of the time but frequently returns to notes.	Student maintains eye contact with audience, seldom returning to notes.	
Elocution	Student mumbles, incorrectly pronounces terms, and speaks too quietly for students in the back of class to hear.	Student's voice is low. Student incorrectly pronounces terms. Audience members have difficulty hearing presentation.	Student's voice is clear. Student pronounces most words correctly. Most audience members can hear presentation.	Student uses a clear voice and correct, precise pronunciation of terms so that all audience members can hear presentation.	
				Total Points:	/20

From https://uni.edu/ietti/impact/experiences_in_inquiry_secondary/evaluation.html

The overall grade will be based on:

Lab technique (perform the experiment in an efficient way as combining incubation time with other tasks as making solution) 51%

Time management (Completing tasks, following deadline, organizing and planning time spent in the lab with class work) 13%

Critical Thinking (the use of literature to interpret the results) 13%

Communication (post presentation) 13%

	1 Did not meet the expectations	2 fairly satisfactory	3 satisfactory	4 good	5 excellent
1 The student will perform immunohistochemistry independently					
2 The student will apply good laboratory technique					
3 The student will be able to describe the hibernation phenomenon.					
4 The student will identify the brain regions in the arctic ground squirrel using a brain rat atlas.					
5 The students will be able to describe the physiological functions of each investigated brain regions					
6 The student will be able to sketch the investigated neuronal pathways.					
7 The student will apply literature-based knowledge to develop a research hypothesis and test it.					
8 The student will collect and analyze data.					
9 The student will compare the results with the initial hypothesis to proof or disproof it					
10 The student will be able to connect the results with the current scientific models of sleep-wake cycle and thermoregulation.					
11 The student will be able to communicate his/her results to peers.					
TOT					

Course policies:

Be punctual and communicate in advance any changes in schedule so we can locate a substitute assistant.

Support services:

Other reading materials will be available when necessary as well as longer discussion time if concepts have not been understood.

Disabilities services:

The instructor will work with the Office of Disabilities Services (208 WHITAKER BLDG, 474-5655) to provide reasonable accommodation to students with disabilities.

Appendix B 4: Neuroendocrinology Syllabus

Course information: Neuroendocrinology

Individual study 2 credits

Instructor:

Course reading materials:

Textbook: An Introduction to Neuroendocrinology Micheal Wilkinson and Richard E. Brown second edition, Cambridge

Papers relevant to the topic

Course description:

Neuroendocrinology investigates the interaction between the endocrine system and the brain. In this introductory class the endocrine system and the central nervous system will be discussed as part of the same integration process that regulates physiological response.

Course Goals:

This course will provide an introduction to the interaction between hormones and brain, to help the student understand neuroendocrine integration. The specific goals of the course are:

- to be able to explain the basic concept of hormone physiology
- to be able to describe the interaction between hormones and CNS
- to apply his/her concepts of hormone physiology to better understand the CNS
- to develop a syllabus for a specific course topic

Student Learning Outcome:

At the end of the class the student will write a Neuroendocrinology class syllabus and develop a class structured on the essential concepts, the important aspects and the interesting topics in neuroscience.

Course Calendar:

	<u>Reading assignments for each week to discuss:</u>	<u>Activity in class:</u>
Week 1	Chapter 1 Classification of chemical messengers Chapter 2 The endocrine glands and their hormones	<ul style="list-style-type: none"> • Identify the basics concepts of the chapters • Develop the learning goals and outcomes for the chapter • Decide the topic to assign a paper for
Week 2	Chapter 3 The pituitary glands and their hormones Chapter 4 The hypothalamic hormones	
Week 3	Chapter 5 Neurotransmitters Chapter 6 Neurotransmitter and neuropeptide control of hypothalamic, pituitary and other hormones	
Week 4	Chapter 7 Regulation of hormone synthesis, storage, release, transport and deactivation Chapter 8 Regulation of hormone levels in the	

	bloodstream	
Week 5	Chapter 9 Steroid and thyroid hormone receptors Chapter 10 Receptors for peptide hormones, neuropeptides and neurotransmitters	
Week 6	Chapter 11 Neuropeptides I: classification, synthesis and co-localization with classical neurotransmitters Chapter 12 Neuropeptides II: function	
Week 7	Chapter 13 Cytokines and the interaction between the neuroendocrine and immune systems Chapter 14 Methods of the study of behavioral neuroendocrinology	
Week 8		Syllabus Outlines
Week 9	Research Paper	Discussion
Week 10	Research Paper	Discussion
Week 11	Research Paper	Discussion
Week 12		Identify which activities would be useful to reach the learning objectives of the class
Week 13		Identify which activities would be useful to reach the learning objectives of the class
Week 14		Final the student would have the syllabus completed with the reading lists of papers

Instructional methods:

This is an individual study course primarily based on discussions, at the end of each class the essential concepts will be highlighted for each chapter.

Evaluation:

The student will be evaluated based on the quality of the discussions and on the final syllabus.

Course policies:

Weekly meetings are required, reading of the chapters before the meetings are essential to develop the discussion.

Support services:

Other reading materials will be available when necessary as well as longer discussion time if concepts have not been understood.

Disabilities services:

The instructor will work with the Office of Disabilities Services (208 WHITAKER BLDG, 474-5655) to provide reasonable accommodation to students with disabilities.

Appendix B 5: Teachable Unit Optogenetics

Topic: **OPTOGENETICS**

Duration: 3 lectures (3 hours)

Goal and outcomes:

1. The student will familiarize with the concept of interdisciplinary using optogenetics as an example and he/she will be able to recognize the importance of cross-talking between disciplines.
 - a) The student will be able to illustrate how the different disciplines in optogenetics are important and how they are linked together.
 - b) The student will be able to apply the concept of interdisciplinary collaboration to other research techniques and in real life (defining the instructor's examples and giving examples themselves).
2. The student will be able to understand the principles and explain the utility of optogenetics. the student will also be able to apply the technique.
 - a) The student will be able to define the different elements required for optogenetics (channel rhodopsin, adenovirus, optic fiber,..).
 - b) The student will be able to describe how the light activates the neurons.
 - c) The student will be able to explain the basic principles and defend the validity of optogenetics.
3. The student will be able to critically discuss scientific papers.
 - a) The student will be able to find papers on the topic using web sources as "pubmed".
 - b) The student will be able to analyze a scientific paper using a template to help them training in identify the key points.
 - c) The student will be able to formulate a critical review on the paper after discussing it with classmates and instructor.

Pre-class assignment: student will read a paper assigned by the instructor about optogenetics technique (pure technique paper) and complete the analysis (following a template) about the paper-paper 1-.

Lecture Day 1:

- Class discussion about paper 1 (15 min)
- Lecture about how different disciplines are used in optogenetics and general overview of the technique (20 min).
- Group Activity: everyone write on a piece of paper an interdisciplinary technique that can think of, the instructor put all of them together and every group gets one. Group discussion and the conclusions of each group will be written and turned in (15 min).
- Last part of the class will be dedicated to a brief web research, using key words to find paper about the topic (10 min).

Pre class assignment: student will write a critical review on paper 1 and complete the analysis (following a template) about paper 2. The student will have a list of three papers on optogenetics found online.

Lecture Day 2:

- Lecture on optogenetics, how channel rhodopsin is delivered in the neurons, how the neurons are activated and the role of the optic fiber. How turning on the light make the neurons release neurotransmitters. How the same structure is used to block neurons response (40 min).
- Discussion on paper 2 (10 min).
- Group activity: the groups choose a common paper between the lists the student brought to class (5 min).
- The instructor will give directions about the group presentations (5 min).

Pre class assignment: student will write a critical review on paper 2 and complete the analysis (following a template) about paper 3. Each group will be ready to present.

Lecture day 3:

- Quiz on optogenetics (15 min)
- Small Group discussion on paper 3 (10 min)
- Group presentations and discussions, each student will have to grade each presentations (it won't count as a grade but they will get point to do so and turn in the grade sheet) (35 min).

Critical review on paper 3 to turn in next class.

Presentations

There will be tow kind of presentation for this unit:

- short 10 min presentations for a non-scientific audience about optogenetics.
- *30 seconds elevator talk* to an expert to convince him/her about the validity of the technique.

Post-assessment of this topic will occur with a short quiz at the end of the teachable unit.

On the final project the students may apply this knowledge on the experimental design for their research topic. On the final exam the students will have to know which the principles of optogenetics and its utility are.

IMMUNOHISTOCHEMISTRY

SHORT INTRODUCTION TO THE BASIC PRINCIPLES OF IMMUNOHISTOCHEMISTRY AND LABORATORY PROTOCOLS

CARLA FRARE

PhD student

For undergraduate teaching purpose, all materials and information were compiled from several online resources. All citations included.

“Immunohistochemistry (IHC) combines anatomical, immunological and biochemical techniques to identify tissue components (e.g. proteins) by the interaction of target antigens with specific antibodies tagged with a visible label. IHC makes it possible to visualize the distribution and localization of specific cellular components within cells (Rogers and Hoffman, 2012).

Introduction

History

IHC takes its name from the roots "immuno", in reference to antibodies used in the procedure, and "histo," meaning tissue. “The principle of IHC has been known since the 1930s, but it was not until 1942 that the first IHC study was reported. Coons *et al.* (1942) used FITC-labeled antibodies to identify *Pneumococcal* antigens in infected tissue. Since then, improvements have been made in protein conjugation, tissue fixation methods, detection labels and microscopy, *making immunohistochemistry a routine and essential tool in diagnostic and research laboratories.* “

(From <https://www.thermofisher.com>)

Applications

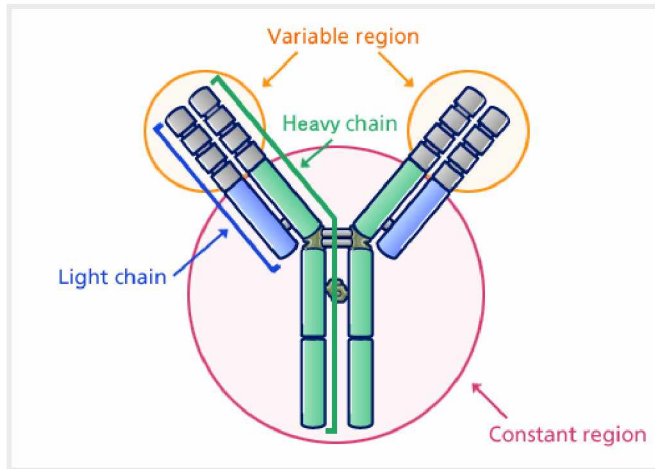
“IHC is used for disease diagnosis, drug development and biological research. Using specific tumor markers, physicians use IHC to diagnose a cancer as benign or malignant, determine the stage and grade of a tumor, and identify the cell type and origin of a metastasis to find the site of the primary tumor. IHC is also used in drug development to test drug efficacy by detecting either the activity or the up- or down-regulation of disease targets. Samples are prepared on individual slides, or multiple samples can be arranged on a single slide for comparative analysis. IHC slides are processed and stained manually. Samples can be viewed by either light or fluorescence microscopy, and advances in the last 15 years have improved the ability to capture images. Visualizing an antibody-antigen interaction can be accomplished in a number of ways. In the most common instance, an antibody is conjugated to an enzyme, such as peroxidase, that can catalyse a colour-producing reaction. Alternatively, the antibody can also be tagged to a fluorophore, such as fluorescein or rhodamine (see immunofluorescence).

Retrieved From *ThermoFisher Scientific and Wikipedia*

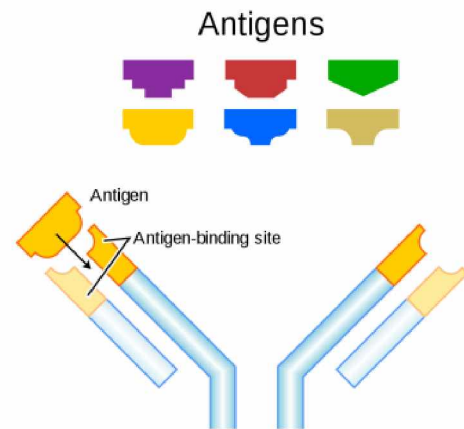
Antibodies

Structure

The immune system is a system of biological structures and processes within an organism that protects against disease. To function properly, an immune system must detect a wide variety of agents, known as pathogens, from viruses to parasitic worms, and distinguish them from the organism's own healthy tissue.



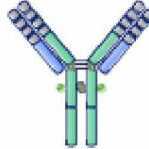
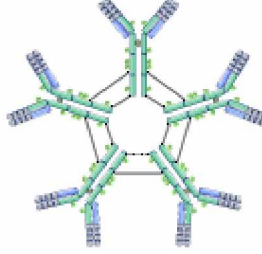
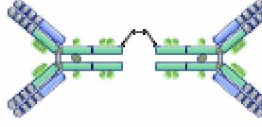
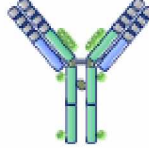
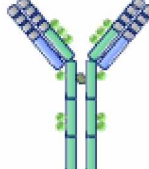
<http://www.kyowa-kirin.com/antibody/basics/structure.html>



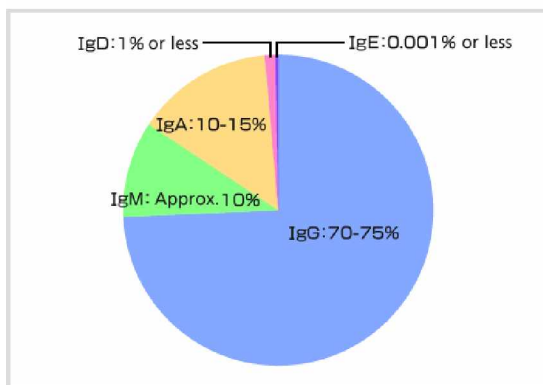
<https://en.wikipedia.org/wiki/Antibody>

“Antibodies are immune system-related proteins called immunoglobulins. Each antibody consists of four polypeptides– two heavy chains and two light chains joined to form a "Y" shaped molecule. The amino acid sequence in the tips of the "Y" varies greatly among different antibodies. This variable region, composed of 110-130 amino acids, give the antibody its specificity for binding antigen. The variable region includes the ends of the light and heavy chains. Treating the antibody with a protease can cleave this region, producing fragment antigen binding (Fab) that includes the variable ends of an antibody. The constant region determines the mechanism used to destroy antigen. Antibodies are divided into five major classes, IgM, IgG, Iga, IgD, and IgE, based on their constant region structure and immune function. There are 5 types of heavy chain constant regions in antibodies. The 5 types - IgG, IgM, IgA, IgD, IgE - (isotypes) are classified according to the type of heavy chain constant region, and are distributed and function differently in the body.”

(From <http://www.biology.arizona.edu/immunology/tutorials/antibody/structure.html>)

IgG	IgG is the main antibody in blood. It is the only isotype that can pass through the placenta, and IgG transferred from the mother's body protects a newborn until a week after birth. IgG widely distributed to the blood and tissue, and protects the body.	
IgM	IgM is made up of 5 antibodies. IgM has a key role in the initial immune system. It is distributed to the blood.	
IgA	Secreted IgA is made up of 2 antibodies. It is distributed to <u>serum</u> , nasal discharge, saliva, breast milk and bowel fluid. Breast milk protects the gastrointestinal tract of newborns from bacterial and viral infection (maternal immunity).	
IgD	IgD is present on the surface of B cells and plays a role in the induction of antibody production.	
IgE	IgE is believed to be related to immunity reactions to parasites, and has recently become known as a key factor of allergies such as pollinosis.	

Population of 5 types of antibodies in blood (%)



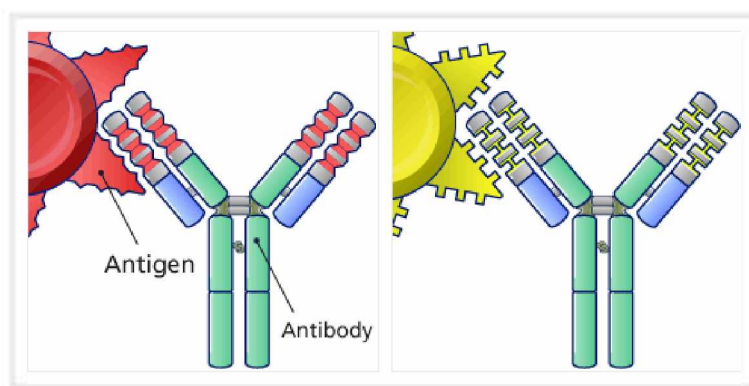
Retrieved From:

<http://www.biology.arizona.edu/immunology/tutorials/antibody/structure.html>

<http://www.kyowakirin.com/antibody/basics/specificity.html>

Antibody-antigen interaction

Antibodies bind to a specific antigen using their variable region. This process is called the specificity of an antibody toward that antigen. An antibody has a pair of variable regions, one on the left and one on the right, and they bind to the same antigen. The binding may involve **electrostatic interactions, hydrophobic interactions, hydrogen bonds and van der Waals forces**. Since these interactive forces are relatively weak, the “fit” between antigen and its complementary site on the antibody must occur over an area large enough to allow the summation of all the possible available interactions. This requirement is the basis for the exquisite specificity observed in immunologic interactions. This fit is often compared to a lock and a key (Benjamini et al., 2000).



(Retrieved From <http://www.kyowa-kirin.com/antibody/basics/specificity.html>)

Antibody Production

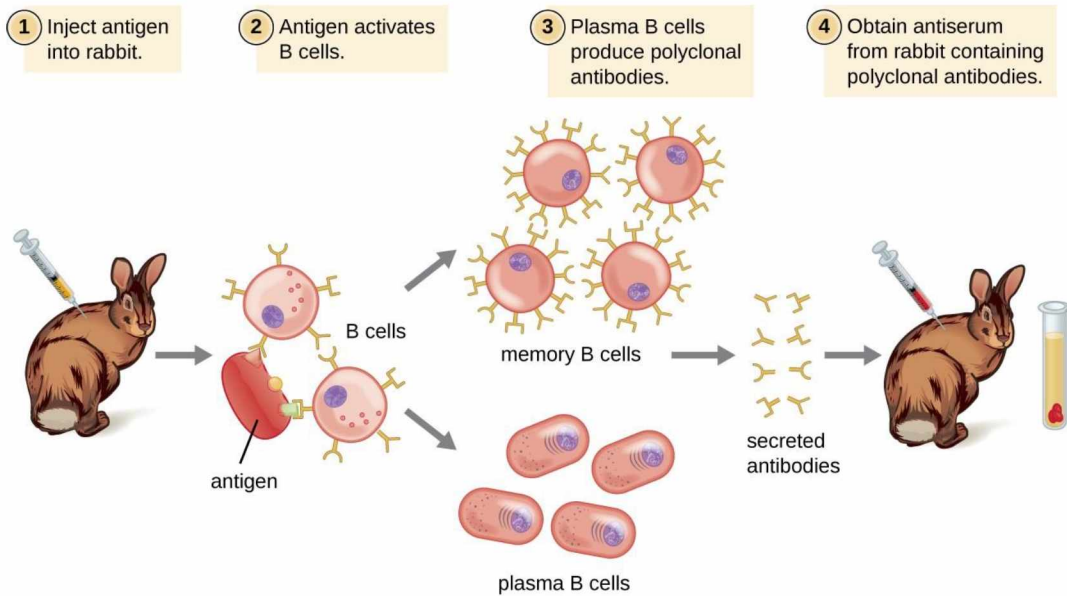
Animals have an immune system that produces antibody corresponding to each foreign substance (antigen) that enters the body. Antigen-antibody Interactions are extremely high specific, each antibody bind only to its target antigen to remove it.

Researcher can produce an antibody against the molecule that is the target of study, as a label to recognize the target molecule.

Polyclonal Antibody

“Antibodies used for research and diagnostic purposes are often obtained by injecting a lab animal such as a rabbit or a goat with a specific antigen. Within a few weeks, the animal’s immune system will produce high levels of antibodies specific for the antigen. These antibodies can be harvested in an antiserum, which is whole serum collected from an animal following exposure to an antigen. Because most antigens are complex structures with multiple epitopes, they result in the production of multiple antibodies in the lab animal. This so-called polyclonal antibody response is also typical of the response

to infection by the human immune system. Antiserum drawn from an animal will thus contain antibodies from multiple clones of B cells, with each B cell responding to a specific epitope on the antigen.



Lab animals are usually injected at least twice with antigen when being used to produce antiserum. The second injection will activate memory cells that make class IgG antibodies against the antigen. The memory cells also undergo affinity maturation, resulting in a pool of antibodies with higher average affinity. Affinity maturation occurs because of mutations in the immunoglobulin gene variable regions, resulting in B cells with slightly altered antigen-binding sites. On re-exposure to the antigen, those B cells capable of producing antibody with higher affinity antigen-binding sites will be stimulated to proliferate and produce more antibody than their lower-affinity peers. An adjuvant, which is a chemical that provokes a generalized activation of the immune system that stimulates greater antibody production, is often mixed with the antigen prior to injection.

Antiserum obtained from animals will not only contain antibodies against the antigen artificially introduced in the laboratory, but it will also contain antibodies to any other antigens to which the animal has been exposed during its lifetime. For this reason, antisera must first be “purified” to remove other antibodies before using the antibodies for research or diagnostic assays.”

(From <https://courses.lumenlearning.com/microbiology/chapter/polyclonal-and-monoclonal-antibody-production/>)

Monoclonal Antibody

“Some types of assays require better antibody specificity and affinity than can be obtained using a polyclonal antiserum. To attain this high specificity, all of the antibodies must bind with high affinity to a single epitope. This high specificity can be provided by **monoclonal antibodies (mAbs)**. Unlike polyclonal antibodies, which are produced in live animals, monoclonal antibodies are produced *in vitro* using tissue-culture techniques. mAbs are produced by immunizing an animal, often a mouse, multiple times with a specific antigen. B cells from the spleen of the immunized animal are then removed. Since normal B cells are unable to proliferate forever, they are fused with immortal, cancerous B cells called myeloma cells, to yield **hybridoma** cells. All of the cells are then placed in a selective medium that allows only the hybridomas to grow (HAT medium); unfused myeloma cells cannot grow, and any unfused B cells die off. The hybridomas, which are capable of growing continuously in culture while producing antibodies, are then screened for the desired mAb. Those producing the desired mAb are grown in tissue culture; the culture medium is harvested periodically and mAbs are purified from the medium. This is a very expensive and time-consuming process. It may take weeks of culturing and many liters of media to provide enough mAbs for an experiment or to treat a single patient. mAbs are expensive.” (From <https://courses.lumenlearning.com/microbiology/chapter/polyclonal-and-monoclonal-antibody-production/>)

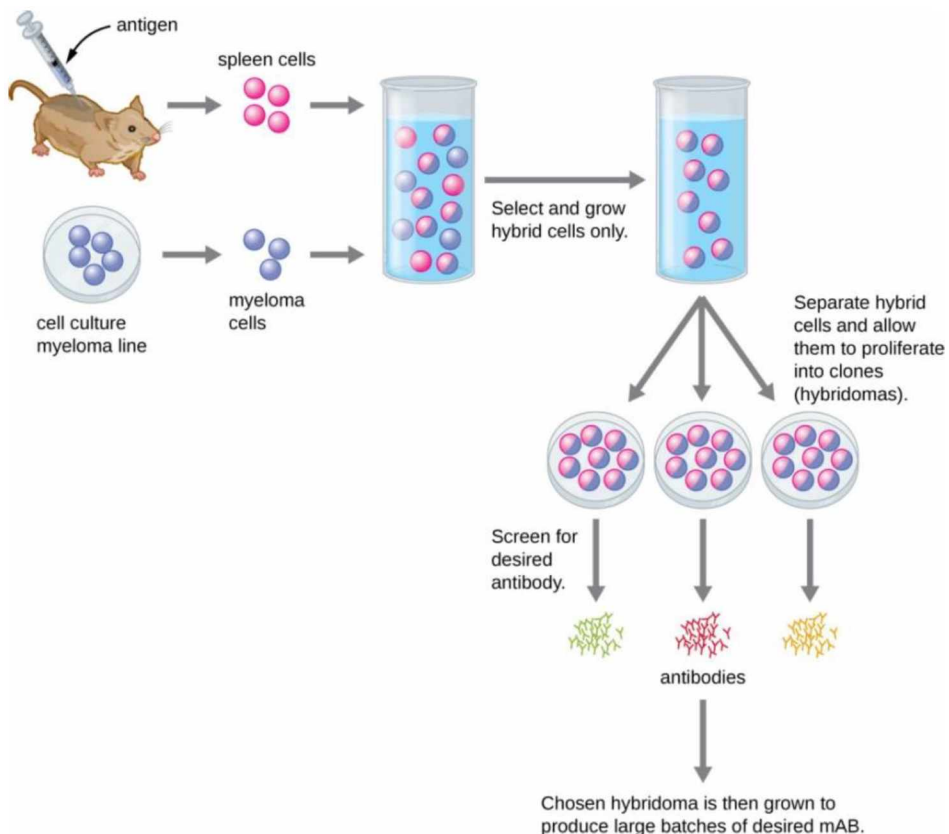


Table 1. Characteristics of Polyclonal and Monoclonal Antibodies	
Monoclonal Antibodies	Polyclonal Antibodies
Expensive production	Inexpensive production
Long production time	Rapid production
Large quantities of specific antibodies	Large quantities of nonspecific antibodies
Recognize a single epitope on an antigen	Recognize multiple epitopes on an antigen
Production is continuous and uniform once the hybridoma is made	Different batches vary in composition

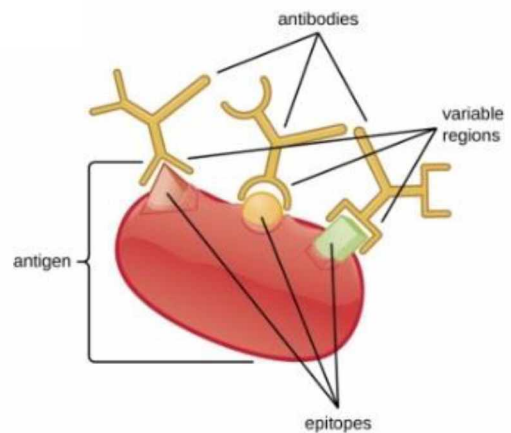
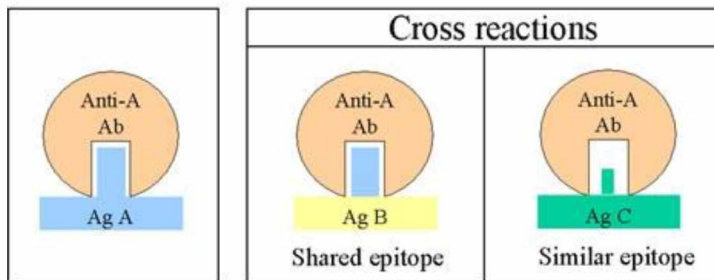
(From <https://courses.lumenlearning.com/microbiology/chapter/polyclonal-and-monoclonal-antibody-production/>)

Cross reactivity

"An antibody's specificity results from the antigen-binding site formed within the variable regions—regions of the antibody that have unique patterns of amino acids that can only bind to target antigens with a molecular sequence that provides complementary charges and noncovalent bonds. There are limitations to antibody specificity, however. Some antigens are so chemically similar that cross-reactivity occurs; in other words, antibodies raised against one antigen bind to a chemically similar but different antigen. Consider an antigen that consists of a single protein with multiple epitopes. This single protein may stimulate the production of many different antibodies, some of which may bind to chemically identical epitopes on other proteins.

Cross-reactivity is more likely to occur between antibodies and antigens that have low affinity or avidity. Affinity, which can be determined experimentally, is a measure of the binding strength between an antibody's binding site and an epitope, whereas avidity is the total strength of all the interactions in an antibody-antigen complex (which may have more than one bonding site). Avidity is influenced by affinity as well as the structural arrangements of the epitope and the variable regions of the antibody. If an antibody has a high affinity/avidity for a specific antigen, it is less likely to cross-react with an antigen for which it has a lower affinity/avidity."

(From <https://courses.lumenlearning.com/microbiology/chapter/polyclonal-and-monoclonal-antibody-production/>)



(From <http://www.microbiologybook.org/mayer/ab-ag-rx.htm>)

Sample preparation

Preparation of the sample is critical to maintain cell morphology, tissue architecture and the antigenicity of target epitopes. This requires proper tissue collection, fixation and sectioning. A common solution is paraformaldehyde.

Tissue Collection and Perfusion

Tissue must be rapidly preserved to prevent protein degradation and tissue architecture damages. Often, the tissue is perfused. Perfusion is performed on anesthetized animals by using a peristaltic pump, tissue is rinsed with sterile saline to eliminate any blood residual and to prevent the detection of hematologic antigens, which may interfere with the detection of target protein. Next, the target organ or tissue is collected for IHC. (From <https://www.scribd.com/document/112873948/IHC>)

Tissue Fixation

“The broad objective of tissue fixation is to preserve cells and tissue components in a “life-like state” and to do this in such a way as to allow for the preparation of thin, stained sections. For practical purposes fixation aims to prevent or arrest the degenerative processes which commence as soon as a tissue is deprived of its blood supply. Loss and diffusion of soluble substances must be avoided as far as possible by precipitation or coagulation of these components or by cross-linking them to other insoluble structural components. Tissues must retain reactivity to stains and other reagents including antibodies and nucleic acid probes.” (From <https://www.leicabiosystems.com/pathologyleaders/fixation-and-fixatives-1-the-process-of-fixation-and-the-nature-of-fixatives/>)

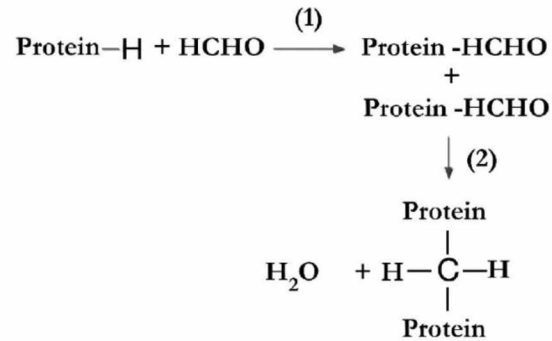
“Fixation chemically crosslinks proteins or reduces protein solubility, which can mask target antigens during prolonged or improper fixation. Therefore, the right fixation method must be optimized based on the application and the target antigen to be stained. The most common fixative is formaldehyde, a semi-reversible, covalent crosslinking reagent that can be used for perfusion or immersion fixation for any length of time, depending on the level of fixation required”. (Retrieved from <https://www.thermofisher.com>)

“The non-coagulant fixing agents chemically react with proteins and other cell and tissue components, becoming bound to them by addition and forming inter-molecular and intra-molecular cross-links, covalent chemical bonds. Because these agents are reactive compounds they bind to a variety of chemical groups in tissues, often affecting the charge at the site of attachment.

These crosslinking fixatives—especially formaldehyde—tend to preserve the secondary structure of proteins and may protect significant amounts of tertiary structure as well. (From <https://www.leicabiosystems.com/pathologyleaders/fixation-and-fixatives-1-the-process-of-fixation-and-the-nature-of-fixatives/>)

<p>Paraformaldehyde is a polymerized form of formaldehyde, usually obtained as a fine white powder</p>	$\text{HO}-\left[\begin{array}{c} \text{H} \\ \\ \text{C}-\text{O} \\ \\ \text{H} \end{array} \right]_{8-100}-\text{H}$
--	--

(Thavarajah et al., 2012)



Sectioning and Mounting

The decision to section tissue is dependent upon the application used; Formalin-fixed tissue is sectioned into slices as thin as 4 to 5µm with a pre-cooled cryostat (−20°C) and mounted to adhesive glass slides or stored in well-plates for free floating immunohistochemistry

Immunohistochemistry

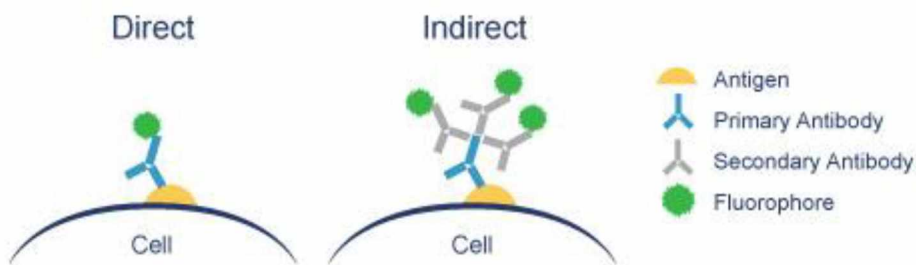
Immunohistochemistry (IHC) is the process of using monoclonal or polyclonal antibodies to detect proteins (antigens) in cells within a tissue section as brain but other tissue as liver, heart.... IHC localizes specific proteins in tissue with labeled antibodies based on antigen-antibody interactions. This method gives information in a spatial manner (e.g. specific proteins are detected in specific brain structures). A marker including fluorescent dyes and enzymes visualizes the immune reactive products.

Direct: Primary Antibody Only

“Direct method is one step staining method, and involves a labeled antibody (i.e. FITC conjugated antiserum) reacting directly with the antigen in tissue sections. This technique utilizes only one antibody and the procedure is short and quick. However, it is insensitive due to little signal amplification and rarely used since the introduction of indirect method.” (From <http://www.abcam.com/secondary-antibodies/direct-vs-indirect-immunofluorescence>)

Indirect: Primary and Secondary Antibodies

“Indirect method involves an unlabeled primary antibody (first layer) which reacts with tissue antigen, and a labeled secondary antibody (second layer) reacts with primary antibody (Note: The secondary antibody must be against the IgG of the animal species in which the primary antibody has been raised). This method is more sensitive due to signal amplification through several secondary antibody reactions with different antigenic sites on the primary antibody. In addition, one labeled second layer antibody can be used with many first layer antibodies (raised from the same animal species) to different antigens. The second layer antibody can be labeled with a fluorescent dye called indirect immunofluorescence method. The second layer antibody may be labeled with an enzyme such as peroxidase, alkaline phosphatase or glucose oxidase, and this is called indirect immunoenzymatic method.” (From <http://www.abcam.com/secondary-antibodies/direct-vs-indirect-immunofluorescence>)



(From <http://www.abcam.com/secondary-antibodies/direct-vs-indirect-immunofluorescence>)

Immunohistochemistry Steps

- Incubate sections with H_2O_2 (hydrogen peroxide). Endogenous peroxide characterized the tissue. To avoid peroxide activity a pre-treatment with H_2O_2 produce an irreversible inactivation. This step will decrease non-specific background.
- Incubate in in blocking solution from the animal used for the secondary antibody. If secondary antibody is made in goat, normal goat serum (NGS) is used. Serum carries antibodies that will bind to the non-specific epitopes in the tissue, thus blocking the antibody used from binding to these non-specific epitopes. Important step when using polyclonal antibodies.
- Incubate sections in *Primary Antibody (Ab)*. Dilution reported in the package is a starting point; the optimal dilution for the sample is identified by titration.
- Incubate sections in biotinylated *Secondary Antibody*. Dilution reported in the package is a starting point; the optimal dilution for the sample is identified by titration.

- Amplification step

Amplification step using the ABC kit (From <https://www.thermofisher.com>):

Biotin, also known as vitamin H, is a small molecule (MW 244.3) that is present in tiny amounts in all living cells and is critical for a number of biological processes. The valeric acid side chain of the biotin molecule can be derivatized in order to incorporate various reactive groups that are used to attach biotin to other molecules. In the context of IHC, biotin is conjugated to antibodies or to the enzyme reporters used to detect target antigens (e.g. Biotinylated Goat Anti-Rabbit IgG Antibody)

The extraordinary affinity of avidin for biotin allows biotin-containing molecules in a complex mixture to be specifically bound to avidin. **Avidin** is a glycoprotein found in the egg white and tissues of birds, reptiles and amphibia. It contains four identical subunits having a combined mass of 67 to 68kDa. Each subunit consists of 128 amino acids and binds one molecule of biotin; thus, a total of four biotin molecules can bind to a single avidin molecule. The extent of glycosylation on avidin is very high; carbohydrates account for about 10% of the total mass of the tetramer. Avidin has a basic isoelectric point (pI) of 10 to 10.5 and is stable over a wide range of pH and temperatures. Extensive chemical modification has little effect on the activity of avidin, making it especially useful for protein purification. However, because of its carbohydrate content and basic pI, avidin exhibits relatively high nonspecific binding properties.

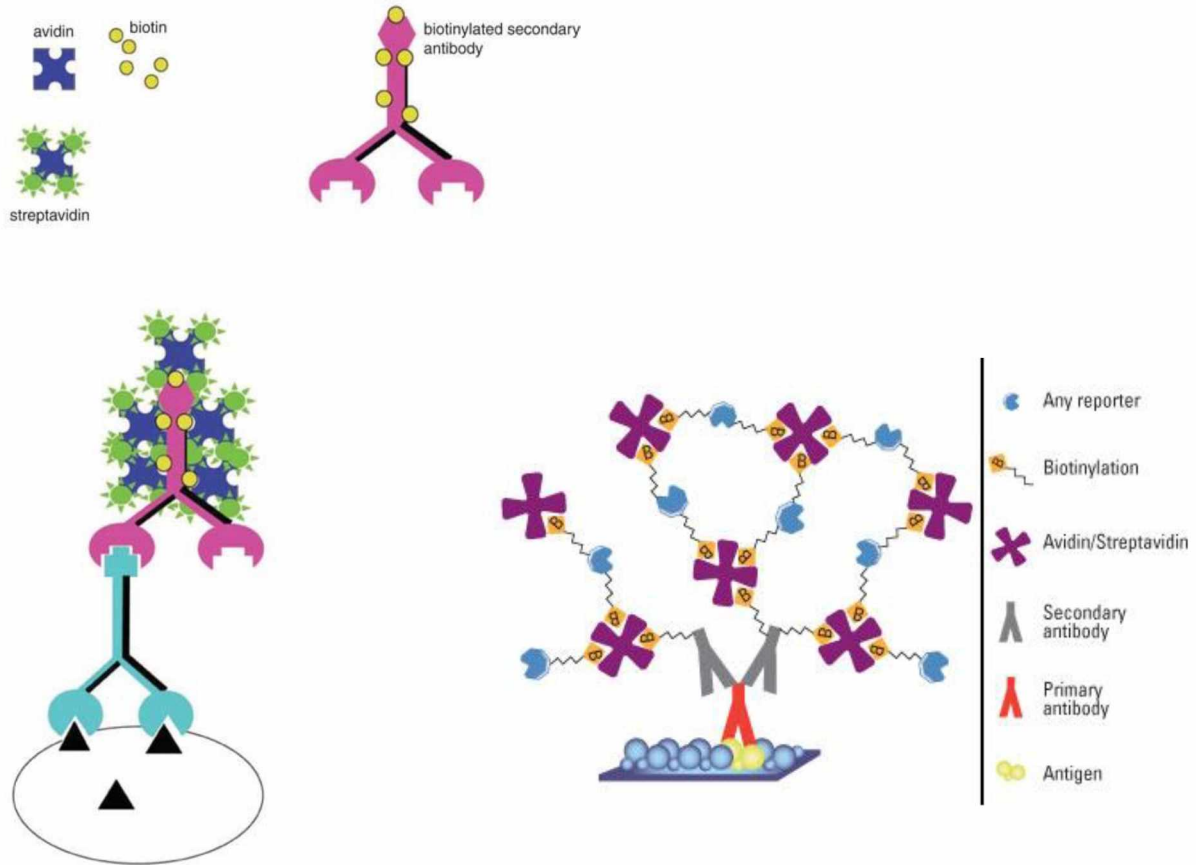
Avidin-biotin binding is the strongest known non-covalent interaction between a protein and ligand. The bond formation between biotin and avidin is very rapid, and once formed, is unaffected by extremes in pH, temperature, organic solvents and other denaturing agents. These features of avidin make detecting or purifying biotin-labeled proteins or other molecules particularly useful for a number of biomedical applications.

Streptavidin is isolated from *Streptomyces avidinii*, and is similar in size and affinity for biotin. In contrast to avidin, though, streptavidin is not glycosylated, which makes the protein less-prone to nonspecific binding in IHC applications. There are considerable differences in the composition of avidin and streptavidin, but they are remarkably similar in other respects. Streptavidin is also a tetrameric protein, with each subunit binding one molecule of biotin with affinity similar to that of avidin. Streptavidin is much less soluble in water than avidin. Guanidinium chloride at pH 1.5 will dissociate avidin and streptavidin into subunits, but streptavidin is more resistant to dissociation.

Reporter intensity is a function of the localized enzyme activity, and improved sensitivity can be achieved by increasing the number of enzyme molecules bound to the target antigen. The multiple biotin binding sites in each tetravalent avidin molecule are ideal for achieving this amplification.

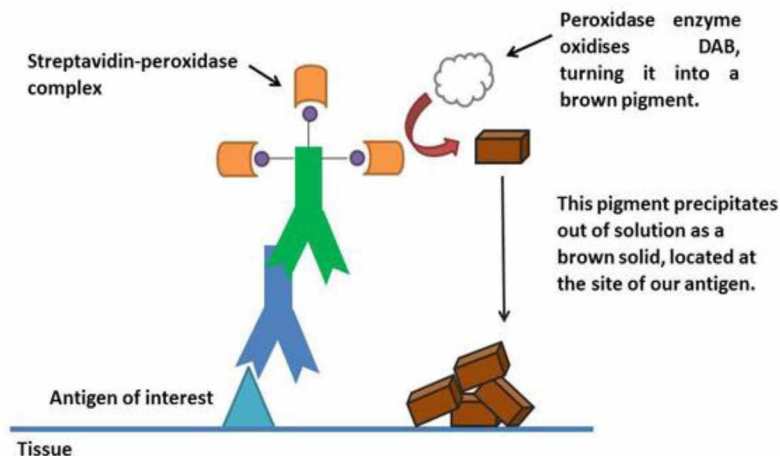
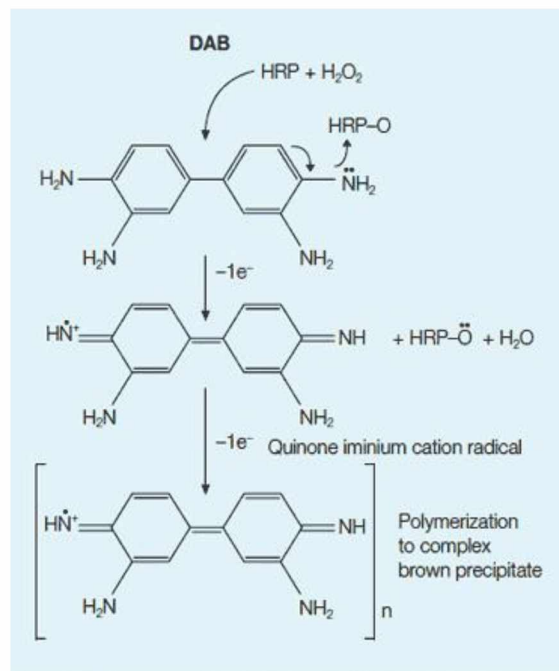
1. The primary antibody is incubated with the tissue sample to allow binding to the target antigen.
2. A biotinylated secondary antibody, with specificity against the primary antibody, is incubated with the tissue sample to allow binding to the primary antibody.
3. **A biotinylated enzyme** (HRP or AP) is pre-incubated with free avidin to form large avidin-biotin-enzyme complexes. Typically, the avidin and biotinylated enzyme are mixed together in a specified ratio (1:1) to prevent avidin saturation and incubated for about 15 minutes at room temperature to form the complex.
4. An aliquot of this solution is then added to the tissue sample, and any remaining biotin-binding sites on the avidin bind to the biotinylated antibody that is already bound to the tissue.

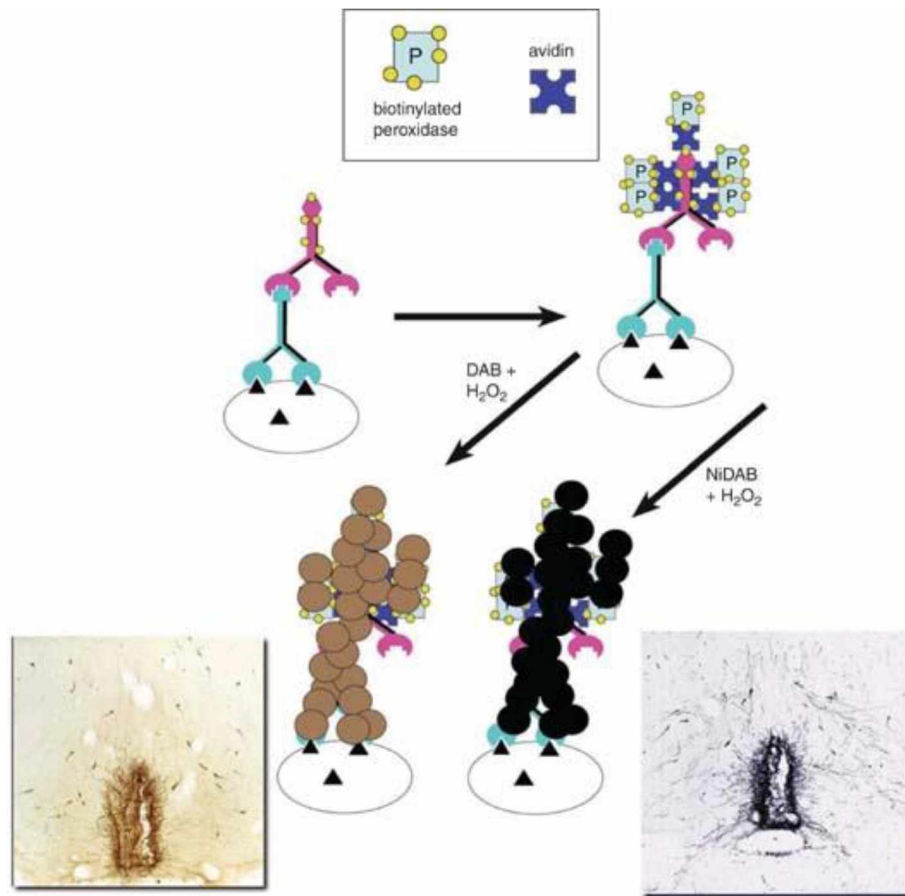
The result is a greater concentration of enzyme (three enzyme molecules to one avidin molecule) at the antigenic site and therefore an increase in signal intensity and sensitivity upon addition of substrate.



(From https://www.researchgate.net/publication/23439986_Current_Protocols_in_Neuroscience/figures?lo=1
<https://www.thermofisher.com/us/en/home/life-science/protein-biology/protein-biology-learning-center/protein-biology-resource-library/pierce-protein-methods/avidin-biotin-complex-method-ihc-detection.html>)

- **Triton-X 100% is a detergent used to improve membrane penetration of antibody. (Do not use when membrane-associated antigens are investigated)**
- DAB (3, 3'-diaminobenzidine), a derivative of benzene, is an organic compound that is used in the staining of nucleic acids and proteins, most commonly for immunohistochemical procedures. Although it is water soluble in its unoxidized form, it forms a water-insoluble brown precipitate when oxidized. In immunohistochemical procedures, the location of proteins can be detected using DAB as a substrate. The secondary antibody is conjugated with a peroxidase enzyme (HRP), and in the presence of hydrogen peroxide (H_2O_2), DAB is readily catalyzed to its oxidized form, forming a brown precipitate.





(From https://www.sheffield.ac.uk/polopoly_fs/1.458351!/file/IHC_bitesize.pdf)

Troubleshooting (From <https://www.abcam.com/protocols/troubleshooting-and-using-controls-in-ihc-and-icc>)

No staining

The primary antibody and the secondary antibody are not compatible

Use a secondary antibody that was raised against the species in which the primary was raised (e.g. primary is raised in rabbit, use anti-rabbit secondary). Be sure that the isotypes of the primary and secondary are compatible (e.g. IgY vs. IgG).

Not enough primary antibody is bound to the protein of interest

Concentrate the antibody more, incubate longer (e.g. overnight) at 4°C.

The antibody may not be suitable for IHC procedures

Check the antibody datasheet to see if it has been validated in IHC, and what type of IHC (formalin/PFA fixation, fresh frozen, etc.).

Test the antibody in a native (non-denatured) WB to make sure it is not damaged.

The primary/secondary antibody/amplification kit may have lost its activity due to improper storage, improper dilution or extensive freezing/thawing

Run positive controls to ensure that the primary/secondary antibody is working properly (see section 4 for more information about controls).

The protein is not present in the tissue of interest

Run a positive control recommended by the supplier of the antibody (see section 4 for more information about controls).

The protein of interest is not abundantly present in the tissue

Use an amplification step to maximize the signal. For example, use a biotin conjugated secondary antibody and a conjugated streptavidin.

The secondary antibody was not stored in the dark (if your detection system is immunofluorescence).

Always prevent the secondary antibody from exposure to light.

Fixation procedures (using formalin and paraformaldehyde fixatives) may be modifying the epitope the antibody recognizes

Use different antigen retrieval methods to unmask the epitope (heat mediated with pH 6 or pH 9 buffer, enzymatic, etc.).

Fix the sections for less time.

The protein is located in the nucleus and the antibody (nuclear protein) cannot penetrate the nucleus

Add a strong permeabilizing agent like Triton X to the blocking buffer and antibody dilution buffer. See our protocol about permeabilization techniques.

The PBS buffer is contaminated with bacteria that damage the phosphate groups on the protein of interest

Add 0.01% azide in the PBS antibody storage buffer or use fresh sterile PBS.

High background

Blocking of non-specific binding might be absent or insufficient

Increase the blocking incubation period and consider changing blocking agent. Abcam recommends 10% normal serum of the species of the secondary antibody for 1 hr, or 1-5% BSA for 30 min for cells in culture.

Another option is to try a secondary antibody that has been pre-adsorbed against the Ig of the species of your samples.

The primary antibody concentration may be too high

Titrate the antibody to the optimal concentration, dilute the antibody further and incubate at 4°C (a slow but targeted binding is best).

Incubation temperature may be too high

Incubate sections or cells at 4°C.

The secondary antibody may be binding non-specifically

Run a secondary control without primary antibody.

If you see staining with your secondary only, change your secondary or use a secondary antibody that has been pre-adsorbed against the Ig of the species of your samples.

Tissue not washed enough, fixative still present

Wash extensively in PBS between all steps.

Endogenous peroxidases are active

Use enzyme inhibitors i.e. Levamisol (2mM) for alkaline phosphatase or H₂O₂ (0.3% v/v) for peroxidase.

Fixation procedures (using formalin or paraformaldehyde fixatives) are causing autofluorescence (if your detection system is immunofluorescence)

Formalin/PFA usually autofluorescence in the green spectrum, so try a fluorophore in the red range.

Use a fluorophore in the infrared range if you have an infrared detection system.

Too much amplification (amplification technique)

Reduce amplification incubation time and dilute the secondary antibody or amplification kit.

Too much substrate was applied (enzymatic detection)

Dilute substrate more and reduce substrate incubation time.

The chromogen reacts with the PBS present in the cells/tissue (enzymatic detection)

Use Tris buffer to wash sections prior to incubating with the substrate, then wash sections/cells in Tris buffer.

Permeabilization has damaged the membrane and removed the membrane protein (membrane protein)

Use a less stringent detergent (e.g.) Tween 20 instead of Triton X). Or simply remove permeabilizing agent from your buffers. See our protocol about permeabilization techniques.

Non-specific staining

Primary/secondary antibody concentration may be too high

Try decreasing the antibody concentration and/or the incubation period. Compare signal intensity against cells or tissue that do not express the target.

Endogenous peroxidases are active

Use enzyme inhibitors i.e. Levamisol (2 mM) for alkaline phosphatase or H₂O₂ (0.3% v/v) for peroxidase.

The primary antibody is raised against the same species as the tissue stained (e.g. mouse primary antibody tested on mouse tissue). When the secondary antibody is applied it binds to all the tissue as it is raised against that species

Use a primary antibody made against a different species than your tissue. Use a biotinylated primary antibody and a conjugated streptavidin for the detection system.

The sections/cells have dried out

Keep sections/cells at high humidity and do not let them dry out.

Using controls

Positive controls

Why positive controls are necessary:

To validate the staining in your sample, use a positive control. This is a section from a cell line or tissue known to express the protein you are detecting. A positive result from the positive control, even if the samples are negative, will indicate the procedure is optimized and working. It will verify that any negative results are valid.

How to know what tissue type or cell line is a suitable positive control:

1. First check the antibody datasheet. This will often provide a suggested positive control. Always ensure the tissue or cell line you use is from a tested species.
2. If the antibody datasheet does not list a positive control, we recommend the following in these circumstances:
 - a. Check to see if there are any Abreviews for the antibody. Any tissues, cells or lysates that have been used successfully by these customers can be considered a suitable positive control.
 - b. Try looking at the Swiss-Prot or Omigene database links on the datasheet. These databases will often have a list of tissues that the protein is expressed in. These can also be considered suitable positive controls.
 - c. Check the GeneCards entry for the protein. This will usually provide you with relative levels of expression in various tissues.

- d. Check the Human Protein Atlas for the protein. This has a database of protein detection in different tissue types, cancers, and cell lines. Find this at www.proteinatlas.org.
- e. If you still have difficulty finding a suitable control, we recommend doing a quick literature search on PubMed to see which tissues and cells express the protein of interest.

Negative controls

Why negative controls are necessary:

Use a section from a cell line or tissue sample known not to express the protein you are detecting. This is to check for non-specific binding and false positive results. Recommended negative control tissues are knock down (KD) or knock out (KO) tissue samples.

No primary controls

This is when the primary antibody is not added to the sample. This indicates if any non-specific binding or false positives may be due to non-specific binding of the secondary antibody.

Antibody dilution buffer containing no antibody is incubated on the same sample in the same way as usual.

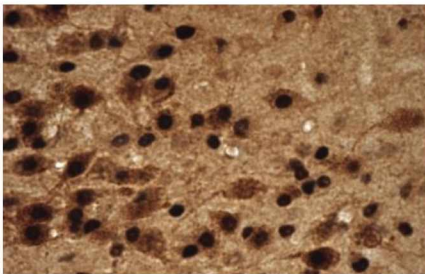
Isotype controls

An isotype control is an antibody of the same isotype (IgG2a, IgY, etc.), clonality, conjugate, and host species as the primary antibody that is raised against a molecule that is non-existent in the sample you are using. Usually this is raised against a chemical or a non-mammalian protein.

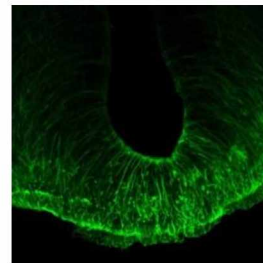
Use the same concentration ($\mu\text{g/ml}$) for the isotype control antibody and the primary antibody. This will determine the level of background in your sample.

Much like the no-primary control step, you would use this on your sample instead of the specific primary antibody. You would then use your secondary antibody as usual.

(From <http://www.abcam.com/protocols/troubleshooting-and-using-controls-in-ihc-and-icc>)



Indirect Immunoenzyme
 Arctic ground squirrel, hypothalamic slice:
 TRH neurons brown DAB, cFos neurons Ni-DAB
 Carla Frare, 2015



Indirect Immunofluorescence
 Arctic ground squirrel, hypothalamic slice:
 Vimentin positive cell (Alex 488)
 Carla Frare, 2013

Resources:

Benjamini, E., Sunshine, G., and Coico, R. (2000). Immunology : a short course (New York ; Chichester : Wiley).

Rogers, G.L., and Hoffman, B.E. (2012). Optimal Immunofluorescent Staining for Human Factor IX and Infiltrating T Cells following Gene Therapy for Hemophilia B. *J. Genet. Syndr. Gene Ther.* *S1*.

Thavarajah, R., Mudimbaimannar, V.K., Elizabeth, J., Rao, U.K., and Ranganathan, K. (2012). Chemical and physical basics of routine formaldehyde fixation. *J. Oral Maxillofac. Pathol. JOMFP* *16*, 400–405.

<http://www.protocolsonline.com/histology/immunohistochemistry-histology/dab-peroxidase-substrate-solution-brown/>

<http://www.bio-rad.com/en-us/applications-technologies/detection-methods>

<http://bitesizebio.com/7619/immunohistochemistry-getting-the-stain-you-want/>

<https://www.thermofisher.com/us/en/home/life-science/protein-biology/protein-biology-learning-center/protein-biology-resource-library/pierce-protein-methods/avidin-biotin-complex-method-ihc-detection.html>

<http://www.kyowa-kirin.com/antibody/basics/specificity.html>

http://csls-text3.c.u-tokyo.ac.jp/active/Appendix_03.html

<https://courses.lumenlearning.com/microbiology/chapter/polyclonal-and-monoclonal-antibody-production/>

<http://www.abcam.com/secondary-antibodies/direct-vs-indirect-immunofluorescence>

Appendix C 2: Undergraduate Research Mentoring Contract

Undergraduate Research Mentoring Contract

This agreement is between the Mentor,, and the Mentee,, and will last for the approximate time period of four months and then informally thereafter.

Both Mentor and Mentee agree to meet daily in the lab setting and once per week to discuss progress and research papers and maintain communication between meetings via communication methods deemed appropriate by both parties.

The Mentor agrees to:

- Maintain communication and be available to provide assistance and support as needed;
- Assist Mentee in identifying goals and projects that would be beneficial to her;
- Advise Mentee as to services at the institution that would benefit her;
- Be honest with the Mentee and give praise as well as constructive criticism; and
- Send articles and reading materials that would benefit the Mentee.

The Mentee agrees to:

- Maintain communication;
- Ask for assistance as the need arises;
- Complete tasks by the established deadlines; and
- Read all the articles and materials sent by the Mentor.

Discussions between the Mentor and the Mentee will be discreet unless otherwise discussed and agreed to by both parties. Both the Mentor and the Mentee agree to follow the guidelines of this agreement for the period specified and to make a good faith effort to resolve any issues that may arise.

Mentor Signature and Date

Mentee Signature and Date

Expected learning outcomes:

1. The student will master the brainstem anatomy and will be able to identify the nuclei of interests in the ground squirrel brain.
2. The student will gain a wide understanding of hibernation through literature review.
3. The student will learn how to perform literature search.
4. The student will learn the brainstem physiological function.
5. The student will learn how to formulate hypotheses and how to link the brainstem functions to the phenomenon of hibernation.
6. The student will master immunohistochemistry, a widely used laboratory technique.
7. The student will be able to confidently use the microscope, learning the basic components and their functions.
8. The student will perform data analysis, first acquiring images, then doing cell counting and at the end performing statistical analysis.

Final products:

- Poster to present at the sleep conference.
- Data will be included in a publication which defines brain nuclei activated by CHA in hypothalamus and brainstem.

Student's Expectation from the research experience:

Approximately number of hours available per week _____

Day and hours when the student will be in the lab

If the student must deviate from the agreed schedule (e.g. to study for an exam), then she/he will communicate this to the mentor at least three days before the change occurs.

Appendix C 3: Student's Performance Evaluation

Student's Performance Evaluation					
Circle one: 1=I understand the skill and work independently, 2= I understand the skill but not effectively independent, 3= I understand the skill with help, 4= I don't understand the skill yet					
1. Knowledge Application	1	2	3	4	n/a
• Ability to apply knowledge to the research field					
• Ability to search independently	1	2	3	4	n/a
• Knowledge of primary scientific literature in the research field	1	2	3	4	n/a
2. Problem Solving Skills	1	2	3	4	n/a
• Ability to identify a problem and suggest solution					
• Ability to use resources (technology, literature) to make decisions and solve problems	1	2	3	4	n/a
• Ability to apply knowledge to solve problems	1	2	3	4	n/a
• Ability to see underlying connections between concepts from different subjects areas	1	2	3	4	n/a
3. Lab Skills	1	2	3	4	n/a
• Use of laboratory equipment					
• Follows laboratory safety procedures	1	2	3	4	n/a
• Lab record keeping and data gathering	1	2	3	4	n/a
• Ability to design and conduct experiment	1	2	3	4	n/a
• Ability to analyze results	1	2	3	4	n/a
• Ability to interpret data by relating to original hypothesis and current literature	1	2	3	4	n/a
4. Teamwork Skills	1	2	3	4	n/a
• Ability to give and receive constructive criticism					
• Ability to take charge of tasks without being asked	1	2	3	4	n/a
• Ability to complete assigned tasks timely	1	2	3	4	n/a

5. Communication Skills	1	2	3	4	n/a
• Presentation Skills					
• Writing Skills	1	2	3	4	n/a
6. General Competencies:	1	2	3	4	n/a
• Take initiative					
• Time management	1	2	3	4	n/a
• Troubleshooting	1	2	3	4	n/a
• Reliability and dependability	1	2	3	4	n/a
• Capacity of improvement	1	2	3	4	n/a
• Resilience and adaptability	1	2	3	4	n/a
• Understanding of professional and ethical responsibilities	1	2	3	4	n/a
Comment on student's strength and Weaknesses					
Other Comments					

Appendix C 4: Mentor-Mentee Closure Assesment

Mentor: _____

Project start date: _____

Mentee: _____

Project end date: _____

This assessment is designed to collect feedback with the purpose to benefit and improve the mentor-mentee relationship. This assessment will not affect any future recommendation letters. Honest and constructive observations and comments are highly appreciated.

Reasons for ending the mentor-mentee relationship:

Mentee Accomplishments (conference presentations, awards, technical skills, soft skills...):

What really worked during your mentee experience?

What was not successful or where did you find difficulties during your mentee experience?

--

Do you think this experience helped you improving the following skills?

	Provide one or more examples that helped you improving the skill	Provide suggestions on how to improve the skill
Knowledge of the Topic (Answering questions, explaining your research..)		
Technical/Lab Skills (Making buffers and reagents, microscopy, using scientific terminology..)		
Communication (Make a poster, presentation, communicate changes on deadlines, inform about problems..)		
Critical Thinking (Understand the information, ask thoughtful questions, suggest novel idea, Self-correct as needed...)		
Problem Solving (Able to identify a problem, provide solutions..)		

Time Management (Meet deadline, good at prioritizing tasks, wisely use of time..)		
Identify Resources (Scientific as journals, people who could answer my questions...)		

Which skills will be more beneficial for your future projects/jobs?

Evaluate your mentor:

My mentor ...	Strongly Disagree	Disagree	Agree	Strongly Agree	
Was accessible and available					N/A
Kept open communication with me					N/A
Showed a reasonable interest/concern towards me					N/A
's behavior and attitude were generally professional					N/A
Gave feedback and constructive criticism					N/A
Encourage me to participate in professional activities outside the University (conferences, science activities..)					N/A
Encourage me to submit proposals, projects..					N/A
Set clear goals and objectives					N/A
Completed the goals planned together					N/A
The relationship met your expectation					N/A
Overall, I would work with my mentor again					N/A

Please provide suggestions to improve your mentor's mentoring style:

What was one of your favorite memories of your mentor-mentee relationship?

Sign and Date
